National Library of Canada
Acquisitions and Bibliographic Services Branch
395 Wellington Street
Ottawa, Ontario
K1A 0N4

Bibliothèque nationale du Canada
Direction des acquisitions et des services bibliographiques
395, rue Wellington
Ottawa (Ontario)
K1A 0N4

Your file Votre référence

Our file Notre référence

NOTICE

The quality of this microform is heavily dependent upon the quality of the original thesis submitted for microfilming. Every effort has been made to ensure the highest quality of reproduction possible.

If pages are missing, contact the university which granted the degree.

Some pages may have indistinct print especially if the original pages were typed with a poor typewriter ribbon or if the university sent us an inferior photocopy.

Reproduction in full or in part of this microform is governed by the Canadian Copyright Act, R.S.C. 1970, c. C-30, and subsequent amendments.

AVIS

La qualité de cette microforme dépend grandement de la qualité de la thèse soumise au microfilmage. Nous avons tout fait pour assurer une qualité supérieure de reproduction.

S'il manque des pages, veuillez communiquer avec l'université qui a conféré le grade.

La qualité d'impression de certaines pages peut laisser à désirer, surtout si les pages originales ont été dactylographiées à l'aide d'un ruban usé ou si l'université nous a fait parvenir une photocopie de qualité inférieure.

La reproduction, même partielle, de cette microforme est soumise à la Loi canadienne sur le droit d'auteur, SRC 1970, c. C-30, et ses amendements subséquents.

Canada

A GENERAL PARAMETRIC OPTIMAL POWER FLOW

by

Katia Campos de Almeida

B.Eng. (Federal University of Juiz de Fora, Brazil)
M.Sc. (State University of Campinas, Brazil)

A thesis submitted to the Faculty of Graduate Studies and Research in partial fulfilment of the requirements for the degree of Doctor of Philosophy

Department of Electrical Engineering
McGill University
Montreal, Canada

ISBN 0-612-05662-7

Canada

ABSTRACT

The objective of an Optimal Power Flow (OPF) algorithm is to find the steady-state operation point of a generation-transmission system which minimizes a pre-specified cost function and meets a set of operational and/or security constraints. OPF algorithms are among the tools present in many Energy Management Systems and their usefulness is increasingly being recognized by power utilities.

This thesis presents an algorithm which uses the parameters existing in the OPF problem to find its solution. These parameters can be in the objective function or the equality or inequality constraints. This algorithm is applied to a parameterized OPF model built according to the following criteria: (i) when all parameters present in the model are relaxed from their given levels, a solution can be trivially found for this parameterized problem and (ii) when all parameters are returned to their original values, the parameterized model is equal to the original OPF. As the initially relaxed parameters are returned to their original values, they define a sequence of OPF problems which converge to the original one. The algorithm is designed to track the optimal solutions of these intermediate problems until the optimum of the original OPF. This tracking is made in a systematic manner. By using a binary search or a linear prediction method, the algorithm finds the maximum increment of the parameters which allow only one inequality to be fixed at its limit or to be released. The parameters are then adjusted to their new values, defining a new OPF problem with known optimal active feasible set. As a consequence, the optimal solution of this new problem can be easily found by solving the first order optimality conditions by Newton's method. In this way, the optimum is tracked from one active feasible set to the next until the parameters reach their original values.

The parameterization permits the solution of the OPF problem for a fixed and variable load using the same mechanism described in the previous paragraph. As a result of this systematic tracking, the method is robust and able to provide a very good insight about the behaviour of the OPF solutions. In addition, the main difficulties encountered in solving the OPF problem are easily visualized and, in particular, the approach permits the differentiation of the potential causes for the failure of the tracking process, including the identification of unsolvable cases. The sensitivities of the optimal solution as a function of the parameters are also by-products of the method; including the Bus Incremental Costs and the System Incremental Cost as functions of the loads. The approach is also flexible enough to permit the simulation of line contingencies and of Flexible AC Transmission Systems (FACTS devices). The algorithm developed was tested in numerous networks with different objective functions and initializations and the results demonstrated the potential of this technique.

RÉSUMÉ

Le but d'un algorithme d'écoulement optimal de puissance (EOP) est de trouver le meilleur point d'exploitation en régime permanent d'un réseau de production-transport d'énergie qui répond à un ensemble de contraintes opérationnelles ou de sécurité. Les algorithmes de EOP sont des outils présents dans les Centres de Conduite de Réseaux et leur utilité est de plus en plus reconnue par les compagnies électriques.

Cette thèse présente un algorithme utilisant les paramètres qui existent dans le problème de EOP dans le but de trouver sa solution. Ces paramètres peuvent être présents dans le critère d'optimisation ou dans les contraintes d'égalité et d'inégalité. Cet algorithme est appliqué à un modèle paramétré de l'EOP bâti selon les critères suivants: (i) quand tous les paramètres du modèle sont relâchés de leurs valeurs données, une solution triviale peut être obtenue et (ii) quand tous les paramètres relâchés sont retournés à leurs valeurs originales, une séquence de problèmes EOP est définie convergeant au problème original. L'algorithme est conçu pour suivre la solution optimale de tous ces problèmes intermédiaires jusqu'au point optimal du problème original. Ce processus est fait d'une façon systématique. En utilisant une recherche binaire ou une méthode de prévision linéaire, l'algorithme trouve l'incrément maximum des paramètres permettant ainsi qu'une seule inégalité soit fixée à sa limite ou soit libérée. Les paramètres sont alors ajustés à leurs nouvelles valeurs définissant ainsi un nouveau problème EOP comportant un ensemble d'inégalités actives connues. Par conséquent, la solution optimale de ce nouveau problème peut être facilement trouvée en solutionnant les conditions optimales de premier ordre par la méthode de Newton. De cette façon, l' optimum est suivi d'un ensemble actif faisable à l'autre jusqu'à ce que tous les paramètres soient arrivés à leurs valeurs d'origine.

La mise en évidence des paramètres permet de solutionner le problème EOP dans le cas des charges fixes ou variables en utilisant le même mécanisme décrit ci-haut. A la

suite de ce processus systématique, il est possible d'obtenir un très bon aperçu du comportement des solutions de l'EOP. Les difficultés principales auxquelles on doit faire face en solutionnant le problème EOP sont facilement visualisées et, en particulier, l'approche permet la différentiation des causes potentielles d'interruption du processus d'optimisation, y compris l'identification des cas sans solution. Les sensibilités de la solution optimale, en fonction des paramètres, sont aussi des produits secondaires du processus, ce qui inclue le coût marginal de la charge du réseau et les coûts marginaux des charges individuelles. L'approche est assez flexible pour permettre la simulation des contingences topologiques et l'optimisation des dispositifs "FACTS" (Flexible AC Transmission Systems). L'algorithme a été validé dans plusieurs réseaux, en considérant différents objectifs d'optimisation et les résultats démontrent le potentiel de cette technique.

ACKNOWLEDGEMENTS

I first would like to express my sincere gratitude to Prof. F.D. Galiana for his expert guidance, support, generosity and friendship during the development of this thesis.

Special thanks to Prof. S. Zlobec for the valuable suggestions and discussions about the theoretical aspects of the thesis.

Thanks are also due to Prof. B.T. Ooi for his constructive comments and constant encouragement.

I also wish to thank Prof. S. Soares for his friendship and support of many years.

In addition, I would like to thank the warm companionship of my friends and colleagues of the Power Group. It has been a great opportunity to meet and share experiences with such a diverse group of people. In particular, many thanks to the System Managers of the laboratory, Lester Loud, Hossein Javidi and Djordje Atanackovic for the ready help with any problem.

The financial support of the Brazilian Research Council, CNPq, the provincial FCAR and the National Sciences and Engineering Research Council of Canada are gratefully acknowledged.

Finally, I would like to thank my family for their continuous encouragement.

TABLE OF CONTENTS

LIST OF SYMBOLS

Symbol	Meaning
a	tap settings ($a \in \mathbb{R}^{nl}$).
aa	linear cost coefficient of c(**pg**) (**aa** $\in \mathbb{R}^{nb}$)
A	bus-line incidence matrix (**A** $\in \mathbb{R}^{(nb \times nl)}$).
Af	starting bus-line incidence matrix (**Af** $\in \mathbb{R}^{(nb \times nl)}$).
At	ending bus-line incidence matrix (**At** $\in \mathbb{R}^{(nb \times nl)}$).
b	vector of variable shunt compensators (**b** $\in \mathbb{R}^{nb}$).
$\mathbf{b}^{sh}$	line shunt capacitors ($\mathbf{b}^{sh} \in \mathbb{R}^{nl}$).
bb	quadratic cost coefficient of c(**pg**) (**bb** $\in \mathbb{R}^{nb}$).
BIC	vector of bus incremental costs (**BIC** $\in \mathbb{R}^{nb}$).
BIC'	vector of reactive bus incremental costs (**BIC'** $\in \mathbb{R}^{nb}$).
c(**x**)	cost function (c: $\mathbb{R}^{nv} \rightarrow \mathbb{R}$).
c(**x**,ε)	parameterized cost function (c: $\mathbb{R}^{nv+1} \rightarrow \mathbb{R}$).
c(**pg**)	generation cost function (c:$\mathbb{R}^{nb} \rightarrow \mathbb{R}$).
c_0	initial cost.
d	vector of real and reactive bus loads (**d** $\in \mathbb{R}^{2nb}$).
e	direction of increment of the decision variables and lagrange multipliers associated with active functional inequalities given by the linear prediction

	($\mathbf{e} \in \mathbb{R}^{nfree}$).
$\mathbf{e}_q$	vector with 1 in the q*th* position and zeros elsewhere ($\mathbf{e}_q \in \mathbb{R}^{m+p-l}$).
E	voltage magnitude.
$\mathbf{g}(\mathbf{x})$	equality constraint ($\mathbf{g}$: $\mathbb{R}^{nv} \rightarrow \mathbb{R}^{m}$).
$\mathbf{g}(\mathbf{x},\varepsilon)$	parameterized equality constraint ($\mathbf{g}$: $\mathbb{R}^{nv+1} \rightarrow \mathbb{R}^{m}$).
$\mathbf{h}(\mathbf{x})$	inequality constraint ($\mathbf{h}$: $\mathbb{R}^{nv} \rightarrow \mathbb{R}^{s}$).
$\mathbf{h}(\mathbf{x},\varepsilon)$	parameterized inequality constraint ($\mathbf{h}$: $\mathbb{R}^{nv+1} \rightarrow \mathbb{R}^{s}$).
H	hessian of the Lagrangian function ($H \in \mathbb{R}^{(nv \times nv)}$).
$\mathbf{HO}(\mathbf{x},\varepsilon)$	homotopy function ($\mathbf{HO}$: $\mathbb{R}^{nv+1} \rightarrow \mathbb{R}^{nv}$).
I	index set of decision variables.
$\mathbf{I}_0$	index set of active limits on decision variables.
$\mathbf{I}_f$	index set of free decision variables.
IC	vector of bus current injections ($\mathbf{IC} \in \mathbb{C}^{nl}$).
ifrom	vector of the starting busses of the system lines (ifrom $\in \mathbb{R}^{nl}$).
ito	vector of the ending busses of the system lines (ito $\in \mathbb{R}^{nl}$).
J	jacobian of the active constraints of P(ε) ($J \in \mathbb{R}^{(m+p \times nv)}$).
J'	jacobian matrix defined after substitution of line q ($J' \in \mathbb{R}^{(m+p \times nv)}$).
K	index set of equality constraints (K={ 1,...,m}).
L	index set of inequality constraints (L ={1,...,s}).
$\mathbf{L}_0(\mathbf{x},\varepsilon)$	index set of active inequalities.
$\mathbf{L}_+(\mathbf{x},\varepsilon)$	index set of active inequalities associated with strictly positive Lagrange multipliers.
$\mathfrak{L}$	Lagrangian function ($\mathfrak{L}$: $\mathbb{R}^{nv+1+m+s} \rightarrow \mathbb{R}$).

$\mathcal{L}^0$	Lagrangian function defined at $\varepsilon=0$ ($\mathcal{L}$: $\mathbf{R}^{nv+1+m} \rightarrow \mathbf{R}$).
lim	superscript - minimum and/or maximum limits.
m	number of equality constraints.
$\mathbf{M}(\varepsilon)$	feasible set of the problem $P(\varepsilon)$.
min	superscript - minimum limit.
max	superscript - maximum limit.
$\mathbf{N}$	index set of the functional inequalities.
$\mathbf{N}_0$	index set of active functional inequality limits.
$\mathbf{N}_f$	index set of the inactive functional inequality limits.
nb	number of buses in a transmission system.
nfree	number of free variables (i.e., not in the limits).
nflfree	number of inactive power flow limits.
nfllim	number of real power flows at their limits.
ng	number of generators.
nl	number of lines.
nqgfix	number of busses with fixed reactive injection.
nqgnf	number of busses with variable reactive injections.
nqglim	number of reactive generations at their limits.
nqgfree	number of free reactive generations.
nv	number of variables.
$\mathbf{p}(\mathbf{V},\delta,\mathbf{a},\phi,\mathbf{xl})$	active power injection.
p	number of active inequality constraints.
pd	active load ($\mathbf{pd} \in \mathbf{R}^{nb}$).

pg	active power generation ($\mathbf{pg} \in \mathbb{R}^{nb}$).
pl	active power flow ($\mathbf{pl} \in \mathbb{R}^{nl}$).
P(ε)	general parameterized OPF model.
q(V,δ,a,ϕ,xl)	reactive power injection.
qg	reactive power generation ($\mathbf{qg} \in \mathbb{R}^{nb}$).
qd	reactive load ($\mathbf{qd} \in \mathbb{R}^{nb}$).
Q(.)	expression representing the second and higher order derivatives of $\mathcal{L}$ with respect to **z** and ε.
r	direction of increment of the Lagrange multipliers associated to the decision variables at the limits given by linear prediction ($s \in \mathbb{R}^{nv-nfree}$).
rl	line resistance ($\mathbf{rl} \in \mathbb{R}^{nl}$).
$\mathbf{r}_q$	vector defined by the difference of the gradients of two inequalities, $\mathbf{h}_p$ and $\mathbf{h}_q$ ($\mathbf{r}_q \in \mathbb{R}^{nv}$).
s	number of inequality constraints.
s	direction of increment of the inactive functional inequalities given by linear prediction ($\mathbf{r} \in \mathbb{R}^{nqgfree+nflfree}$).
S	vector of complex power injections ($\mathbf{S} \in \mathbf{C}^{nb}$).
Sl	vector of complex power flows ($\mathbf{Sl} \in \mathbf{C}^{nl}$).
$\mathbf{Sl}_1$	vector of complex power flows disregarding the flows on the line shunt capacitors ($\mathbf{Sl}_1 \in \mathbb{R}^{nl}$).
SIC	system incremental cost.
ST	vector of sensitivities of the objective function to changes in variable bounds or functional inequality limits ($\mathbf{ST} \in \mathbb{R}^{nv+nl}$).
t	vector of complex transformer settings ($\mathbf{t} \in \mathbf{C}^{nl}$).
T	superscript - transpose.

$\mathbf{T}$	plane tangent to the set of active constraints.
$\mathbf{u}$	vector of control variables.
$\mathbf{U}$	matrix composed by the vectors which span the range space of W ($\mathbf{U} \in \mathbb{R}^{(nv+m+p \times nv+m+p-l)}$).
$\mathbf{v}$	vector belonging to the null-space of $\mathbf{W}$ ($\mathbf{v} \in \mathbb{R}^{nv+m+p}$).
$\mathbf{V}$	vector of voltage magnitudes ($\mathbf{V} \in \mathbb{R}^{nb}$).
$\mathbf{VC}$	vector of complex voltages ($\mathbf{VC} \in \mathbf{C}^{nb}$).
w	weighting factor associated with the quadratic parameterized term of the objective function.
w_1	weighting factor associated with the generation costs.
w_2	weighting factor associated with the term representing transmission losses.
w_3	weighting factor associated with the term representing the deviation of the voltage magnitudes from normal.
W	hessian of the Lagrangian function ($W \in \mathbb{R}^{(nv+m+p \times nv+m+p)}$).
W_f	submatrix of W composed only by the indices of the free variables ($W_f \in \mathbb{R}^{(nfree+m+p \times nfree+m+p)}$).
$\mathbf{x}$	vector of decision variables ($\mathbf{x} \in \mathbb{R}^{nv}$).
$\mathbf{xl}$	vector of line series reactances ($\mathbf{xl} \in \mathbb{R}^{nl}$).
$\mathbf{y}$	vector of control variables (Chapter 2) and vector belonging to the null space of J ($\mathbf{y} \in \mathbb{R}^{m+p}$) (Chapter 3).
$\mathbf{Y}$	admittance matrix ($\mathbf{Y} \in \mathbf{C}^{(nb \times nb)}$).
$\mathbf{Yl}$	diagonal of line series admittances ($\mathbf{Yl} \in \mathbf{C}^{(nl \times nl)}$).
$\mathbf{z}$	vector composed by the solutions of the first order optimality conditions $\mathbf{z}^T=[\mathbf{x}^T,\lambda^T,(\mu_{L0})^T]$.
α	vector of Lagrange multipliers associated with the active power balance equations ($\alpha \in \mathbb{R}^{nb}$).

β	vector of Lagrange multipliers associated with the reactive power balance equations at the load busses ($\beta \in \mathbb{R}^{nqgfix}$).
γ	vector of Lagrange multipliers associated with the active power generations ($\gamma \in \mathbb{R}^{nb}$).
δ	vector of voltage angles ($\delta \in \mathbb{R}^{nb}$).
Δ, Δ	increment on a variable or a vector.
ε	continuation parameter ($0 \leq \varepsilon \leq 1$).
ζ	vector of Lagrange multipliers associated with the general functional inequalities ($\zeta \in \mathbb{R}^{(nqglim+nfllim)}$).
η	vector of Lagrange multipliers associated with the phase shifter angles ($\eta \in \mathbb{R}^{nl}$).
θ	scalar multiplying **U**.
λ	vector of Lagrange multipliers associated with general equality constraints ($\lambda \in \mathbb{R}^{m}$).
$\Lambda(.)$	function composed by the first derivatives of the Lagrangian with respect to $\mathbf{x}$, λ, ζ_{N0} and ν_{I0}.
$\Lambda_f(.)$	partition of Λ composed by the indices related to the free variables and the Lagrange multipliers of the active constraints.
μ	vector of Lagrange multipliers associated with general inequality constraints ($\mu \in \mathbb{R}^{s}$).
ν	vector of Lagrange multipliers associated with lower and upper limits on the decision variables ($\nu \in \mathbb{R}^{2nv}$).
ξ	vector of Lagrange multipliers associated with the tap settings ($\xi \in \mathbb{R}^{nl}$).
π	vector of Lagrange multipliers associated with the voltage magnitudes ($\pi \in \mathbb{R}^{nb}$).
ρ	vector of Lagrange multipliers associated with the reactive power balance equations at the PV busses ($\rho \in \mathbb{R}^{nqgfix}$).

σ	Lagrange multiplier associated with the active power flows ($\sigma \in \mathbb{R}^{nflim}$).
τ	vector of Lagrange multipliers associated with variable series reactances ($\tau \in \mathbb{R}^{nl}$).
υ	vector composed by all lagrange multipliers of the OPF model (Appendix A)
ϕ	vector of phase shifter angles ($\phi \in \mathbb{R}^{nl}$).
ψ	vector of Lagrange multipliers associated with variable shunt compensators ($\psi \in \mathbb{R}^{nb}$).
*	superscript - conjugate.

Note: All vectors are column vectors. Matrices and vectors are represented in bold letters while scalars are represented in normal letters. Unless described in the list above, subscripts indicate an element of a vector or a matrix. Superscripts, on the other hand, represent values of a variable at a specific iteration.

LIST OF TABLES

LIST OF FIGURES

LIST OF ABBREVIATIONS

Abbreviation	Meaning
AC	Alternating Current
AL	Augmented Lagrangian
DC	Direct Current
ED	Economic Dispatch
EHV	Extra High Voltage
EICC	Equal Incremental Cost Criterion
EMS	Energy Management System
FACTS	Flexible AC Transmission Systems
GRG	Generalized Reduced Gradient
GTO	Gate Turn-Off Thyristor
KT	Kuhn-Tucker
LICQ	Linear Independence Constraint Qualification
LP	Linear Programming
MFCQ	Mangasarian-Fromovitz Constraint Qualification
PQ	Power-Reactive Power (i.e., at PQ buses, real and reactive power are specified in the load flow equations).
PV	Power-Voltage (i.e., at PV buses, real power and voltage magnitude are specified in the load flow equations).

QP	Quadratic Programming
SQP	Sequential Quadratic Programming

CHAPTER 1

INTRODUCTION

1.1 General

Power utilities nowadays place great importance on the secure-economic operation of their systems. The savings that can be obtained by an economical operation have been proven to be considerable [Maria and Findley, 1987 and Bridenbaugh et al., 1992]. With increased restrictions in the construction of new power plants and transmission lines (in spite of a continuous increase in the demand), it becomes even more necessary to obtain the best possible performance out of existing systems.

The problem of optimal steady-state operation of a generation-transmission system is represented through a mathematical model broadly known as the Optimal Power Flow (OPF) problem. The OPF problem can be defined as a "general mathematical tool used to find the instantaneous optimal operation of a power system under constraints which meet operating feasibility and, optionally, security constraints" [Carpentier, 1987]. The first mathematical formulation of the OPF problem was proposed almost four decades ago and, since then, has been used almost with no modifications in numerous studies.

All research on the OPF problem can be rationalized if we consider that, by solving this problem, all state variables of a power system can be optimally controlled (according to some pre-specified criterion, e.g., minimum cost or minimum transmission losses) while satisfying a very complex set of equality and inequality constraints. The OPF problem is a power engineers' answer to society's demand for the minimum possible waste of energy with a high quality of service. An OPF forms part of the specifications in any project submitted today for the energy management system (EMS) of a power

system. Nevertheless, the OPF is still is not broadly used, mainly because of the difficulties of using such a tool in control centres [Stott et al., 1987 and Heinz et al., 1993]. The reasons for these difficulties are various. In spite of the extensive research made in OPF, still today there are cases where OPF algorithms fail to find an optimal solution. More important, some of the constraints present in day-to-day operation cannot yet be properly modelled. As a consequence, solutions provided by the OPF algorithms are not always realistic and it still constitutes a risk to rely entirely in OPF algorithms in daily operation of a power system. In addition, unlike load flow programs that are broadly used by the power utilities (and considered reliable tools for operation), the implementation and use of OPF programs is not trivial. The fact that there must be specialized personnel to use an OPF package and the sophistication of such a tool accounts for a general reluctance in the power utilities about the advantages of using an OPF program in daily operation.

Unfortunately (and perhaps predictably), the task of optimizing the steady-state operation of a generation-transmission system is not easily tractable. The laws that rule power generation and transmission transform the OPF into a mixed integer-nonlinear (non-convex) problem which can defy the most sophisticated optimization methods. Because of its numerous potential applications in power as well as its complexity, the OPF problem can be classified among classical optimization problems such as the "knapsack problem" or the "travelling salesman problem". Surprisingly, until today, in spite of the huge bibliography that exists about the OPF, no attempt has been made to condense the many different aspects of this problem in a book where, usually, one finds only the theory of some of the more elementary versions of the OPF, e.g., the Equal Incremental Cost Economic Dispatch and the classical load flow problem. This, together with the basic characteristic of the OPF, which requires a good knowledge in both power systems operation and mathematical programming, has led to the lack of a consensus in the literature as to the best way to approach this problem.

Presently, different OPF packages are available in the market [Burchett et al., 1984; Sun et al., 1984; Alsaç et al, 1990 and Bertran et al., 1990]. Computational programs exist that find the optimal operation state of a power system in seconds,

contradicting the previous general perception that the steady-state optimization could not be done on-line. Nevertheless, in spite of all the advances achieved in terms of computational speed, many theoretical aspects of the OPF problem have not been sufficiently studied. Consequently, causes of failure or difficult convergence of OPF algorithms are not always known. This is a difficult area which could not yet be properly studied, in part because of the tools available to solve the problem.

The research being carried out nowadays in this area is mainly concerned with implementing fast algorithms that provide reliable solutions for the OPF problem where the system demands and topology are considered fixed. Ideally, a method that would represent the changes in the operation environment should be employed in order to be as close as possible to the day-to-day operation of a power system. With this in mind, we propose in this thesis the use of a method that would be able to represent to some extent the changes that could occur in the power system. Here, a parametric optimization method is used to solve the OPF problem. This approach was also motivated by a desire to investigate the behaviour of OPF solutions with respect to variations in problem parameters such as loads and variable limits.

1.2 The Present Thesis

The OPF model, as any other mathematical model, is composed of decision variables which can be controlled and a set of variables over which usually one has no control: the *parameters*. Active and reactive generation are some examples of the decision variables while load demand, line characteristics and operational limits are examples of parameters.

Parametric optimization characterizes the behaviour of the optimal solution of a problem for a range of parameter variations. Thus, the use of a parametric optimization approach in the OPF serves to analyze the optimal behaviour of the decision variables as some of the model parameters vary. This variation can be due to normal time behaviour such as daily load changes. Parameter variation can also be artificially imposed to examine the behaviour of the OPF solution with respect to coefficients such as variable

limits and cost data. The latter type of parameter variation is interesting to study on its own merits, however we found that it can be the basis for a new approach to solve the OPF.

Different parametric approaches have been used to solve the OPF problem. The present thesis is an extension and generalization of previous research pursued at McGill University. The studies developed thus far using parametric methods to solve the OPF problem were limited by the specific nature of the models and algorithms used. Typically, they minimize a cost subject to linear constraints by parametric quadratic programming. Alternatively, they can be based on models consisting of non-linear constraints and costs that are linearized and solved through sequential quadratic programming. Here we propose a general parametric OPF model where the full nonlinear load flow equalities and inequalities are enforced while minimizing an arbitrary objective function. Furthermore, in this work, the OPF problem can be independently parameterized by relaxing one or more of the following : (a) the objective function; (b) the inequality limits and (c) the equalities. This feature enables the tracking and analysis of the OPF behaviour in terms of general parameter variations and also a systematic solution of the OPF from an arbitrary initial condition.

The strategy proposed here can be divided into two main phases. Phase I finds the OPF solution for a given load level starting from an arbitrary initial condition. Phase II tracks the OPF solution as a function of the load level over a given interval starting from the Phase I solution.

In Phase I, the objective function, the equality and inequality constraints are parameterized by a single parameter. The parameterized OPF is then relaxed by modifying this parameter in such a way that an arbitrary initial solution is forced to be optimal. The variation of the parameter produces a sequence of nonlinear optimization problems, with known active constraint set, whose solutions converge to the solution of the original OPF problem. Since for each problem in the sequence the active set is always known, the corresponding solutions are reduced to simply solving the set of equations arising from the first order optimality conditions. Thus, starting from an arbitrary initial solution, the

optimum is tracked through a strategy that consists of two steps: (i) the variation of the parameter that brings the initial relaxed problem progressivelly closer to the original one and (ii) the solution of the various intermediate optimization problems by Newton's method. The key of this strategy is step (i). The variation of the parameter must be done in a way that only one change at a time takes place in the optimal active set. This approach leads to the systematic tracking of the optimal solution and permits an easy detection of the causes of failure of the optimization process whenever this occurs.

In Phase II, after obtaining an optimal solution for Phase I, the algorithm tracks the OPF solution trajectory as a function of the load over a given interval. The ability to track the OPF solution in terms of the load has potential in an on-line environment by allowing system operators to pre-calculate the optimal dispatch strategies based on a load forecast.

1.2.1 Outline of the Thesis

The chapters of this thesis are organized as follows:

Chapter 2, first of all, presents a general description of the OPF problem: the different formulations, variables, constraints and objective functions used. Next, an analysis is made of the OPF literature, emphasizing the most recent publications and also some important work done in the past. These publications are classified according to the optimization techniques used to solve the problem and some of the strong and weak points of the different methods are discussed. Following this, a general idea of parametric methods is given through the discussion of some mathematical examples. Finally, the various publications in power system operation using parametric methods are presented emphasizing the work done in Economic Dispatch and OPF.

Chapter 3 presents the theoretical aspects of the parametric approach used in this thesis. The discussion starts with a description of the parameters existing in the OPF model. Next are presented the first and second order optimality conditions of a general nonlinear parametric optimization problem whose feasible set satisfies a set of regularity

constraints. These optimality conditions are then used to explain the parameterized models used in this thesis to solve the OPF problem for fixed and variable system load. With the parametric models described, the process of tracking the optimal solution is studied in detail and the various causes for the failure of the parametric approach are explained. In the last section is introduced the concept of "structural stability" of a parametric mathematical problem. The special case of the Parametric-OPF is then analyzed and some conclusions are drawn about the behaviour of the OPF solution in a varying load environment.

Chapter 4 presents the Parametric-OPF algorithm implemented in this thesis. To describe this algorithm, detailed parameterized models for solving the OPF are introduced and the associated optimality conditions are derived. The algorithm is divided into two main stages which are discussed separately: the definition of a feasible set which is active at the optimal solution of the parameterized model, and the resolution of the first order optimality conditions defined for this specific active feasible set. First, an explanation is given about how an optimal active feasible set is obtained through the use of a binary search or a linear prediction method. The Newton method based approach used to solve the system of equations composed of the optimality conditions of the parameterized problem is then described.

Some special applications of the algorithm described in Chapter 4 are presented in Chapter 5. First of all, a methodology for the simulation of line contingencies is described. Next, using quantities which are by-products of the Parametric-OPF algorithm, we derived expressions of the sensitivities of the OPF solutions for an interval of load variation, including the Bus Incremental Costs and the System Incremental Cost. Following this, a methodology is described to study the behaviour and influence of Flexible AC Transmission Systems (FACTS) devices in the optimal steady-state operation of generation-transmission systems.

In Chapter 6 the results of tests made with the Parametric-OPF algorithm are presented and analyzed. The systems tested here are: the 14, 30 and 118-bus IEEE test networks and a 34-bus network with 64 lines characterized by high levels of reactive

power and voltage instability. The results are organized in two parts. In the first part, the computational aspects of the method are discussed by comparing its performance for different initializations, strategies to find the optimal active feasible set and type of constraints and variables existing in the problem. In the second part, some analysis are made regarding the behaviour of the OPF variables during the solution of the problem for fixed or variable load; in some cases, also supposing line contingencies. In addition, some economical aspects of the optimal steady-state operation are also discussed. Next, some tests with FACTS devices are presented and their influence in the OPF solution is studied

Finally, Chapter 7 provides an overview of the present thesis and recommendations are made regarding future work.

1.2.2 Claim of Originality

To the best of the author's knowledge, the following are the main results and contributions of this thesis:

1. The formulation of a general parametric OPF model where the objective function, equality and inequality constraints are parameterized.

2. The implementation of a parametric algorithm where the full OPF problem is solved by systematically tracking the active set and without recourse to sequential linear or quadratic programming. Two versions are developed, one for the OPF with fixed loads and a second for load tracking.

3. A detailed study of the behaviour of the OPF solution for both fixed and variable system loads, in particular an analysis of the potential causes for the failure of the method.

4. The definition of a *region of structural stability* for the OPF problem (i.e., a region where there is a continuous change in the optimal solution of the problem for a change in the system load or any operational limit).

5. The study of the algorithm in a number of test cases including the influence and behaviour of Flexible A.C Transmission System (FACTS) devices in the OPF problem.

CHAPTER 2

BACKGROUND

2.1 Introduction

The optimal power flow (OPF) problem can be defined as a "general mathematical tool used to find the instantaneous optimal operation of a power system under constraints which meet operating feasibility and, optionally, security constraints" [Carpentier, 1987].

The OPF is becoming nowadays an important tool in Energy Management Systems (EMS); it is increasingly replacing the classical load flow algorithms to perform operation and planning tasks.

The OPF can be classified among very general and difficult mathematical problems such as the "travelling salesman" or the "knapsack" problems. While it is possible to find books devoted entirely to the last two problems, the different details of modelling, approximations and solution methods for the OPF are only superficially treated in books devoted to power systems planning and control where, usually, one finds only the theory of some of the more elementary versions of the OPF, e.g. the Equal Incremental Cost Economic Dispatch and the classical load flow problem. The lack of textbooks on OPF is surprising since the OPF has been the subject of an enormous amount of research for over thirty years and its importance has been more and more recognized by the power utilities. The original model has engendered many different OPF formulations and almost every mathematical optimization method has been applied to its solution; but the general problem, as conceived today, remains a challenge.

In this chapter, first of all, the OPF problem is characterized and the various details and extensions of the basic model are presented. After that, the various works that have been published in this field in recent years as well as some important earlier results are discussed, so as to give an idea about the state of the art in OPF. Subsequently, the mathematical approach used in this thesis to solve the OPF - a parametric optimization technique - is introduced and the reasons for this choice are presented together with some general applications of parametric approaches in power system analysis.

2.2 The Optimal Po er Flow Problem

2.2.1 Basic Formulation

The OPF optimizes the static operating condition of a power generation-transmission system. A scalar function is to be minimized subject, in some cases, to thousands of sparse equality and inequality constraints.

An OPF algorithm has found many applications in modern power systems operation and planning. As examples, in operation, the OPF can be used for on-line (secure or basic) control of the decision variables as a component of a Hydrothermal Dispatch [Luo et al., 1989] or even as a tool to calculate the "spot price" of both active and reactive power being traded among utilities and consumers [Shirmohammadi et al., 1991] In planning, the OPF is slowly substituting the classical load flow, because of the increasing concern with security and economy of a power system [Hong et al., 1990].

Mathematically, the problem can be generally stated as:

$$\underset{x}{Min} \quad c(x) \tag{2.1}$$

subject to

$$g(x) = 0 \tag{2.2}$$

$$h(x) \leq 0 \tag{2.3}$$

The variable vector **x** can be divided into a set of controls **u** and a set of dependent variables **y**.

The control variables can include some active power generations, the voltage magnitudes or reactive power of generating units and synchronous condensers, the variable transformer tap and phase-shifter settings, other reactive power sources such as capacitors and reactors, DC link power flows and, in special conditions, line switching operations and load shedding.

The dependent variables can include the voltage phase angles, the voltage magnitudes at load buses, line flows and losses.

The scalar objective function (2.1) can measure economic and performance aspects of the system operation such as generation cost, transmission losses, voltage profile deviation from normal, aggregation of control actions or even the number of controls actions.

The equality constraints (2.2) usually represent the power balance equations at the load buses while the inequality constraints (2.3) typically depict both the functional inequalities, such as power flows, and the bounds on **x**.

The reader is referred to Appendices A and B for a detailed description of the mathematical OPF formulation.

In its most general formulation, the OPF is a mixed non-linear (non-convex) integer programming problem whose solution is extremely difficult and time consuming to find. Most of the approaches developed thus far have considered only continuous variables in their formulation. Even though approximate methodologies have been proposed to represent discrete variables [Liu et al., 1992], this is an area that still needs development.

In a similar way to what is done with the load flow equations, the variables and constraints of the OPF can be divided into active and reactive subsets. These subsets are usually weakly coupled, so that two subproblems can be defined: the "active power OPF" and the "reactive power OPF" [Stott et al., 1980].

For Extra High Voltage (EHV) systems with short transmission lines, the transmission losses are sometimes neglected and the voltages approximated by 1.0 p.u, resulting in the linearized or DC load flow model where the energy balance in the network buses is represented only in terms of active power and voltage angles. If, in the OPF problem, such a linearized model is used to represent the system power balance, the model is called Economic Dispatch with Network Constraints or DC OPF. Considerable research has been conducted with the DC OPF since its formulation, leading to some of the best known methods for the complete model that exist today [Alsaç et al., 1990 and Bertran et al., 1990].

As pointed out in some literature reviews [Carpentier, 1987; Huneault and Galiana, 1990], accurate and fast OPF methods exist for the active power problem, whereas the complete active-reactive and reactive power problems, being more intricate, has posed greater difficulties in finding efficient solution methods. Extensive research in the past years has been, in fact, devoted to the proper modelling and solution strategy for the reactive power OPF [Kirshen and Van Meeteren, 1988; Alsaç et al., 1990; Salgado et. al., 1990]. The basic problem is related to the sequential solution of the decoupled formulation of the OPF: The active problem is optimized and the results are given as constants to the reactive subproblem, which will optimize the reactive part of the network using only the remaining controls (that were not "optimized" by the active subproblem). In this iterative solution, sometimes the reactive subproblem is not able to correct new violations on the constraints only by adjusting the available reactive controls, thus compromising the convergence of the overall algorithm. A general approach to correct this deficiency is to include in the active model those additional reactive constraints that cannot be met with reactive means only. In addition, in the objective function of the reactive subproblem, the binding constraints of the active subproblem are added as penalty terms [Carpentier, 1987]. Numerous variations of this general approach can be found, as

can be seen in the references mentioned above.

Regarding the treatment of the types of variables, the OPF problem can be written in two different ways [Carpentier, 1987]:

(i)- Sparse Modelling

Equations (2.1)-(2.3)

In this sparse model, no distinction is made between dependent and controllable variables. All variables are treated as decision variables and optimized simultaneously, resulting in very sparse constraints.

(ii)- Compact or Reduced Modelling

$$Min \quad c(u,y[u]) \tag{2.4}$$

subject to

$$g(u,y[u]) = 0 \tag{2.5}$$

$$h(u,y[u]) \leq 0 \tag{2.6}$$

In this reduced model, the optimization is performed with respect to the controllable variables, **u**. The dependent variables are treated as explicit functions of **u**. In this formulation, there are fewer variables and constraints but at the expense of a decrease in sparsity.

With the reduced model, the solution of the OPF is decomposed into two parts: a load flow solution to find **y** as a function of **u** and the optimization of the reduced problem over **u**. A large number of procedures used to solve the OPF problem is based on the reduced model [Carpentier, 1987].

2.2.2 The Security Constrained OPF

An important application of OPF algorithms is in security constrained optimal control of a power system.

An operationally secure power system is one which " can withstand, without serious consequences, any of a preselected list of credible disturbances (contingencies)" [Balu et al., 1992].

Unfortunately, the problem of identifying the most suitable corrective actions for those contingencies which are found to cause overloads, voltage limit violations or instability in a power system is not a trivial one. However if, associated with each corrective action, there is a "cost", the problem of optimal secure control of a power system can be mathematically stated as a modified OPF whose constraints consider not only operational aspects of the actual generation-transmission system but also of contingency states. In expanding the basic OPF formulation to include contingency constraints, two levels of security can be represented [Stott et al., 1987]:

(i)- Security under contingencies without corrective actions (Preventive Control).

An optimal set of controls is sought to guarantee that no operating limits are violated in the system before or after each contingency. In this conservative approach, it is assumed that no adjustment in the control variables occurs after any of the possible contingencies. That is, the pre-contingency control is sufficient to ensure that, even if the contingency occurs, no violations take place. This problem can be formulated as:

$$Min \quad c(u_0,y_0) \tag{2.7}$$

subject to

$$g(u_0,y_0) = 0, \quad h(u_0,y_0) \leq 0 \tag{2.8}$$

and

$$g(u_0,y_k) = 0, \quad h(u_0,y_k) \leq 0 \tag{2.9}$$

for every contingency k.

(ii)- Security under contingencies with corrective actions (Corrective Control)

Here, no operating limit is violated in the system, before or after contingency, assuming that a corrective action can be applied after the contingency occurs. The security constrained OPF for this case becomes:

$$Min \quad c(u_0,y_0) \tag{2.10}$$

subject to

$$g(u_0,y_0) = 0, \quad h(u_0,y_0) \leq 0 \tag{2.11}$$

and

$$g(u_k,y_k) = 0, \quad h(u_k,y_k) \leq 0 \tag{2.12}$$

$$a \leq |u_0 - u_k| \leq b \tag{2.13}$$

for every contingency k.

Thus, for every contingency k, the $\mathbf{u}_k$ are unknown quantities which can be adjusted to perform a corrective action within the interval **[a,b]**.

The final operational cost of the Preventive Control approach can be very high due to the fact that there are fewer controls. The final operational cost of the Corrective Control formulation is lower, but the problem becomes enormous due to the increased number of control variables. There is, of course, a trade-off between operational cost and security and, in the end, it is up to the utility to define when one is more important than the other.

In practice, applying an optimal secure control strategy to a generation-transmission system involves much more than just finding the solution of a secure-OPF. Normally, the implementation of such control starts with the definition of a number of "likely" contingencies, specifying their expected severity, and whether they would be considered in preventive or corrective control actions. After this initial phase, it is important to define, through some kind of sensitivity analysis, the set of controls that would be operated (in preventive or corrective actions) to guarantee the security of the system after each contingency. This is specially important if we consider the large number of control variables involved in the corrective control. With a control set defined, it is then necessary to specify the maximum amplitude of each control adjustment. Finally, the sequence of control actions may be significant in order to ensure that no violations occur during the implementation of the sequence of actions.

Some aspects in the formulation of a secure-OPF must be considered as well. Security constraints may be treated as "hard" or "soft" constraints where the latter may tolerate some violations. This is specially useful when feasibility is not found for a problem with hard constraints. By "softening" some hard constraints, the algorithm can be made to move towards an optimal solution if the relative importance of the specific violations is defined correctly by the user (i.e. the definition reflects the utility's policy) [Alsaç et al., 1990]. Also, the determination of a proper balance between security and economy is an important issue [Lereverend et al., 1990].

2.2.3 Applications

Many OPF programs, with and without security constraints, are currently implemented in utility control centres in both off-line studies as well as in the on-line environment. These two OPF modes have different features. The OPF programs used in off-line studies are basically applied in operation planning. In this off-line application, in addition to the standard use of the OPF, the ability to provide sufficient information for analysis of infeasible cases is very important - for instance, the correct detection of bottlenecks in a transmission network or the loadability limit. Another desirable characteristic would be the ability to provide sensitivities of the objective function and variables with respect to changes in the parameters. In this application, higher computational costs can be compensated by a more rigorous formulation and solution of the problem.

An OPF intended for on-line execution needs to be compatible with other aspects of the on-line environment. The power system state is, in general, changing through time and the (secure) optimal state changes correspondingly. Thus, the solution speed of the program should be high enough so that it finds a solution before the power system has changed significantly, which implies being fast enough to run several times per hour. The secure-OPF is specially complicated because its formulation (i.e., the list of contingencies or the mode of operation (preventive/corrective)) may change with time as well.

In recent years utilities have reported experiences in the application of OPF to the operation of their systems [Bridenbaugh et al. 1992 and Heinz et al., 1992]. It seems that numerous improvements are still needed, even in commercial OPF packages, in order to conform the optimal control actions with other requirements of the daily operation of a power system. There also exist concerns regarding the efforts in training, maintenance and tuning necessary to implement the OPF in a control centre [Papalexopoulos et al., 1993]. In any case, the OPF found in control centres is presently implemented only in an "advisory" mode, i.e., the control actions that constitute the OPF solution are offered only as recommendations to the dispatcher. The on-line OPF programs working in a closed-loop are limited to some very specific functions such as constrained economic dispatch

[Balu et al., 1992]. Nevertheless, it seems inevitable that the OPF will eventually become accepted and used just as much as the conventional load flow is used today. There is still a need for further improvement, and the feedback from the utility companies' experience will continue to bring valuable insight and refinements to the modelling and strategy of solution of the problem of optimal (secure) control of a power system.

2.3 Literature Review

Since it was first formulated in 1962 [Carpentier, 1962], the optimal power flow problem has been the subject of extensive research, most of it devoted to numerical algorithms for its solution. The early methods were directed towards applications in the area of transmission planning and their utilization in operation was prohibitive due to the high computational solution time. The development of powerful computers and numerical methods in recent years has made possible the utilization of an OPF algorithm in on-line operation tasks as well.

Literature reviews of OPF have been published on a regular basis. The first of these is a very interesting review by Happ [Happ, 1977] that traces the development of the OPF starting with the early methods used to reduce operating costs of a generation-transmission system. Another useful review was published by Stott and colleagues [Stott et al., 1980] emphasizing the numerical methods applied in OPF solutions. Carpentier also published a very general paper concerning on-line operation of a power system, classifying and discussing important results in the field [Carpentier, 1987]. Finally, a more recent paper by Huneault and Galiana [Huneault and Galiana, 1990] made a very thorough classification of the works published in the area until 1989. In addition, reviews regarding recent advances and trends in power system optimization and security control were published by Stott and colleagues [Stott et. al., 1987] and also by Balu and colleagues [Balu et al., 1992].

The formulation of the optimal power flow problem had its basis on an older power system operation problem: the Economic Dispatch (ED).

The ED tries to allocate the total generation required among the generating units, so that some constraints are satisfied and the total generating cost is minimized. This problem was first formulated in the early 20's when there was already a concern about how to economically divide the total load amongst the available generating units. Before 1930, various methods were in use, e.g., the "base load method", where the units were loaded to the maximum capability following the criteria of efficiency; or the "best point loading method" where the units were successively loaded to their lowest heat rate following the same criterion of efficiency. In the early 30's, the "Equal Incremental Cost Criterion (EICC)" was already considered the best approach, a fact that was proved in 1934 [Happ, 1977]. Since then, sustained research has been carried out in ED [Huneault and Galiana, 1990 and Chowdhury and Rahman, 1990]. In the classical load flow formulation, the system incremental cost represents the minimal change in generation cost per unit change in the system total demand, with this demand located at the slack bus. The participation factors load flow permits an interesting variation of the optimal dispatch via EICC. This modified load flow includes the participation factors to distribute the power mismatch into the complex power balance equations [Guoyu et al., 1985]. By using it to calculate the transmission penalty factor, Meisel [Meisel, 1993] demonstrated that the associated system incremental cost represented the minimal incremental change in generation costs, per unit change in the system total demand, with this demand distributed according to the specified participation factor vector.

The solution of the economic dispatch by the EICC was a precursor of the OPF. In the late 50's some work was done to improve the transmission loss representation and minimization through the ED. At the same time, the load flow was implemented in digital computers. The OPF was a "natural" outcome of these developments since the load flow equations and the idea of minimizing costs (or any other criteria) were formulated in the same problem. In the early 60's, Carpentier placed the optimal power flow on a firm mathematical basis [Carpentier, 1962]. Much of the work in OPF, since then, has been based on his formulation. In spite of being able to model the problem of optimal power system operation in a compact way, Carpentier was not successful with his original solution algorithm based on a Gauss-Seidel method [Happ, 1977].

Gradient Based Approaches

The first efficient solution of the OPF was accomplished using gradient methods. In 1968, Dommel and Tinney published an approach based on the reduced gradient method that would become a benchmark in the area [Dommel and Tinney, 1968]. They extended the Newton's load flow method to the OPF by dividing the variables into unknowns or dependent variables **y**, consisting of voltage magnitudes and angles for PQ buses and voltage angles for PV buses; fixed parameters **p** consisting of the active and reactive power injections for PQ buses and the voltage angle of the slack bus; and control variables **u** representing the voltage magnitudes on the generator buses, generator real power and transformer tap ratios. The unknowns were expressed in terms of the controls and, by linearizing the power flow equations, a gradient method was applied to optimize the control variables **u**. After every change in the controls, the non-linear load flow equations were solved by the Newton method. Inequality constraints were handled by the projection approach (for the control variables) or via a penalty approach (for **y** and functional limits). The method was very flexible but the penalty function and gradient step mechanisms required careful tuning.

OPF algorithms based on the Generalized Reduced Gradient (GRG) method were proposed both by Peschon and colleagues [Peschon et al., 1971] and Carpentier [Carpentier, 1973]. In Peschon's approach, penalty functions were used for the inequalities only in the beginning (to force the initial solution into a feasible region). Thereafter, whenever a functional quantity violated a limit, it entered the set **u** as a control variable at its limit. In exchange, by linear sensitivity analysis, an existing member of **u**, that could become a dependent variable **y** without violating its limits, was taken out of the set **u**. A gradient step was then taken in the new **u** and a load flow was solved, like in the Dommel-Tinney approach. Because of these exchanges between **y** and **u**, the load flow equations were not the standard ones, which led to modified sparsity solution techniques. Since the method did not use penalties, it required less tuning than the Dommel-Tinney approach, but each iteration was more time consuming [Stot et al., 1980].

Carpentier's methodology also expressed the dependent variables in terms of the control variables which are then optimized via GRG. However, this approach expressed, through linear sensitivity analysis, the violated and near violated functional inequalities in terms of **u**, so that no penalties were used. In this reduced model the cost is minimized subject to the linearized critical inequalities and to the active power balance equation.

Gradient based methods are still in use nowadays, particularly in algorithms that are based on sequential optimization of the linearized active and reactive optimal power flows followed by a load flow solution. Lee and colleagues [Lee et al., 1988] used a gradient projection method to solve a linearized decoupled OPF where both active and reactive subproblems minimized the cost of active generation. In the reactive subproblem, the reactive generations were expressed in terms of the active ones, with the cost coefficients modified accordingly. The same sequential optimization strategy was used by Salgado and colleagues [Salgado et al., 1990], with the difference that the objective function of the reactive subproblem was the transmission losses or minimal deviation of reactive generation. Both papers did not report any special care to perform the reactive optimization, but no line limits were considered. The reactive subproblem of the decoupled OPF algorithm implemented at Electricité de France is also solved via a GRG based approach [Carpentier, 1987 and 1993].

Penalty Based Approaches

Another early attempt to solve the OPF problem was based on techniques of transforming a constrained optimization problem into an unconstrained one: the Penalty and Barrier methods. These methods were used by Sasson [Sasson et al., 1969], to transform the OPF into an unconstrained problem and solve it via the Fletcher-Powell method. The better performance of the Penalty methods led to subsequent studies [Sasson et al, 1971]. In this last work, penalties were used to represent both equality and inequality constraints of the OPF problem and the modified unconstrained OPF was solved via the Newton method. Because of the fine tuning necessary on the penalty factors, the convergence of the method was long and the reliability not very good.

Although the experiences with penalty functions were not encouraging, another approach developed from the idea of transforming constrained problems into unconstrained ones: the Augmented Lagrangian (AL) method. The first OPF based on this method was published in 1988 [Santos Jr. et. al., 1988], in an application to minimize active transmission losses. In this work, both equality and inequality constraints are treated via the Augmented Lagrangian and a Newton solver is applied to the unconstrained modified problem. Another application of AL to minimize power system losses was published shortly after [Rehn et al., 1989]. In this work, the dependent variables of the OPF were expressed in terms of the control variables using the load flow equations and the optimization, using a quasi-Newton method, was made over an augmented Lagrangian function that considered only the active inequalities (also expressed in terms of the control variables). Recently, a variation of the previous approaches was presented [da Costa and Santos Jr., 1992]. In it, the Lagrangian of the original problem is "augmented" only by terms corresponding to the inequality constraints (the equalities are not penalized), and a quadratic approximation of the modified Lagrangian is solved via the Newton method. The computational time reported in all these works is very short and the penalty factors associated with the Augmented Lagrangian (the Lagrange multipliers) are incremented via a dual procedure. Still, some tuning is necessary to assure convergence, and the difficulties associated with such tuning are not discussed in the papers.

Linear Programming Based Approaches

Linear programming (LP) applications for the OPF problem were initially used in real power dispatching. Works like that of Wells [Wells, 1968] were already very complete, with piecewise-linear objectives and constraints on all variables. Presently, there are numerous LP-based algorithms for the OPF. This class of methods can be defined by the following steps [Stott et al, 1980]:

(i)- solve the standard load flow for **y** in terms of a guess of **u**;
(ii)- linearize the problem constraints;
(iii)- minimize the objective function subject to these constraints;

Generally speaking, the active subproblem is sufficiently linear and therefore very few iterations will be enough. In some power systems, the reactive power varies almost linearly with the voltage, but not in others [Stott et al., 1980]. This can lead to difficulties for convergence. Many publications in linear programming applied to the OPF were presented between 1970 and 1980 [Huneault and Galiana, 1990], the best known being those of Stott and colleagues [Stott and Hobson, 1978 (a) and (b)]. In this work, a dual simplex approach is applied to the compact model of the linear active OPF. In the beginning, the constraints are relaxed and, as the process develops, only the violated ones are added to the working set of constraints. The approach proved to be very efficient, giving very fast and reliable results.

In the late 80's, some key problems in using LP for solving the reactive OPF were tackled. To control voltage magnitudes, Kirchen [Kirchen and Van Meeteren, 1988] proposed an ingenious implementation of a sequential LP based OPF that allowed the addition of voltage constraints to the active subproblem via a sensitivity matrix. This made possible the correction of voltage constraints violations via the rescheduling of the active power controls, in case it was not possible to correct all voltage violations in the reactive subproblem through reactive controls only.

Sequential LP has been extensively used to solve the OPF problem. The package by PCA corporation [Alsaç et al., 1990] is completely based on the decoupling of the active and reactive OPF and basically uses the same dual approach described previously by Stott [Stott and Hobson ,1978 (a) and (b)]. The approach is claimed to be suitable for a on-line environment and is also capable of handling security constraints. The reported CPU times are extremely low, even for large systems, notwithstanding that, in the cases reported, very few constraints had to be enforced. ESCA corporation also released a LP based OPF package, also based on decoupling and a similar dual approach to solve the reduced model that can include security constraints [Bertram et al., 1990]. Once more, the results show a very high performance, but no details were given concerning the number of active inequalities in the case study.

Another branch of LP based approaches for the linearized OPF is based on network flow programming techniques. Previous works applied such methods to active linear OPF only, with the transmission losses represented as bus-loads [Lee et al., 1981]. Recently, an application to the complete OPF was reported by Rice and colleagues [Rice et al., 1991]. In this implementation, the active generations are optimally scheduled via a generalized network flow programming based algorithm and, subsequently, a load flow calculation handles the reactive part of the problem. In spite of being very efficient to solve the active subproblem, the reactive OPF still could not be efficiently solved via network flow programming.

Linear programming is also the basis of geographic decomposition approaches. Such decomposition is specially useful in reactive power optimization because of the localized impact of reactive power. In a recent work [Deeb and Shahidehpour, 1990], a Dantzig-Wolfe decomposition method is used with such intent. The network is divided into areas of influence of specific reactive controls. A LP problem is formulated considering only constraints related to a specific area and a "master problem" is used to model the linking constraints of all areas. The solution is done in two levels: first, the optimization of each area's controls is carried out separately; then, the results of each subproblem are passed to the master problem that makes the necessary adjustments to the controls in order to meet linking constraints and send back new initial solutions for the subproblems.

In the solution of an OPF with security constraints, general decomposition approaches offer the possibility of separation the security-constrained problem into subproblems, each of them defined for a specific contingency under study. The first application of such methods to the complete secure OPF was based on a Benders decomposition scheme [Monticelli et al., 1987]. Each subproblem was solved separately and provided new constraints to the master problem, so that the final solution respected the corresponding contingency. The modelling also considered the system corrective capabilities after the outage occurred. A more recent methodology to solve the security-constrained reactive OPF, with corrective actions, was also based on a decomposition approach [Terra and Short, 1991]. First of all, some pre-specified contingencies were

evaluated and the sensitivities of the control variables to those contingencies were calculated. Then, a non-linear subproblem is defined for each contingency, considering only the control devices most effective in eliminating any violation related to that contingency. The subproblems are solved separately via a reduced-gradient approach and coordinated by a linear master problem.

LP based algorithms have also been used to solve OPF fuzzy models. Fuzzy variables were introduced in the OPF very recently. Miranda [Miranda and Saraiva, 1992] used the formulation on a DC optimal power flow by considering the system active load as fuzzy variables. Applications to the reactive power problem were presented later considering the voltage limits as fuzzy quantities [Tomsovic, 1992 and Abdul-Rahman and Shahidehpour, 1993]. Fuzzy modelling is a very new approach and no study has been made to assess its impact and potential contribution to the problem of optimal power system operation.

Quadratic Programming Based Approaches

Another class of algorithms for the OPF can be characterized by the use of Quadratic Programming (QP) techniques. Here we will define as a QP based approach every method used to solve linearized quadratic OPF models, or to solve quadratic approximations of the Lagrangian of the non-linear OPF. This includes the sequential quadratic programming (SQP) and Newton methods.

An early attempt to directly solve the first order optimality condition equations - the Kuhn-Tucker (KT) conditions - for the OPF was made by Peschon [Peschon et al., 1969]. The authors applied a Newton-Raphson solver to the KT equations of the reactive subproblem and used some rules to define the variables fixed at the limits. The same idea of solving the KT equations simultaneously is, nowadays, the basis of some of the most successful approaches to the OPF problem. There are numerous implementations of this kind [Huneault and Galiana, 1990]. Among all the different programs used, it is the General Electric package [Burchett et al., 1984 and 1988], the ESCA package [Sun et al., 1984] and a utility developed software [Maria and Findlay, 1987].

The program made by Sun and colleagues was the first implementation of a QP based algorithm powerful enough to be used in real systems. The authors directly solved a quadratic approximation of the Lagrangian of the OPF via a Newton method. The KT conditions were solved, for all the unknowns, considering only the set of equality and active inequality constraints. Techniques were used to improve convergence characteristics: the size of the hessian was kept constant throughout the process by the use of dummy elements to compensate for changes in the active set, special storage and factorization of the hessian was used to preserve sparsity and penalty terms corresponding to variable at limits were added to the objective function. Functional inequalities of VAR dispatchable sources were introduced to the feasible set when violated and other functional inequalities were treated with penalties. The computational times were very good, but, in spite of all the progress achieved, the identification of the correct optimal feasible set was not systematic.

The program developed by Gamal Maria and colleagues, also used a Newton solver with a active set strategy for the KT conditions of the OPF problem. The main difference between this implementation and the ESCA package was the use of linear predictions to define the binding inequalities at a certain iteration. After a possible violation is identified by linear prediction, a LP algorithm calculates the increments in all decision variables and Lagrange multipliers due to the introduction of this new inequality in the active set. The possible violated inequalities are tested with the same procedure until the correct set is identified.

Burchett and colleagues took a different approach to solve the KT conditions. Instead of directly solving the system of equations, an equivalent quadratic optimization problem (with linear constraints) is solved. The methodology, known as SQP, was composed of two loops. The outer loop linearized the KT system, setting up the quadratic subproblem that would be minimized in the inner loop. After the solution of the inner loop was found, all variables were updated and the KT equations were checked. If the resulting errors were bigger than a specified tolerance, new linearizations would be performed and the program returned to the inner loop. This initial implementation was later extended to the secure-OPF using a decomposition approach. Each quadratic

subproblem was decomposed in a master (quadratic) and slaves (linear) problems, each of the latter defined for one contingency. The master problem was solved via a QP method while the slaves were solved via LP techniques.

In the last five years, a great number of OPF implementations were based in quadratic programming. Newton based algorithms were used in studies carried out by utilities and universities. Sun [Sun et al., 1988] discussed the implementation of the ESCA package in a real transmission system to optimize the reactive power scheduling, also presenting a criterion to detect infeasibilities based on the value of the Lagrange multipliers. The Newton method is also the basis of an algorithm for optimal voltage and reactive control proposed by Bjelogrlić and colleagues [Bjelogrlić et al., 1990]. Here, once more, the network is divided into control zones each with a reduced set of control variables, chosen according to their influence on the bus voltage magnitudes of a specific zone. A suboptimal power flow is defined by using the reduced set of controls and constraints related only to that zone. The objective function used is composed of a term which represents transmission losses and another term to guarantee reactive power reserves.

Many SQP-based strategies were proposed. Lu and colleagues [Lu et al., 1988] proposed a methodology to incorporate HVDC equations in a SQP based optimal power flow algorithm. Nanda and colleagues [Nanda et al., 1989] linearized and decoupled the OPF to solve it via Fletcher's quadratic programming method. The method was compared with an algorithm based on Beale's method and a LP based algorithm adapted to quadratic programming, showing better performance, both in terms of computational speed and memory requirements. Chang [Chang et al., 1990] separated the OPF problem into two distinct modes. They suggested the utilization of a LP based OPF for fast corrective generation rescheduling and treatment of infeasibility, together with a SPQ-based strategy to minimize transmission losses, in case of no limit violations.

Some deficiencies and pitfalls of the Newton approach were discussed in an interesting paper by Monticelli and Liu [Monticelli and Liu, 1992]. The paper addresses some cases of non-convergence of the Newton method due to the temporary ill-

conditioning of the hessian of the Lagrangian. The "adaptative movement penalty method" proposed by the authors was conceived with the purpose of guaranteeing well-conditioning of the hessian matrix during the factorizations existing on a Newton iteration. The method does not affect the convergence of the algorithm and no tuning is necessary to assure positive definiteness due to ill-conditioning, but the problem of loss of positive-definiteness due solely to changes in the active set is not addressed.

Other improvements on the original Newton algorithm have been proposed. Hong [Hong, 1992] discussed some factorization strategies of the hessian matrix to improve the CPU time and suggested schemes to avoid ill-conditioning and heuristics to treat inequalities. Also, Crisan [Crisan and Mohtadi, 1992] presented a method for enforcement of the inequality constraints based on the sensitivity of the Lagrangian to changes in OPF the variables.

Multiobjective Approaches

It is also possible to find multi-objective models for the problem of optimal control of a generation-transmission system. In reality, trade-offs between different objectives, such as economic operation, reliability, security and minimal impact on environment, can be impossible. The usual approach taken by the researchers is to assign distinct weights to each objective, allowing for relative importance among goals. However, sometimes different objectives cannot be evaluated under a common measure. With this in mind, some authors have applied multiobjective optimization techniques to solve the OPF. Yokoyama [Yokoyama et al., 1988] used the ε-constrained technique to obtain the set of non-inferior solutions of a OPF problem, whose objective functions were the generation cost, the environmental impact and a penalty for line overload. After the set of non-inferior solutions was found, the optimal solution of the problem was selected using a preference index which reflected the static system security. Another interesting application was proposed by Fouad [Fouad and Jianzhong, 1993]. The optimal rescheduling of power generation was formulated as a multiobjective problem, taking into consideration also stability constraints, represented via the transient energy function. The solution strategy incorporated Goal Programming techniques and a knowledge base.

Interior Point Methods

Interior point methods based OPF algorithms have appeared in the literature recently. Granvile [Granvile, 1993] used such approach to solve the reactive power dispatch and Wu [Wu et al., 1993] applied it to the general problem. In both works, the OPF was transformed into a equality constrained problem by the introduction of slack variables in the inequalities and the addition of logarithmic barrier functions on the objective function to guarantee their non-negativity. The authors proposed a pure and a predictor-corrector primal-dual interior point algorithm. Both methods had performances that can be compared to LP-based OPF methods in terms of computational speed.

Parallel Implementation

In the search for computational speed, there are also attempts to solve the OPF in parallel processors. An interesting formulation for the secure-OPF suitable for such implementation was presented by Talukdar [Talukdar and Ramesh, 1993]. In this formulation, a contingency is represented by a correction time and a constraint relating all correction times is introduced in the model. The overall problem is decomposed into a set of smaller subproblems - each of them related to one contingency - and these subproblems are solved in parallel.

Discrete Controls Representation

Some of the controls available to optimize a transmission system operation are better represented by discrete variables. To consider these controls as such in a OPF implementation would increase considerably the complexity of the problem. For this reason, researchers have been concentrating in finding approximate representation for these discrete controls. One of these controls, is the switching operation, i.e., changes in the network topology to improve the system state. Some authors have proposed approaches to incorporate corrective switching actions on the OPF, mainly to meet security constraints. Schnyder and Glavitsch [Schnyder and Glavitsch., 1988 and 1990] treated switching actions as contingencies in the network and represented them by current

injections applied to the original system. Carpentier [Carpentier, 1993] also proposed the replacement of branch switching by equivalent dummy injections. In his work, he also suggested a Branch and Bound process to find the optimal solution of the OPF incorporating switching actions.

Most of the work done in OPF considers the shunt capacitors and inductors as continuous variables, what can cause discrepancies in the final solutions. Linear programming based methods permit recognition of control discreteness, however, nonlinear programming methods do not model discrete controls properly. An approach to treat these discrete controls on a nonlinear OPF was introduced by Liu [Liu et al., 1992] in their penalty based discretization algorithm. In it, a quadratic penalty function is associated to every discrete variable (which is modelled as continuous) and some rules are used to correctly apply these penalties. The results are very close to those obtained by an OPF where all controls are treated as continuous, but the tuning of the penalties seems difficult.

Miscellaneous

Some deficiencies in the current OPF implementation were discussed in an paper by Tinney and colleagues [Tinney et al., 1988]. The authors highlighted the importance of correctly modelling the external network and the discrete OPF variables, and discussed methods to reduce the number of control actions in OPF applications. The importance of correctly representing discrete variables was also studied by Papalexopoulos [Papalexopoulos et al., 1989]. This paper showed, through extensive numerical testing with a SQP based OPF algorithm, the closeness of coupled and decoupled OPF solutions, the robustness of the method with respect to different starting points and the negligible effects of discretization of transformer tap settings.

The effects of load modelling in OPF and secure-OPF implementations were discussed by Dias [Dias and El-Hawary, 1989 and 1991]. The OPF without security constraints but including load modelling was found, in some cases, to give unrealistic results for generation cost minimization due to the tendency of decreasing the bus voltage

magnitudes to decrease power consumption, thus reducing the final cost. According to the authors, the secure-OPF solution did not present such characteristic if the load models were included during contingencies only.

The probabilistic and deterministic modelling of the OPF problem were also studied with Newton based implementations to minimize generation cost [El-Hawary and Mbamalu, 1991]. The probabilistic OPF results were compared with a probabilistic solution based on the use of four different deterministic OPF results plus one OPF solution for the mean loading condition of the system. The results of the probabilistic OPF were found to be more accurate, but the differences between the two models were not significant.

Industry Implementations

Many utilities have implemented OPF algorithms in their EMS centres. Various studies with this tool have been reported, with emphasis either on the final results of such an application or the problems associated with its implementation.

Before implementing its own OPF algorithm, Ontario Hydro conducted a study on the potential savings that such a tool would provide. The results showed that up to $ 2.5 million per year could be saved if a OPF was used in operation control [Maria and Findlay, 1987]. Following the policy of using the OPF in operation, a later publication reported the optimization of fixed tap transformer settings the Newton based OPF [Kellermann et al., 1991]. In this work, the OPF algorithm was applied to a fictitious system composed by subsystems defined at different load scenarios, and the optimal tap setting were calculated for the resulting model. The approach can be extended to all control variables whose settings are required to be valid and optimal for an extended period of time, but, due to the size of the resulting problem, the number of different scenarios is very limited.

Through the optimization of transformer tap settings and capacitor allocation, made by the GE OPF package, Bridenbaugh and colleagues [Bridenbaugh et al., 1992]

researched the minimization of the transmission losses and improvement of the voltage regulation between light load and peak load periods of the Ohio Edison utility. The optimization of the transformer tap settings and capacitors was performed by an iterative process. The former were optimized for light load conditions; after a tentative transformer tap schedule had been established, the optimal capacitor bank allocation was determined for the peak-load model. The authors reported, as a result, annual reductions of 34.5% on the reactive power imports, of 1.3% on the active power losses and of 4.3% for the reactive power losses.

German utilities also have reported the improvements gained by the utilization of OPF algorithms in operation. Through the use of a SQP based OPF to minimize active losses considering only reactive controls, Denzel and colleagues [Denzel et al., 1988] could reduce the network active losses by up to 5%, improving also the system voltage profile. Also VEW reported savings of 3 to 6% of the annual power system losses associated with an improvement of the voltage profile [Heinz et al., 1992].

Problems concerning the introduction of an OPF algorithm on EMS centres were studied by several authors. Vaahedi [Vaahedi and Zein El-Din, 1989], discussed the influence of load models on a OPF and studied some dynamic security implications of applying the package in on-line operation. Heinz [Heinz et al., 1992] studied the problem of voltage reduction at light-load periods of operation due to the use of an OPF package, proposing strategies for the use of the algorithm. In a recent publication Hong [Hong, 1993] analyses different strategies to apply the corrective control actions, given by an OPF algorithm, to alleviate VAR violations. Also, a cost/benefit analysis of the on-line use of an OPF was presented for an application to minimize production cost, considering only active power controls [Papalexopoulos et al., 1993].

As could be seen in the literature review, the techniques to solve the optimal power flow problem have been continuously developing and branching out into different directions. Among the approaches suitable for on-line OPF implementations are those using parametric optimization approaches. These optimization strategies, in reality, belong to class of methods that are based on the idea of solving a mathematical problem by a

smart manipulation of its parameters: parametric methods. In the next section, we will give a general idea of such methods and discuss previous works in power systems analysis based on them.

2.4 Parametric Methods

2.4.1 Basic Concepts

Many physical systems are operated under restrictions that can be formulated as a finite number of equality and inequality constraints. A common feature of these systems is that they have two different sets of variables. One is composed of the *parameters*, which normally cannot be directly controlled (e.g., the power system load, variable limits, line resistances and reactances, etc). When the parameters of a physical system are fixed, they partially or completely determine the behaviour of the other set of variables: the *decision variables* (e.g., the voltage magnitudes). It can be of great interest to determine the behaviour of a set of decision variables with respect to parameter variations (e.g., the behaviour of voltage magnitudes as the load varies), or it might be possible that, by conveniently introducing parameters in a complicated mathematical model and varying them, we are able to transform the original problem into a simpler one, solve it, and by returning progressively the parameters to their original values, "track" the initial solution until the solution of the original problem. Parametric methods were conceived with the purpose of tracking solutions of problems that are "embedded" into a broader class of problems by the use of parameters.

A straightforward application of the concept of parameterization is in the solution of nonlinear equations [Garcia and Zangwill, 1981]. These equations are "parameterized" in a way that, when the introduced parameter ε is equal to zero, they are easily resolvable, and at ε equal to one, they become the original equation. After the initial equation is solved, the parameter is incremented until 1 and the solution path (that is now a function of the parameter) is tracked until the final solution.

The following example, taken from [Garcia and Zangwill, 1981], illustrates the process:

Example 2.1

Suppose we want to solve the nonlinear system

$$\begin{aligned} (x_1)^3 - 3(x_1)^2 + 8x_1 + 3x_2 - 36 &= 0 \\ (x_1)^2 + x_2 + 4 &= 0 \end{aligned} \tag{2.14}$$

If we take, as our initial system of equations,

$$\begin{aligned} (x_1)^3 + 8x_1 + 3x_2 &= 0 \\ x_2 &= 0 \end{aligned} \tag{2.15}$$

The only solution is $(x_1^0, x_2^0)= (0,0)$.

Using the parameter ε, we construct a system that yields the original system for ε=1 and system (2.15) for ε=0:

$$\begin{aligned} (x_1)^3 + 8x_1 + 3x_2 - \epsilon[3(x_1)^2 + 36] &= 0 \\ x_2 + \epsilon[(x_1)^2 + 4] &= 0 \end{aligned} \tag{2.16}$$

The solution of (2.16) is a function of ε:

$$\begin{aligned} x_1(\epsilon) &= 6\epsilon \\ x_2(\epsilon) &= -36\epsilon^3 - 4\epsilon \end{aligned} \tag{2.17}$$

The point $(x_1(\varepsilon), x_2(\varepsilon))$ describes a path as ε increases from 0 to 1. Following this path leads us directly to the solution $(x_1(1), x_2(1))=(6,-40)$.

Equation (2.16) is called *homotopy function* , **HO**(ε), and the methods used to track as the parameter varies are called homotopy, path-following or continuation methods.

In general, suppose that $\mathbf{F}(\mathbf{x})$: $\mathbb{R}^{nv} \rightarrow \mathbb{R}^{nv}$ and nonlinear. Using the homotopy process, we want to solve

$$F(x) = 0 \tag{2.18}$$

First of all, it is necessary to set up a simple system, for which we have a solution x^0:

$$E(x) = 0 \tag{2.19}$$

Then, we define a homotopy function $\mathbf{HO}(\mathbf{x},\varepsilon)$: $\mathbb{R}^{nv+1} \rightarrow \mathbb{R}^{nv}$, which has the original nv variables plus ε. **HO** must be constructed so that

$$\begin{aligned} HO(x,0) &= E(x) \\ HO(x,1) &= F(x) \end{aligned} \tag{2.20}$$

Following the solutions $\mathbf{x}(\varepsilon)$ of $\mathbf{HO}(\mathbf{x},\varepsilon)$ from ε=0 to ε=1, we find the solution of the original problem (2.18).

In the same way that it is possible to track the solution path of a system of equations, it is also possible to follow the solution of an optimization problem. Generally speaking, parametric optimization deals with the characterization of the optimal decision variables for a range of parameter variations. The potential of parametric approaches in nonlinear optimization is broad. In addition to their ability to track optimal solutions as some of the parameters of the problem change, parametric approaches can also find applications in transforming complicated optimization problems into convex ones and to derive globally convergent algorithms for non-convex problems. Also, they can be used

in global optimization or to provide means of improving the optimal solutions of specific systems by proposing variations to the parameters of the model [Guddat et al., 1990 and Zlobec, 1985].

The optimal solution of a minimization problem (P), whose feasible set fulfils some general properties (the constraint qualifications), must satisfy the set of first order optimality conditions for optimality. The opposite is not always true: the solution of this set of equations must also satisfy the so-called sufficient conditions for optimality in order to be an optimal solution of (P) [Luenberger, 1984]. Nevertheless, if we want to verify the behaviour of the optimal solution of (P) as some of its parameters change, we can track the solutions of the set of necessary optimality conditions, provided that these are tested for the sufficient conditions for optimality as well. This idea is the basis of some of the parametric optimization methods. The following example illustrates the potential of such approach in the optimal control of power systems.

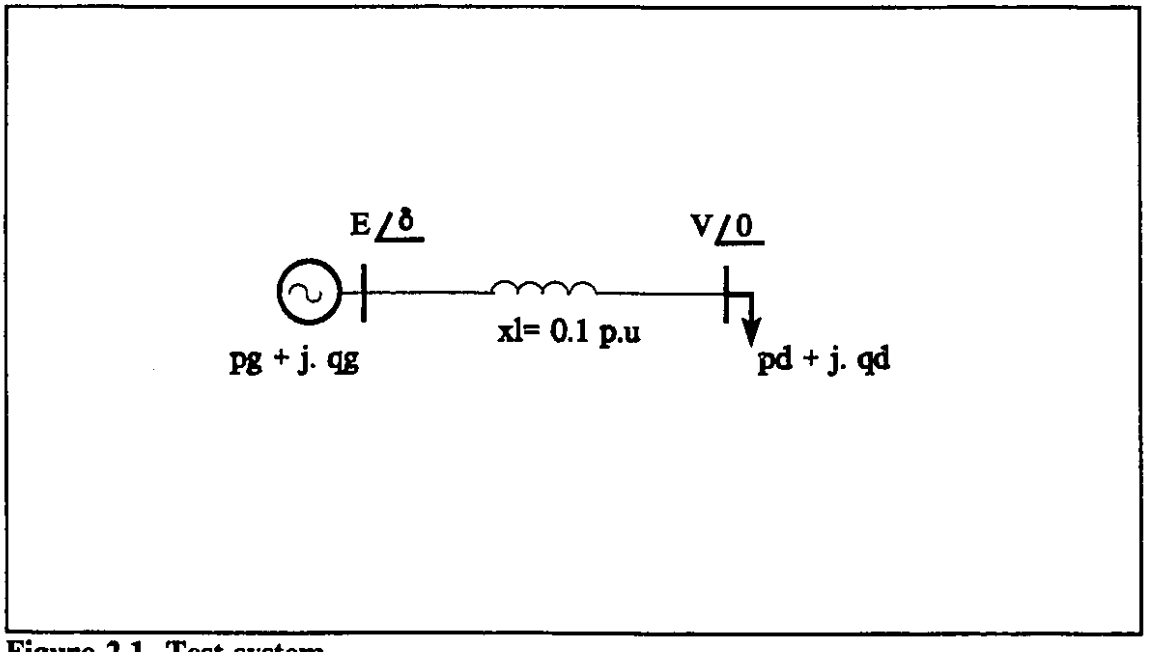

Figure 2.1- Test system.

Example 2.2

We want to study the behaviour of the optimal bus voltages of the system of Figure 2.1 as the system load (pd + j.qd) varies with time.

Suppose that pd= ε.Δpd and qd= ε.Δqd; i.e., pd and qd vary with time, starting from zero, and increasing until Δpd and Δqd as ε varies from 0 to 1. Thus, pd=pd(ε) and qd=qd(ε). The OPF problem for the system of Figure (2.1) is defined as

$$Min \quad \frac{1}{2}[(V-1)^2 + (E-1)^2] \tag{2.21}$$

subject to

$$\frac{EV\sin(\delta)}{xl} = pd(\epsilon) \tag{2.22}$$

$$\frac{-V^2 + EV\cos(\delta)}{xl} = qd(\epsilon) \tag{2.23}$$

The Lagrangian of the problem (which is a function of the parameter ε) can be written as

$$\begin{aligned} \mathcal{L}(V,E,\lambda_p,\lambda_q,\epsilon) &= \frac{1}{2}(V-1)^2 + \frac{1}{2}(E-1)^2 + \\ &+ \lambda_p\left(pd(\epsilon) - \frac{VE\sin(\delta)}{xl}\right) + \lambda_q\left(qd(\epsilon) + \frac{V^2 - VE\cos(\delta)}{xl}\right) \end{aligned} \tag{2.24}$$

Therefore, the Lagrangian conditions are:

$$\frac{\partial \mathcal{L}}{\partial \delta} = -\lambda_p \frac{VE\cos(\delta)}{xl} + \lambda_q \frac{VE\sin(\delta)}{xl} = 0 \tag{2.25}$$

$$\frac{\partial \mathcal{L}}{\partial V} = (V-1) - \lambda_p \frac{E\sin(\delta)}{xl} + \lambda_q \frac{2V - E\cos(\delta)}{xl} = 0 \tag{2.26}$$

$$\frac{\partial \mathcal{L}}{\partial E} = (E-1) - \lambda_p \frac{V\sin(\delta)}{xl} - \lambda_q \frac{V\cos(\delta)}{xl} = 0 \tag{2.27}$$

$$\frac{\partial \mathcal{L}}{\partial \lambda_p} = pd(\epsilon) - \frac{EV\sin(\delta)}{xl} = 0 \tag{2.28}$$

$$\frac{\partial \mathcal{L}}{\partial \lambda_q} = qd(\epsilon) - \frac{-V^2 + EV\cos(\delta)}{xl} = 0 \tag{2.29}$$

From (2.28) and (2.29), we have

$$\frac{[pd(\epsilon)xl]^2}{(EV)^2} + \frac{[qd(\epsilon)xl + V^2]^2}{(EV)^2} = \sin^2(\delta) + \cos^2(\delta) = 1 \tag{2.30}$$

Which will give

$$V = \left(-2qd(\epsilon)xl + E^2 \pm \frac{\sqrt{E^4 - 4qd(\epsilon)xlE^2 - 4pd(\epsilon)^2xl^2}}{2} \right)^{\frac{1}{2}} \tag{2.31}$$

Also,

$$\delta = \sin^{-1}\left(\frac{pd(\epsilon)xl}{EV}\right) \tag{2.32}$$

Solving equations (2.26) and (2.27) for λ_p and λ_q, we have:

$$\lambda_p = \frac{1}{2pd(\epsilon)}\left[\frac{V^4 - V^3 - qd(\epsilon)xl(E - E^2)}{V^2} + qd(\epsilon)xl + E^2 - E\right] \tag{2.33}$$

$$\lambda_q = \frac{xl}{2(qd(\epsilon)xl + V^2)}\left[E^2 - E - qd(\epsilon)xl - \frac{V^4 - V^3 - qd(\epsilon)xl(V + E^2 - E)}{V^2}\right] \tag{2.34}$$

Now, using (2.28), we can express λ_p and λ_q in terms of E, x, pd(ε) and qd(ε). If we substitute the modified expressions of the λ_p and λ_q into (2.25), we will end up with

two sets of non-linear equations in terms of E, pd(ε) and qd(ε); each one defined for one solution of (2.31):

$$E^3 - 2qd(\epsilon)xlE \pm (3E - 2)[E^4 - 4qd(\epsilon)xlE^2 - 4pd(\epsilon)^2xl^2]^{\frac{1}{2}}$$
$$- 2E\left[-2qd(\epsilon)xl + E^2 \pm \frac{\sqrt{E^4 - 4qd(\epsilon)xlE^2 - 4pd(\epsilon)^2xl^2}}{2}\right]^{\frac{1}{2}} = 0 \qquad (2.35)$$

When ε=0, the (relaxed) problem above has a trivial solution: V=1 p.u, E=1 p.u. and δ= 0.

As ε is varied from 0 to 1 (i. e., the pd and qd vary from 0 to Δpd and Δqd), equation (2.35) can be solved numerically, giving two solutions E(ε), only one of these satisfying the sufficient conditions for optimality. Substituting the values of E(ε) in (2.31) and (2.32) we have the expression of V(ε) and δ(ε). Finally, the expressions of $\lambda_p(\epsilon)$ and $\lambda_q(\epsilon)$ can be obtained by substituting the values of E(ε) and V(ε) in (2.33) and (2.34). As a result, for specified Δpd and Δqd, we obtain the solution trajectories of the voltages of the system represented in Figure (2.1) as ε is varied from 0 to 1. Figure 2.2 depicts the optimal values of E and V as the system load increases from pd=0 and qd=0 until pd=0.8 p.u. and qd=0.1 p.u.. It is interesting to note that, as the load increases, the voltage magnitude at the generator bus increases and the voltage magnitude at the load bus decreases. If there was a maximum limit for E, for pd greater than 0.62 p.u., E would be fixed and, as consequence, V would drop much faster.

In the example above, the system of KT equations (2.25)-(2.29) is the homotopy function **HO**(V,E,pg,qg,λ_p,λ_q,ε) that connects the minimization problem defined for pd=0 and qd=0 with the problem defined for pd=0.8 and qd=0.1. As the system load was increased, we followed this homotopy function to obtain the optimal solution paths of E and V.

Although the idea of tracking the solution is quite simple, the existence of a *path*, defined here as a piecewise differentiable curve in space, is not always guaranteed. To

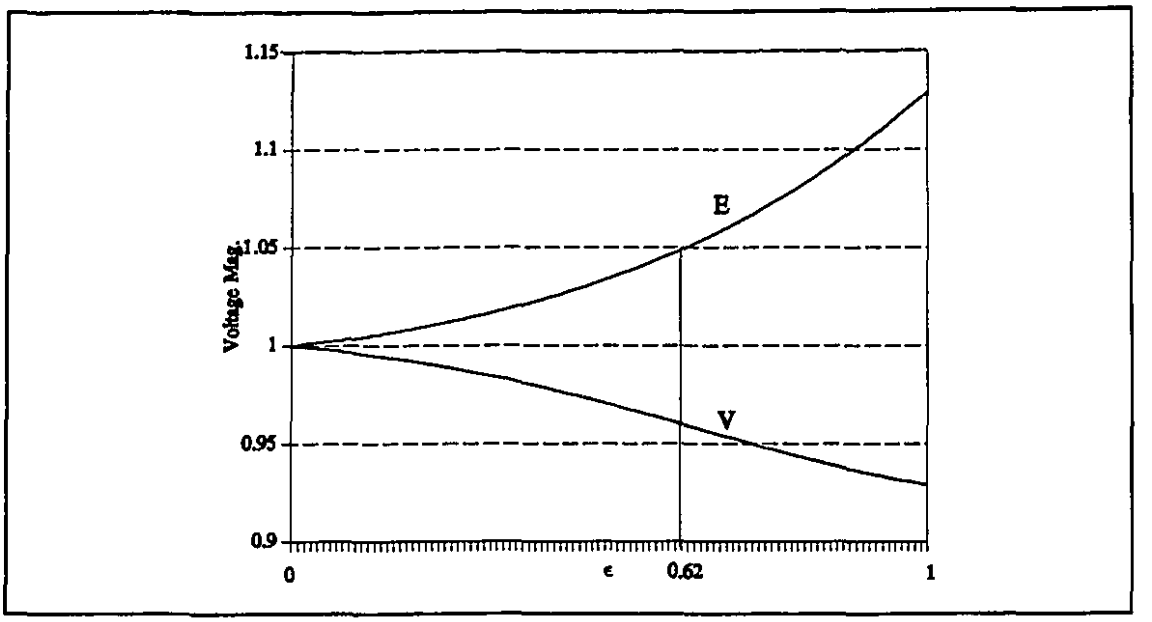

Figure 2.2- Optimal trajectories.

assure the existence of a path, the jacobian of the homotopy function of each example must satisfy a set of conditions for all $\varepsilon \in [0,1]$. The solution of optimization problems can be specially complicated when inequality constraints exist in the model (as they exist in the OPF). For such problems, the behaviour of the active feasible set is of special importance, since there are situations were even a very small change in the parameter can produce a "collapse" of this set, interrupting the solution process.

In this thesis we will work with a OPF model in which all individual data involved depend only on one parameter. The tool that we use for a solution algorithm is a path-following method. Since the behaviour of such methods depends heavily on the structure of the set of all local minimizers of the parametric problem, the concepts of stability of a feasible set and of degeneracies (here called critical points) will be important throughout the development of the theoretical basis of the approach. Although there is a considerably large literature about parametric optimization, for the theoretical aspects of the problem we will refer, most of the time, to the book of Guddat and colleagues [Guddat et al., 1990] and to some additional publications by the same research group.

2.4.2 Parametric Techniques in Power System Analysis

General Applications

Parametric methods have been used in many studies in power system analysis. As early as in 1971, a parametric approach was used to generate load flow solution trajectories and to calculate points of singularities in the load flow jacobian [Thomas et al., 1971]. Since then, many different homotopy methods were applied with basically the same intent: find the voltage collapse point (also called bifurcation point or maximum loadability point) in the power system steady state operation. In the late 80's, an attempt to calculate multiple solutions of the load flow equations was based in the so-called Simplicial Methods [Okumura et al., 1989]. Since then, other related work has been based on a parameterization of the load flow equations which augments by 1 the dimension of the system jacobian. During the process, different variables are alternately treated as the parameter of the problem, which, according to the authors, keeps the load flow jacobian well conditioned near the point of voltage collapse (contrary to what happens with other methods based on the pure system jacobian). Among the publications are the works of Iba [Iba et al., 1991], Ajjarapu [Ajjarapu and Christy, 1992] and Cañizares [Cañizares and Alvarado, 1992]. A very recent paper in the area introduced a different type of parameterization of the load flow equations that preserves the dimension of the jacobian; only adding some non-zero elements to the original matrix [Jean-Jumeau and Chiang, 1993]. Basically, the interesting characteristics of these approaches in the calculation of the maximum loadability limit is that they are not exhausting cut-and-try processes and that the numerical difficulties that exist near a system loading limit are overcome.

Parametric Methods in OPF Studies

Parametric optimization techniques have been previously used in studies in OPF, both as a means of performing sensitivity analysis and of tracking the power system variables optimal behaviour. The first work in OPF that used parameter variations was published in the early 80's [Dillon, 1981]. This work was also a Newton-based

OPF implementation but, in it, the sensitivities of the optimal solutions to parameter (load) variations were used to find the changes in the OPF constraints, so that the Newton solver could be applied together with a feasible set strategy. Since then, several extensions of the approach have been proposed.

Aoki [Aoki and Satoh, 1982] published a work in ED with security constraints using a model where the transmission losses were represented as a quadratic function of the real power, added to the objective function of the problem as a penalty, and the associated Lagrange multiplier was treated as a parameter. A parametric quadratic programming method was applied to solve the modified problem. Later, Carpentier [Carpentier, 1983] presented some results of another application of parametric quadratic programming to the real power dispatch. In his model, however, the system load was treated as a parameter and the optimal solution was found for a range of load variations. Later, the method was applied in a solution strategy for the full OPF [Carpentier, 1987]. At the same time, Blanchon [Blanchon et al., 1983] also applied the same technique to find the point of voltage collapse in a reactive power dispatch. Parametric optimization methods were also used by a group from the Italian power utility ENEL to solve the real power dispatch, to solve both linear and quadratic formulations of the real power dispatch [Innorta et al., 1985 and 1987].

Bacher [Bacher and Van Meeteren, 1988] also reported results on the use of a parametric quadratic programming technique for real time generation control while Gribik [Gribik et al., 1990] described a parametric OPF formulation to perform sensitivity analysis of the system losses with respect to the load. Finally, the concept of parameterization was used by Venkatesh [Venkatesh et al., 1992] to calculate the sensitivities of OPF solutions with respect to variable limits.

At McGill University, research in parametric optimization applied to the problem of optimal system operation was first done by Vojdani [Fahmideh-Vojdani and Galiana, 1983]. In this first application, the continuation method was used to track the optimal solution of the linearized OPF throughout an entire interval of variation. Later, Galiana [Galiana et al., 1983] proposed a parametric technique for the OPF based on a varying

limits strategy. In Ponrajah's work [Ponrajah and Galiana, 1989], this varying limits strategy, together with the restart homotopy continuation algorithm, was applied to the economic dispatch problem where the losses were treated as a non-linear function of the control variables. More recently, Huneault [Huneault and Galiana, 1991] suggested a successive linearization solution for the full OPF problem where each linearized subproblem is solved by a continuation method that considered the load and the variables' limits as parameters. An extension and generalization of these previous works was presented in the past year [Almeida et al., 1993, (a) and (b)]. In these results, a general parametric model was examined considering the full non-linear load flow equations and inequalities and an arbitrary objective function. The present thesis details the investigation summarized by these two publications.

2.5 Motivation for Thesis Research

The present thesis is an extension and generalization of previous studies in OPF done at McGill University. The first of these works used the continuation method to follow the solution of the ED with network constraints as the system load varied with time [Fahmideh-Vojdani, 1982]. In it, the only variable considered as a parameter was the system load, an initial solution for the problem was found for a constant load, whose level did not affect any of the variable limits existing in the model (i.e., generation and line limits). Subsequently, the load (parameter) was varied and the initial optimal solution was tracked until the feasibility limit was reached.

As an extension of this first work, the thesis of Ponrajah [Ponrajah, 1987] applied the continuation method to an economic dispatch problem with network constraints represented by the full load flow equations. Initially, both the functional and the variable limits were relaxed through the parameterization of their limits, so that an initial optimal solution is easily found for the ED. Subsequently, these limits were progressively returned to their initial values and the initial solution was tracked until the optimal solution of the original problem using the restart homotopy continuation method.

Finally, in a later work, Huneault [Huneault, 1988] solved a parameterized OPF, with a quadratic objective function (the generation cost), via a mix of SQP and continuation method. For a specified load level, the OPF was first of all linearized. The inequalities of the linear subproblem were then relaxed through the parameterization of their limits. As the limits were returned to their original values, the initial solution was tracked until the final solution of the linear subproblem. If the solution of the linear subproblem satisfied the non-linear constraints of the original problem, the final solution was found; if not, a new linearization was made at this point and the process was repeated. After the OPF was solved for the initial load level, the load was varied and the whole process repeated.

The research developed thus far concerning the application of parametric methods to the OPF has been restricted to some specific formulations of the general problem. From the literature review, it is easy to see that most of the applications were restricted to the active linearized OPF. Even in the cases where the non-linear network constraints were considered, either only the active OPF was solved [Carpentier, 1987], or the solution procedure was made specific to solve one of the OPF tasks (that is, minimize the generation cost) [Ponrajah, 1987], or even the approach was based in successive linearizations of the original problem [Huneault, 1988]. The full nonlinear problem, with a general objective function, was never solved directly, i.e., without linearizations. This is the objective of the present thesis.

In this work, we parameterize a complete OPF problem where all the variables are treated as continuous, considering both functional inequalities and bounds on the problem variables. The non-linear parameterized problem is solved by Newton method (i.e., the problem is solved directly, without applying the strategy of successive linearizations used by Huneault). The choice for direct solution was motivated by the fact that successive linearizations can lead to intermediate subproblems whose solution is very far from the region defined by the original non-linear constraints, compromising the performance of the algorithm.

Four important factors were considered in the choice of the parametric method:

(i)- Many different approaches have been used to solve the OPF, some of them being very successful in terms of computational speed. Nevertheless, the non-linear methodologies used so far rely either on penalty factors or on heuristics to define the optimal feasible set. Parametric methods provide a way of systematically controlling the changes in the active set throughout the optimization process.

(ii)- The treatment of the system load as a parameter allows very fast solution of the OPF problem for varying load. In addition, the parametric algorithm is capable of exactly tracking the load curve. These two characteristics make such approach very suitable for on-line use.

(iii)- Parametric methods are powerful tools for analysis of mathematical models. Although many algorithms have been successful in solving the OPF problem, most of the times it is very difficult to determine causes for non-convergence of the algorithms (i.e., to distinguish between infeasible and feasible cases when an optimal solution cannot be found). Parametric approaches give us valuable information about weak points and bottlenecks of a power system. This characteristic is particularly useful in planning studies, not only because parametric methods show very clearly the evolution of all variables as the system load is varied, but also can provide the trajectories of these quantities as *any* parameter of the system varies.

(iv)- As it was previously discussed, the OPF is a important tool for power system operation. It is a more general model than the classical load flow because, in principle, no control is considered fixed. It is, thus, of great interest to observe the behaviour of the OPF variables as some parameters of the system varies because this can give us a valuable insight about the main problems for its operation. A parametric method allows a very good understanding of the generation-transmission system optimal behaviour.

In the next chapter we will introduce the parametric OPF model and discuss in more detail the theoretic aspects of the implementation.

CHAPTER 3

THEORETICAL BASIS OF THE PARAMETRIC OPTIMAL POWER FLOW

3.1 Introduction

As was shown in the previous chapter, a smart parameterization of a complicated mathematical problem provides a means for its solution and for analysis of its behaviour with respect to parameter variations. The use of such an approach to solve the OPF gives us a very good understanding of the optimal power system operation (see example 2.2) not possible with other solution methods. The OPF is a complicated problem, and the application of a parametric technique for its solution highlights (and explains) many of the difficulties that have been encountered by researchers, this being so because the parametric approach "dismembers" the original OPF into a sequence of simplified problems that "converges" to the original one. This property will become clearer as the chapter progresses.

In this chapter, we will introduce a general parametric OPF model (Parametric-OPF) and examine some theoretical aspects of the methodology. In addition, we will discuss some problems that are identified when a parametric approach is used to solve the OPF, emphasizing their relation to optimal power system operation.

3.2 Parameterization of the OPF Problem

3.2.1 Parameters of the OPF

We can consider as parameters every quantity that usually cannot be directly controlled. In the OPF model, parameters can be found in the objective function, equality and inequality constraints.

The objective function of the OPF is composed of "costs" which measure the quality of a solution from the operational as well as economical point of view. Any cost coefficient associated with the decision variables can be seen as a parameter and thus can be used as a means of controlling the optimization process. In addition, the shape of the objective function can be modified through the use of parameters to facilitate the optimization process; for example by the introduction of some quadratic parameterized terms (see section 3.2.3).

The equality constraints of the OPF model are also composed of parameters and decision variables. The most commonly used parameter is the system load which was considered in several previous applications of parametric methods to OPF (see section 2.3). Also, we can consider as parameters the line reactances, susceptances and resistances. While the parameter "system load" makes it possible to track the load variation throughout an interval of time, the relaxation of some of the line parameters allows us to represent even topological changes in the system network. As a result, the parameterization of the equality constraints of the OPF allows us to simulate the optimal behaviour of a system whose topology and total load varies with time which is consistent with the day-to-day operation of a generation-transmission system.

Finally, all limits on the decision variables and functional inequalities can also be considered as parameters. The study of the system optimal behaviour, as some of these parameters vary, can give us a good idea of the operational cost imposed by such limits and of their influence on the power system steady state operation.

In general, thus, the parameterization of the objective function, equality and inequality constraints of the OPF, not only provides a methodology for the solution of this problem but offers a means to carry out OPF analysis for a broad range of operational conditions. These two strong points of parametric approaches are used here in the solution of the OPF problem for both constant and variable system load. The method of solution proposed in this thesis is based on the relaxation of parameters appearing in the objective function, equality and inequality constraints of the OPF. We can subdivide our methodology into two phases: in Phase I the OPF problem is solved for a specified load level, subsequently, in Phase II, a load curve is tracked starting from the optimal solution of Phase I. At the beginning of Phase I, both equalities and inequalities are relaxed (so that the feasible set is made as broad as necessary) and the objective function is reshaped through a smart parameterization. A trivial initial optimal solution can then be found and tracked until the final optimal solution as the initially relaxed problem is returned to its original form. Since we start Phase II of the algorithm at the optimal solution of Phase I, the parameterization required at this point is a simplification of that used during Phase I. For this reason, we chose to discuss the theoretic aspects of the methodology for both parameterized models together.

3.2.2 Parameterized OPF and Optimality Conditions

If we want to solve an optimization problem via any numerical method, the first step is the definition of an initial guess sufficiently close to the solution of the original problem. This is crucial since, in general, numerical methods have local convergence only. Parametric techniques can be used to globalize locally convergent algorithms for the solution of non-linear optimization problems [Guddat et al., 1984].

Our goal in this thesis is to propose an algorithm that, in principle, is able to find the optimal solution of the OPF problem, starting from *any* initial solution.

First, let the general parametric OPF problem $P(\varepsilon)$ be defined as

$$\underset{x}{Min} \quad c(x,\epsilon) \tag{3.1}$$

subject to

$$g_k(x,\epsilon) = 0,\ k \in K \tag{3.2}$$

$$h_l(x,\epsilon) \leq 0,\ l \in L \tag{3.3}$$

where $\mathbf{x} \in \mathbb{R}^{nv}$, $\varepsilon \in [0,1]$, c, $\mathbf{g}_k$ and $\mathbf{h}_l$ are real valued functions, K={ 1, ..., m }, m < nv, and L= {1,...,s}.

The idea is to modify the OPF model so that, at ε=0, *any* initial solution ($\mathbf{x}^0$, λ^0, μ^0) is optimal (which implies that it is also feasible). To be an optimal solution, ($\mathbf{x}^0$, λ^0, μ^0) must satisfy a certain set of conditions at ε=0 discussed below. Since we are interested in tracking the optimal solution from ε=0 until ε=1, ideally these conditions must be satisfied throughout this interval of variation. Unfortunately, this is not always the case and, as a consequence, the algorithm is not able to arrive at the optimal solution. The failure of the continuation process can be due to two main reasons: (i) No solution exists beyond a certain ε or (ii) failure of the algorithm to find an optimum even when one exists.

In the following sections we discuss in more detail the conditions which allow us to characterize ($\mathbf{x}^0$, λ^0, μ^0) as an optimal solution and to track this initial optimum over the entire interval of ε. In addition, we will pay particular attention to cases where the continuation process fails.

Constraint Qualifications

Throughout this work, we will characterize the optimal solutions of the Parametric-OPF using the first order optimality conditions (the Kuhn-Tucker conditions) and the second order sufficiency conditions [Luenberger, 1984]. In the same way that it was done

in example (2.2), where the necessary optimality conditions were tracked, the methodology proposed here is based on the tracking of the Kuhn-Tucker conditions as the parameter ε is varied from 0 to 1. To be able to track the Kuhn-Tucker conditions, we impose some additional assumptions, called *constraint qualifications* [Fiacco, 1983]. Cases where the tracking process cannot continue, including OPF infeasibility, are often related to the violation of the constraint qualifications. Some definitions are now introduced.

Let the feasible set of the parametric OPF problem, P(ε), be

$$M(\epsilon) = \{x \in \mathbf{R}^{nv} \mid g_k(x,\epsilon) = 0,\ k \in K,\ h_l(x,\epsilon) \le 0,\ l \in L\} \tag{3.4}$$

Also, for a fixed ε, let $L_0(\mathbf{x},\varepsilon)$ be the set of active inequality constraints. Thus,

$$L_o(x,\epsilon) = \{l \in L \mid h_l(x,\epsilon) = 0\} \tag{3.5}$$

In this study, two constraint qualifications are specially significant:

(i)- the linear independence constraint qualification (LICQ);
(ii)- the Mangasarian-Fromovitz constraint qualification (MFCQ).

The first set is more restrictive than the second set of constraints.

At a point $x \in M(\epsilon)$, the linear independence constraint qualification (LICQ) is said to hold if the vectors $\frac{\partial g_k}{\partial x}(x,\epsilon)$, $k \in K$, and $\frac{\partial h_l}{\partial x}(x,\epsilon)$, $l \in L_0(x,\epsilon)$, are linearly independent.

At $x \in M(\epsilon)$, the Mangasarian-Fromovitz constraint qualification (MFCQ) is said to hold if:

(i)- the vectors $\frac{\partial g_k}{\partial x}(x,\epsilon),\ k \in K$ are linearly independent;

(ii)- there exists a non-zero vector $\varpi \in \mathbb{R}^{nv}$ such that

$$\frac{\partial^T g_k}{\partial x}(x,\epsilon).\varpi = 0,\ k \in K \tag{3.6}$$

$$\frac{\partial^T h_l}{\partial x}(x,\epsilon)\varpi < 0,\ l \in L_0(x,\epsilon) \tag{3.7}$$

Note that equation (3.6) implies linear dependence of the columns of $\frac{\partial g}{\partial x}(x,\epsilon)$ and therefore does not contradict supposition (i) of MFCQ . The geometrical interpretation of MFCQ is that the gradients of the active inequality constraints at x form a pointed cone (i.e., a cone with an angle smaller than 90^2) and there exists a vector in this cone that is tangent to the surface formed by the equality constraints. Also, note that every point that satisfies LICQ also satisfies MFCQ.

The importance of these constraint qualifications will become clearer when we discuss the tracking process and the possible ways in which it can fail.

Optimality Conditions

Let the Lagrangian function of P(ε) be defined as

$$\mathfrak{L}(x,\epsilon) = c(x,\epsilon) + \sum_{k\in K} \lambda_k g_k(x,\epsilon) + \sum_{l\in L_0} \mu_l h_l(x,\epsilon) \tag{3.8}$$

Supposing that, at (**x**,ε) , either LICQ or MFCQ is satisfied. Then, **x** is the local optimal solution of P(ε), if and only if [Luenberger, 1984],

(i)- the Kuhn-Tucker equations hold:

$$\frac{\partial c}{\partial x}(x,\epsilon) + \sum_{k \in K} \lambda_k \frac{\partial g_k}{\partial x}(x,\epsilon) + \sum_{l \in L_0} \mu_l \frac{\partial h_l}{\partial x}(x,\epsilon) = 0 \tag{3.9}$$

$$g_k(x,\epsilon) = 0,\ k \in K \tag{3.10}$$

$$h_l(x,\epsilon) = 0,\ l \in L_0 \tag{3.11}$$

$$h_l(x,\epsilon) \leq 0,\ l \notin L_0 \tag{3.12}$$

$$\mu_l \geq 0 \tag{3.13}$$

(ii)- the second order sufficient conditions hold ; i.e., the second derivative of the Lagrangian with respect to **x** (the hessian matrix),

$$H(z,\epsilon) = \frac{\partial^2 \mathcal{L}}{\partial x^2} = \frac{\partial^2 c}{\partial x^2}(x,\epsilon) + \sum_{k \in K} \lambda_k \frac{\partial^2 g_k}{\partial x^2}(x,\epsilon) + \sum_{l \in L_0} \mu_l \frac{\partial^2 h_l}{\partial x^2}(x,\epsilon) \tag{3.14}$$

is positive definite on the sub-space

$$T_* = \{ y \mid \frac{\partial g}{\partial x}(x,\epsilon)y = 0,\ \frac{\partial^T h_l}{\partial x}(x,\epsilon)y = 0,\ l \in L_*(x,\epsilon) \} \tag{3.15}$$

where

$$L_*(x,\epsilon) = \{ l \in L_0(x,\epsilon) \mid \mu_l > 0 \} \tag{3.16}$$

Under the assumption that at least one of the constraint qualifications holds at $\varepsilon=0$, the first and second order optimality conditions provide sufficient means for making $(\mathbf{x}^0, \lambda^0, \mu^0)$ optimal at $\varepsilon=0$. That is, we "optimize" the OPF model for $\varepsilon=0$ by forcing the first and second order optimality conditions to be met at this point. Besides being an "optimal model" for $\varepsilon=0$, our parameterized OPF must become the original OPF problem at $\varepsilon=1$, making it possible to use the principle of homotopy methods for its solution. To accomplish these objectives, three relatively simple modifications are introduced in the original OPF, to solve it both for constant and variable load. For the reasons explained previously, the parameterized models for Phase I and Phase II are somewhat different. Therefore, the two models are discussed separately in the next sections.

3.2.3 Parameterized Model for Constant Load - Phase I

Let $\mathbf{x}^0$ and λ^0 be initial values of $\mathbf{x}$ and λ, respectively (how to select these initial values for the Parametric-OPF is described in section 4.3.1). By construction, we define the parametric optimal power flow (Parametric-OPF) problem as:

$$\underset{x}{Min}\ c(x,\epsilon) \tag{3.17}$$

subject to

$$g_k(x,\epsilon) = g_k(x) - (1 - \epsilon)g_k(x^0) = 0,\ k \in K \tag{3.18}$$

$$h_l(x,\epsilon) = h_l(x) - (1 - \epsilon)\Delta h_l \le 0,\ l \in L \tag{3.19}$$

where

$$c(x,\epsilon) = c(x) - (1 - \epsilon)c_0^T x + \frac{1}{2}(1 - \epsilon)w\|x - x^0\|^2 \tag{3.20}$$

$$c_0 = \frac{\partial c}{\partial x}(x^0) + \sum_{k\in K} \lambda_k^0 \frac{\partial g_k}{\partial x}(x^0) \tag{3.21}$$

and

$$\begin{aligned} \Delta h_l &= 0 \quad if \quad h_l(x^0) \le 0 \\ \Delta h_l &> h_l(x^0) \quad if \quad h_l(x^0) > 0 \end{aligned} \tag{3.22}$$

It is easy to see that, at ε=0, no inequality constraint is active. Therefore, LICQ (and, consequently, MFCQ) is satisfied if, at $\mathbf{x}^0$, the gradients of the equality constraints are linearly independent. Provided that this condition is met, we can characterize the optimal solution through equations (3.9)-(3.16). Using these equations we can verify that the above parameterization achieves four objectives:

(i)- It relaxes the inequality limits according to (3.19) and (3.22) so that, at ε=0 they are strictly inactive. This, therefore implies that the corresponding Lagrange multipliers $\boldsymbol{\mu}^0 = \mathbf{0}$ (See Figure 3.1).

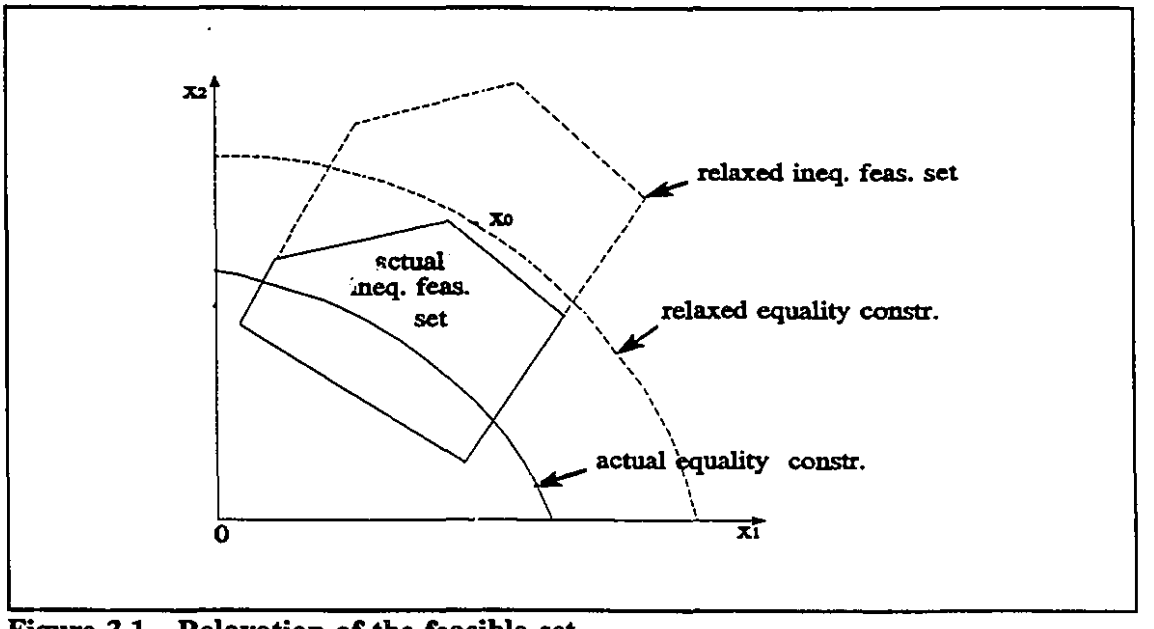

Figure 3.1 - Relaxation of the feasible set.

(ii)- It modifies the equality constraints (by essentially relaxing the load) according to (3.18), so that, at $\epsilon = 0$, the equalities are exactly satisfied (see Figure 3.1). The Lagrange multipliers associated with the equalities are set to the arbitrary value λ^0.

(iii)- It translates the cost function by adding a parameterized linear term, so that the first order optimality conditions (3.9)-(3.13) are satisfied at $\epsilon = 0$ (see Figure 3.2).

(iv)- It adds a quadratic term to the cost function, so that the second order optimality conditions are met near $\epsilon = 0$ for a sufficiently large w (see Figure 3.3).

For a x^0 that satisfies the constraint qualifications at and near $\epsilon = 0$, the second order optimality conditions are met for a sufficiently large coefficient w (see equation (3.20)), which makes the hessian matrix diagonally positive dominant. As the parameter is varied from 0 to 1, the objective function, the equality and inequality constraints are returned to their original form, so that, at $\epsilon = 1$, the parametric

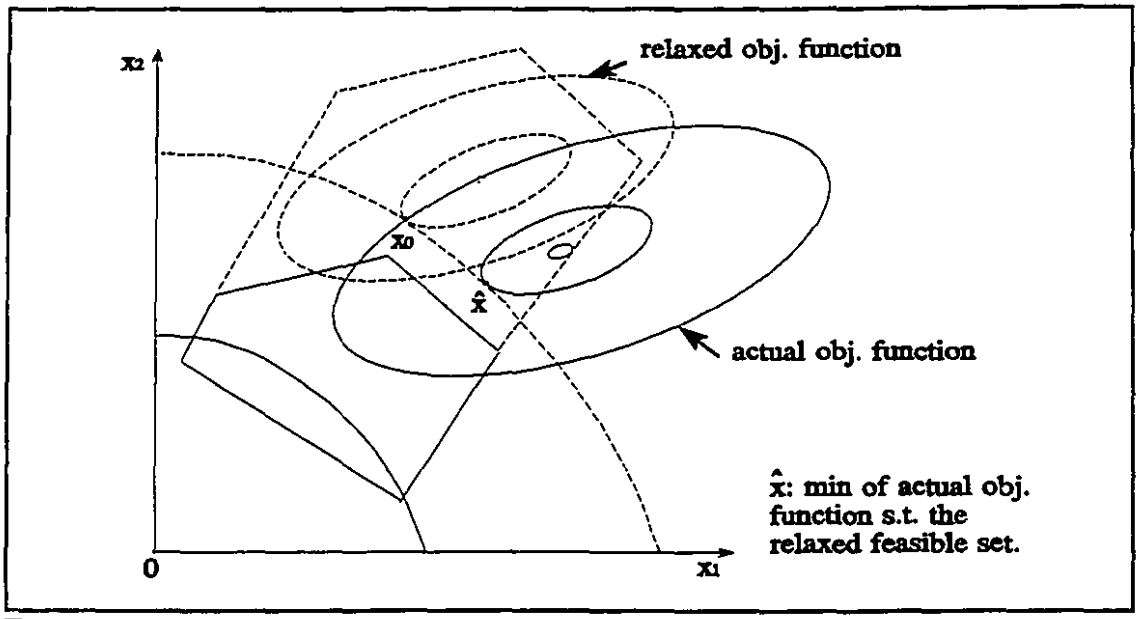

Figure 3.2 - Translation of the objective function.

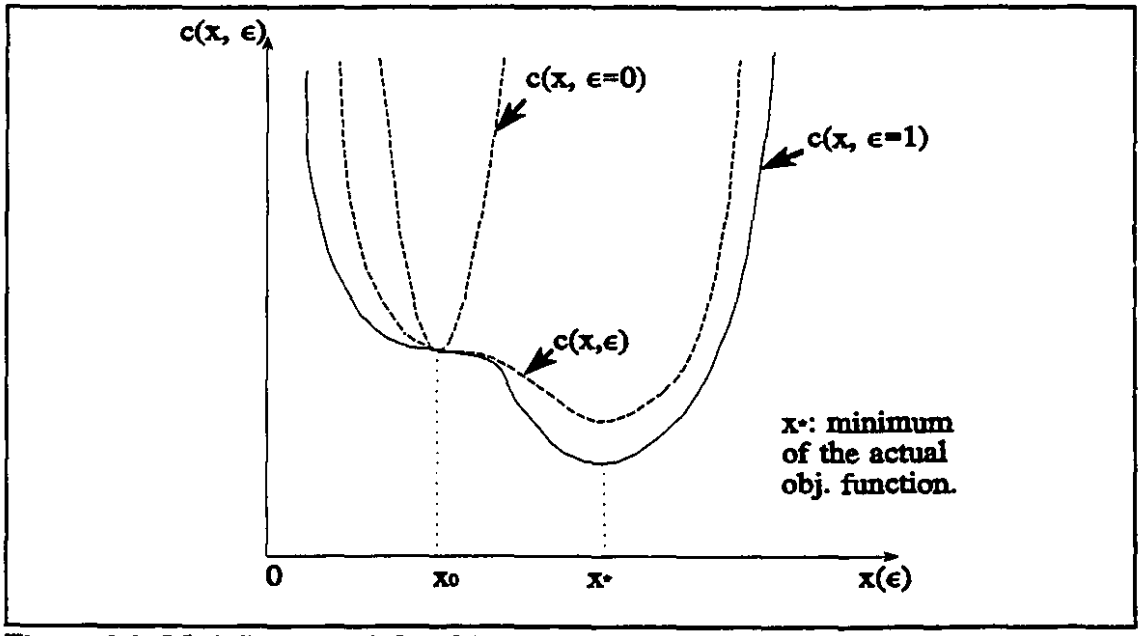

Figure 3.3- Modification of the objective function.

problem coincides with the original OPF. Thus, if we are able to track the initial solution (made optimal) until $\epsilon = 1$, we solve the original problem. Although the idea is quite simple, the tracking process requires that some conditions be met throughout the interval $0 \leq \epsilon \leq 1$. The difficulties associated with the tracking of the optimal solution as ϵ is varied from 0 to 1 are discussed in section 3.3.2.

3.2.4 Parameterized Model for Load Tracking - Phase II

As was discussed in the previous section, the linear and quadratic terms added to the objective function of the original OPF problem translates and reshapes the objective function at $(\mathbf{x}^0, \lambda^0)$ so the initial guess becomes optimal, whereas the parameterization of the equalities and inequalities makes our initial guess feasible. Since the load tracking process supposes that we already have an optimal solution for the initial load level, the parameterization of the objective function and of the inequalities is not necessary at the beginning of the tracking process. However, since we will assume a variable load, the parameterization of the power balance equations is still necessary. In this way, the starting problem (defined for the actual load level) and the goal problem (defined for the next load level) are related by means of the parameterization of the equality constraints. Theoretically, this is the only parameterization needed for load tracking. Nevertheless, the quadratic term added to the objective function plays an important role in the performance of a numerical solution algorithm since it makes $c(\mathbf{x},\varepsilon)$ more convex near $\varepsilon=0$. For this reason, this term is kept in the parameterized model used in Phase II.

Suppose that the vector of load levels, $\mathbf{d}$, for Phase I is $\mathbf{d}^0$ and suppose that the next point of the load curve is $\mathbf{d}^0+\Delta\mathbf{d} \triangleq \mathbf{d}^1$. Then, the Parametric-OPF for load tracking between $\mathbf{d}^0$ and $\mathbf{d}^1$ can be formulated by,

$$\underset{x}{Min} \quad c(x,\epsilon) \tag{3.23}$$

subject to

$$g_k(x,d(\epsilon)) = g_k(x,d^0 + \epsilon\Delta d) = 0, \quad k \in K \tag{3.24}$$

$$h_l(x,d(\epsilon)) = h_l(x,d^0 + \epsilon\Delta d) \leq 0, \; l \in L \tag{3.25}$$

where

$$c(x,\epsilon) = c(x) + (1 - \epsilon)\frac{1}{2}w \| x - x^o \|^2 \tag{3.26}$$

and where $\mathbf{x}^0$ is the optimal solution for the initial load level. The weighting factor, w, can have the same or a different value from the one used in Phase I.

The parameterization of the equality constraints becomes clearer when we explicitly represent $\mathbf{g}_k(\mathbf{x},\mathbf{d}(\varepsilon))$, $k \in K$, as the power balance equations for the load buses of the power system (see Appendix A and B). If $\mathbf{pd}^0_k$ and $\mathbf{qd}^0_k$ are the real and reactive loads at bus k for Phase I, equation (3.24) can be rewritten as:

$$g_k(x,d(\epsilon)) = \begin{bmatrix} p_k(x) - (pd_k^0 + \epsilon \Delta pd_k) \\ q_k(x) - (qd_k^0 + \epsilon \Delta qd_k) \end{bmatrix} \tag{3.27}$$

Therefore, for $\varepsilon=0$, the power balance equations is satisfied for the demand $\mathbf{d}^0$ whereas, at $\varepsilon=1$, they are satisfied for the new demand $\mathbf{d}^0+\Delta\mathbf{d}$. More importantly, for any $0 < \varepsilon < 1$, these equations are satisfied for the load level $\mathbf{d}^0+\varepsilon\Delta\mathbf{d}$, that is, the optimum is found for the entire load trajectory.

The situation of the inequality constraints is similar. The functional inequalities representing the power generations are of the same type as (3.27). Other functional inequalities that do not have the bus loads explicitly represented in their expressions such as line power flows are not parameterized by ε. Note that this is a significant difference from Phase I, where the line flows have their limits parameterized. In Phase II this is not required as the flow limits are satisfied by the initial conditions. For this reason, it is easy to see that *Phase II is a special case of Phase I.*

Thus, the tracking process in Phase II between any $\mathbf{d}=\mathbf{d}^0$ and any $\mathbf{d}=\mathbf{d}^0+\Delta\mathbf{d}$ is equivalent to a Phase I problem with load equal to $\mathbf{d}^0+\Delta\mathbf{d}$ but where the initial solution corresponds to a load level equal to $\mathbf{d}^0$ and meets all the inequalities.

Since the parametric models used in the two phases will be based on the tracking of the optimal trajectory for $0 \leq \varepsilon \leq 1$, we will discuss the tracking process for both models together.

3.3 Tracking the Optimal Trajectory for $0 \leq \varepsilon \leq 1$

3.3.1 Conditions for Continuity of the Trajectories

As was discussed in the previous chapter, parametric methods are based on the tracking of the solution trajectories defined by the homotopy function, $\mathbf{HO}(\mathbf{x},\varepsilon)$, which "connects" the initial, relaxed problem with the problem we want to solve.

As ε is varied starting from 0, the corresponding optimal solutions form a set of optimal solution trajectories that must be tracked until $\varepsilon=1$. The success or failure of the parametric method, therefore, depends heavily on the characteristics of the optimal solution trajectories formed in the interval $0 \leq \varepsilon \leq 1$. More specifically, to be able to apply a numerical method to follow the solutio. of the KT equations until the optimal solution of the original problem, we must guarantee that, in the entire interval $0 \leq \varepsilon \leq 1$,

(i)- the KT equations can be used to represent an optimal solution for the Parametric-OPF. Moreover, the Lagrange multipliers associated with the equality and inequality constraints are uniquely defined;

(ii)- the solutions of the KT equations satisfy the second order sufficient conditions for optimality;

(iii)- the trajectories are piecewise continuously differentiable (with respect to $\mathbf{x}$).

Therefore, suppose that, at some value of ε, $\bar{\epsilon}$, we know the optimum, $\bar{x}$, then for all ε in some neighbourhood around $\bar{\epsilon}$ there exists an optimal solution provided that:

(A)- At the point $\bar{x}$, LICQ is satisfied (this guarantees that (i) above is satisfied [Fiacco, 1983];

(B)- The active inequality constraints remain active;

$$\mu_l(\epsilon) > 0,\ l \in L_0 \tag{3.28}$$

(C)- The inactive inequalities are not violated;

$$h_l(x(\epsilon),\epsilon) < 0,\ l \notin L_0 \tag{3.29}$$

(D)- The second order sufficient conditions for optimality (equations (3.14)-(3.16)) are satisfied.

If conditions (A)-(D) are satisfied, then for all ε in the neighbourhood of $\bar{\epsilon}$, the jacobian of the first order optimality conditions (3.09)-(3.11), that is,

$$W(z,\epsilon) = \begin{bmatrix} H(z,\epsilon) & J^T(x,\epsilon) \\ J(x,\epsilon) & 0 \end{bmatrix} \tag{3.30}$$

is non-singular. Where

$$J(x,\epsilon) = \begin{bmatrix} \dfrac{\partial g}{\partial x}(x,\epsilon) \\ \dfrac{\partial h_{L_0}}{\partial x}(x,\epsilon) \end{bmatrix} \tag{3.31}$$

is the jacobian of the active constraints and where $\mathbf{z} = [\mathbf{x}^T, \lambda^T, \boldsymbol{\mu}^T_{L0}]^T$ [Kojima, 1980]. Then, by the Implicit Function Theorem [Garcia and Zangwill, 1981], all points $\mathbf{z}(\epsilon)$ =

$[\mathbf{x}^T(\varepsilon),\ \lambda^T(\varepsilon),\ \boldsymbol{\mu}^T_{L0}(\varepsilon)]^T$ that satisfy the homotopy function $\mathbf{HO}(\mathbf{x},\varepsilon)=\mathbf{0}$ (defined by equations (3.09)-(3.11)) are on a single continuously differentiable path through $(\bar{x},\bar{\epsilon})$.

The basic idea of tracking the optimal trajectory is to start with a known optimum for some ε and find the maximum possible increase in ε which does not violate any of the above conditions. If conditions (B) or (C) establish such a maximum, the resulting point is called a *break-point* and corresponds to either the release of an active inequality or the binding of a previously inactive inequality. The tracking process consists of following the optimal path from one break-point to another until ε=1. It is this procedure which enables the method to systematically identify the final active set. Furthermore, the active set throughout the path is also determined which has important implications in understanding when and how constraints become activated or deactivated in terms of the continuation parameter. These changes in the active set together with the non-linear characteristic of the Parametric-OPF, can lead, however, to situations where the tracking process cannot continue to the final solution. These situations are basically characterized by the violation of conditions (A) or (D) above. In some of the cases where this problem happens, there is no solution of the OPF beyond the point where the violation occurs. In other cases, even if there is an optimum, the method fails to find it. In the next section, we present a systematic discussion of the points of the optimal path where the tracking process of the optimal trajectory cannot continue. Such points are called critical points.

3.3.2 Critical Points in the Tracking Process

It has been shown that, through a smart parameterization of the OPF problem, followed by a progressive return of the parameters to their initial values, we may be able to track any initial estimate of the OPF problem until the optimum. It can be expected, however that a non-linear problem such as the OPF presents difficulties for its solution which, when using parametric methods, translate into loss of optimality of the solution trajectories or into discontinuities of the feasible set. These problems are inherent in the OPF and some of them were reported previously [Sun et al., 1984; Monticelli and Liu, 1992]. We do not have, at the present, a solution for all the cases where the parametric method fails to find a solution, but this thesis provides insight into this important and

difficult aspect which has, up to now, received little attention. We will classify the critical points into seven different types. The first four types are discussed in detail in [Jongen et al., 1986, (a) and (b) and Guddat et al., 1990] for a general nonlinear parametric optimization problem. In addition, Poore and Tiahrt published an extensive study of the first type of critical points [Poore and Tiahrt, 1987]. The last three types of critical points are more particular to the Parametric-OPF algorithm.

Type 1: Release of an active inequality leads to a saddle point

Suppose that at $\varepsilon = \bar{\epsilon}$, the solution $\bar{z}$ of the Kuhn-Tucker equations satisfies the following properties:

(i)- At $\bar{x}$ LICQ is satisfied;

(ii)- $L_0(\bar{x},\bar{\epsilon}) \neq \varnothing$

(iii)- In (3.09), exactly one of the Lagrange multipliers, $\bar{\mu}_p$, vanishes, whereas all the others (if they exist) $\bar{\mu}_l \neq 0$. Let,

$$T = \{ y \mid \frac{\partial g}{\partial x}(\bar{x},\bar{\epsilon})y = 0, \frac{\partial^T h_l}{\partial x}(\bar{x},\bar{\epsilon})y = 0, l \in L_0(\bar{x},\bar{\epsilon}) \} \qquad (3.32)$$

$$\hat{T} = \{ \hat{y} \mid \frac{\partial g}{\partial x}(\bar{x},\bar{\epsilon})\hat{y} = 0, \frac{\partial^T h_l}{\partial x}(\bar{x},\bar{\epsilon})\hat{y} = 0, l \in L_0(\bar{x},\bar{\epsilon}), l \neq p \} \qquad (3.33)$$

(iv)- The projection of the hessian matrix (equation (3.14)) is non-singular in (3.32).

(v)- The projection of the hessian matrix is non-singular in (3.33).

(vi)- The derivative of $\mathbf{h}_p$ with respect to ε does not vanish.

According to (vi), after the critical point, $\mathbf{h}_p$ will not remain equal to zero, and therefore can either be released (in case its derivative with respect to ε is negative), or it can be kept at its limits (in case its derivative with respect to ε increases). According to (i), (iv) and (v), the jacobian of the Kuhn-Tucker conditions (equation (3.30)) remains non-singular both before and after $\mathbf{h}_p$ is released. Therefore, in the neighbourhood of this critical point we have three possible situations: (a) the solution of the KT equations remains optimal after $\mathbf{h}_p$ is released (that is, $\boldsymbol{H}$ has only positive eigenvalues in (3.33)), (b) the solution of the KT equations remains optimal after $\mathbf{h}_p$ is fixed at its limit and (c) the solution of the KT equations loses optimality (i.e., $\boldsymbol{H}$ has one or more negative eigenvalues in (3.33)). In the first two cases, although the trajectory is not smooth at this point [Jongen et al., 1986 (b)], the tracking can proceed normally. In the last situation however, the optimal solution trajectory stops at $(\bar{x},\bar{\epsilon})$. Thus, at this point there is at least one descent direction, $\tilde{y}$, for the Parametric-OPF which is associated with the negative eigenvalue of the projected hessian. If we are able to find such a direction, we can find a local minimizer $\hat{x}$ for the Parametric-OPF at $\bar{\epsilon}$ (see Figure 3.4). Of course $\hat{x} \neq \bar{x}$ and we can continue to follow the optimal path through the point $(\hat{x},\bar{\epsilon})$. This descent direction can be found by an approach proposed in [Guddat et. al., 1990].

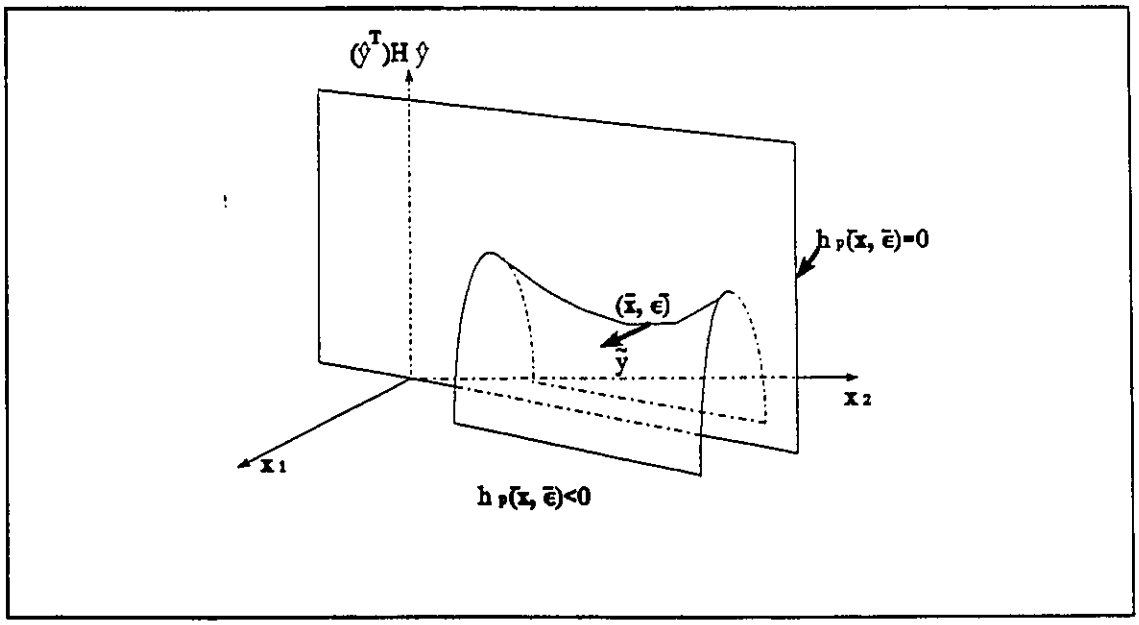

Figure 3.4- Critical point of type 1.

Example of type 1 critical point

Critical points of this type are often observed during the load tracking process when the system load is decreasing because some of the previously active limits on the system variables have a tendency to be released, thus augmenting the space of optimization and transforming previous minimum points into saddle points. In addition, such critical points can also occur during Phase I if we have a system with a great number of variables. This is the case presented in Figures 3.5.a-c. In this application we are trying to find the operating point which optimizes generation cost and voltage profile considering that some of the line series reactances are variable (i.e., supposing that some FACTS devices exist in the system), (Figure 3.5.a). At ε=0.286, the reactance of line 55 is released from its minimum limit, according to the sign of its Lagrange multiplier (Figure 3.5.b). At this point, the minimum eigenvalue of the projected hessian becomes negative and the solution loses optimality (Figure 3.5.c). It is interesting to observe that, beyond ε=0.286, although the variable was to be released from its limit (because the associated Lagrange multiplier became positive), the variable violates this limit, showing that interpretation of the Lagrange multiplier as the sensitivity of the objective function with respect to changes on the variable limit is not valid after the solution of the KT equations loses optimality.

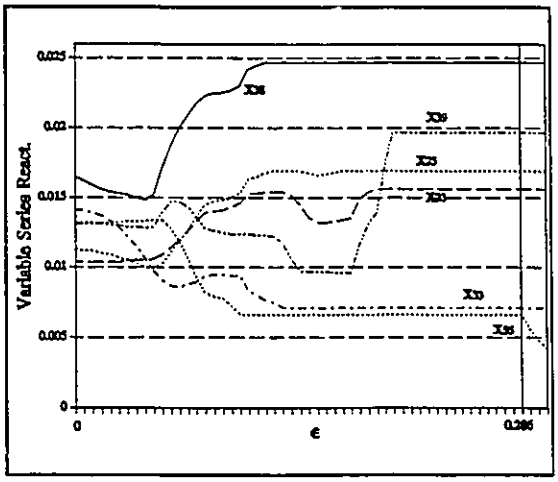

Figure 3.5.a - Variable series react.

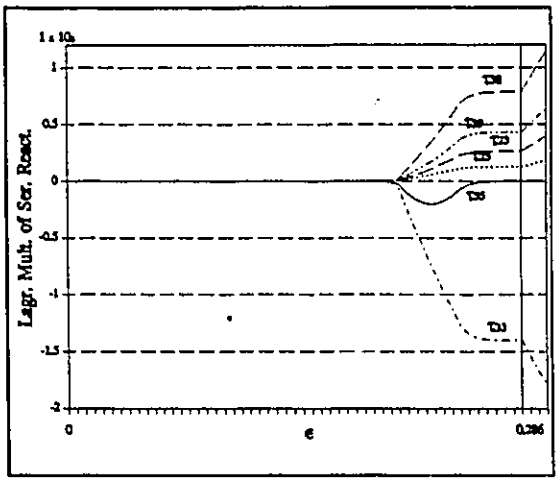

Figure 3.5.b - Lagrange Multipliers

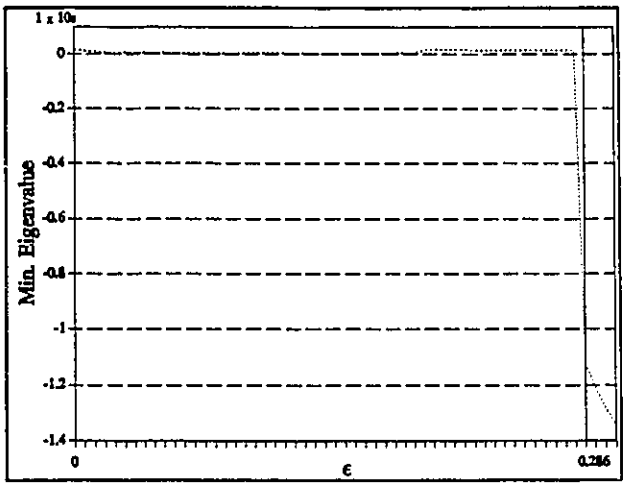

Figure 3.5.c - Minimum Eigenvalue

Type 2: Singular projection of the hessian matrix

Now, suppose that at $\varepsilon = \bar{\epsilon}$, the solution $\bar{z}$ of the Kuhn-Tucker equations satisfies the following conditions:

(i)- At $\bar{x}$ LICQ is satisfied.

(ii)- $\mu_l \neq 0$ for all $l \in L_0(\bar{x},\bar{\epsilon})$

(iii)- Exactly one eigenvalue of the projection of the hessian $\boldsymbol{H}$ (equation (3.14)) on the subspace $\boldsymbol{T}$ (equation (3.32)) vanishes.

To study the behaviour of the KT set around $\bar{\epsilon}$, first of all we must notice that the derivative of the KT equations (3.09)-(3.11) with respect to ε must satisfy, at and near $(\bar{x},\bar{\epsilon})$,

$$\frac{d}{d\epsilon}\left(\frac{\partial \mathcal{L}}{\partial z}\right) = \frac{\partial^2 \mathcal{L}}{\partial z^2}\cdot\left(\frac{dz}{d\epsilon}\right) + \frac{\partial^2 \mathcal{L}}{\partial z \partial \epsilon} = 0 \qquad (3.34)$$

which implies from equation (3.30) that,

$$\frac{dz}{d\epsilon}(\bar{z},\bar{\epsilon}) = -\begin{bmatrix} H(\bar{z},\bar{\epsilon}) & J^T(\bar{x},\bar{\epsilon}) \\ J(\bar{x},\bar{\epsilon}) & 0 \end{bmatrix}^{-1}\begin{bmatrix} \frac{\partial^2 \mathcal{L}}{\partial z \partial \epsilon}(\bar{z},\bar{\epsilon}) \end{bmatrix} \qquad (3.35)$$

Now, by (iii) the matrix $W(\bar{z},\bar{\epsilon})$ is singular at this point [Kojima, 1980], thus dz/dε goes to infinity as we approach $(\bar{x},\bar{\epsilon})$. To characterize the curve of optimal solution near this point we must impose an additional condition (iv) on the second derivative of the Kuhn-Tucker conditions, that is,

(iv)- The second derivative of the Lagrangian with respect to **z** and ε does not vanish. In addition, the third derivative of the Lagrangian with respect to **z** does not vanish.

These four conditions ensure that the trajectories can locally be represented by a parabola and that after the point $(\bar{x},\bar{\epsilon})$ one of the eigenvalues of the projected hessian becomes negative [Jongen et al., 1986,(a) and (b)]. See also Appendix C.

Example of type 2 critical point

This situation is illustrated by the 5-bus system represented in Figure 3.6. In this example we used the parametric approach to optimize the transmission losses of the system. From Figures 3.7.a-f we notice that, as ε approaches 0.405, the minimum eigenvalue of the projected hessian approaches 0 at the same time as the optimal trajectories of the voltage magnitude and angles, as well as real and reactive power generations reach a turning point. In this example, we are able to pass through the point where the minimum eigenvalue vanishes and continue the tracking (i.e., reach an optimal trajectory that reaches ε=1) by jumping to another path. However, in general, it is not possible to track the solution beyond such a critical point because of ill-conditioning problems near the turning point. This example illustrates a case where before ε=0.405 the solution trajectories of the KT equations were not optimal, whereas after ε=0.405 they became optimal. The opposite situation may also occur (i.e., loss of optimality) and we must find other means to continue the tracking process along another path, if one exists.

As in the first type of critical point, the resolution of this case is not easy, however one method proposed in [Guddat et al., 1990] but not tested here uses a descent direction to search for a local minimizer $\hat{x}$ for the same $\bar{\epsilon}$ which lies on another optimal path. Then, starting at $(\hat{x},\bar{\epsilon})$ the pathfollowing process can be exploited again (see Figure 3.8).

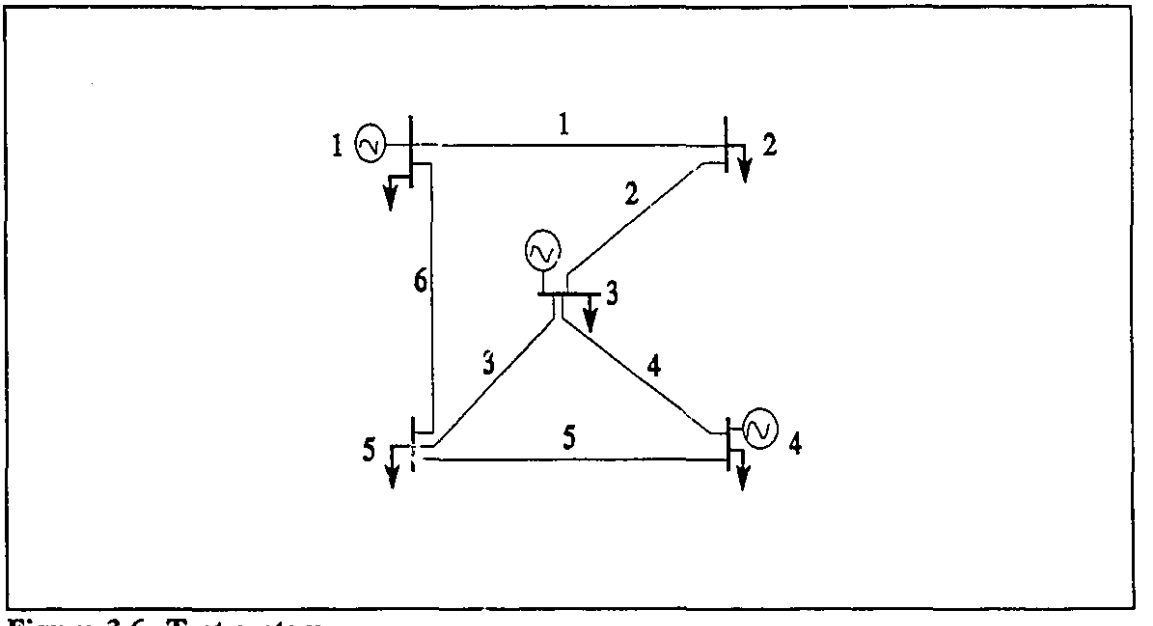

Figure 3.6- Test system.

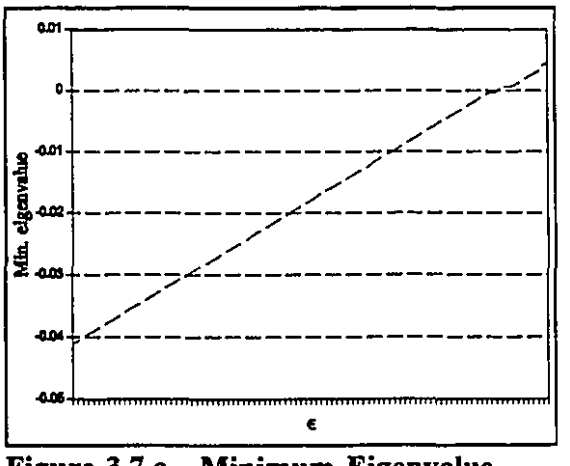

Figure 3.7.a - Minimum Eigenvalue.

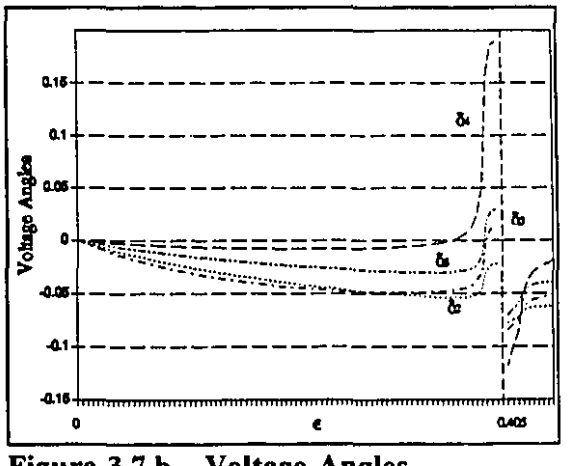

Figure 3.7.b - Voltage Angles.

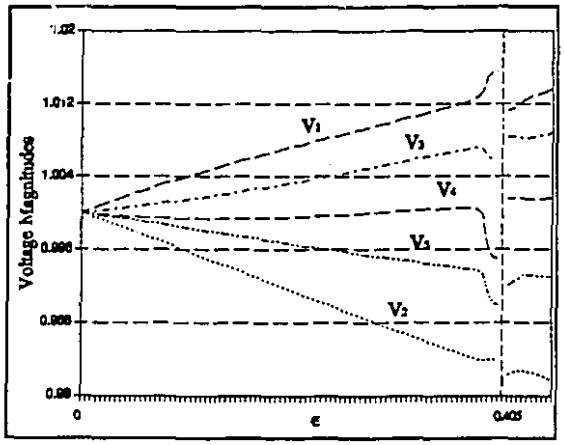

Figure 3.7.c - Voltage Magnitudes.

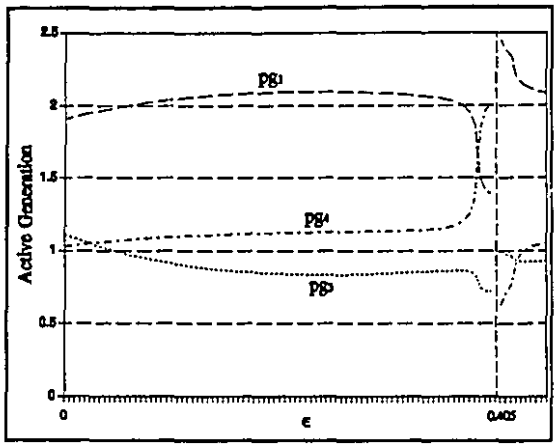

Figure 3.7.d - Active Generation.

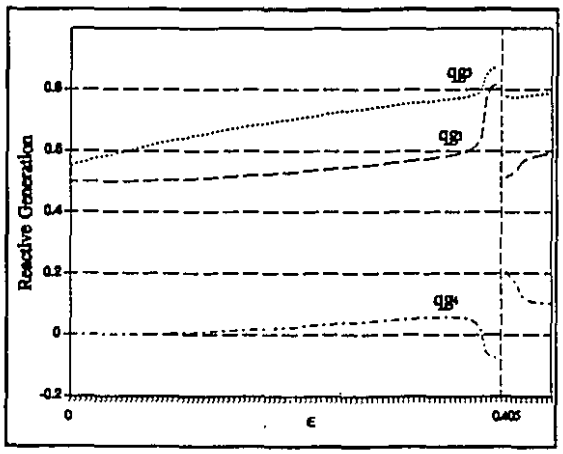

Figure 3.7.e - Reactive Generation.

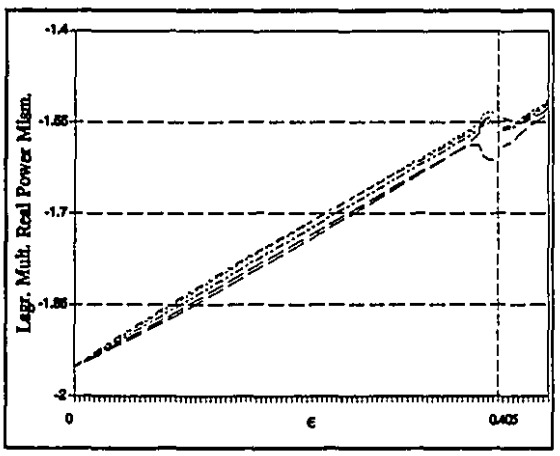

Figure 3.7.f - Lagrange Multipliers.

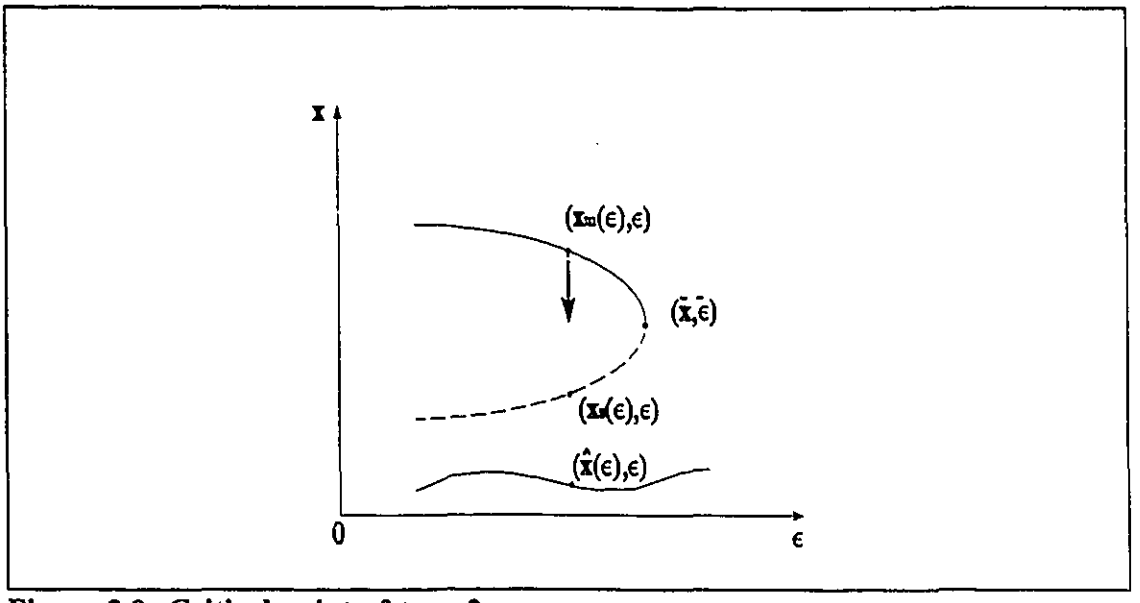

Figure 3.8- Critical point of type 2.

Type 3: Jacobian of the active set is rank deficient

A point $(\bar{x},\bar{\epsilon})$ of the solution trajectory of the Kuhn-Tucker equations is a critical point of type 3 if the following conditions are fulfilled:

(i)- The rank of $J(\bar{x},\bar{\epsilon})$ is incomplete and less than nv.

From (i) and (3.31) we see that there exist λ_k, μ_l, $k \in K$, $l \in L_0(\bar{x},\bar{\epsilon})$, not all zero such that

$$\sum_{k\in K} \lambda_k \frac{\partial g_k}{\partial x}(\bar{x},\bar{\epsilon}) + \sum_{l\in L_0} \mu_l \frac{\partial h_l}{\partial x}(\bar{x},\bar{\epsilon}) = 0 \qquad (3.36)$$

(ii)- If the set of active inequalities $L_0(\bar{x},\bar{\epsilon})$ is not empty then all corresponding Lagrange multipliers $\mu_l > 0$.

Here, as in the previous type of critical points, the matrix $W(\bar{z},\bar{\epsilon})$ is singular [Kojima, 1980]. To characterize the behaviour of the optimal solution trajectory in this case, we need the following additional suppositions (see Appendix C):

(iii)- The second derivative of the Lagrangian with respect to **z** and ε does not vanish. In addition, the third derivative of the Lagrangian with respect to **z** does not vanish.

Since the matrix $W(\bar{z},\bar{\epsilon})$ is singular at $(\bar{x},\bar{\epsilon})$ as a consequence of (i), at this point dz/dε goes to infinity. By (iii), the parameter ε of the optimal solution trajectory has a (non-degenerate) local maximum and can be represented locally by means of a parabola (see Figure 3.9). As a consequence of (i) and (ii), the Lagrange multipliers associated with the active constraints go to infinity as we approach $(\bar{x},\bar{\epsilon})$ [Gauvin, 1977 and Jongen et al., 1986 (b)]. It can also be demonstrated that the "lower" part of the parabolic trajectory near the critical point $(\bar{x},\bar{\epsilon})$ describes maximum rather than by minimum points [Jongen et al., 1986 (b)].

As we progress along the optimal solution path toward the critical point, the objective function c(**x**,ε), can either decrease or increase with ε. In case it decreases, it is possible to compute a point on the "lower" side of the parabola, $\mathbf{x}_{max}(\varepsilon)$, with $\varepsilon < \bar{\epsilon}$ but close to $\bar{\epsilon}$(see Figure 3.9). Then, one can start at $\mathbf{x}_{max}(\varepsilon)$ with a descent method to find a new local minimizer for the problem, say, $\hat{x}(\epsilon)$, if it exists. If the objective function, c(**x**,ε), decreases with ε along the original path, then $\hat{x}(\epsilon)$ will differ from $\mathbf{x}_{min}(\varepsilon)$ (see Figure 3.9)), that is, we will be assured to lie on a different path. However, in the case where the objective function increases with ε, it is not possible to continue the tracking beyond $\bar{\epsilon}$ because the feasible set in the neighbourhood becomes empty. In this last case, therefore, by starting at $\mathbf{x}_{max}(\varepsilon)$ with any descent direction method we will eventually return to $\mathbf{x}_{min}(\varepsilon)$ again [Guddat et al., 1988 and 1990].

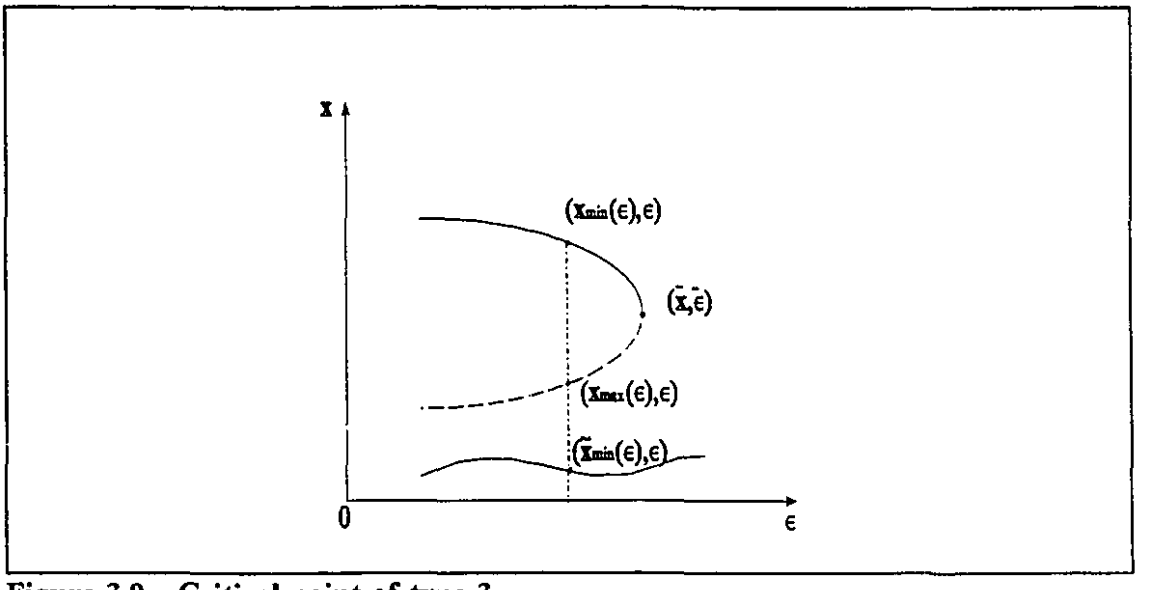

Figure 3.9 - Critical point of type 3.

Example of type 3 critical point

During the solution of the parametric OPF, critical points of type 3 are found mainly during Phase II (where the parameter is the system load) for situations where the system load is increasing. Since, for these cases, the objective function increases as well, we can conclude that, beyond such critical points, the feasible set becomes empty in the neighbourhood. As a consequence, a feasible solution, if it exists, will lie in a region of the feasible set that is distant from the actual operating point.

A critical point of type 3 is illustrated by the same system represented in Figure 3.6 but with a different set of limits (only line flows have limits in this example). In this application, we want to optimize the generation cost and improve the system voltage profile. At ε=0.985, the transmission limits of lines 1 and 2 are active and it is not possible to satisfy the load connected to bus 2 even by increasing the voltages at both ends of the lines to reduce the transmission losses. It is easy to verify that there is no feasible solution for this problem because as the two lines feeding bus 2 saturate, the bus essentially becomes isolated from the network and cannot receive any additional power to meet its load.

Unlike the two previous critical situations where loss of optimality was the underlying cause, this type of critical point is related to cases where there is no solution for the OPF. It is interesting to notice that such a critical situation is a consequence of the local structure of the feasible set thus highlighting its close relation to infeasibility. In fact, one can understand this critical situation as a generalization of load flow infeasibility [Galiana and Zeng, 1990]. In Figures 3.10.a-f, we show the behaviour of the optimal solution for this case. Note that the Lagrange multipliers associated with the line flows (Figure 3.10.f) tend to infinity as we approach ε=0.985, contrary to the Lagrange multipliers represented in Figure 3.7.f.

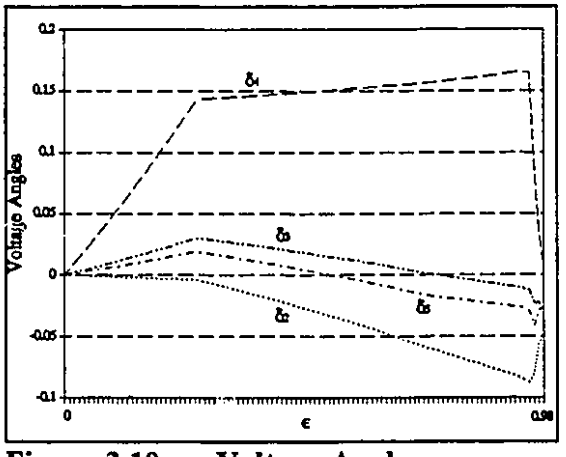

Figure 3.10.a - Voltage Angles

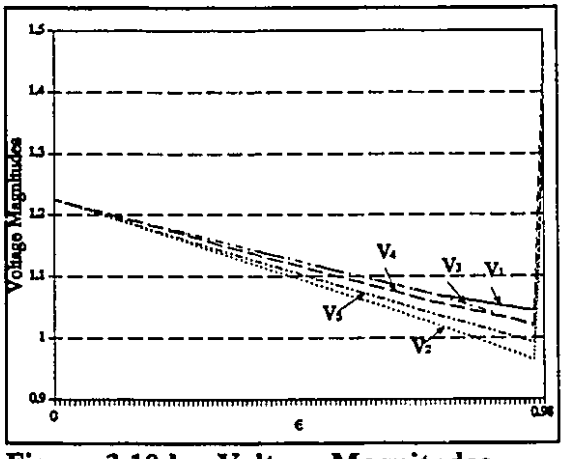

Figure 3.10.b - Voltage Magnitudes.

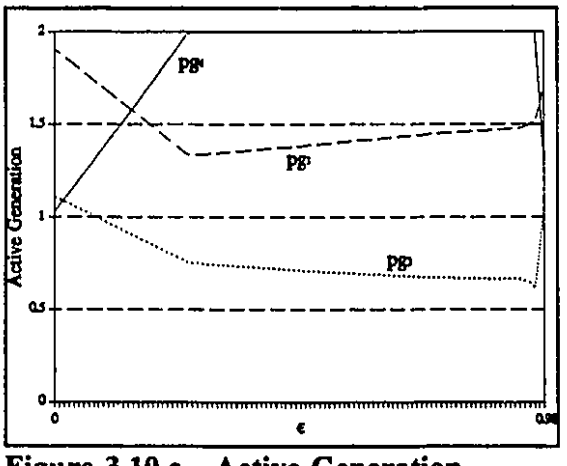

Figure 3.10.c - Active Generation.

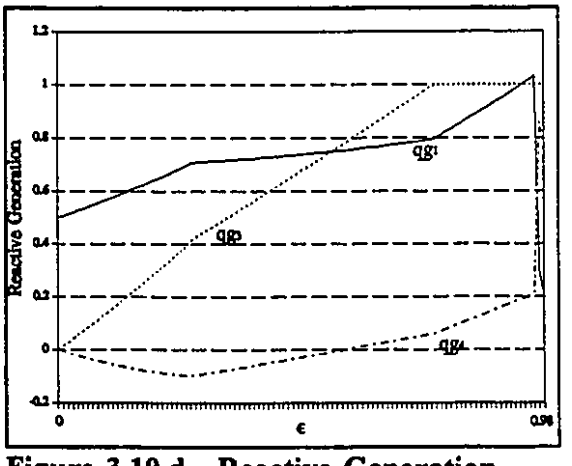

Figure 3.10.d - Reactive Generation.

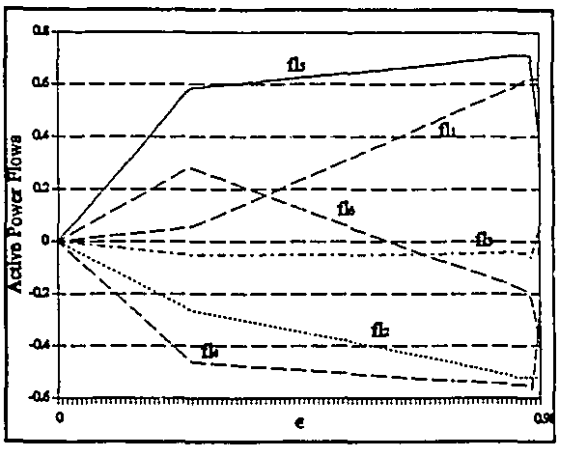

Figure 3.10.e - Power Flows.

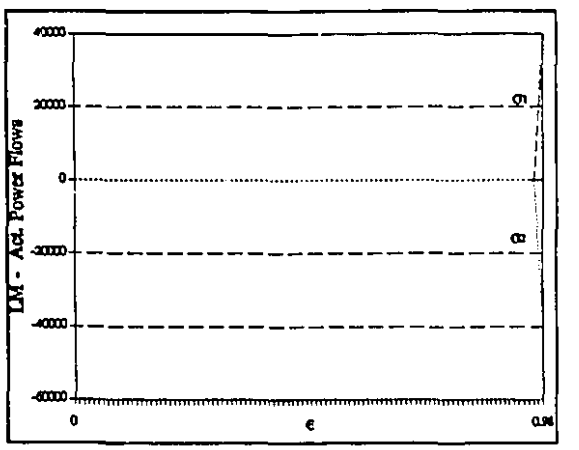

Figure 3.10.f - Lagrange Multipliers.

Type 4: Number of active constraints exceeds the number of free variables by one

A point $(\bar{x},\bar{\epsilon})$ is of type 4 if the following conditions hold:

(i)- m+p = nv+1 (i.e., the number of active constraints is equal to the number of variables plus one). Thus, since m < nv, the total number of active inequality constraints, $p \geq 2$.

(ii)- There exist λ_k, μ_l, $k \in K$, $l \in L_0(\bar{x},\bar{\epsilon})$, not all vanishing such that:

$$\sum_{k \in K} \lambda_k \frac{\partial g_k}{\partial x}(\bar{x},\bar{\epsilon}) + \sum_{l \in L_0} \mu_l \frac{\partial h_l}{\partial x}(\bar{x},\bar{\epsilon}) = 0 \qquad (3.37)$$

(iii)- In (3.37), it is assumed that all $\mu_l \neq 0, l \in L_0(\bar{x},\bar{\epsilon})$.

(iv)- The gradients of the equalities and active inequalities are different from zero.

From conditions (i)-(iv) it follows that for every $q \in L_0(\bar{x},\bar{\epsilon})$ the set

$\left\{\frac{\partial g_k}{\partial x}(\bar{x},\bar{\epsilon}),\ \frac{\partial h_l}{\partial x}(\bar{x},\bar{\epsilon}),\ k\in K,\ l\in L_0(\bar{x},\bar{\epsilon}),\ l\neq q\right\}$ is linearly independent. To be able to proceed with the tracking process, we must find a $\mathbf{h}_q$, $q \in L_0(\bar{x},\bar{\epsilon})$, such that, when deleted from the active set, the new values of $\mu_l > 0$, $l \in L_0(\bar{x},\bar{\epsilon})$, $l \neq q$ and $\mathbf{h}_q \leq 0$ (Note that after deleting $\mathbf{h}_q$ from the active set, it is not necessary to test the projection of the hessian since the dimension of $\mathbf{x}$ is equal to the number of active inequalities and equalities). If there is no such inequality function, $\mathbf{h}_q$, the feasible set becomes empty beyond $(\bar{x},\bar{\epsilon})$. To find the correct inequality to delete from the active set a method, such as the one proposed in Appendix D, can be used.

Example of type 4 critical point

A type 4 critical point occurs in a situation that is similar to the one found in type 3 where part of the network becomes isolated. A typical situation can be seen in an application from the 5-bus system of Figure 3.6. In this application, the limits on the generation at bus 1 are tightened whereas the generation limits on buses 3 and 4 are broadened. Here we set the generation cost for bus 1 much higher than the other generation costs and we want to find an operating point which minimizes the total generation cost plus deviations of the voltage profile from normal. At ε=0.949, $\mathbf{qg}_1$, $\mathbf{pg}_4$, $\mathbf{V}_3$ and $\mathbf{V}_4$ are at their maximum values and $\mathbf{V}_1$ is at the minimum. When $\mathbf{qg}_3$ reaches its maximum, the number of active constraints (equals to 13) becomes greater than the number of variables (equals to 12), thereby reaching a type 4 critical point. Figures 3.11.a-f show the optimal trajectories for this case. In this example, it was possible to continue the tracking beyond ε=0.949 by releasing $\mathbf{pg}_4$ from its maximum limit at the same time that $\mathbf{qg}_3$ was fixed at the minimum. The occurrence of this critical point can be explained by the difference that exists between the generation costs of buses 1,2 and 4. Because the cost of generation is much smaller at bus 4, the optimization process will make $\mathbf{pg}_4$ generate its maximum permissible amount. However, because of a reactive problem at bus 3, it is not possible to find an operating point inside the feasible limits of the problem. Therefore, the program is forced to use the more expensive generation of bus

1. Note in Figures 3.11- b,d and f that the Lagrange multipliers have a discontinuity in their values across the critical point.

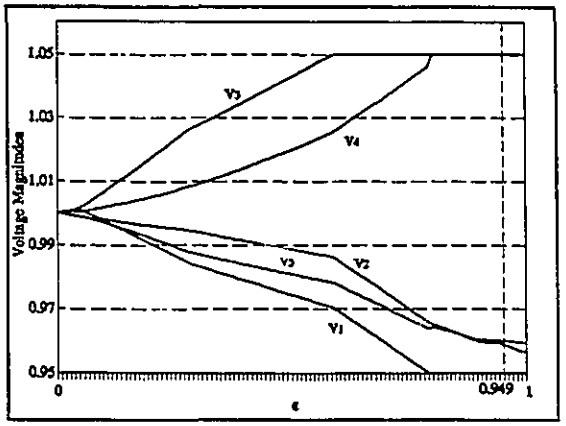

Figure 3.11.a - Voltage Magnitudes.

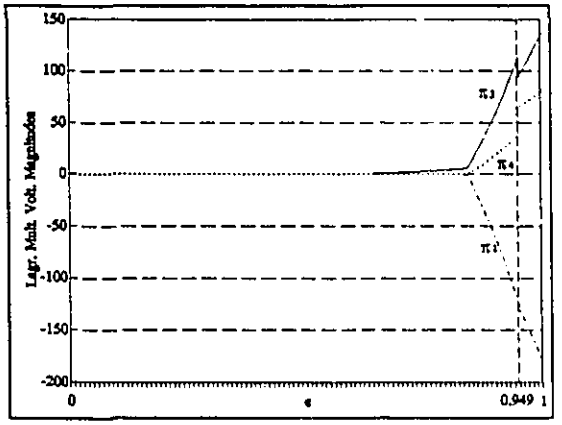

Figure 3.11.b - Lagrange Multipliers.

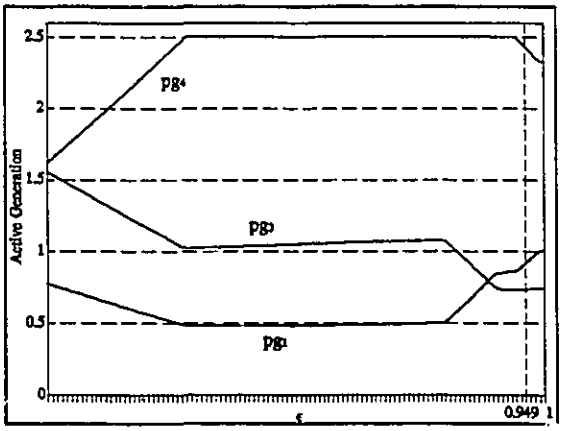

Figure 3.11.c - Active Generation.

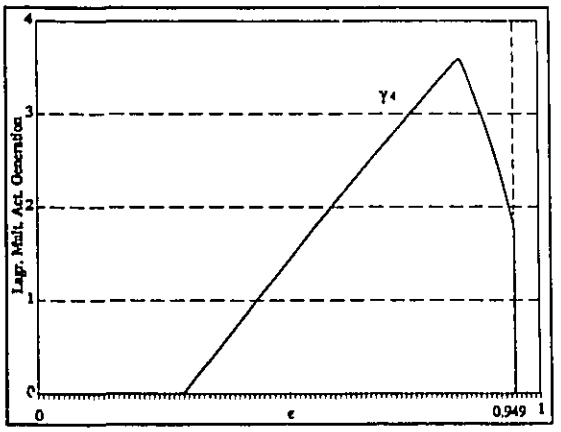

Figure 3.11.d - Lagrange Multipliers.

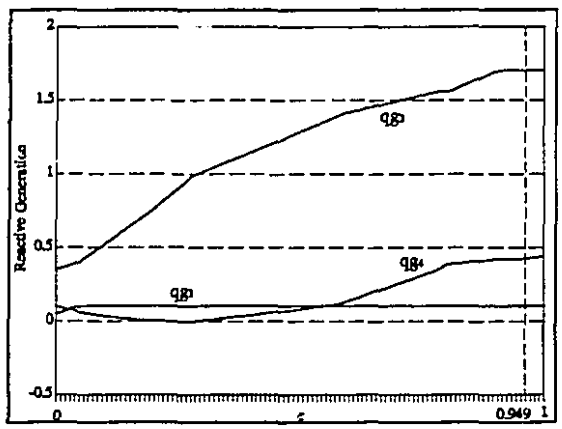

Figure 3.11.e - Reactive Generation.

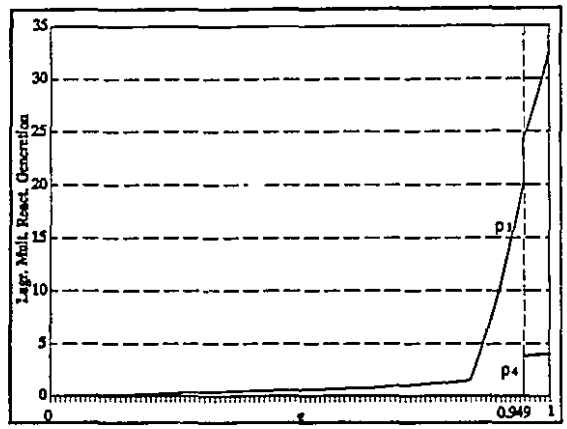

Figure 3.11.f - Lagrange Multipliers.

The last two types of critical points are important in our study because they may coincide with the feasibility limit of the OPF which in Phase II corresponds to the maximum loadability limit. The method used here, since it tracks the optimal solution from one break-point to another (i.e., no multiple changes in the active set are permitted) is capable to point out clearly where the bottlenecks are situated in the transmission system by checking for critical points of type 3 or 4.

In addition to the critical situations described above, during the tracking process other conditions may occur that prevent the tracking method from proceeding toward $\varepsilon=1$. Most of these situations can be described as a combination of two of the different types of critical points discussed previously. Because of their nature, it is difficult to propose "jumps" to other sets of local minimizers when these critical points occur. Throughout the solution of the Parametric-OPF we also encountered some points of this mixed kind. There are basically 3 different "composed" critical points which, as with types 1 to 4, are classified here by the type of violation they lead to in conditions (A)-(D) (see page 14):

Type 5: Two or more active inequalities released at the same ε

At this type of critical point, $(\bar{x},\bar{\epsilon})$, the following conditions hold:

(i)- LICQ is satisfied.

(ii)- $L_0(\bar{x},\bar{\epsilon}) \neq \varnothing$

As in type 1, here we have,

$$\frac{\partial c}{\partial x}(\bar{x},\bar{\epsilon}) + \sum_{k\in K} \lambda_k \frac{\partial g_k}{\partial x}(\bar{x},\bar{\epsilon}) + \sum_{l\in L_0} \mu_l \frac{\partial h_l}{\partial x}(\bar{x},\bar{\epsilon}) = 0 \qquad (3.38)$$

(iii)- In (3.38) two or more (r) Lagrange multipliers associated with active inequalities vanish. Assume that μ_i=0, i=1,...,r

(iv)- The second order sufficient conditions for optimality (equations (3.14)-(3.16)) are met.

(v)- The derivatives of the inequality constraints $\mathbf{h}_i$, i=1,...,r, with respect to ε are different from zero.

By (iii) we see that, at this critical point, two or more inequality constraints can be released. Following the release of some combination of these constraints, the projected hessian may remain positive definite, that is, the critical $(\bar{x},\bar{\epsilon})$ may remain optimal, or the projected hessian may become indefinite, indicating loss of optimality. If the critical point loses optimality after the $\mathbf{h}_i$ are released other combinations may be attempted to continue the tracking. The problem here, therefore, is to determine which constraints to release, a combinatorial problem whose solution by trial and error is computationally expensive. This is specially problematic in OPF since, normally, the constraints being simultaneously released are of the same type (e.g., limits on reactive sources geographically close to each other) and the release of one of them is almost certain to affect the others.

Type 6: Two or more inequalities to be fixed at the same ε

A critical point $(\bar{x},\bar{\epsilon})$ is of type 6 if the following conditions hold:

(i)- At $(\bar{x},\bar{\epsilon})$ LICQ is satisfied. Hence as for the previous types,

$$\frac{\partial c}{\partial x}(\bar{x},\bar{\epsilon}) + \sum_{k\in K} \lambda_k \frac{\partial g_k}{\partial x}(\bar{x},\bar{\epsilon}) + \sum_{l\in L_0} \mu_l \frac{\partial h_l}{\partial x}(\bar{x},\bar{\epsilon}) = 0 \qquad (3.39)$$

(ii)- In (3.39) $\mu_l > 0$ for all $l \in L_0(\bar{x},\bar{\epsilon})$

(iii)- There exit r inequalities $h_i(\bar{x},\bar{\epsilon})$, $i \notin L_0(\bar{x},\bar{\epsilon})$ simultaneously reaching their limits.

(v)- The derivatives of $\mathbf{h}_i$, i=1,...,r, with respect to ε are different from zero.

At this point, unless one or more of the inequalities reaching their limit are fixed, multiple violations of the optimality condition C (page 14) will occur for $\varepsilon > \bar{\epsilon}$. Thus, one or more of these inequalities must be fixed. If the new jacobian $\boldsymbol{J}$ (formed by the previously active constraints plus the new ones) has full rank and no new violations occur, then $(\bar{x},\bar{\epsilon})$ will remain optimal in a neighbourhood of the critical point. As in type 5, this is a combinatorial problem.

Critical points of type 6 are often followed by critical points of type 5 in the tracking process. The power system configuration can play an important role in such kinds of critical points. Figure 3.12 illustrates one such possible situation. At bus 2 of this system, a synchronous condenser and a static compensator supply reactive power to the network and they tend to increase or decrease their VAr outputs in unison. Depending on their operational limits, these components may have to be fixed at the same value of ε. Even if they are not to be fixed at their limits at the same ε, changes in the active set

may occur throughout the tracking process which force both variables to be released at the same point. This is the case depicted in Figures 3.13.a-b, where the Lagrange multipliers associated with a shunt compensator and a synchronous condenser connected at the same bus reach zero at ε=0.88. Other trivial cases would be transmission limits on parallel lines or generation units connected to the same bus (in applications where generation cost is not considered). Although sometimes it is possible to resolve these critical situations by introducing small changes in the limits of the problem data, in general we must rely on heuristics to find the correct combination of active constraints and continue the tracking.

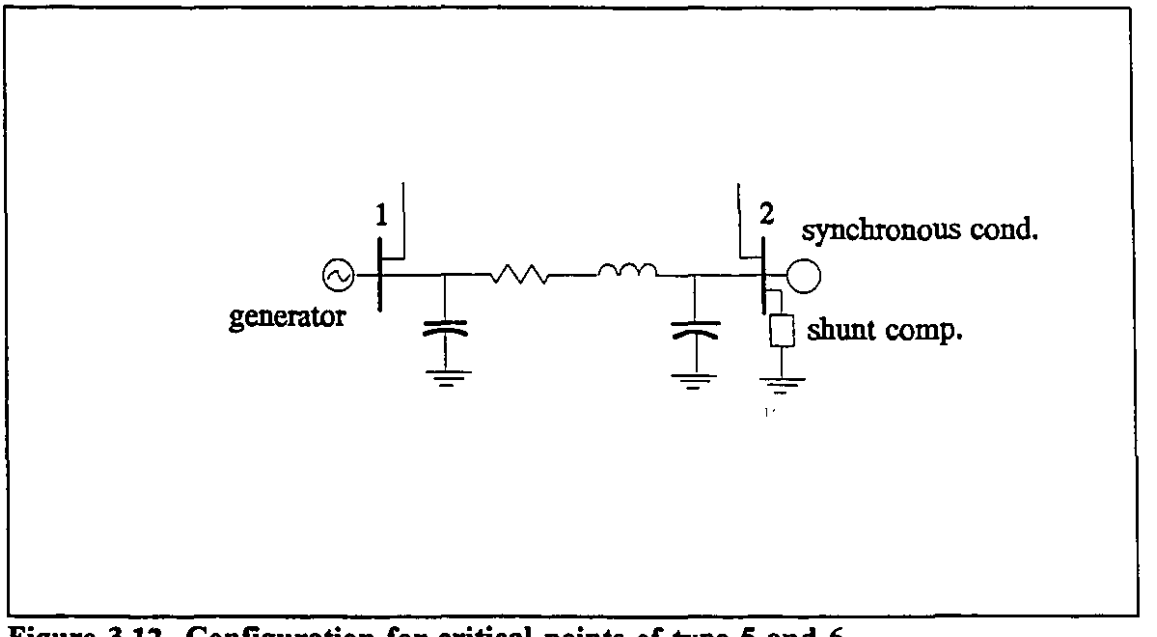

Figure 3.12- Configuration for critical points of type 5 and 6.

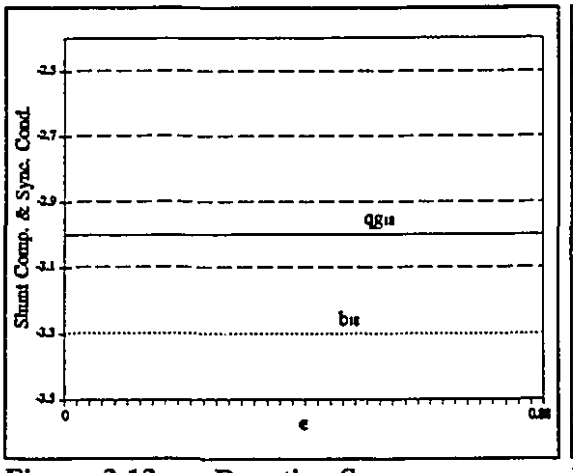

Figure 3.13.a - Reactive Sources.

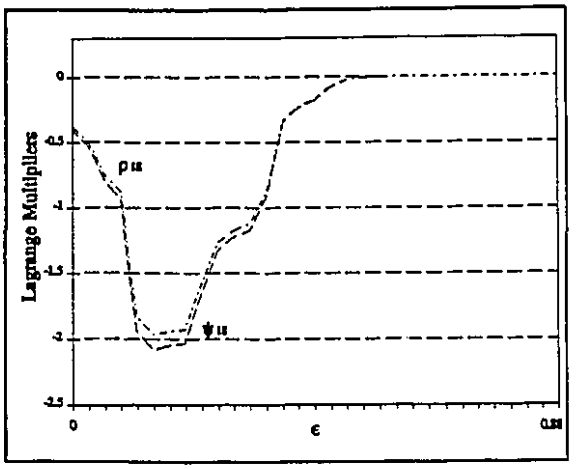

Figure 3.13.b Lagrange Multipliers.

Type 7: Release of an active inequality leads to a singular projected hessian

This is a special case of Type 2. It is assumed here that at $(\bar{x},\bar{\epsilon})$, the following conditions hold

(i)- Conditions (i)-(iv) and (vi) of critical points of type 1 are satisfied

(ii)- For all $\hat{y}$ as defined in (3.33), exactly one eigenvalue of $\hat{y}^T \frac{\partial^2 \mathcal{L}}{\partial x^2}(\bar{x},\bar{\epsilon})\hat{y}$,

vanishes.

This situation indicates that, at some $\bar{\epsilon}$, when a μ_p reaches zero and the corresponding inequality constraint is released, the problem has multiple solutions. For our problem, this situation has been found to occur at the end of the tracking process and it indicates that, although the weighting factor associated with the quadratic term of the objective function was able to force the solution of the KT equations to be optimal for all $0 \leq \varepsilon < 1$, near $\varepsilon = 1$, a new variable is released and the final optimal solution is not unique. As with critical points of type 1 and 2, this type of behaviour is typical of problems where the degrees of freedom are very high (i.e., where the number of free

variables is very large compared to the number of active constraints), and, moreover, where not all variables are present in the objective function. An example would be the optimization of the voltage profile considering all real and reactive sources free (within limits) as depicted in Figure 3.14.a-c. In these figures, we show the optimal trajectories of variable shunt compensator, $\mathbf{b}_{27}$, for $0 \leq \varepsilon \leq 1$. At $\varepsilon=1$, when $\mathbf{b}_{27}$ is released from its minimum limit, the minimum eigenvalue of the projected hessian vanishes, characterizing the existence of multiple optimal solutions. For this situation, a descent direction of improvement cannot be found (in contrast to what occurs in type 1). Figure 3.15 shows a geometrical interpretation for this type of critical point.

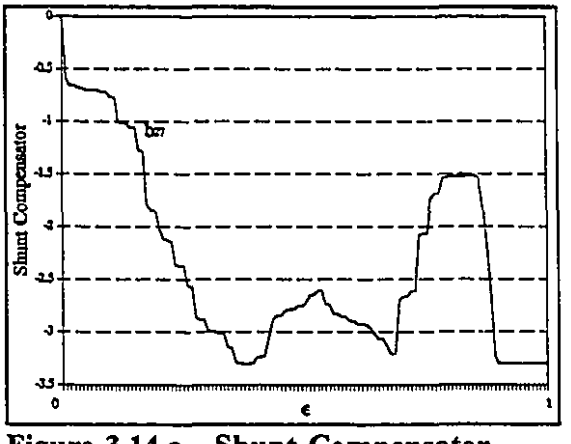

Figure 3.14.a - Shunt Compensator.

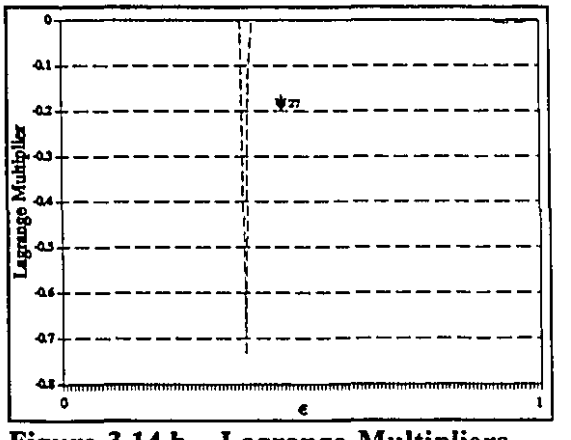

Figure 3.14.b - Lagrange Multipliers.

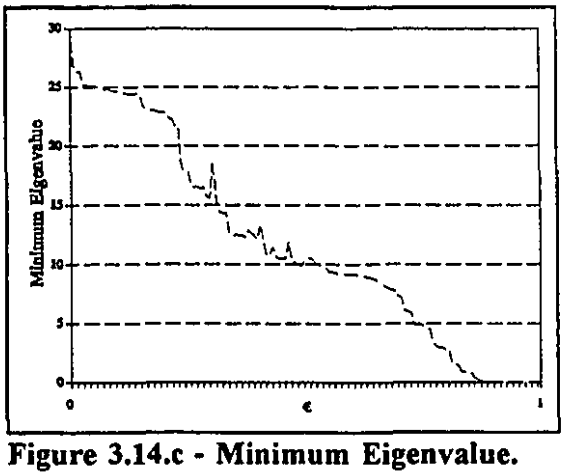

Figure 3.14.c - Minimum Eigenvalue.

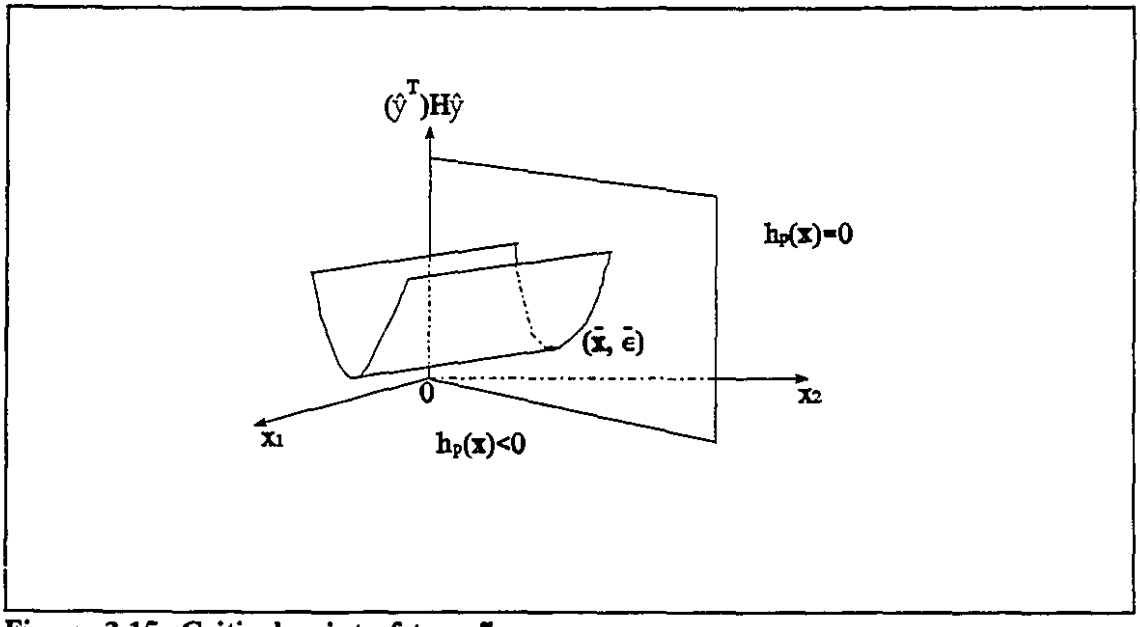

Figure 3.15- Critical point of type 7.

Table 3.1 below presents the 7 different types of critical points and the corresponding types of violation of conditions (A)-(D).

Table 3.1- Summary of critical points.

Type	Violation	Consequence
1	The Lagrange multiplier μ_p associated with an active inequality, h_p, vanishes.	After h_p is released, the projection of the hessian has one negative eigenvalue. To continue the tracking, there must be a jump to another optimal path for the same value of ε.
2	Projection of the hessian of the Lagrangian, H, on the null space of J has a vanishing eigenvalue.	W is singular. Quadratic turning point of the KT trajectories. To continue the tracking, there must be a jump to another optimal path. If the critical point occurs at ε=1, there exist multiple optimal solutions.
3	LICQ is violated; J has incomplete rank.	W is singular. Quadratic turning point of the KT trajectories. The Lagrange multipliers μ_l, $l \in L_0$ go to infinity. If the objective function is decreasing near the critical point, it might be possible to jump to another optimal path to continue the tracking. Otherwise, the feasible set becomes locally empty beyond the critical point.
4	$h_p = 0$, $p \notin L_0$. If h_p is introduced in the feasible set, the number active constraints is bigger than the number of variables.	J has incomplete rank if h_p is fixed at its limit. In case some previously fixed inequality can be released, there is a discontinuity in the optimal trajectories of the Lagrange multipliers and the tracking can proceed. Otherwise, the feasible set becomes locally empty beyond the critical point.
5	Two or more Lagrange multipliers associated with the active inequalities vanish at the same ε.	Combinatorial problem: which inequalities to release.
6	Two or more inequality constraints reach their limits at the same ε.	Combinatorial problem: which inequalities to fix at the limit.
7	Special case of type 2. μ_p=0, $p \in L_0$ and after h_p is released the projection of the hessian H has a vanishing eigenvalue.	If the critical point occur at $\varepsilon < 1$, the solution path loses optimality and it is not possible to find a direction of descent to continue the tracking. If the critical point occurs at ε=1, the problem has multiple solutions.

3.4 Stability of the Feasible Set

As can be seen by the formulation of the Parametric-OPF, each new value of the parameter ε defines a new OPF problem. As ε is varied from 0 to 1, a family of problems is created. This family connects the initial (relaxed) problem to the problem we want to solve. In the previous section, we discussed the various types of critical points of the KT equations that can occur during the tracking process and showed that some of them are related to the collapse of the feasible set. This brings us to the concept of *structural stability of the feasible set* M(ε) (equation (3.4)).

The idea behind the parameterization of the OPF and the tracking of optimal solutions is based on the fact that the problem defined for a small parameter variation is close to the problem for which we have a solution and, therefore, a numerical method is able to easily find the new optimum. In this way, even if we start from an initial point which is very distant from the final solution, by solving a sequence of problems that are close to each other (even if the initial an the final one are very different) we are able to eventually reach the optimum. The efficiency of the method, however, is entirely dependent of the fact that a small perturbation on the parameter does not cause abrupt changes in the feasible set. In other words, we want to guarantee that a problem P(ε) is equivalent to all slightly perturbed ones. If this happens, P(ε) is said to be *structurally stable*.

The importance of structural stability becomes clear in the example below. Suppose that we want to solve the following optimization problem:

$$\underset{x}{Min}\ x \tag{3.40}$$

subject to

$$\epsilon x = 0 \tag{3.41}$$

$$-10 \le x \le 10 \tag{3.42}$$

The feasible set of this problem is $M(\varepsilon)= \{0\}$ if $\varepsilon \neq 0$ and $M(\varepsilon)= [-10,10]$ if $\varepsilon = 0$. Also, the optimal solution $x(\varepsilon)=0$ if $\varepsilon \neq 0$ and $x(\varepsilon)= -10$ if $\varepsilon = 0$. Thus, as ε varies in the neighbourhood of 0 the solution changes drastically.

Although the example above illustrates a very unlikely situation, loss of stability can occur in practical applications of parametric optimization. During the solution of the Parametric-OPF, situations of loss of structural stability are known to occur, and in all cases it prevented the tracking process from continuing. A formal definition of structural stability is as follows:

Definition [Guddat et al., 1990]: The feasible set $M(\varepsilon)$ is said to be structurally stable at $(\bar{x},\bar{\epsilon})$ if there exists a neighbourhood O of $(\bar{x},\bar{\epsilon})$ such that for every $(\hat{x},\hat{\epsilon}) \in O$ the corresponding set $M(\hat{\epsilon})$ is homeomorphic with $M(\bar{\epsilon})$.

Note: Two subsets $\mathbf{A}, \mathbf{B} \subset \mathbf{R}^k$ are said to be homeomorphic if there exists a bijective mapping Φ: $\mathbf{A} \rightarrow \mathbf{B}$ (i.e., Φ is both one-to-one and onto) with both Φ and Φ^{-1} continuous.

From what is written above, it can be seen that structural stability implies that if $\bar{x} \in M(\bar{\epsilon})$, we are always able, using Φ, to reach a point $\hat{x} \in M(\hat{\epsilon})$ in the neighbourhood (and vice-versa). This is the basic supposition behind the tracking process. Without structural stability, as ε is varied from 0 to 1, we cannot reach 1 because, at some point (say ε_1), we will not be able to find a mapping that connects our present optimal solution with the optimal solution of the OPF problem defined for some $\varepsilon_2 > \varepsilon_1$.

An interesting real-life example to illustrate the concept of structural stability can be formulated for the same 2-bus system of Figure 2.1 of the previous chapter. Suppose now that we want to minimize the voltage profile deviation form 1 p.u. imposing a maximum limit on the voltage magnitude E. The problem can be formulated as

$$Min\ \frac{1}{2}[(E-1)^2 + (V-1)^2]$$

subject to

$$\frac{VE\sin\delta}{xl} = pd(\epsilon)$$

$$\frac{-V^2 + VE\cos\delta}{xl} = qd(\epsilon)$$

$$E \le 1.05$$

The new Lagrangian function is

$$\mathcal{L} = \frac{1}{2}(E-1)^2 + \frac{1}{2}(V-1)^2 + \lambda_p\left(pd(\epsilon) - \frac{VE\sin\delta}{xl}\right) + \lambda_q\left(qd(\epsilon) + \frac{V^2 - VE\cos\delta}{xl}\right) + \mu_E(E - 1.05)$$

and the KT equations are

$$\frac{\partial\mathcal{L}}{\partial\delta} = -\lambda_p\frac{VE\cos\delta}{xl} + \lambda_q\frac{VE\sin\delta}{xl} = 0 \qquad (3.43)$$

$$\frac{\partial\mathcal{L}}{\partial V} = V - 1 - \lambda_p\frac{E\sin\delta}{xl} + \lambda_q\frac{(2V - E\cos\delta)}{xl} = 0 \qquad (3.44)$$

$$\frac{\partial\mathcal{L}}{\partial E} = E - 1 - \lambda_p\frac{V\sin\delta}{xl} - \lambda_q\frac{V\cos\delta}{xl} + \mu_E = 0 \qquad (3.45)$$

$$\frac{VE\sin\delta}{xl} - pd(\epsilon) = 0,\ \forall\ \lambda_p \qquad (3.46)$$

$$\frac{-V^2 + VE\cos\delta}{xl} - qd(\epsilon) = 0, \forall \lambda_q \tag{3.47}$$

$$\mu_E(E - 1.05) = 0, \mu_E \geq 0 \tag{3.48}$$

For pd(ε) and qd(ε) defined as before, at ε=0, E=1 p.u. and V=1 p.u is the (trivial) optimal solution, therefore, by (3.48), μ_E=0 and we can solve the problem as it was previously solved. When E reaches the maximum limit (at ε=0.62 from Figure 2.2), we can continue to use equations (2.31) and (2.32) to calculate V and δ , but the expressions of the Lagrange multipliers will change. Solving (3.43) and (3.44) for λ_p and λ_q (and remembering that E=1.05) we have:

$$\lambda_p = \frac{xl(1 - V)\sin\delta}{2V\cos\delta - 1.05} \tag{3.49}$$

$$\lambda_q = \frac{xl(1 - V)\cos\delta}{2V\cos\delta - 1.05} \tag{3.50}$$

Finally, from (3.45),

$$\mu_E = 1 - 1.05 + \frac{V(1 - V)}{2V\cos\delta - 1.05} \tag{3.51}$$

The behaviour of V and E as the system load is varied can be calculated as in the previous chapter for E < 1.05, and using the algorithm above when E reaches 1.05. The optimal trajectories of V and E for this example are represented in Figure 3.16. Note that V has a sharp decrease after E is fixed at its limit. Beyond ε=0.97 the solutions of equation (2.31) are complex, which means that there are no real values for V for this load level. At this point the feasible set loses its structural stability. Note that, when E=1.05, the OPF becomes a load flow and that the structural stability limit is, in reality, the point of voltage collapse. At ε=0.97, there is a bifurcation on the optimal trajectory of V and

two different values for this voltage can be found.

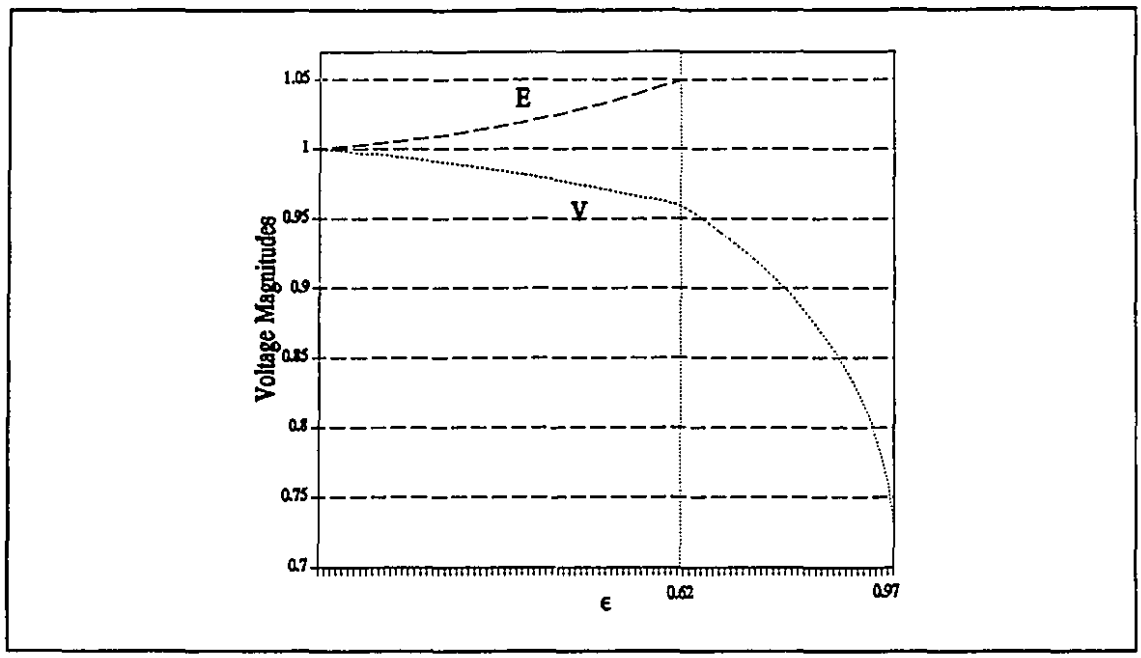

Figure 3.16- Loss of structural stability.

From the definition, we can see that structural stability of the feasible set is a local property (i.e., a set is said to be structurally stable around some specific point). Because the OPF is a non-convex problem the assurance of structural stability for all ε $\in$ [0,1] is impossible for all study cases. As we discussed in the previous section, in the optimal solution trajectories that we must track in order to reach the final solution, critical points may occur and there is no guarantee that the tracking process can continue until ϵ=1. Some of these critical points are mathematically associated with loss of structural stability; and, from a practical point of view, associated with physical limits present in the generation-transmission system under study. The question is, therefore, how to characterize loss of structural stability and how to physically interpret this loss during the tracking process. Because structural stability is a characteristic of the feasible set, we can expect that it is connected with some of the constraint qualifications presented in section (3.2.2). The MFCQ is strongly related with structural stability. If a feasible set is

compact[1], then it is structurally stable if and only if MFCQ is satisfied in all its points [Guddat et al., 1986]. Now, consider two OPF problems that are continuously connected by means of the parameter ε, $\varepsilon \in [0,1]$. All variables present in the OPF model are bounded by maximum and minimum limits, therefore the feasible set $M(\varepsilon)$ for a specified ε is bounded. In addition, by the form of the constraints, it can be seen that the feasible set $M(\varepsilon)$ is closed. Then, we can say that there is a compact set $\boldsymbol{A}$ containing the feasible set $M(\varepsilon)$ for all $\varepsilon \in [0,1]$. Now, if MFCQ is satisfied at every point of $M(\varepsilon)$ for all $\varepsilon \in [0,1]$, then the final feasible set $M(1)$ is homeomorphic with $M(0)$. Conversely, if the topological structure of the set $M(1)$ differs from $M(0)$, then, for some $\varepsilon \in [0,1]$, at some $\mathbf{x} \in M(\varepsilon)$, MFCQ must be violated.

To ensure that $M(0)$ is structurally stable, consider the following arguments. In the Parametric-OPF problem (equations (3.17)-(3.22)), at $\varepsilon=0$ all inequality constraints are relaxed, thus, to guarantee that the initial feasible set $M(0)$ is stable, our initial guess $\mathbf{x}^0$ must be such that the jacobian of the equality constrains has complete rank and that there exists a ϖ such that $\boldsymbol{J}(\mathbf{x}^0,0).\varpi = \mathbf{0}$. The first condition implies that the jacobian of the energy balance equations for the load buses is of full rank (see OPF model in Appendix A), a condition which is normally satisfied if $\mathbf{x}^0$ is a typical load flow solution. The second condition is satisfied by construction because, initially, the number of variables in the OPF model is normally much bigger that the number of the equality constraints (remember that no inequality is active at this point). As the tracking progresses towards 1, however, there is no guarantee that MFCQ will be satisfied. Since near every $(\bar{x},\bar{\epsilon})$ where conditions (A)-(D) are fulfilled, there is an optimal solution of the Parametric-OPF (see section 3.2.1), then the only way in which the feasible set loses its stability is if some of the critical points described above occur. It has been demonstrated that only at points of type 3 or type 4 (where all μ_l in (3.37) are greater than zero and, consequently, no inequality can be released) is the feasible set not stable [Jongen et al., 1986, (b)]. This is not surprising since both critical points occur when the active feasible set does not have a good structure. The example discussed when we presented type 3 of critical points is,

[1] A set $\boldsymbol{A}$ is said to be closed if every point that is arbitrarily close to $\boldsymbol{A}$ is a member of $\boldsymbol{A}$. A set $\boldsymbol{A}$ is compact if it is both closed and bounded (that is, if it is closed and contained within a sphere of finite radius) [Luenberger, 1984].

therefore, an example of loss of structural stability, whereas in the example of type 4 stability is preserved. These examples as well as the last one give a good idea of what loss of structural stability means in the physical model. It does not mean loss of feasibility (in the strict sense) but, as in the load flow model and its so-called point of voltage collapse, loss of stability indicates that operation (optimal or not) near such a point is not stable to parameter variations.

The characterization of the regions where the changes in the feasible set with respect to parameter variations are continuous (regions of structural stability) can be of great importance. To see this, take for example the behaviour of the optimal solution of the OPF problem as the system load varies. If the optimal operating point is near an unstable point, any variation on the load level will cause an abrupt change in the optimal operating point which cannot be accomplished in the operation. Also, in special cases, the variation of the load can lead even to the nonexistence of an optimal or feasible solution. In an on-line environment the assurance of structural stability is vital to guarantee a reliable operation of the power system.

Although there exists a significant amount of publications concerning structural stability, most of them are theoretical. Researchers started to introduce some of the theoretical results in non-linear optimization algorithms in the last decade (see, for example, [Fiacco, 1983]), however, these early implementations included mostly sensitivity analysis. Only recently, with the study of critical points in parametric optimization, some of the theory regarding structural stability could be formalized in a more applicable manner.

Recently, there have been some studies of the sensitivities of the OPF solutions to small changes in bus loads, flow limits, bus voltage limits and other OPF constraints [Venkatesh et al., 1992]. In addition, the question of infeasibility of the OPF problem has been gaining considerable attention in the past years because the recognition of unfeasible cases is a necessary characteristic of any OPF package [Stott et al., 1987; Sun et al., 1988]. Nevertheless, a systematic study of OPF feasibility and structural stability has not been done yet. This is a little surprising, since there have been many studies concerning

concerning the bifurcation (voltage collapse) regions of the load flow solutions, but, from the study of critical points, it is easily seen that the study of stability regions for the OPF problem is not trivial. Nevertheless, the discussion of structural stability raises an interesting question regarding the optimal operation of a power system: is it more desirable to establish a "structural stability region" or a "feasibility region" for the OPF problem?

3.5 Conclusion

The theory associated with the Parametric-OPF is both rich and difficult. The parameterization provides means for a greater understanding of the OPF problem. At the same time, it highlights the difficulties associated with the problem itself, being able to differentiate the obstacles that have been encountered by researchers for the solution of the OPF. The OPF continues to be a difficult problem and this is reflected in the various kinds of "critical points" of the optimal solution trajectories. In spite of all the difficulties associated with the process of tracking an optimal solution, the discussion presented throughout this chapter gives us a basis to draw important conclusions concerning the approach:

(i)- The Parametric-OPF allows us, in principle, to solve the OPF problem from any initial solution and to exactly track a pre-specified load curve;

(ii)- The parameterization provides means of solving the OPF problem in a systematic way, without using heuristics to find the optimal active set;

(iii)- The approach can give us a very good understanding of the different kinds of problem that exist in the OPF solution, and, more importantly, permits the analysis of cases where an optimal solution cannot be found;

(iv)- Since the method is able to differentiate the various causes for the interruption of the tracking process, it gives us means of suggesting solutions for some of the critical points;

(v)- In particular, the approach permits the definition of regions of *structural instability* for the OPF problem, which is a generalization of the concept of voltage collapse region for the classical load flow problem. This has special importance during the load tracking, since it can define a (local) maximum loadability limit for the system under study, thus providing valuable information about the system "weak points", where improvements (e.g. new reactive sources) must be introduced.

The theory presented in this chapter, therefore, demonstrates that the parametric approach, can be very useful for the solution and analysis of the OPF problem. In view of the potential of the approach, an algorithm for the solution of the Parametric-OPF was implemented. The details of the implementation are discussed in the next chapter.

CHAPTER 4

PARAMETRIC-OPF SOLUTION ALGORITHM

4.1 Introduction

The solution algorithm for the Parametric-OPF was formulated mainly with the intent of systematically controlling the changes in the optimal feasible set, thus making it possible to exactly track the solution trajectories and to detect critical points. In a summarized manner, after the initialization is carried out (transforming the initial solution guess into an optimal solution) the Parametric-OPF algorithm can be subdivided into two main steps: (i) the increment on the parameter (creating a new OPF problem) and (ii) the solution of this newly formulated OPF. The performance of the algorithm, therefore, depends on a good implementation of the two steps. A detailed description of the methodology is given in this chapter.

From all aspects involved in the tracking process discussed in the previous chapter, it can be easily seen that the parametric approach is able to very clearly identify, differentiate and analyze the main difficulties that have been encountered by researchers in solving the OPF, namely variations of: loss of optimality, loss of feasibility and ill-conditioning. These difficulties are reflections of the different types of critical points of the optimal trajectory. Up to now, no solution has been proposed for all the types of critical points that may appear during the tracking process. Therefore, solution algorithms for the critical points are not included in the implementation of the method and, as a consequence, the Parametric-OPF algorithm is not able to arrive at the optimal solution in all cases. Nevertheless, we are able to detect multiple optimal solutions or even reasons for non-convergence of the method by analyzing the different critical points.

4.2 Detailed Modelling and Optimality Conditions

The parametric algorithm implemented in this thesis is based on the tracking of the homotopy function defined by the KT conditions for the Parametric-OPF. In order to better explain the implementation, we will introduce a more detailed formulation for the Parametric-OPF where the functional inequalities and limits on the decision variables are represented separately.

Let **I** denote the index set of decision variables and **N** the index set of functional inequalities. Additionally, let $\mathbf{I}_0(\mathbf{x},\varepsilon)$ be the set of active limits on decision variables and $\mathbf{N}_0(\mathbf{x},\varepsilon)$ be the set of active functional inequalities. Throughout the derivation, we will call a variable which lies strictly within its limits, $\mathbf{x}_i^{min} < \mathbf{x}_i < \mathbf{x}_i^{max}$, $i \in \mathbf{I}$ a *free variable*. Let $\mathbf{I}_f(\mathbf{x},\varepsilon)$ be the set of free variables and $\mathbf{N}_f$ be the set of inequality constraints not at the limit. These index sets will be used to derive the Parametric-OPF algorithm.

4.2.1 Problem Definition and Optimality Conditions for Phase I

In Phase I, it always possible to define a vector $\mathbf{x}^0$ which is inside its operational limits. To ensure that the functional equalities and inequalities are satisfied at $\mathbf{x}^0$ an appropriate parameterization is implemented as discussed below. Note that $\mathbf{x}^0$ is already within its limits and does not need to be included in the parameterization. Similarly, the parameterization is such that there are no binding functional inequalities. The Lagrange multiplier associated with the equality constraints λ^0 can assume any value.

Thus, for a pair $(\mathbf{x}^0,\lambda^0)$ which satisfies the conditions above, we define the Parametric-OPF for Phase I as,

$$Min\ c(x,\epsilon) \tag{4.1}$$

subject to

$$g_k(x,\epsilon) = g_k(x) - (1 - \epsilon)g_k(x^0) = 0,\ k \in K \tag{4.2}$$

$$h_n(x,\epsilon) = h_n(x) - (1 - \epsilon)\Delta h_n \le 0,\ n \in N \tag{4.3}$$

$$x_i^{min} \le x_i \le x_i^{max},\ i \in I \tag{4.4}$$

where $c(\mathbf{x},\varepsilon)$ is defined in equations (3.20) and (3.21) of the previous chapter, $\mathbf{h}_n(\mathbf{x},\varepsilon) \in \mathbb{R}^{(1 \times nv+1)}$, $n \in \mathbf{N}$, represents the functional inequalities (the reactive generation and the active power flows) (see Appendix A for a detailed definition of all problem variables and constraints). The parameter ε assumes values from 0 to 1.

Splitting equation (4.4) into two inequalities $\mathbf{x} \ge \mathbf{x}^{min}$ and $\mathbf{x} \le \mathbf{x}^{max}$, and associating a Lagrange multiplier vector, ν, with this set of inequalities, we can represent the upper and lower limits on $\mathbf{x}$ together in the Lagrangian function of the problem. Note that, at the optimum, the sign of ν_i must be + or - depending on whether $\mathbf{x}_i$ is at the maximum or minimum limit. Thus, the Lagrangian function of the problem (4.1)-(4.4) can be defined as

$$\mathcal{L} = c(x,\epsilon) + \sum_{k \in K} \lambda_k g_k(x,\epsilon) + \sum_{n \in N_0} \zeta_n h_n(x,\epsilon) + \sum_{i \in I} \nu_i (x_i - x_i^{lim}) \tag{4.5}$$

where $\mathbf{x}^{lim}=[(\mathbf{x}^{min})^T,(\mathbf{x}^{max})^T]^T$ and ζ is the Lagrange multiplier associated with the active functional inequalities (initially, the set of active functional inequalities is empty).

The KT conditions for the Parametric-OPF model of Phase I are, then:

$$\frac{\partial \mathcal{L}}{\partial x} = \frac{\partial c}{\partial x}(x) + \sum_{k \in K} \lambda_k \frac{\partial g_k}{\partial x}(x) + \sum_{n \in N_0} \zeta_n \frac{\partial h_n}{\partial x}(x) + \nu - (1 - \epsilon)\left\{\frac{\partial c}{\partial x}(x^0) + \sum_{k \in K} \lambda_k{}^0 \frac{\partial g_k}{\partial x}(x^0) - w(x - x^0)\right\} = 0 \tag{4.6}$$

$$\frac{\partial \mathcal{L}}{\partial \lambda_k} = g_k(x) - (1 - \epsilon) g_k(x^0) = 0, \; k \in K \tag{4.7}$$

$$\frac{\partial \mathcal{L}}{\partial \zeta_n} = h_n(x) - (1 - \epsilon) \Delta h_n = 0, \; n \in N_0 \tag{4.8}$$

$$\frac{\partial \mathcal{L}}{\partial \nu_i} = x_i - x_i^{\lim} = 0, \; i \in I_0 \tag{4.9}$$

$$h_n(x) < 0, \; n \in N_f \tag{4.10}$$

$$x_i < x_i^{\lim}, \; i \in I_f \tag{4.11}$$

$$\zeta_n \geq 0, \; n \in N_0 \tag{4.12}$$

$$\left.\begin{array}{l} \nu_i = 0, \; i \in I_f \\ \nu_i \geq 0 \; for \; x_i = x_i^{\max} \\ \nu_i \leq 0 \; for \; x_i = x_i^{\min} \end{array}\right\} i \in I_0 \tag{4.13}$$

4.2.2 Problem Definition and Optimality Conditions for Phase II

In the same way that it was done for Phase I, a new formulation for Phase II can

be introduced. Since we have an optimal active feasible set at the end of Phase I, the inequality constraints for Phase II do not have to have their limits parameterized. Let $\mathbf{d}^0$ be the load level during Phase I. Let $\mathbf{x}^0$ be the associated optimal solution at the end of Phase I, that is, for ε=1, and let $\Delta\mathbf{d}$ be the difference between $\mathbf{d}^0$ and the next load level[1]. The Parametric-OPF for this case is defined as

$$Min\ c(x,\epsilon) \tag{4.14}$$

subject to

$$g_k(x,d(\epsilon)) = g_k(x,d^0+ \epsilon\Delta d) = 0,\ k \in K \tag{4.15}$$

$$h_n(x,d(\epsilon)) = h_n(x,d^0 + \epsilon\Delta d) \le 0,\ n \in N \tag{4.16}$$

$$x_i^{\min} \le x_i \le x_i^{\max},\ i \in I \tag{4.17}$$

where $c(\mathbf{x},\varepsilon)$ is defined as in (3.26).

The Lagrangian function for the problem (4.14)-(4.17) can be written as:

$$\mathcal{L} = c(x,\epsilon) + \sum_{k\in K} \lambda_k g_k(x,d(\epsilon)) + \sum_{n\in N_0} \zeta_n h_n(x,d(\epsilon)) + \sum_{i\in I} \nu_i(x_i - x_i^{\lim}) \tag{4.18}$$

Substituting $c(\mathbf{x},\varepsilon)$ from equation (3.26), the KT conditions can be expressed as

[1] In the implementation of the Parametric-OPF for Phase II, it was assumed linear trajectories for the system loads. However, trajectories that are nonlinear in ε can also be easily implemented.

$$\frac{\partial \mathcal{L}}{\partial x} = \frac{\partial c}{\partial x}(x) + (1 - \epsilon)w(x - x^0) + \sum_{k \in K} \lambda_k \frac{\partial g_k}{\partial x}(x, d^0 + \epsilon \Delta d) + \sum_{n \in N_0} \zeta_n \frac{\partial h_n}{\partial x}(x, d^0 + \epsilon \Delta d) + \nu = 0 \tag{4.19}$$

$$\frac{\partial \mathcal{L}}{\partial \lambda_k} = g_k(x, d^0 + \epsilon \Delta d) = 0, \; k \in K \tag{4.20}$$

$$\frac{\partial \mathcal{L}}{\partial \zeta_n} = h_n(x, d^0 + \epsilon \Delta d) = 0, \; n \in N_0 \tag{4.21}$$

$$\frac{\partial \mathcal{L}}{\partial \nu_i} = x_i - x_i^{\lim} = 0, \; i \in I_0 \tag{4.22}$$

$$h_n(x, d^0 + \epsilon \Delta d) < 0, \; n \in N_f \tag{4.23}$$

$$x_i < x_i^{\lim}, \; i \in I_f \tag{4.24}$$

$$\zeta_n \geq 0, \; n \in N_0 \tag{4.25}$$

$$\left.\begin{array}{l} \nu_i = 0, \; i \in I_f \\ \nu_i \geq 0 \; for \; x_i = x_i^{\max} \\ \nu_i \leq 0 \; for \; x_i = x_i^{\min} \end{array}\right\} i \in I_0 \tag{4.26}$$

The models defined by (4.1)-(4.4) and (4.14)-(4.17) will be used to derive the Parametric-OPF algorithm implemented in this thesis. Because these models are only slightly different, the solution algorithms implemented for Phase I and Phase II do not vary considerably.

The KT conditions for both cases can be simplified if we substitute the decision variables at their limit, $\mathbf{x}_i=\mathbf{x}_i^{lim}$, directly into equations (4.6)-(4.8) for Phase I and (4.19)-(4.21) for Phase II. In this way, constraints (4.9) and (4.22) are implicitly satisfied.

4.3 Basic Solution Strategy

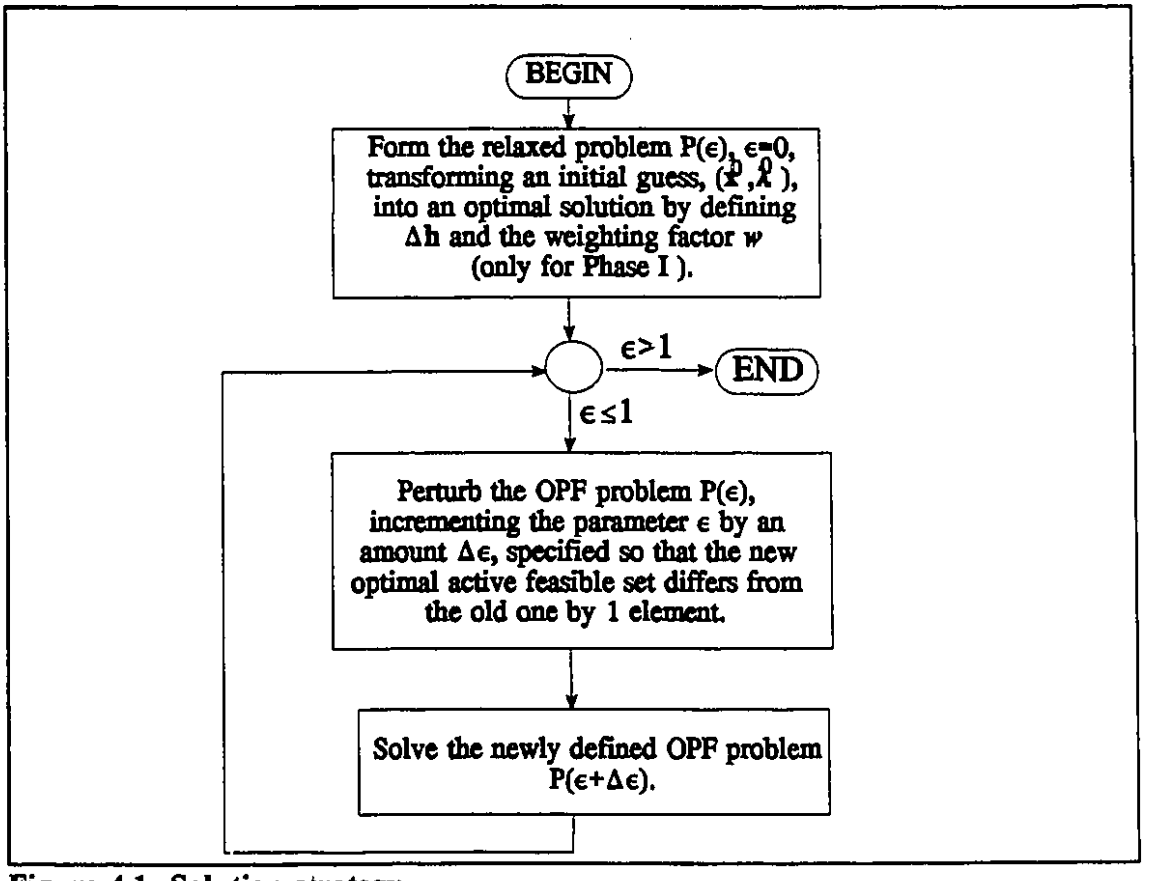

Figure 4.1- Solution strategy.

The formulation of the KT conditions depends on the knowledge of the active sets $\mathbf{N}_0(\mathbf{x},\varepsilon)$ and $\mathbf{I}_0(\mathbf{x},\varepsilon)$ Although for Phase I, at $\varepsilon=0$, these active sets are empty, they change throughout the tracking process as ε is increased. The values of ε where these changes occur (break-points) must be determined so that the KT equations can be formulated and solved. Therefore, in addition to a method for solving the KT equations, the Parametric-OPF algorithm (both for Phase I and II) must have a strategy to find the break-points. As a result, the methodology used here can be decomposed into three main steps for Phase

I and, since the initialization is not necessary, two main steps for Phase II (see Figure 4.1). The overall performance of the method depends, therefore, on the efficient solution of the problems related to the different steps. Each step, namely, initialization, increment of the parameter, and solution of the optimality conditions is discussed separately in the following sections.

4.3.1 The Initialization

To initialize the Parametric-OPF algorithm four quantities need to be specified: $\mathbf{x}^0$, λ^0, $\Delta\mathbf{h}$ and the weighting factor w.

Although any $\mathbf{x}^0$ that satisfies $\mathbf{x}^{min} < \mathbf{x} < \mathbf{x}^{max}$ in principle can be used as an initial guess for the Parametric-OPF solution, the choice of this vector will greatly affect the performance of the methodology because, basically, this initial choice will define a parametric problem that, at ε=0, can be "far" or "close" to the original problem to be solved (at ε=1). As a general rule, the closer $\mathbf{x}^0$ is to solving the load balance equations of the original problem, the better. A close initial guess will translate into a smaller number of changes in the optimal active set and, as a consequence, into a reduced computational effort. In fact, in the tests made, a good initial choice for $\mathbf{x}$ could decrease the number of changes in the active set by as much as half.

The influence of the Lagrange multipliers λ^0 on the performance of the algorithm, on the other hand, was found to be less significant than the influence of $\mathbf{x}^0$. This is an interesting point since the choice of the Lagrange multipliers can affect considerably the convergence characteristics of other optimization methods such as dual methods [Rehn et al., 1989; Santos Jr. et al., 1988]. Different initial values for λ^0 were tested (see section 6.2.2). It was found that a reasonable initialization would be to set the Lagrange multipliers associated with the active power balance equations equal to the average of the generation incremental cost and the Lagrange multipliers associated with the reactive power balance equal to 1. However, other values for λ^0 can also be used without compromising the convergence of the Parametric-OPF.

In practice, $\Delta\mathbf{h}$ is usually selected to be the same for every violated functional inequality and equal to the maximum violation on the inequality limits at ε=0. The choice of $\Delta\mathbf{h}$ does not significantly affect the performance of the algorithm, therefore other choices of $\Delta\mathbf{h}$ are possible. For example, for every $n \in N_0$, $\Delta\mathbf{h}_n$ can be made equal to $\mathbf{h}_n(\mathbf{x}^0)$ minus a constant which is equal to the average of the maximum and minimum limits of $\mathbf{h}_n(\mathbf{x})$.

Finally, the weighting factor w must be carefully chosen because it reshapes the objective function by adding to it a quadratic term depending on the deviation of the decision variables from their initial values. A large w, therefore, will keep $\mathbf{x}$ close to $\mathbf{x}^0$ until ε is very close to 1 and, as a consequence, all the changes in the active set necessary for optimization will occur in a narrow interval of ε negatively impacting on the convergence of the algorithm.

4.3.2 Step I - Incrementing the Parameter ε

Since we are following the optimal solution trajectory from one break-point to the next starting from ε=0, we basically increment the parameter ε until the first violation occurs among all inactive inequalities or on the sign of the Lagrange multipliers associated to the active inequalities. As a consequence, after the increment in ε, the new OPF will have a known optimal active set and can be easily solved by any optimization method.

Although the approach of incrementing ε until the next violation occurs is a very conservative (and, therefore, slow) one, the choice of such an approach was based on the fact that it is difficult to know a priori the effect that a newly fixed inequality constraint will have in the non-active inequalities. More importantly, if we want to analyze causes for an eventual non-convergence of the method, the precise tracking of the changes in the optimal active set is necessary. Thus, the computational speed was compromised in order to built a tool that is able to systematically find the changes in the active feasible set and is more suitable for analysis studies.

The two methods used in this work to find the next violated inequality limit are based on:

(i)- Binary Search.
(ii)- Linear Prediction.

Binary Search

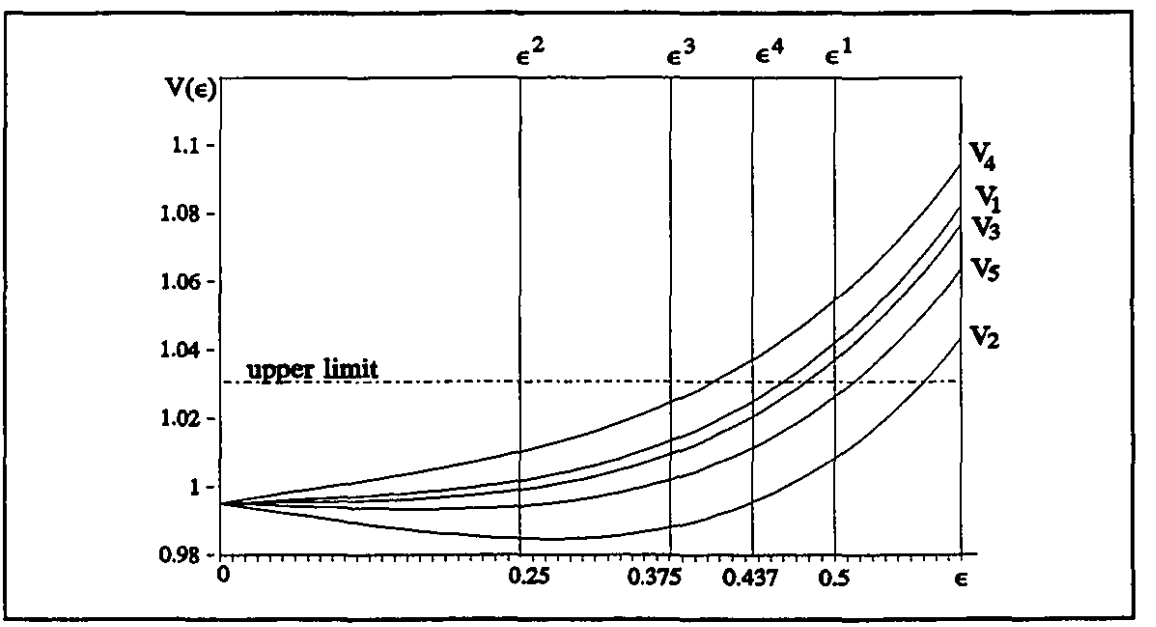

Figure 4.2- Binary search mechanism.

The binary search mechanism is the simplest way found to predict changes in the active set. The algorithm is quite straightforward and can be explained with the help of Figure 4.2 above showing five typical optimal trajectories as a function of ϵ. These five voltage magnitudes are from the same 5-bus system example presented in chapter 3 (Figure 3.5), all of which have a maximum limit of 1.03 p.u.. The sequence of vertical lines denoted by ϵ^1 to ϵ^4 indicates the values of ϵ tried by the binary search to localize the first break point. For each value of ϵ, the optimality conditions (4.6)-(4.8) are solved and the number of violations noted. When there is only 1 violation, this is fixed at its limit. Observe that it is not necessary to find the exact location of the break-point to stop the binary process, but simply to ensure that

only 1 violation exists. In this example, the first break-point occurs near $\epsilon = 0.4$ and requires that V_4 be fixed at the upper limit.

Figure 4.3 illustrates, for the same example, the optimal trajectories (dotted lines) based on the initial active set, $\mathbf{I}_0(\mathbf{x},0)$, and how these trajectories drastically change when one variable is fixed and the active set is modified to $\mathbf{I}_0^0,\ldots,\mathbf{I}_0^3$ (solid lines). This figure also shows the complete optimal trajectory with all the break-points included. One can observe, for example, that if the initial active set were maintained until $\epsilon = 1$, then several voltages would have violated the upper limit of 1.03 p.u. An aggressive but non-systematic approach could have fixed all violations at $\epsilon = 1$, however, from the Figure, we see that this does not correspond to the optimal solution. In fact, the optimum requires that only three of the voltages be fixed at $\epsilon = 1$.

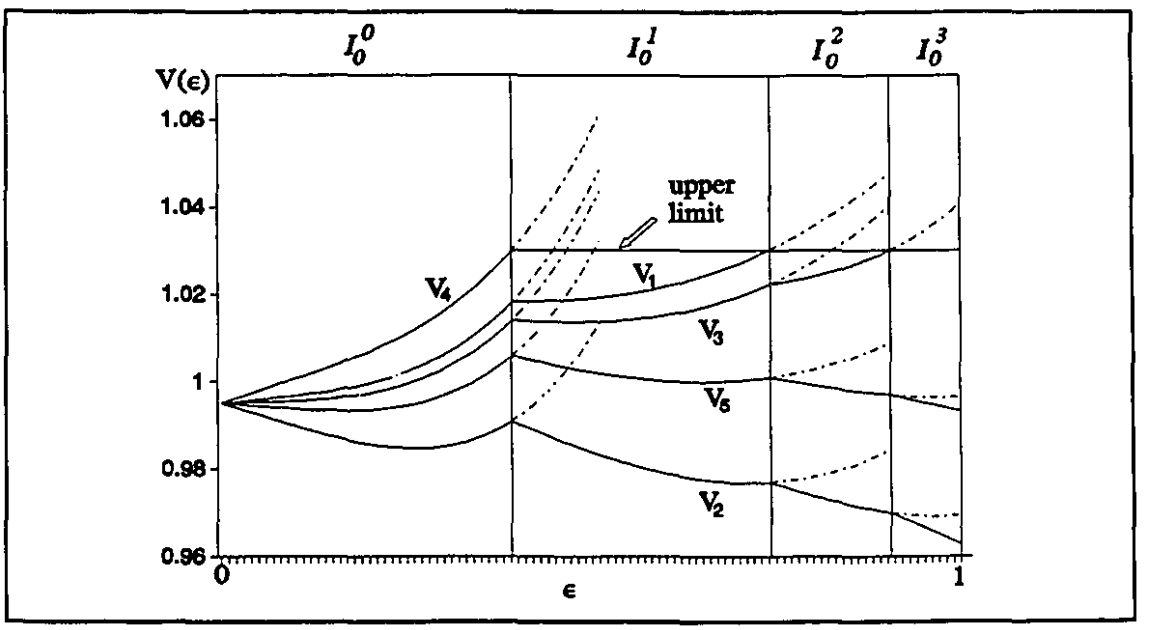

Figure 4.3- Optimal trajectories with break-points.

The binary search mechanism is very simple to implement and, in many cases, quite efficient. However, if the number of evaluations of the system of K'T equations to check the inequality limits is very large, the binary process will be considerably slow. For this reason, a second method of finding the optimal active set changes was developed based on linear approximations of the optimal trajectories.

Linear Prediction

In this method, a linear approximation of the optimal solution trajectories is used to find the next constraint to be fixed at the limit or the next active constraint to be released. First of all, a linear approximation of the free variables and the Lagrange multipliers of the equalities and active functional inequalities must be obtained. For this, let the function $\Lambda(z,\epsilon)$ be defined as

$$\Lambda(z,\epsilon) = \left[\frac{\partial^T \mathcal{L}}{\partial x}(z,\epsilon) , \frac{\partial^T \mathcal{L}}{\partial \lambda}(z,\epsilon) , \frac{\partial^T \mathcal{L}}{\partial \zeta_{N_0}}(z,\epsilon) , \frac{\partial^T \mathcal{L}}{\partial \nu_{I_0}}(z,\epsilon) \right]^T = 0 \quad \textbf{(4.27)}$$

that is, (4.27) corresponds to system (4.6)-(4.9) for Phase I or system (4.19)-(4.22) for Phase II. In (4.27) $z = [x^T, \lambda^T, (\zeta_{N_0})^T, (\nu_{I_0})^T]^T$, with $\zeta_{N_0} = \{ \zeta_n, \forall n \in N_0 \}$ and $\nu_{I_0} = \{ \nu_i, \forall i \in I_0 \}$.

The last term of (4.27), $\frac{\partial \mathcal{L}}{\partial \nu_{I_0}}$, can be implicitly represented by replacing x_i by x_i^{lim}, for all $i \in I_0$ in the expressions of all other terms of the equation. Thus, (4.27) can be rewritten as

$$\Lambda(z,\epsilon) = \left[\frac{\partial^T \mathcal{L}}{\partial x}(z,\epsilon) , \frac{\partial^T \mathcal{L}}{\partial \lambda}(z,\epsilon) , \frac{\partial^T \mathcal{L}}{\partial \zeta_{N_0}}(z,\epsilon) \right]^T = 0 \quad \textbf{(4.28)}$$

In (4.28) the linear prediction must be made only for the free variables. By (4.13) (or (4.26) for Phase II) the Lagrange multipliers associated with the free variables $\nu_{I_f} = \{ \nu_i, \forall i \in I_f \}$ are equal to zero. Thus, let $z_f = [(x_{I_f})^T, (\lambda)^T, (\zeta_{N_0})^T]^T$, where $x_{I_f} = \{ x_i, \forall i \in I_f \}$. Define

$$\Lambda(z_f,\epsilon) = \left[\frac{\partial^T \mathcal{L}}{\partial x_{I_f}}(z,\epsilon) , \frac{\partial^T \mathcal{L}}{\partial \lambda}(z,\epsilon) , \frac{\partial^T \mathcal{L}}{\partial \zeta_{N_0}}(z,\epsilon) \right]^T \tag{4.29}$$

A linear approximation for $\Lambda(z_f, \epsilon)$ at a point $(\bar{z},\bar{\epsilon})$ can, then, be written as,

$$\Lambda(\bar{z}_f+\Delta z_f,\bar{\epsilon}+\Delta\epsilon) = \Lambda(\bar{z}_f,\bar{\epsilon}) + \left[\frac{\partial \Lambda}{\partial z_f}(\bar{z}_f,\bar{\epsilon}) , \frac{\partial \Lambda}{\partial \epsilon}(\bar{z}_f,\bar{\epsilon}) \right] \begin{bmatrix} \Delta z_f \\ \Delta\epsilon \end{bmatrix} = 0 \tag{4.30}$$

Since, for the optimal trajectories, $\Lambda(\bar{z}_f,\bar{\epsilon}) = 0$ and $\Lambda(\bar{z}_f+\Delta z,\bar{\epsilon}+\Delta\epsilon) = 0$,

$$\frac{\partial \Lambda}{\partial z_f}(\bar{z}_f,\bar{\epsilon})\Delta z_f + \frac{\partial \Lambda}{\partial \epsilon}(\bar{z}_f,\bar{\epsilon})\Delta\epsilon = 0 \tag{4.31}$$

The increment on z_f, Δz_f, is, thus,

$$\Delta z_f = e\,\Delta\epsilon \tag{4.32}$$

where

$$e = -\left[\frac{\partial \Lambda}{\partial z_f}(\bar{z}_f,\bar{\epsilon}) \right]^{-1} \frac{\partial \Lambda}{\partial \epsilon}(\bar{z}_f,\bar{\epsilon}) \tag{4.33}$$

The derivative of $\Lambda(\bar{z}_f,\bar{\epsilon})$ with respect to z_f is equal to $W(\bar{z}_f,\bar{\epsilon})$ defined in equation (4.50) for Phase I or (4.53) for Phase II, whereas $\frac{\partial \Lambda}{\partial \epsilon}(\bar{z}_f,\bar{\epsilon})$ is given by the derivative of equations (4.6)-(4.8) (or (4.19)-(4.21), for Phase II) with respect to ϵ, which is given by (4.52), for Phase I, or (4.55), for Phase II.

Equation (4.32) is valid for the decision variables x_i $i \in I_f$, the Lagrange multipliers associated with the equality constraints, λ_k, $k \in K$, and active functional

inequalities, ζ_n, $n \in N_0$. To obtain the linear prediction for the Lagrange multipliers ν_i, $i \in I_0$, we must use the KT conditions as defined for the variables fixed at the limits. For Phase I we have, from equation (4.6):

$$\nu_{I_0} = -\left\{\frac{\partial c}{\partial x_{I_0}}(x) + \sum_{k\in K}\lambda_k\frac{\partial g_k}{\partial x_{I_0}}(x) + \sum_{n\in N_0}\zeta_n\frac{\partial h_n}{\partial x_{I_0}}(x) - (1-\epsilon)\left\{\frac{\partial c}{\partial x_{I_0}}(x^0) + \sum_{k\in K}\lambda_k^0\frac{\partial g_k}{\partial x_{I_0}}(x^0) - w(x_{I_0}-x_{I_0}^0)\right\}\right\} \tag{4.34}$$

Similarly, for Phase II, from equation (4.19),

$$\nu_{I_0} = -\left\{\frac{\partial c}{\partial x_{I_0}}(x) + \sum_{k\in K}\lambda_k\frac{\partial g_k}{\partial x_{I_0}}(x, d^0+\epsilon\Delta d) + \sum_{n\in N_0}\zeta_n\frac{\partial h_n}{\partial x_{I_0}}(x, d^0+\epsilon\Delta d) + (1-\epsilon)w(x_{I_0}-x_{I_0}^0)\right\} \tag{4.35}$$

where $\nu_{I_0} = \{\nu_i, \forall i \in I_0\}$,

Since $\nu_{I_0} = \nu_{I_0}(x, \lambda, \zeta_{N_0}, \epsilon)$, a linear approximation for ν_i, $i \in I_0$, for both Phases I and II, will be given by

$$\Delta\nu_{I_0} = \left[\left(\frac{\partial\nu_{I_0}}{\partial x_{I_f}}\right)\frac{dx_{I_f}}{d\epsilon} + \left(\frac{\partial\nu_{I_0}}{\partial\lambda}\right)\frac{d\lambda}{d\epsilon} + \left(\frac{\partial\nu_{I_0}}{\partial\zeta_{N_0}}\right)\frac{d\zeta_{N_0}}{d\epsilon} + \frac{\partial\nu_{I_0}}{\partial\epsilon}\right]\Delta\epsilon \tag{4.36}$$

where the derivatives of ν are taken with respect to the free decision variables x_i, $i \in I_f$, λ_k, $k \in K$ and ζ_n, $n \in N_0$. More explicitly, equation (4.36) can be written as,

$$\Delta v_{I_0} = r\Delta\epsilon \tag{4.37}$$

where, for Phase I,

$$r = -\left[\frac{\partial^2 \mathcal{L}}{\partial x_{I_0}\partial x_{I_f}}(\bar{z},\bar{\epsilon}) \;,\; \frac{\partial^T g}{\partial x_{I_0}}(\bar{x},\bar{\epsilon}) \;,\; \frac{\partial^T h_{N_0}}{\partial x_{I_0}}(\bar{x},\bar{\epsilon})\right] e + \frac{\partial^T g}{\partial x_{I_0}}(x^0) + \frac{\partial^T h_{L_0}}{\partial x_{I_0}}(x^0) - w(x_{I_0} - x^0_{I_0}) \tag{4.38}$$

with

$$\frac{\partial^2 \mathcal{L}}{\partial x_{I_0}\partial x_{I_f}}(\bar{z},\bar{\epsilon}) = \frac{\partial^2 c}{\partial x_{I_0}\partial x_{I_f}}(\bar{x}) + (1-\bar{\epsilon})w + \frac{\partial^2 (g^T\lambda)}{\partial x_{I_0}\partial x_{I_f}}(\bar{x}) + \frac{\partial^2 (h_{N_0}{}^T\zeta_{N_0})}{\partial x_{I_0}\partial x_{I_f}}(\bar{x}) \tag{4.39}$$

On the other hand, for Phase II,

$$r = -\left[\frac{\partial^2 \mathcal{L}}{\partial x_{I_0}\partial x_{I_f}}(\bar{z},d(\bar{\epsilon})) \;,\; \frac{\partial^T g}{\partial x_{I_0}}(\bar{x},d(\bar{\epsilon})) \;,\; \frac{\partial^T h_{N_0}}{\partial x_{I_0}}(\bar{x},d(\bar{\epsilon}))\right] e - w(x_{I_0} - x^0_{I_0}) \tag{4.40}$$

with

$$\frac{\partial^2 \mathcal{L}}{\partial x_{I_0}\partial x_{I_f}}(\bar{z},d(\bar{\epsilon})) = \frac{\partial^2 c}{\partial x_{I_0}\partial x_{I_f}}(\bar{x}) + (1-\bar{\epsilon})w + \frac{\partial^2 (g^T\lambda)}{\partial x_{I_0}\partial x_{I_f}}(\bar{x},d(\bar{\epsilon})) + \frac{\partial^2 (h_{N_0}{}^T\zeta_{N_0})}{\partial x_{I_0}\partial x_{I_f}}(\bar{x},d(\bar{\epsilon})) \tag{4.41}$$

Note that e in (4.38) and (4.40) is obtained from equation (4.33).

Finally, a linear approximation for the functional inequalities not fixed at the limit can be written as

$$h_{N_f}(\bar{x} + \Delta x, \bar{\epsilon} + \Delta \epsilon) = h_{N_f}(\bar{x}, \bar{\epsilon}) + s\Delta \epsilon \tag{4.42}$$

where

$$s = \left(\frac{\partial h_{N_f}}{\partial x_{I_f}}(\bar{x}, \bar{\epsilon}) \right) \frac{dx_{I_f}}{d\epsilon} + \frac{\partial h_{N_f}}{\partial \epsilon}(\bar{x}, \bar{\epsilon}) \tag{4.43}$$

Note that $\frac{dx_{I_f}}{d\epsilon}$ in (4.43) is obtained from (4.33).

The expression of $\frac{dh_{N_f}}{d\epsilon}$ is different for Phase I and II. For Phase I, it is equal to Δh_{N_f}, whereas, for Phase II, it varies according to the type of inequality limit. For the functional limits on the reactive generations, which depend directly on the load level, this derivative will be equal to $\Delta \mathbf{qd}$, whereas, for the active power flows, this derivative is equal to zero because their expressions do not depend directly on ε (see appendix A).

The increment in ε, Δε, that yields the maximum of one violation of the inequality limits, is then given by

$$\Delta \epsilon = \min \{ \Delta \epsilon_z \geq 0, \Delta \epsilon_v \geq 0, \Delta \epsilon_h \geq 0 \} \tag{4.44}$$

where

$$\Delta \epsilon_z = [\Delta \epsilon_{x_i}, \Delta \epsilon_{\lambda_k}, \Delta \epsilon_{\zeta_n}], \quad i \in I_f,\ k \in K,\ n \in N_0 \tag{4.45}$$

In (4.45) we have that

$$\Delta\epsilon_{x_i} = \frac{x_i^{\min} - x_i}{e_i}, \; if \; e_i < 0$$

$$\Delta\epsilon_{x_i} = \frac{x_i^{\max} - x_i}{e_i}, \; if \; e_i > 0 \qquad (4.46)$$

$$\Delta\epsilon_{\zeta_n} = -\frac{\zeta_n}{e_n}$$

$\Delta\varepsilon_\lambda$ is considered to be infinite since λ can assume any value.

In addition,

$$\Delta\epsilon_{\nu_i} = -\frac{\nu_i}{r_i}, \qquad i \in I_0 \qquad (4.47)$$

and

$$\Delta\epsilon_{h_n} = -\frac{h_n(\bar{x},\bar{\epsilon})}{s_n}, \qquad n \in N_f \qquad (4.48)$$

Note that $\Delta\varepsilon_\zeta$ $\Delta\varepsilon_\nu$ and $\Delta\varepsilon_h$ can be found to be negative. In this case only the positive values must be checked. Note also that, in (4.47), ν_i can assume positive or negative values (depending on whether $\mathbf{x}_i$ is at the maximum or minimum limit). In both cases, however, we want to check whether the Lagrange multiplier reaches zero so that the associated variable can be released.

As a consequence of the linear approximation for the optimal trajectories, after ε is incremented by $\Delta\varepsilon$ calculated in (4.44), it may happen that more than one variable violates its limits. If this situation occurs, a decrement in ε may be obtained at the new point $\mathbf{z}(\varepsilon + \Delta\varepsilon)$. All expressions obtained to increment ε are still valid in this case with the difference that, now, $\Delta\varepsilon$ will be made equal to the minimum (negative) $\Delta\varepsilon$ obtained from equations (4.46)-(4.48). Also, to reduce the computational effort, only violated quantities can be considered, thus decreasing the dimension of (4.32), (4.37) and (4.42).

Figure 4.4 illustrates the process for two variables $\mathbf{x}_1$ and $\mathbf{x}_2$ whose minimum limits are 0. In this Figure, starting from ε=0, the next break-point was predicted to occur at ε^1 but at this point both $\mathbf{x}_1 < 0$ and $\mathbf{x}_2 < 0$. Thus, at the new values $\mathbf{x}_1=\mathbf{x}_1(\varepsilon^1)$ and $\mathbf{x}_2=\mathbf{x}_2(\varepsilon^1)$, a new linearization is made to decrement ε until ε^4 where only the limit of $\mathbf{x}_1$ is violated.

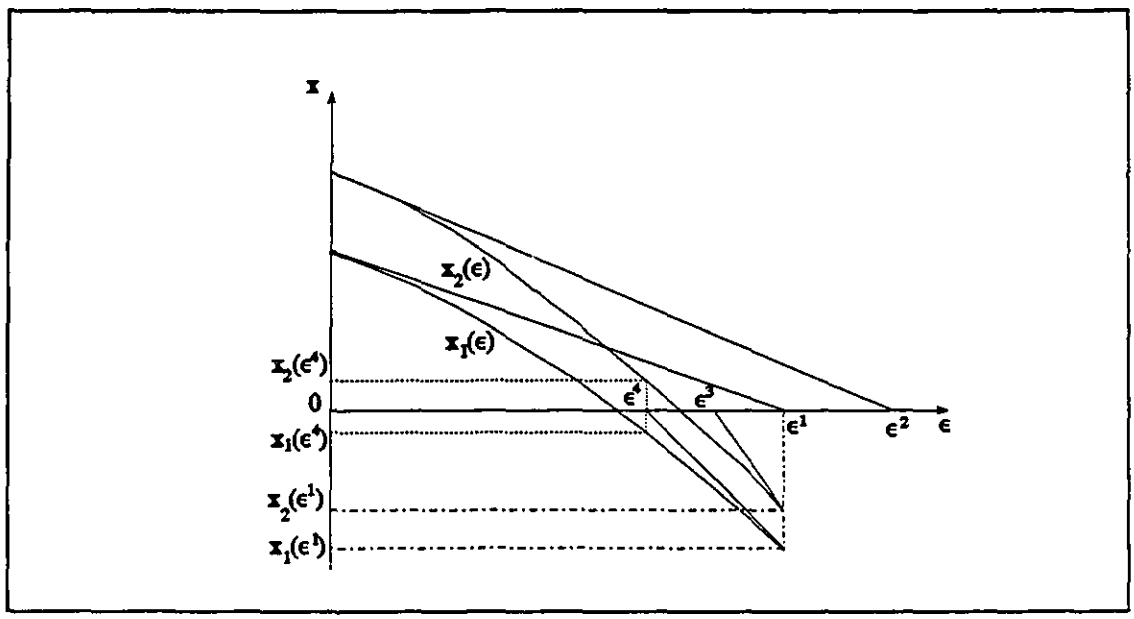

Figure 4.4- Linear prediction.

Tests (see Chapter 6) have demonstrated that linear prediction improves considerably the performance of the Parametric-OPF algorithm because they are not "blind" searches, being able to find the next break-point in fewer iterations when compared with binary search. The good performance is also due to the fact that the trajectories between two break-points are approximately linear, as can be seen in Figure 4.3. There are, however, two important points to be considered when using a linear prediction. The first is related to the characteristic of the curve being approximated by a straight line. To understand this, a typical example is represented in Figure 4.5. In this Figure, $\mathbf{x}_1$ reaches its minimum limit (equal to 0) at ε^*. Because of the shape of the optimal trajectory, however, the linear predictions will yield a sequence of approximations to this break-point (ε^1, ε^2, ε^3, etc). As the algorithm proceeds, there will be infinitely small increments in ε and, in the end, the algorithm will not be able to proceed beyond this point. To avoid this kind of situation, the Parametric-OPF uses a convergence

tolerance for the linear prediction. If the increment $\Delta\varepsilon$ is smaller than a tolerance, *tol*, this increment is multiplied by a pre-specified constant c and the KT equations are evaluated at the new $\varepsilon+c\Delta\varepsilon$. The values of the tolerance and of c must be defined for each system being tested and depend on the proximity of the break-points in the optimal trajectories. Based on the tests made, we found reasonable per unit values of $10^{-2} \leq tol \leq 10^{-4}$ and $2 \leq c \leq 4$. A more "intelligent" (and also more computationally expensive) methodology to solve such situations would be to make $\Delta\varepsilon$ equal to the average of the two minimum increments of the set $\{\Delta\varepsilon_z, \Delta\varepsilon_\zeta, \Delta\varepsilon_h\}$. A second option would be to use a mixed strategy composed by binary search and linear prediction. In this case, a linear prediction would be used to make an initial guess of the break point and a binary search would be applied subsequently to define the first violation. So far, these strategies have not been implemented in the algorithm.

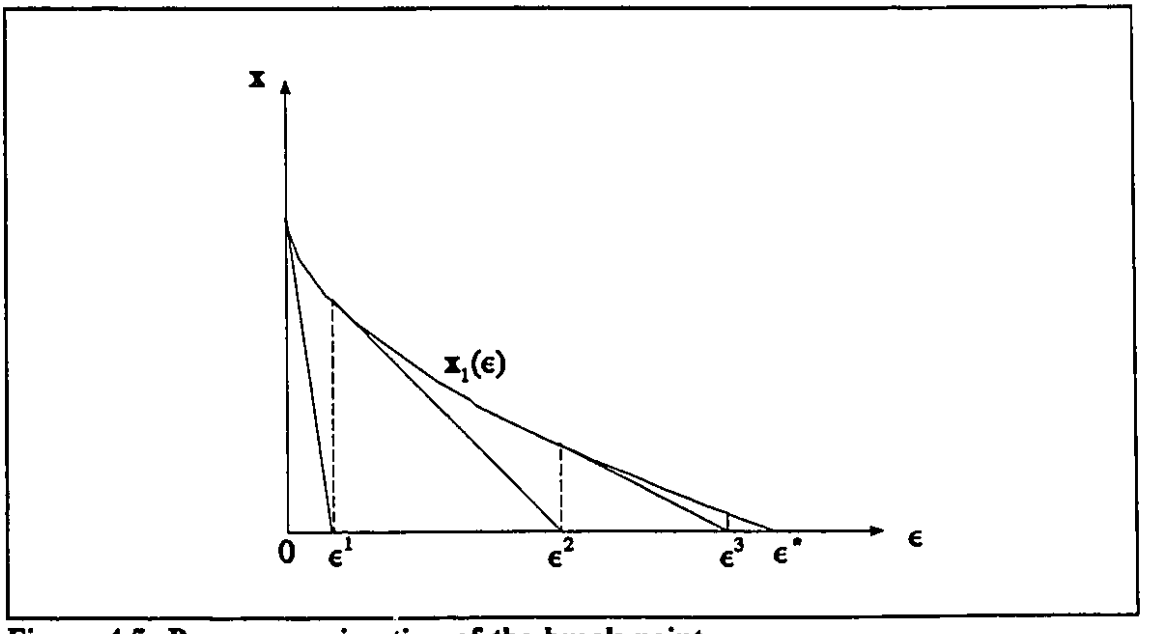

Figure 4.5- Poor approximation of the break-point.

The second point that must be discussed in this type of search is related to the "backwards" prediction. Because this prediction is made at points that do not satisfy the operational limits, it may happen that, between the actual ε and $\varepsilon+\Delta\varepsilon$ calculated by the linear prediction, there is a critical point of type 2 (see section 3.3.1). This situation is represented in Figure 4.6 below. In this Figure, the new point $\mathbf{x}_1(\varepsilon^1)$ corresponds to the

value of x_1 at the incremented ε. Because of the critical point, however, $x_1(\varepsilon^1)$ lies on a different path defined by the KT equations (remember that, at critical points of type 2, the function defined by the KT equations has a quadratic turning point). If there are other violations at ε^1, a new linear prediction may give an increment in ε, (resulting in ε^2) instead of the decrement that is sought. Since this kind of situation is related to the occurrence of critical points in the optimal trajectories, there is no easy solution. However, it is important to note that the critical point may not have happened if, before the critical point, a new variable is fixed at its limit (remember that, at ε^1, where the linear prediction is made, the limits are not considered). This implies that, even if the linear prediction fails, the binary search may succeed because it is not based on approximations of the optimal trajectories.

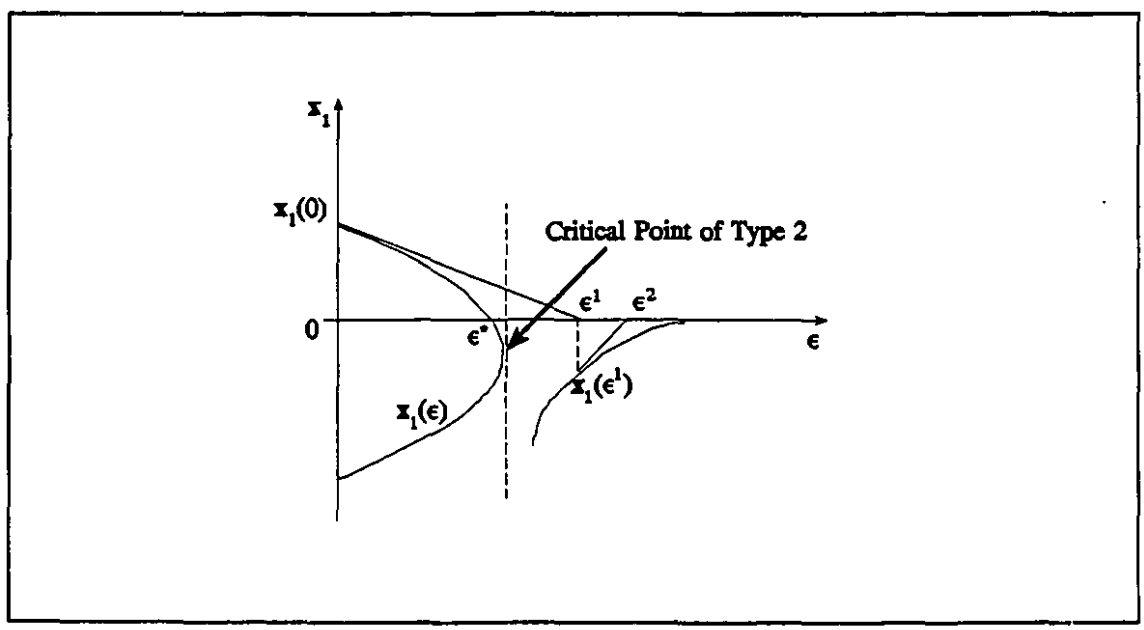

Figure 4.6- Linear prediction with a critical point.

Based on the above discussion, a combination of the two strategies (binary search and linear prediction) to find the break-points of the optimal trajectories was also implemented. In all, three strategies were used:

- binary search;
- forwards and backwards linear prediction;

- forwards linear prediction and backwards binary search.

Among these three strategies, the last one is the most efficient if we consider computational speed and robustness. The second strategy is usually the fastest one but it may also fail in the backwards search whereas the first mechanism is the slowest one.

Although the third strategy discussed above presented the best performance, even this strategy will fail in case a critical point occurs during the tracking process because, in such situations, when there is a solution, either the trajectories themselves lose optimality or multiple violations occur, no matter how many evaluations are made to find the break-points. The solution for the critical points that occur in the optimal trajectories rely on the "jumps" proposed in the previous chapter, however, as was previously mentioned, these jumps are still not implemented in the computational program that solves the Parametric-OPF.

It must also be emphasized that each one of the mechanisms presented here to find the break-points can be used together with some heuristics that would immediately fix certain types of violation that happen at approximately the same ε (without new searches). This heuristic is based on the fact that, for some types of violations, after the first violation is fixed, the remaining ones must also usually be fixed. Similar heuristics are presently used in any OPF algorithm based on the active feasible set strategy. This would increase considerably the computational speed of the parametric method, but at the expense of losing the systematic calculation of the changes in the optimal active feasible set. As a result, the causes for the failure of the algorithm would not be so easy to analyze. In fact, one of the biggest problems encountered by researchers when studying the OPF problem is to discover the causes of occasional failure of the solution algorithms. This is easily understandable considering that most of the solution algorithms are based on heuristics to find the active set.

The obstacles encountered in defining the correct optimal active set are understandable in view of the optimal trajectories depicted in Figure 4.3, where the influence that a variable fixed at its limit has on the behaviour of the free variables is

easily verified. In general, there is no guarantee that the fixing of a variable at its limit will not cause additional violations. As a consequence, it is very difficult to implement a heuristic strategy that considers all possibilities.

A final comment regarding the strategies to find the break-points must be made concerning the load tracking phase. In normal situations, the system loads do not vary considerably during a short period of time. This fact, when viewed by the parametric model, signifies a small change in the optimal solution for a change in ε. As a consequence, a more aggressive approach can be used during Phase II to perform the tracking of the solution trajectories. Since the solution is not likely to vary much, an attempt can be made initially to increase ε from 0 directly to 1. After this initial trial, if multiple violations occur, either the linear prediction or the binary search can be used to find the break-points.

After a successful increment in ε is made (and an optimal active set is defined) the algorithm passes to the next stage, where the KT equations are solved and the optimality of the solution is tested. This final stage is discussed next.

4.3.3 Solution of the Kuhn-Tucker Equations by Newton Method

Once the active feasible set is estimated, the KT equations (4.6)-(4.9) and (4.19)-(4.22) can be easily solved by a numerical method. In this thesis, because of its quadratic convergence characteristics, the Newton method was used to find the new candidate for optimal solution. Applying the Newton method to the set of KT equations (4.6)-(4.8) (or (4.19)-(4.21)), the increment in $\mathbf{z}_f$ can be obtained by solving the same system represented in equation (4.31):

$$\left[W(z_f,\epsilon)\right]\begin{bmatrix}\Delta x_{I_f}\\ \Delta\lambda\\ \Delta\zeta_{N_0}\end{bmatrix} = -\begin{bmatrix}\Delta\left(\frac{\partial \mathcal{L}}{\partial x_{I_f}}\right)\\ \Delta\left(\frac{\partial \mathcal{L}}{\partial \lambda}\right)\\ \Delta\left(\frac{\partial \mathcal{L}}{\partial \zeta_{N_0}}\right)\end{bmatrix} \tag{4.49}$$

where, for Phase I, we have

$$W(z_f,\epsilon) = \begin{bmatrix}\frac{\partial^2 \mathcal{L}}{\partial x_{I_f}^2}(z,\epsilon) & , & \frac{\partial^T g}{\partial x_{I_f}}(x,\epsilon) & , & \frac{\partial^T h_{N_0}}{\partial x_{I_f}}(x,\epsilon)\\ \frac{\partial g}{\partial x_{I_f}}(x,\epsilon) & , & 0 & , & 0\\ \frac{\partial h_{N_0}}{\partial x_{I_f}}(x,\epsilon) & , & 0 & , & 0\end{bmatrix} \tag{4.50}$$

with

$$\frac{\partial^2 \mathcal{L}}{\partial x_{I_f}^2}(z,\epsilon) = \frac{\partial^2 c}{\partial x_{I_f}^2}(x) + (1-\epsilon)w + \frac{\partial^2 (g^T(x,\epsilon)\lambda)}{\partial x_{I_f}^2} + \frac{\partial^2 ({h_{N_0}}^T(x,\epsilon)\zeta_{N_0})}{\partial x_{I_f}^2} \tag{4.51}$$

and

$$\begin{bmatrix}\Delta\left(\frac{\partial \mathcal{L}}{\partial x_{I_f}}\right)\\ \Delta\left(\frac{\partial \mathcal{L}}{\partial \lambda}\right)\\ \Delta\left(\frac{\partial \mathcal{L}}{\partial \zeta_{N_0}}\right)\end{bmatrix} = \begin{bmatrix}\frac{\partial c}{\partial x_{I_f}}(x^0) + \frac{\partial^T g}{\partial x_{I_f}}(x^0)\lambda^0 - w(x_{I_f} - x_{I_f}^0)\\ g(x^0)\\ \Delta h_{N_0}\end{bmatrix}\Delta\epsilon \tag{4.52}$$

In the same way, for Phase II, in equation (4.49) we have

$$W(z_f, d(\epsilon)) = \begin{bmatrix} \frac{\partial^2 \mathcal{L}}{\partial x_{I_f}^2}(z, d(\epsilon)) & , & \frac{\partial^T g}{\partial x_{I_f}}(x, d(\epsilon)) & , & \frac{\partial^T h_{N_0}}{\partial x_{I_f}}(x, d(\epsilon)) \\ \frac{\partial g}{\partial x_{I_f}}(x, d(\epsilon)) & , & 0 & , & 0 \\ \frac{\partial h_{N_0}}{\partial x_{I_f}}(x, d(\epsilon)) & , & 0 & , & 0 \end{bmatrix} \tag{4.53}$$

with

$$\frac{\partial^2 \mathcal{L}}{\partial x_{I_f}^2}(z, d(\epsilon)) = \frac{\partial^2 c}{\partial x_{I_f}^2}(x) + (1-\epsilon)w + \frac{\partial^2 (g^T(x, d(\epsilon))\lambda)}{\partial x_{I_f}^2} + \frac{\partial^2 (h_{N_0}{}^T(x, d(\epsilon))\zeta_{N_0})}{\partial x_{I_f}^2} \tag{4.54}$$

and

$$\begin{bmatrix} \Delta\left(\frac{\partial \mathcal{L}}{\partial x_{I_f}}\right) \\ \Delta\left(\frac{\partial \mathcal{L}}{\partial \lambda}\right) \\ \Delta\left(\frac{\partial \mathcal{L}}{\partial \zeta_{N_0}}\right) \end{bmatrix} = \begin{bmatrix} -w(x_{I_f} - x_{I_f}^0) \\ \begin{pmatrix} -\Delta pd \\ -\Delta qd \end{pmatrix} \\ \begin{pmatrix} \Delta qd \\ 0 \end{pmatrix} \end{bmatrix} \Delta\epsilon \tag{4.55}$$

In (4.55) the equality constraints are the active power balance equations for all buses of the system and the reactive power balance equations for the load buses, whereas the inequality constraints are composed by the active limits on the reactive generation and on the power flows (see appendix A). Since the power flow limits do not depend directly on epsilon, $\Delta(\partial\mathcal{L}/\partial\zeta_n) = 0$, for n belonging to the set of active power flow limits.

After systems (4.6)-(4.8) or (4.19)-(4.21) are solved, the new values of the Lagrange multipliers associated with the decision variables can be obtained directly from (4.34) or (4.35), thus assuring the fulfilment of all KT equations.

System (4.49) is very similar to the system solved by classical Newton based OPF methods. The only important difference here is the introduction of the weighting factor w on the main diagonal, which improves the conditioning of $W(z,\varepsilon)$ and the convergence of the Newton iterations.

4.3.4 Ill-Conditioning of the Newton Method Jacobian Matrix

The derivatives present in (4.49) are considered only with respect of the free variables. This fact, together with the changes in N_0 throughout the tracking process will result in modifications on the size of this system every time any quantity is fixed or released from its limit. As was discussed in the previous chapter, the non-linear characteristic of the OPF problem and the changes in the optimal active set can lead to critical situations where $W(z,\varepsilon)$ is singular. This implies also that, at points in the neighbourhood of a critical point, $W(z,\varepsilon)$ is ill-conditioned and as a consequence, the Newton iterations may not converge.

Ill-conditioning of the Newton matrix has been recognized as one of the biggest problems of this method when applied to the OPF. Some strategies to avoid temporary ill-conditioning can be found in the literature [Monticelli and Liu, 1992]. In general, we can differentiate between two types of ill-conditioning: temporary or permanent. The first type is caused by temporarily fixing two incompatible variables at their limits, an example of which is shown in Figure 4.7.

Figure 4.7 represents a transmission corridor between buses k and l. Suppose that, at some point of the optimization process, the voltage magnitudes V_k is at its maximum and V_l reaches its maximum. With both V_k and V_l fixed, only a considerable difference in the voltage angles will allow the transmission of real and reactive power between these two buses. If, under these conditions, the transfer of reactive power is required (because

local Var sources are at a limit), this can result in an ill-conditioned matrix $W(z,\varepsilon)$. If there is a solution to such a situation, immediately the algorithm will "ask" for the release of V_k. In terms of the parameter, this implies that the break point defined by the release of V_k is at an ε which is very close to the ε value at which V_l was fixed. The effect that the parameter ε has on the active constraints of the OPF is basically to initially relax and subsequently return the load to its original value in an "ordered" manner. This implies that the Parametric-OPF will allow a very small increase in the load before the voltage magnitude V_k is released.

We can view the classical Newton approach as a parametric approach for which ε=1 (always). Comparing both methods, it can be seen that the Parametric-OPF will, first of all, find the point (that is the load) where both variables can be at their limits (that is, the point where V_l just reached its limit and its Lagrange multiplier is close to zero) and then modify the load very little (that is, slightly increase ε) with these two variables at their limits before releasing V_k. The classical Newton, however, will try to solve the original problem with both voltage magnitudes at their limits. As a consequence it is expected that the matrix $W(z,\varepsilon)$ associated with Newton will be very ill-conditioned during the iteration where both voltages are fixed. Therefore, methods such as the one presented in [Monticelli and Liu 1992] will be of great importance. On the other hand, for the Parametric-OPF such ill-conditioning is much less severe due to the process of gradually incrementing the parameter. In other words, the parametric process is less affected by the temporary ill-conditioning than a classical Newton approach for the OPF would be.

Now, suppose that the situation depicted in Figure 4.7 occurs during the load tracking phase at a point where the system load is increasing. As the load increases, there may be a need to transmit more power between buses k and l and as a consequence their voltage magnitudes tend to increase to reduce the losses. If both voltage magnitudes reach their maximum limits and the load continues to increase it is unlikely that any of these voltages will be released. In mathematical terms, the ill-conditioning caused by both voltages fixed will be permanent and eventually the tracking process will not be able to continue. Regardless of whether the load tracking is solved via a classical Newton method

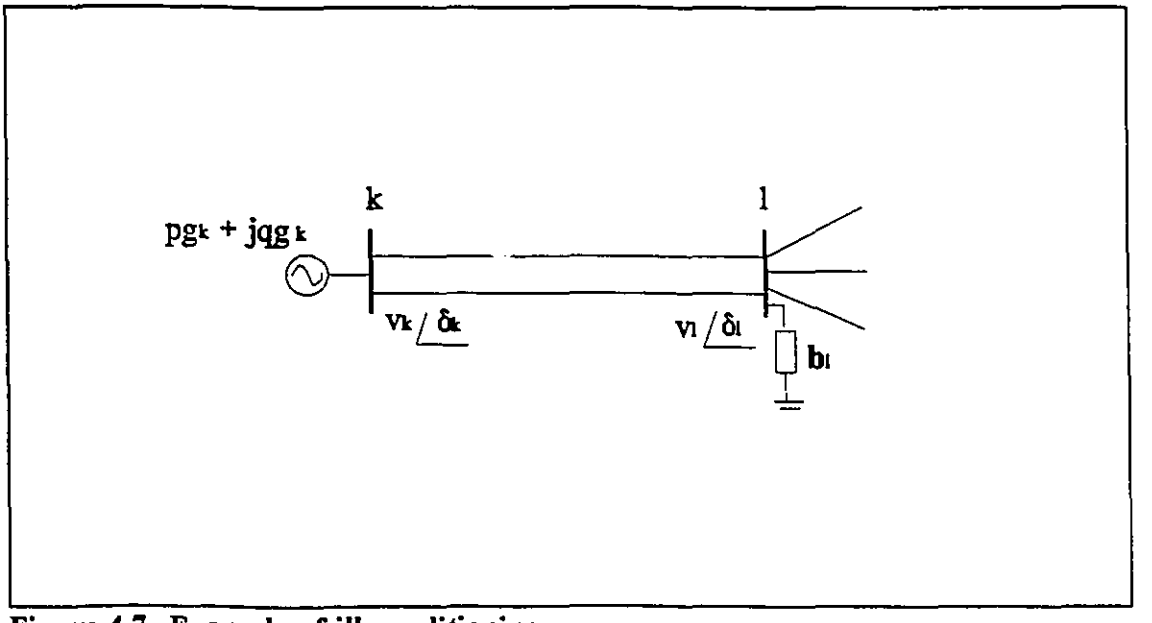

Figure 4.7- Example of ill-conditioning.

or the parametric method, the conditioning of matrix $W(z\varepsilon)$ will deteriorate in such cases. This is a typical situation where we reach a critical point of type 3 or 4. If there are enough degrees of freedom, eventually the matrix will become singular. If we run out of degrees of freedom, one of the fixed variables must be released to continue the tracking. If this is not possible, system (4.49) cannot be solved and the process, no matter if governed by the classical Newton or by the parametric method, must stop.

From the discussion of critical points in the previous chapter, it can be seen that near critical points of type 2 or 3 (that is, in a region where the minimum is not well defined or in a unstable region) $W(z\varepsilon)$ is ill-conditioned. The above example of permanent ill-conditioning is related to a critical point of type 3 (note that beyond this point there is no local solution for the problem). The causes for the other type of permanent ill-conditioning, related to the existence of multiple solutions, are mainly a consequence of a poor formulation of some OPF cases. This situation may occur in cases where there are too many control variables to be optimized (e.g. a bus with both variable synchronous condenser and shunt reactor). In some cases it is possible to bypass this problem by fixing some variable at an appropriate limit or by combining two variables into one. In general, however, unless the formulation of the case under study is improved, it is not possible to find a unique optimal solution [Stott et al., 1987].

4.4 Algorithm Flow Chart

The parametric algorithm for the solution of the OPF is summarized in Figure 4.8. In the solution algorithm, the strategies for incrementing ε will depend on the type of search used and also on the operational mode (Phase I or II). For the binary search, the initial (tentative) increment in ε is constant and equal to $\Delta\varepsilon^{sp}$. For Phase I, the value of $\Delta\varepsilon^{sp}$, will depend on the system being tested. During Phase II, for systems with an approximate linear behaviour $\Delta\varepsilon^{sp}=1$ whereas for systems with problems of voltage instability $\Delta\varepsilon^{sp} < 1$. Conversely, when using linear prediction, the value of $\Delta\varepsilon$ will vary between iterations according to equation (4.44). In the same way, the decrement on the value of ε will depend on the search used.

The four cases differentiated by the algorithm when incrementing ε are consequences of the strategy of making only one change in the active feasible set at a specific parameter value. Therefore, in Case I, when there is no violation, the active set is kept constant and ε is incremented, whereas, in Case IV, of multiple violations, ε is decremented and the algorithm returns to the last acceptable solution to initialize the tracking (that is, a new increment in ε is specified starting from the last acceptable solution). When there is only one violation, Case II, the solution and the active feasible set is updated and again the KT equations are solved to verify if the updated solution is optimal. If the solution satisfies the inequality limits (Case I) the algorithm proceeds with the new increment in ε. However, if new violations occur (Case III), both the solution point and the active feasible set must be made equal to their last acceptable values. Case III, therefore, occurs when a variable fixed at its limit causes new violations on the inequality limits or on the sign of the Lagrange multipliers.

After every change in the active set, increment or decrement in ε, the algorithm must test for the optimality of the KT solutions. This test is associated with the test for critical points. After or at critical points of type 1, 2 or 7 the solution of the KT equations loses optimality. Near or at critical point of type 2 or 3 matrix $\boldsymbol{W}$ becomes ill-conditioned and Newton method does not converge. Additionally, the KT equations cannot be solved

beyond critical points of type 3 (for increasing objective function) or 4 (when it is not possible to release any inequality) because the feasible set becomes locally empty. Finally, an active feasible set cannot be analytically defined at critical points of type 5 or 6.

Figure 4.9 depicts the flow-chart of the Parametric-OPF for both Phase I and II. Initially, for the load level $\mathbf{d}^0$, Phase I is solved starting from an initial guess $\mathbf{z}^0$. Subsequently, the algorithm returns to the main loop (represented in detail in Figure 4.8) for every new load level $\mathbf{d}^j$, $j \in [1, inter]$. In this process, the final solution for a load level is used as a starting point for the tracking of the optimal solution in the next load interval, which considerably increases the computational speed of the method.

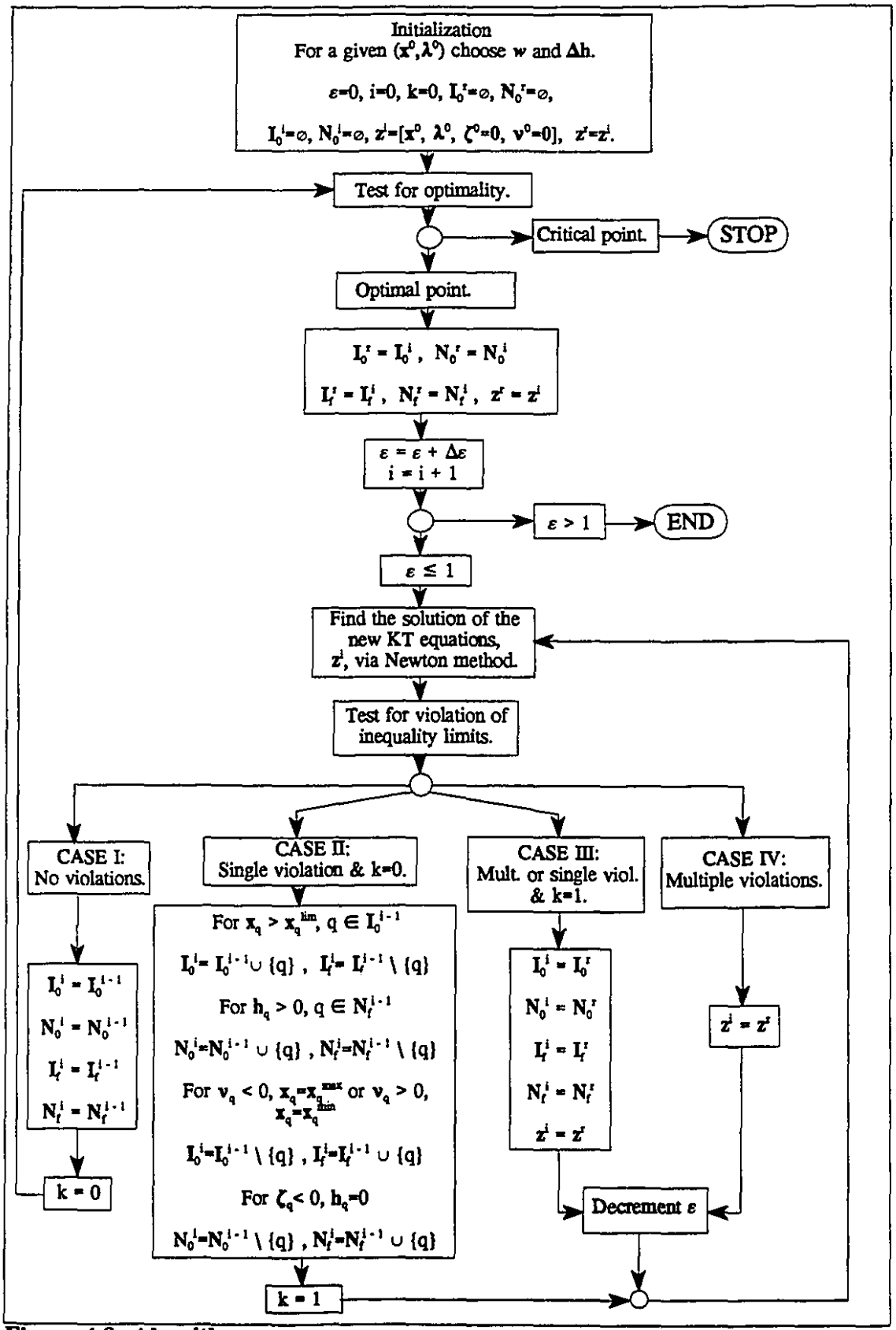

Figure 4.8- Algorithm.

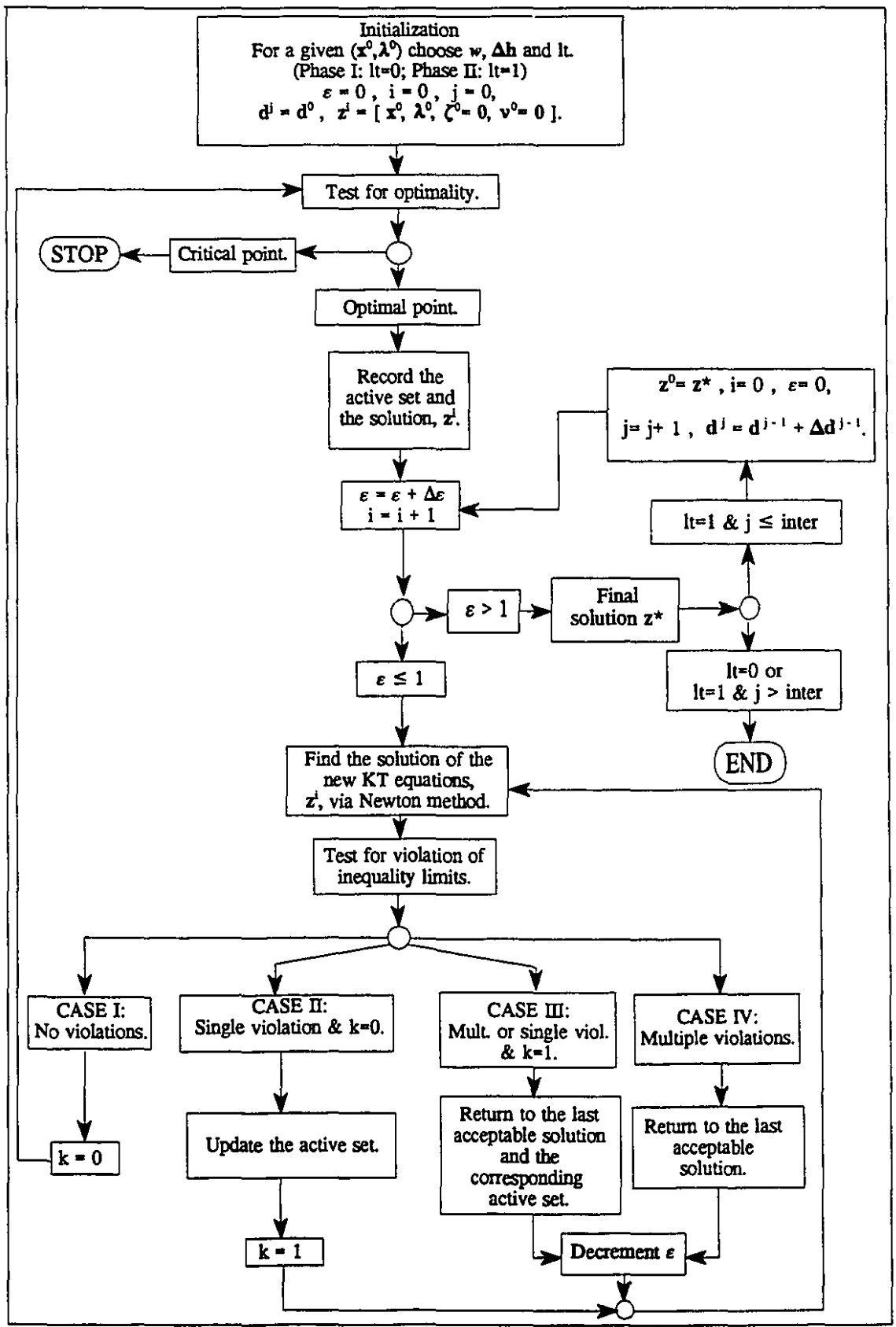

Figure 4.9- Flow Chart of Phase I and Phase II.

4.5 Conclusion

Although it can be used in two different scenarios (constant or variable load), the Parametric-OPF algorithm is basically the same for both cases. This characteristic is a consequence of the concept of parameterization of an optimization problem and its usefulness is significant, as can be seen in the study of the OPF. Although the algorithm relies on the Newton method to solve the KT conditions, some of the difficulties associated with this method, namely the problem of temporary ill-conditioning and the problem of correctly defining the optimal active feasible set, are successfully overcome by the Parametric-OPF. The mechanisms used by the algorithm to find the optimal active feasible set are quite straightforward and systematic. As a consequence, the tuning necessary to apply the algorithm to different test cases is small and the method is reasonably robust. As a conclusion, we may say that the Parametric-OPF offers a flexibility and a robustness that is not easily encountered in OPF algorithms.

In the next chapter we make use of the flexibility of the parametric approach to do some special studies in the optimal operation of a generation-transmission system.

CHAPTER 5

SPECIAL APPLICATIONS OF THE PARAMETRIC-OPF

5.1 Introduction

From what was discussed up to this point, is easy to see that the Parametric-OPF permits the analysis of the influence of every parameter existing in the OPF model. This fact indicates that the Parametric-OPF can be a useful tool to perform some special studies on the optimal operation of generation-transmission systems. In this chapter, we make use of this special characteristic to study three particular aspects of economic and secure operation of power systems. First of all, the method is applied to the simulation of loss of lines during load tracking. Next, it is shown that the method is good for sensitivity analysis, being able to provide the Bus Incremental Costs and the System Incremental Cost throughout the interval of load variation. This is useful for making economic decisions in bus load management or power transactions. Finally, the algorithm is used to analyze the behaviour and influence of FACTS devices in the optimal operation of a power system under fixed and varying load conditions.

5.2 Simulation of Line Contingencies

The first special application of the Parametric-OPF is in contingency analysis. The simulation of contingencies is important to identify vulnerabilities in the power system to the loss of some component.

The strategy adopted by the Parametric-OPF for the study of line outages during the load tracking phase is based on the alternate use of the two different parametric models of Phase I and Phase II. If during the load tracking, at a specific load level d^j, a contingency occurs, the last optimal solution found by the algorithm loses both its optimality and its feasibility. To continue the tracking, it is necessary to use this last solution as an initialization for a Phase I procedure that will find the optimal operation point for that specific load level. After finding the optimal solution, the algorithm returns to the load tracking mode. Figure 5.1 illustrates the process. To simulate contingencies during Phase I, one applies the Phase I algorithm to the modified network starting with the optimum point before the contingency.

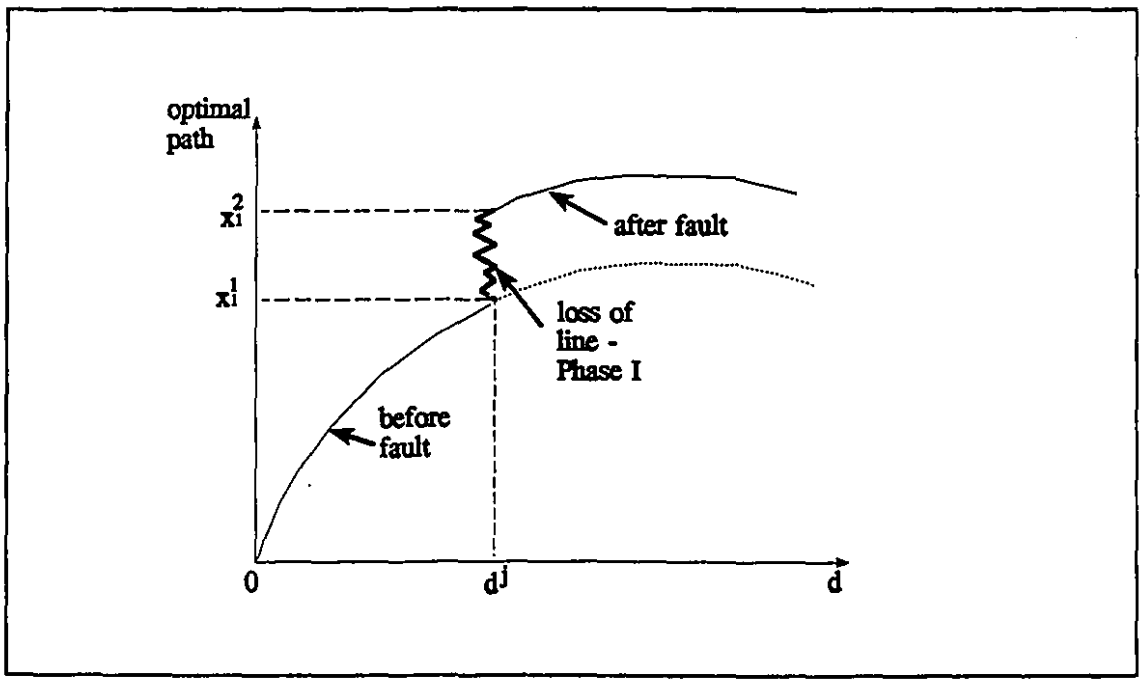

Figure 5.1- Simulation of contingencies.

The simulation of loss of lines is done by the modification of the impedance matrix **Y** defined in Appendix B. The method used is the classical one, very similar to that used by Monticelli [Monticelli, 1983].

5.3 Sensitivity Analysis

The calculation of the optimal operating states alone does not provide all necessary information about the operating conditions of a generation-transmission system. The knowledge of the sensitivities of the optimal solution to any parameter variation can be of great value when considering transmission transactions or upgrades in the system. Ideally, an optimization method must be able to provide us with information regarding the sensitivity of the operating condition with respect to any change in the model parameters without expensive additional calculations.

The Parametric-OPF method is capable of providing the trajectories of sensitivities of the optimal cost with respect to changes in system load or to the variable limits. In particular, during the load tracking (Phase II), the trajectories of the bus incremental costs and of the system incremental cost corresponding to all points of the load curve can be obtained without any additional calculation. These quantities are very helpful when dealing with energy transactions.

In recent years, there has been considerable discussion concerning the unbundling of the services provided by the utilities. Under regulations adopted recently by different countries, power utilities may have to live with energy exchanges with numerous non-utility generators as well as to accept wheeling transactions throughout its network. As a consequence of these changes in the policy of energy supply, there have been many discussions about how to cost such transactions. These costs can be classified into four categories [Shirmohammadi et al., 1991]:

- Operating cost: production cost due to generation redispatch and rescheduling resulting from the transmission transaction;

- Opportunity cost: benefits of all transactions that the utility foregoes due to operating constraints that are activated by the transmission transactions (cost of lost opportunities);

- Reinforcement cost: capital cost of new transmission facilities needed to accommodate the transmission transaction;

- Existing system cost: the allocated cost of existing transmission facilities used by the transmission transaction.

The type of transmission transactions also vary according to their duration and continuity. Thus, some transactions take place over a period spanning several years while others are of shorter duration. Also, the transactions can be classified as "firm" (that is, continuous or not subject to discretionary interruptions) or "non-firm". The above mentioned four cost components vary with the type of transaction. For non-firm transmission transactions, there is usually no need to consider the reinforcement cost and the existing system cost when calculating the total cost. The reinforcement and existing system costs are associated with general improvements of the system network and therefore are subject to planning studies over a long term horizon. The opportunity and operating costs, however, are associated with daily operation of a power system and must be considered in most types of transmission transactions. The opportunity cost, itself, is partially due to unrealized savings in production cost if the utility cannot bring in cheaper energy as a result of operating limits. In addition, the opportunity cost is also caused by the unrealized contribution to the cost of the existing system by potential firm transactions that could not be made because of operating constraints.

The transmission transactions cost components can all be obtained with the help of OPF algorithms since they suppose optimal operating conditions for the system under study [Shirmohammadi at al., 1991]. In this thesis, however, we will restrict ourselves to the study of operating cost only.

The marginal operating cost incurred by energy transactions is affected not only by changes in load and generation but must also take into consideration system security, VAr requirements and voltage profile limits. For this reason, an analytical tool suitable to address these issues is the OPF. LP based OPF algorithms [Fahd and Sheblé, 1992] and sequential quadratic programming based OPF algorithms which also consider security

constraints [Mukerji et al., 1992] have been proposed to estimate the marginal operating cost associated with wheeling or non-utility generation. Although this marginal cost can be obtained by comparing the OPF results with and without the possible transactions, a faster method is based on the use of the bus incremental costs.

The total marginal cost of transacted power can be estimated as follows

$$\Delta C = \sum_{i \in \Omega} BIC_i \Delta p_i \tag{5.1}$$

where ΔC is the marginal operating cost of the transaction, Ω is the set of all buses involved in the transaction, $\mathbf{BIC}_i$ is the bus incremental cost at bus i and $\mathbf{\Delta p}_i$ is the change in the net real power injection at bus i due to the transaction. The change in the net injection is positive if the transaction involves a change in load and negative if it involves a change in generation. Equation (5.1) can also be extended to include bus incremental costs associated with VAr changes.

The adoption of a parametric approach to calculate ΔC may be quite helpful because the method exactly tracks the load curve and, therefore, is able to provide the trajectories of the bus incremental costs and of **pg** for an entire interval of load variation. The bus incremental costs can be easily obtained by the method using information that is already available throughout the tracking process, as is shown in the following paragraphs.

The sensitivity of the objective function with respect to changes in the active load at bus i is called the incremental cost of bus i ($\mathbf{BIC}_i$). From the parameterized model used in Phase II, represented in Chapter 3 (equations (3.24)-(3.27)), these quantities can be represented as

$$BIC_i = \frac{\partial c(x,\epsilon)}{\partial pd_i} = \frac{\partial}{\partial pd_i}\left[c(x) + (1-\epsilon)\frac{1}{2} w \| x - x^0 \|^2\right] \tag{5.2}$$

They are interpreted as follows: " Fixing the value of ϵ, let the load at bus i vary arbitrarily keeping all other bus loads constant." Thus, in the above partial derivatives, ϵ is treated as a constant parameter.

The objective function represented in (5.2) is a function of **x**. Therefore,

$$\frac{\partial c}{\partial pd_i} = \frac{\partial^T c}{\partial x}\frac{\partial x}{\partial pd_i} \tag{5.3}$$

From the KT conditions (see equation (3.10)) we know that

$$\frac{\partial^T c(x,\epsilon)}{\partial x} = -\sum_{k\in K}\lambda_k\frac{\partial^T g_k(x,\epsilon)}{\partial x} - \sum_{l\in L_0}\mu_l\frac{\partial^T h_l(x,\epsilon)}{\partial x} \tag{5.4}$$

Substituting (5.4) into (5.3) therefore gives

$$\frac{\partial c(x,\epsilon)}{\partial pd_i} = -\sum_{k\in K}\lambda_k\frac{\partial^T g_k(x,\epsilon)}{\partial x}\frac{\partial x}{\partial pd_i} - \sum_{l\in L_0}\mu_l\frac{\partial^T h_l(x,\epsilon)}{\partial x}\frac{\partial x}{\partial pd_i} \tag{5.5}$$

or

$$\frac{dc(x,\epsilon)}{dpd_i} = -\sum_{k\in K}\lambda_k\frac{\partial g_k(x,\epsilon)}{\partial pd_i} - \sum_{l\in L_0}\mu_l\frac{\partial h_l(x,\epsilon)}{\partial pd_i} \tag{5.6}$$

From equation (A.42) we have, for all k ∈ K,

$$g_k(x,\epsilon) = pg_k - p_k(V,\delta,a,\phi,xl) = pd_k \qquad (5.7)$$

Thus, $\partial \mathbf{g}_k / \partial \mathbf{pd}_i$ vanishes for all k≠i and is equal to 1 for k=i. In the parameterized model, the Lagrange multiplier associated with (5.7) is α_k (see equation (A.42)). Also, from the parameterized model we have that $\partial \mathbf{h}_l / \partial \mathbf{pd}_i = 0$, $\forall$ l (see equations(A.44)-(A.51)). Consequently,

$$\frac{\partial c(x,\epsilon)}{\partial pd_i} = -\alpha_i \qquad (5.8)$$

As was explained in the previous chapter, the parametric algorithm uses the Newton method to obtain the optimal solutions for every new problem defined after an increment in the parameter ε. As a consequence, the Lagrange multipliers associated with the equalities (that is, the real power balance equations of every bus of the system and the reactive power balance equations for the load buses), as well as the Lagrange multipliers associated with the active inequalities are automatic by-products of the algorithm. During Phase II, an increment in ε is in reality an increment in the load buses (see section A.3.1) and the algorithm exactly tracks the load curve. Therefore, the Parametric-OPF is able to provide the Lagrange multiplier optimal trajectories for the whole interval of load variation and the exact of trajectories of the bus incremental costs are also known with no extra calculation.

In addition to the extra operating costs due to the increase of active load, cases may happen where the incremental cost of transmitting additional reactive power must also be considered [Li and David, 1993]. Although reactive generation is not explicitly present in the cost function, it affects both real line losses and voltage magnitudes and therefore its influence on the final cost may be not negligible. Tc take into consideration this additional operating cost, one can extend the definition of marginal cost of transacted

power to the reactive transacted power. In this case, in equation (5.1), the real power balance is substituted by the reactive power balance and the bus incremental cost is defined as the increment on the total cost due to an increment in the reactive load, that is,

$$BIC'_i = \frac{\partial c(x,\epsilon)}{\partial qd_i} = \frac{\partial}{\partial qd_i}\left[c(x) + (1-\epsilon)\frac{1}{2}w\|x - x^0\|^2\right] \qquad (5.9)$$

where $\mathbf{BIC'}_i$ is the increment in the total cost due to a unit increment in $\mathbf{qd}_i$.

As with the bus incremental costs associated with real power, the trajectories of **BIC'** can be easily calculated by the parametric algorithm. In the Parametric-OPF model used during Phase II, the reactive power balance at the load buses as well as the functional inequality defined for the reactive generation are dependent on **qd** (see equations (A.43) and (A.44)). Thus, the **BIC'** will depend on the Lagrange multipliers associated with the reactive power balance equations, β, (defined only for the load buses) or on the Lagrange multipliers associated with the limits on **qg**, $\rho^{lim} = [(\rho^{min})^T, (\rho^{max})^T]^T$. Following the same steps as before,

$$BIC'_i = \begin{cases} \beta_i, & \textit{if } i \textit{ is a load bus} \\ \rho_i^{lim}, & \textit{if } i \textit{ is a generation bus} \end{cases} \qquad (5.10)$$

where, ρ_i^{lim} will be equal to zero if none of the limits on $\mathbf{qg}_i$ are active, positive if $\mathbf{qg}_i = \mathbf{qg}_i^{max}$ and negative if $\mathbf{qg}_i = \mathbf{qg}_i^{min}$.

Besides being used in (5.1), the vector of (active) bus incremental costs, **BIC**, is also necessary for the calculation of the system incremental cost. While the bus incremental costs give us an idea of the effect on the total cost of generation of a unit increment of load at each bus, the system incremental cost tells us the effect that an increment in the total system load has on the total generation cost. The system

incremental cost serves as a reference value when discussing power transactions. As a general rule, a utility would not consider selling power for a price that is inferior to its system incremental cost. However, this rule is not always valid if line flow limits are active and transmission losses are high because it may happen that the system incremental cost is higher than some bus incremental costs. In such cases, it would be possible to sell energy through those buses for a price inferior to the system incremental cost and still make a profit. Knowing the bus incremental costs provides new information that can be used by utilities to buy and sell power in a more economical manner taking into account all types of constraints.

The system incremental cost is defined as ,

$$SIC = \frac{dc(x,\epsilon)}{d\left(\sum_{i=1}^{nb} pd_i\right)} \tag{5.11}$$

or, if we call pd_{tot} the summation of the active loads of all buses,

$$SIC = \frac{dc(x,\epsilon)}{dpd_{tot}} \tag{5.12}$$

The total cost, $c(\mathbf{x},\epsilon)$, in (5.12) is a function of all the OPF model variables, $\mathbf{x}$, which in turn are functions of pd_{tot} through the load vector $\mathbf{pd}$. Thus, SIC can be rewritten as

$$SIC = \frac{\partial^T c}{\partial x}\frac{\partial^T x}{\partial pd}\frac{dpd}{dpd_{tot}} \tag{5.13}$$

Now, since, from equation (5.3), we have

$$\frac{\partial^T c}{\partial x}\frac{\partial^T x}{\partial pd} = BIC^T \tag{5.14}$$

then, for an increment **Δpd** in the active load vector and an increment Δpd_{tot} in the total load, the system incremental cost is written,

$$SIC = \frac{1}{\Delta pd_{tot}} BIC^T \Delta pd \tag{5.15}$$

During the load tracking, equations (5.8), (5.10) and (5.15) define the trajectories of **BIC**, **BIC'** and SIC. Since the Parametric-OPF precisely tracks the load variation, these trajectories correspond exactly to all points of the load curve. Note that these quantities correspond to the changes in the (parameterized) objective function caused by changes in the loads.

So far, the discussion about sensitivities was restricted to the influence of the (parameter) system load. Although these sensitivities are directly related to the question of transmission transactions, they alone do not provide a complete picture of the system optimal operating point. Basically, all parameters existing in the OPF model affect the optimal solution (and the optimal cost). The second type of parameter that must be considered is the operating limit. The sensitivity of the objective function to changes in the limits of both functions and variables can give us valuable insight about bottlenecks in the power system, where considerable savings could me made if improvements were introduced.

Representing an inequality constraint in the Phase II Parametric-OPF model as

$$h_i(x, d(\epsilon)) \le h_i^{lim} \tag{5.16}$$

we want to calculate the sensitivity of the objective function to changes in $\mathbf{h}_i^{lim}$, $\mathbf{ST}_i$:

$$ST_i = \frac{\partial c(x,\epsilon)}{\partial h_i^{\lim}} = \frac{\partial}{\partial hl_i^{\lim}}\left[c(x) + (1-\epsilon)\frac{1}{2}w\|x - x^0\|^2\right] \qquad (5.17)$$

As in the previous calculations, in (5.17),

$$\frac{\partial c}{\partial h_i^{\lim}} = \frac{\partial^T c}{\partial x}\frac{\partial x}{\partial h_i^{\lim}} \qquad (5.18)$$

Substituting the values of $\partial^T c/\partial \mathbf{x}$ into (5.18) and following the same steps as before yields

$$\frac{\partial c(x,\epsilon)}{\partial h_i^{\lim}} = -\mu_i \qquad (5.19)$$

Therefore, the sensitivities of the optimal operation cost to changes on operating limits depend on the negative of the Lagrange multipliers associated with these inequalities. Since the approach provides the trajectories of the Lagrange multipliers, no additional calculation is needed to obtain these sensitivities.

As a conclusion, we may say that the parametric method yields valuable additional information about the optimal operation of the generation-transmission system. Because the full nonlinear OPF model is used, in the values of the sensitivities are included both active and reactive related constraints (that is, MW, MVAr, voltage magnitudes, tap settings, phase shifters and power flows limits). Thus, if the method is used together with a load forecast algorithm, a very good approximation of the bus incremental costs and system incremental cost can be obtained.

5.4 Representation of FACTS Devices in the OPF Model

The last special application of the Parametric-OPF is to study the behaviour and influence of FACTS (Flexible AC Transmission System) devices on the optimal operation of a power system.

The operation of a transmission system is described by physical laws (the Kirchoff Laws) which limit the degree of control that can be exercised on such systems. Basically, the available controls apply to generated power and to changes in the system topology. In addition, the span of the control actions is severely limited by other constraints (e.g.: the amount of reactive power in the network must be carefully chosen so that the phenomenon of voltage collapse does not occur; or the disconnection of a line must be made so that it does not lead to overloaded lines in the region). This plus the fact that, at every instant, it is necessary to assure an equilibrium between generation and demand, transform the control of a power system into a difficult task. In recent years, the increase in load demand has not been accompanied by a corresponding growth in the existing transmission facilities. The expansion of the transmission networks has been restricted by cost and/or more general economical or environmental issues. This discrepancy between the growth of power demand and the generation-transmission networks has given rise to problems that were not a concern in the past, increasing further the difficulties associated with an appropriate control of the system [Le Du, 1992].

It has, therefore, become necessary to operate existing transmission systems at load levels beyond the design limit, as well as to transmit power over longer distances. These factors motivated research on new mechanisms of control that came to be known as FACTS devices. Contrary to more commonly used control devices (e.g. phase-shifting transformers), FACTS devices are electronically controlled based on thyristor (or GTO) technology which has a much higher operating speed and broader controllability [Hingorani, 1991]. This technology offers utilities the ability to control power flows in their transmission routes and to allow transmission lines to be loaded closer to their thermal limits without compromising security. FACTS devices presently being developed or conceived are [Le Du, 1992]:

- variable series compensators;
- thyristor-switched phase shifters;
- generalized phase shifters/voltage regulators.

So far, some studies have been made on the impact of variable series capacitors using the load flow model [Maliszewiski et al., 1990] or the linearized OPF model [Taranto et al., 1992].

The model for the FACTS devices used in this thesis is represented in Figure 5.2. It is basically a variable transformer tap and/or phase shifter in series with a variable reactance. This represents a type of device which does not yet exist but which demonstrates the potential capability of a very general FACTS technology which includes devices such as thyristor-controlled variable series capacitors as a special case. We wanted here to investigate how such a device could be optimally controlled by an OPF.

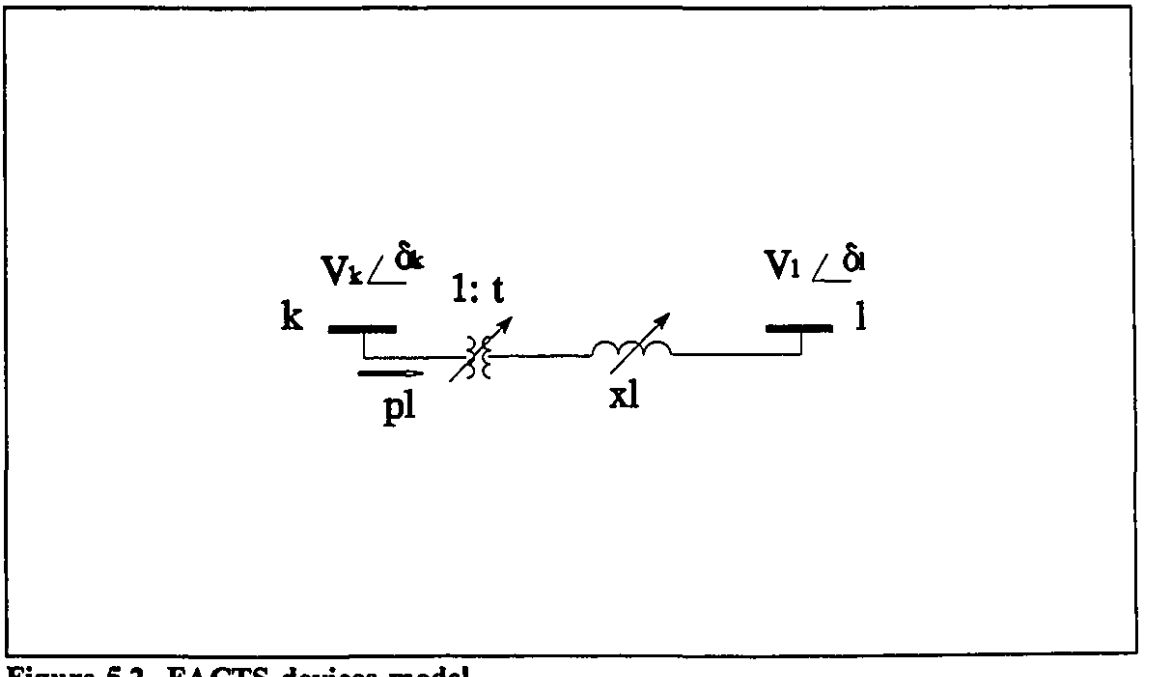

Figure 5.2- FACTS devices model.

For the OPF studies, the FACTS device variables are subjected to minimum and maximum limits, with the reactance supposed to vary from capacitive to inductive (that

is, a positive maximum limit and a negative minimum limit). The variables present in the FACTS model (that is, the series reactance and the transformer complex turns ratio) are directly represented in the parametric algorithm. Thus, the optimal trajectories of these variables are known both in Phase I as in Phase II, as well as the Lagrange multipliers associated with their operating limits (that is, the sensitivity of the optimal cost to the operating limits).

To help the reader understand the motivation for the choice of this general FACTS device consider the following discussion. For extra high voltage systems, the power transfer across a line connecting buses k and l of a transmission network can be approximated by the expression

$$pl = \frac{V_k V_l}{xl} \sin(\delta_k - \delta_l) \tag{5.20}$$

where V_k and δ_k are the voltage magnitude and angle of bus k, V_l and δ_l are the voltage magnitude and angle of bus l and xl is the series reactance of the line.

An increment in the transmitted power, therefore depends on the voltage magnitudes and angles of the connected buses and on the reactance of the line. Therefore, the control of the power flow can be done by the modification of the voltages, the inductive reactance, xl or the relative phase angle ($\delta_k - \delta_l$). While the inductive reactance of the transmission line can be reduced by changing the conductor, the idea is to introduce an external component to vary xl according to the operation needs. The introduction of a device such as the one represented in Figure 5.2 can provide the required control. By varying the phase shifter angles and the series reactances it is possible to increase or to limit the power flow on the line without causing great changes in the operating points of the variables in neighbouring buses.

The power flow through the FACTS device represented in Figure 5.2 is written

$$pl = \frac{aV_kV_l}{xl}\sin(\delta_k - \delta_l + \phi) \tag{5.21}$$

where the complex turns ratio t is given by,

$$t = ae^{j\phi} \tag{5.22}$$

and where V_k and δ_k are the voltage magnitude and angle of bus k, V_l and δ_l are the voltage magnitude and angle of bus l and xl is the variable series reactance.

Thus, by appropriately choosing a, ϕ and xl, one can control the power flow. Because these quantities affect both with the real and reactive power in the network, an OPF algorithm is the correct tool tc be used to study the impact and controllability of the FACTS devices in steady-state operation. In this study, the questions we want to answer regarding the FACTS devices are:

- How difficult it is to control such devices via an OPF algorithm?
- What is the influence of such devices have on the control of line flows?
- To what extent can they increase the loadability limit of a transmission system?
- What is the influence can they have on the total operating cost?

To answer these questions, the Parametric-OPF was used to study the FACTS devices in different test systems under fixed and varying load conditions.

Two important factors must be kept in mind when studying the optimal behaviour of FACTS devices. First of all, the network power injections depend on the admittance matrix (that is, on the inverse of the reactance of the lines), therefore, the derivatives appearing in the Newton method will be sensitive to changes in the series reactance (see Appendix B). Second, the introduction of a new variable **xl** on the OPF problem increases the already large optimization space, which may increase the occurrence of saddle points.

For these reasons, it can be expected that the optimal control of FACTS devices via an OPF algorithm is not an easy task. The tests performed did indeed confirm this point. The convergence of the Newton iterations proved to be slow and there were also cases where optimality was lost during the tracking process (occurrence of critical points of type 1 or 2). In spite of these difficulties, the parametric algorithm was able to answer all the above questions. The results are summarized in the next chapter.

5.5 Conclusion

The use of an optimization algorithm in the operation of a transmission system is valuable not only because of the resulting optimal operating states. Ideally, an optimization must be able to provide us with information regarding the behaviour of the operating condition in case of changes in the conditions defining the problem. In addition, it is desirable that an optimization approach yield some insight into the optimal behaviour of the control variables. With the parametric approach, it is possible to gain a good understanding about the system operation in case of changes in the network topology, in the load demand and in the operational limits. While the simulation of contingencies is important to define a more secure operating state, sensitivity analysis is essential for making economical decisions. Throughout the load tracking, the approach provides us with the trajectories of the sensitivities of the total cost with respect to changes in the system load or in the operational limits. With this information, the cost of transmission transactions can be easily evaluated. In addition, it becomes easy to identify expensive bottlenecks in the system, whose elimination could produce important savings.

The special characteristics of the parametric approach also makes it a suitable tool to analyze the impact and steady-state optimal behaviour of new control mechanisms. In this thesis we used the Parametric-OPF to study the influence of FACTS devices. The method allows the direct representation of the variables present in the model, also providing the sensitivity of the optimal cost to changes in the operational limits of the variables existing on the FACTS model.

With this chapter we finish the description of the basic Parametric-OPF algorithm and of the special applications of the method. The results of the simulations performed in different test systems for Phase I and II, as well as for the special applications described in this chapter are presented in the next chapter.

CHAPTER 6

TESTS RESULTS

6.1 Introduction

The implementation of an OPF algorithm to solve real-life examples demands a considerable amount of time. If we consider that the number of variables existing in a real-life example is on average three times the number of buses in the network, then it can easily be seen that problems with more than two thousand variables are not unusual. This, together with the nonlinear (non-convex) characteristic of the problem are key factors of the difficulties associated with implementing an OPF algorithm. In these applications, the use of sparsity techniques or other procedures which can improve the computational time are a necessity. As a consequence, the interval of time between the conception of a new OPF method and the implementation of an algorithm that is efficient enough to be used by the power utilities can be of several years.

Although the parametric approach has been previously used in simplified formulations of the OPF problem, this thesis presents the first implementation of a general (nonlinear) parametric OPF algorithm. The main objective of this thesis was therefore to investigate the potential of this general OPF approach. The implementation of a commercially acceptable tool was not one of our objectives.

In this chapter, to analyze the performance of the approach, we first discuss the computational aspects of the Parametric-OPF algorithm. This is done by presenting the results of tests made in different systems considering different initial conditions, solution strategies for finding the optimal active set and objective functions. Next, we turn our

attention to the behaviour of the OPF solution during Phase I and II, considering contingencies as well as analyzing unsolvable cases. In addition, some results on sensitivity analysis are presented, emphasizing some aspects of economic transactions. Finally, some test results with FACTS devices are analyzed.

6.2 Computational Aspects

The Parametric-OPF was implemented in a SUN Sparc 10 workstation using MATLAB version 4.0. In the implementation, we took advantage of the facilities provided by MATLAB, specially the sparse matrix and the matrix manipulation facilities. However, in the Parametric-OPF algorithm, no higher level MATLAB functions such as the optimization toolbox or nonlinear equation solvers were used. Such higher level functions were programmed from basic functions. The MATLAB sparsity techniques used in the implementation are designed for a general mathematical problem, therefore, they do not take full advantage of the particular characteristics of the OPF problem. In addition, it is important to note that MATLAB is an environment rather than a programming language. As a consequence, the computational time of the MATLAB implementation of our OPF algorithm could almost certainly be sharply improved with other implementations using computer languages such as C or Fortran.

The Parametric-OPF method was tested in power systems of up to 118 buses under fixed and variable load conditions. The transmission and generation data of the systems used can be found in Appendix E.

In all the results shown, the termination criterion for the convergence of the Newton method was fixed at 10^{-6} p.u. for the errors on the first order optimality conditions.

The first group of tests presented in this section are organized as follows. For every one the three strategies used to find the optimal active set, that is, (i) binary search, (ii) forwards and backwards linear prediction and (iii) forwards linear prediction combined with backwards binary search, the method was tested with three different objectives: (a)

generation cost plus voltage profile deviation from normal, (b) transmission losses, (c) voltage profile deviation from normal. Combinations of these objective functions were also tested but are not included here for lack of space. Each simulation was carried out considering two different values for the initial guess of the optimum vector of decision variables, x^0, namely, flat voltage and an approximate AC load flow solution[1].

The second group of tests verifies the influence of the initial guesses of the vector of Lagrange multipliers λ^0 on the convergence of the algorithm. In these tests, different values of λ^0 were combined with the objective functions (a) and (b) described above while using binary search to find the active set.

The third group of tests analyzes the influence of the weighting factor w on the convergence of the algorithm. Here, some of the previous tests were repeated with a different value of w. For these tests, forwards and backwards linear prediction was used as the strategy to find the active set.

In the next group of tests, we analyze the influence of active line flow limits on the overall convergence of the Parametric-OPF by repeating some of the previous tests with more restrictive power flow limits. For these tests, only strategy (iii) was used to find the break-points of the optimal trajectories.

Finally, the convergence characteristics of the Phase I algorithm are tested considering variable series reactances. Here, some of the tests previously carried out with the binary search strategy were repeated.

Some of the tests conducted on Phase I of the algorithm were repeated in the load tracking phase (Phase II) in order to compare their respective computational effort. In these comparative tests, only the 34-bus and the IEEE 118-bus systems were used. The objective function was the transmission losses.

---

[1] Since the algorithm does not parameterize the limits on the decision variables, any variable, which in the load flow solution is outside its limits must be modified in order to satisfy the constraints.

6.2.1 Tests With Different Types of Predictors and x^0

The results presented in this subsection are for Phase I only. This study is not required for Phase II since the initial condition here is defined by the results of Phase I. The results presented here are related to four test systems of varying sizes, total load and reactive power levels. For every system, the tests with each mechanism used to control the changes in the active set are shown in a different Table. The first Table shows the results using the binary search mechanism. In the tests shown in the second Table, forwards and backwards linear prediction was used. Finally, in the third Table all tests were made with linear prediction forwards plus binary search backwards. The tests with binary search were done for two different $\Delta\varepsilon^{sp}$ in order to verify the sensitivity of the method to this quantity. In all tests, the initial Lagrange multipliers associated with the real power balance equations were set to the average of the generation incremental cost whereas the Lagrange multipliers associated with the reactive power balance equations were made equal to 1.

In the Tables below, an ε-*iteration* is any of the main loops present in Figure 4.8. A *trial* ε-iteration is defined as one where no changes in the active feasible set are implemented, in spite of existing violations (Cases III and IV of Figure 4.8). Normally, after a trial iteration, the value of ε is decreased until only one single violation occurs. A *good* ε-iteration is defined as one where the active feasible set could be kept constant or successfully updated (Cases I and II). The number of iterations of the Newton method associated with all ε-iterations, *NR-iter.*, is also presented in the Tables. The column *Time per* ε-*iteration* shows the average computational time of an ε-iteration in seconds, while the column *Total time* indicates the total computational time excluding initialization or the output. Finally, *Flat* and *L. flow* indicate whether the initial guess, x^0, is equal to the flat voltage profile or an approximate load flow solution.

The results for the 14-bus system are summarized in the next three Tables. For this network, in each Newton iteration, a system of a maximum of 53 equations must be solved.

Table 6.1- 14 bus system - binary search.

Case	X^0	# Good ε-iter.	# Good NR-iter.	# Trial ε-iter.	# Trial NR-iter.	Time per ε-iter. (sec.)	Total Time (sec.)
w_1=1 w_3=100 $\Delta\varepsilon^{sp}$=.1	Flat	13	39	2	9	5.18	93.3
	L. Flow	12	35	1	7	5.09	81.45
w_1=1 w_3=100 $\Delta\varepsilon^{sp}$=.2	Flat	9	27	4	19	5.03	84.88
	L. Flow	8	23	3	17	5.44	76.27
w_2=1 w=10 $\Delta\varepsilon^{sp}$=.1	Flat	22	85	6	24	5.30	174.93
	L. Flow	20	62	3	11	4.79	134.13
w_2=1 w=10 $\Delta\varepsilon^{sp}$=.2	Flat	No convergence of the NR method for $\varepsilon \approx 0.8$ due to ill conditioning.					
	L. Flow	16	47	4	15	4.77	119.28
w_3=1 w=10 $\Delta\varepsilon^{sp}$=.1	Flat	25	89	11	42	5.15	226.95
	L. Flow	22	81	11	40	5.17	217.3
w_3=1 w=10 $\Delta\varepsilon^{sp}$=.2	Flat	19	62	11	45	5.12	184.5
	L. Flow	18	59	12	45	5.06	197.56

The first thing to be noticed in Table 6.1 is that, although a larger $\Delta\varepsilon^{sp}$ generally led to a decrease in the number of good ε-iterations, the number of trials increased. In the case of loss minimization (4th case in Table 6.1), the larger $\Delta\varepsilon^{sp}$ even prevented the process to converge. This shows that a compromise exists between the value of the default increase in the parameter and the overall performance of the method.

Comparing the number of good Newton iterations presented in the three tables, is

Table 6.2- 14 bus system - linear prediction.

Case	x^0	# Good ε-iter.	# Good NR-iter.	# Trial ε-iter	# Trial NR-iter.	Time per ε-iter. (sec.)	Total time (sec.)
w_1=1 w_3=100	Flat	10	26	1	4	5.89	82.53
	L. Flow	12	33	0	0	6.31	94.70
w_2=1 w=10	Flat	15	39	6	24	6.37	165.65
	L. Flow	19	59	2	7	6.36	165.46
w_3=1 w=10	Flat	17	46	3	17	6.41	166.78
	L. Flow	16	38	3	15	6.37	165.66

Table 6.3- 14 bus system - linear prediction & binary search.

Case	x^0	# Good ε-iter.	# Good NR-iter.	# Trial ε-iter	# Trial NR-iter.	Time per ε-iter. (sec.)	Total time (sec.)
w_1=1 w_3=100	Flat	12	33	1	4	5.54	88.75
	L. Flow	12	33	0	0	6.03	90.50
w_2=1 w=10	Flat	16	45	6	24	5.80	157.20
	L. Flow	19	59	2	7	5.97	155.23
w_3=1 w=10	Flat	17	46	4	21	5.56	150.16
	L. Flow	22	60	4	18	5.70	188.35

also noticeable that this number is smaller for the linear prediction forwards and backwards, indicating that this mechanism provides the best prediction for the break-points. From the number of trial iterations, it can be seen that it is easier to minimize the generation costs plus voltage profile deviation from normal than to minimize transmission losses or the voltage profile deviation alone (probably because of the good convexity of the generation cost function). Also, note that the CPU time per ε-iteration is smaller for the binary search since this mechanism does not require the additional calculations needed by the linear prediction. The total CPU time in the binary search, on the other hand, can

be larger than the CPU times of the other strategies due to the better performance of the linear prediction. For these examples, although the number of trial iterations for the second strategy was the smallest, the best CPU times were obtained with the third strategy, suggesting that the computational expense of a backwards linear prediction is not worth using.

The following Tables 6.4-6.6 summarize the results for the 30-bus network. For this example, in each Newton iteration, a system of a maximum of 118 equations must be solved.

Table 6.4- 30 bus system - binary search.

Case	X^0	# Good ε-iter.	# Good NR-iter.	# Trial ε-iter.	# Trial NR-iter.	Time per ε-iter. (sec.)	Total Time (sec.)
w_1=1 w_3=100 $\Delta\varepsilon^{sp}$=.1	Flat	13	39	3	11	8.10	186.38
	L. Flow	13	37	7	27	8.88	231.00
w_1=1 w_3=100 $\Delta\varepsilon^{sp}$=.2	Flat	9	25	7	26	8.47	203.36
	L. Flow	9	25	9	35	9.19	220.77
w_2=1 w=10 $\Delta\varepsilon^{sp}$=.1	Flat	23	80	20	72	8.39	453.25
	L. Flow	15	46	5	19	9.73	272.72
w_2=1 w=10 $\Delta\varepsilon^{sp}$=.2	Flat	19	56	20	71	8.07	403.71
	L. Flow	12	34	9	42	10.61	307.83
w_3=1 w=10 $\Delta\varepsilon^{sp}$=.1	Flat	24	77	9	34	8.54	341.98
	L. Flow	19	68	2	8	10.29	277.83
w_3=1 w=10 $\Delta\varepsilon^{sp}$=.2	Flat	20	54	11	46	8.38	318.48
	L. Flow	16	50	5	22	10.30	288.55

The tests with different strategies using the 30-bus network suggest that the binary search mechanism becomes comparatively less efficient for a larger network. This is mainly due to the increase in the number of trial ε-iterations (and associated NR iterations) which does not compensate for a smaller CPU time per ε-iteration. For this network, the second mechanism of tracking the active set was found to be the most efficient one in terms of CPU time and number of good ε-iterations. In addition, $\mathbf{x}^0$ was found to have a stronger influence when using binary search because it yielded a

Table 6.5- 30 bus system - linear prediction.

Case	x^0	# Good ε-iter.	# Good NR-iter.	# Trial ε-iter	# Trial NR-iter.	Time per ε-iter. (sec.)	Total time (sec.)
w_1=1 w_3=100	Flat	11	24	0	0	9.02	153.48
	L. Flow	11	21	0	0	8.34	141.93
w_2=1 w=10	Flat	19	49	3	9	8.45	270.58
	L. Flow	16	42	2	6	10.23	255.77
w_3=1 w=10	Flat	20	55	3	13	10.69	310.22
	L. Flow	15	41	1	4	9.99	219.88

Table 6.6- 30 bus system - linear prediction & binary search.

Case	x^0	# Good ε-iter.	# Good NR-iter.	# Trial ε-iter	# Trial NR-iter.	Time per ε-iter. (sec.)	Total time (sec.)
w_1=1 w_3=100	Flat	11	24	0	0	8.86	150.70
	L. Flow	11	22	0	0	8.70	147.98
w_2=1 w=10	Flat	20	52	3	9	9.03	298.08
	L. Flow	20	56	2	6	9.63	279.43
w_3=1 w=10	Flat	20	55	3	13	9.63	279.53
	L. Flow	15	41	1	4	10.80	237.65

considerable difference in the number of trial iterations between the flat and load flow starts.

The following Tables 6.7 - 6.9 show the results for the 34-bus system. For this example, in each Newton iteration, a system of a maximum of 147 equations must be solved.

Table 6.7- 34 bus system - binary search.

Case	X^0	# Good ε-iter.	# Good NR-iter.	# Trial ε-iter.	# Trial NR-iter.	Time per ε-iter. (sec.)	Total Time (sec.)
w_1=200 w_3=1000 w=10 $\Delta\varepsilon^{sp}$=.05	Flat	62	210	82	341	6.20	1176
	L. Flow	39	171	48	314	8.17	956
w_1=200 w_3=1000 w=10 $\Delta\varepsilon^{sp}$=.1	Flat	61	204	119	528	6.50	1458
	L. Flow	34	149	71	463	8.40	1137
w_2=1000 w=20 & w=600 $\Delta\varepsilon^{sp}$=.05	Flat	78	272	177	750	6.30	2098
	L. Flow	51	231	57	319	7.60	1150
w_2=1000 w=20 & w=600 $\Delta\varepsilon^{sp}$=.1	Flat	No convergence of the NR method for $\varepsilon \approx 0.9$ due to ill-conditioning.					
	L. Flow	45	206	74	451	7.7	1268
w_3=1000 w=10 $\Delta\varepsilon^{sp}$=.05	Flat	At $\varepsilon \approx 0.48$ critical point of type 4.					
	L. Flow	33	145	18	81	6.74	445
w_3=1000 w=10 $\Delta\varepsilon^{sp}$=.1	Flat	At $\varepsilon \approx 0.48$ critical point of type 4.					
	L. Flow	24	92	19	87	6.53	379

The 34-bus system is characterized by high levels of reactive power and voltage instability. In spite of its relatively small size, this system posed the greatest difficulties for the convergence of the Parametric-OPF algorithm. This is noticeable from the CPU times shown in Tables 6.7-6.9. For this system, only the case of minimization of generation cost plus voltage profile deviation from flat was successfully solved by all

Table 6.8- 34 bus system - linear prediction.

Case	x^0	# Good ε-iter.	# Good NR-iter.	# Trial ε-iter	# Trial NR-iter.	Time per ε-iter. (sec.)	Total time (sec.)
w_1=200 w_3=1000 w=10	Flat	74	224	6	19	7.31	885
	L. Flow	39	164	3	17	10.02	691
w_2=1000 w=20 & w=600	Flat	94	302	9	28	7.50	1222
	L. Flow	62	351	12	51	9.3	1036
w_3=1000 w=10	Flat	At ε≈ 0.42 critical point of type 4.					
	L. Flow	24	68	11	50	7.31	365.68

Table 6.9- 34 bus system - linear prediction & binary search.

Case	x^0	# Good ε-iter.	# Good NR-iter.	# Trial ε-iter	# Trial NR-iter.	Time per ε-iter. (sec.)	Total time (sec.)
w_1=200 w_3=1000 w=10	Flat	76	241	7	23	7.21	894
	L. Flow	43	183	3	17	9.08	663
w_2=1000 w=20 & w=600	Flat	96	313	6	19	7.00	1129
	L. Flow	71	377	14	56	8.80	1076
w_3=1000 w=10	Flat	At ε≈0.42 critical point of type 4.					
	L. Flow	27	94	7	39	6.83	321

strategies for the two adopted initial solutions. The minimization of transmission losses starting from flat voltage profile could not be done using $\Delta\varepsilon$=0.1 because of ill-conditioning of the Newton method matrix, H. Since a smaller increment in ε solved this problem, this is a case of ill-conditioning which does not occur with small increments or when linear prediction is used, showing the better precision of this last approach when compared with the binary search. The difficulty of the minimum loss problem also led to

different values of the weighting factor, w, depending on the initial guess. When $\mathbf{x}^0$ is made equal to the flat voltage, w=10 is enough to guarantee a initial optimal solution and good convergence of the Newton process; however, for $\mathbf{x}^0$ equal to the approximate load flow solution, w=600 must be used to assure the success of the tracking process. The case of minimization of the voltage deviation from normal also posed difficulties. Because the optimization space for this test system is considerably larger than the one of the 30-bus network, the occurrence of saddle points increases. This is the case with the optimization of the voltage profile. When all variables of the problem are free, at ε=1 we have a critical point of type 7. Thus, to be able to perform the optimization, some of the variables had to be fixed. For the case shown in Tables 6.7-6.9, **qg**(18), **qg**(27), **b**(18) and **b**(27) were fixed at the minimum. Although this recourse made possible the optimization process, it also created another problem for the tracking: the appearance of a critical point of type 4 in the optimal trajectory originated at $\mathbf{x}^0$ equal to flat voltage. In such situation a strategy such as described in Appendix D may be useful to permit the continuity of the tracking process, but even when the tracking can proceed, the computational time is much higher than in normal cases.

A comparison of the computational times and number of trial iterations shows once more the better performance of the strategies based on forwards linear prediction. In addition, when comparing the number of NR iterations of Tables 6.8 and 6.9, it can be seen that the forwards and backwards linear prediction provides a better guess for the break-point. In spite of this fact, the computational time of the third strategy (forward linear prediction and backwards binary search) is smaller in half of the cases studied due to the smaller CPU time per ε- iteration.

The results of the tests made with the IEEE 118-bus system are summarized in the next three Tables. For this example, in each Newton iteration, a system of a maximum of 490 equations must be solved

Table 6.10- 118 bus system - binary search.

Case	X^0	# Good ε-iter.	# Good NR-iter.	# Trial ε-iter.	# Trial NR-iter.	Time per ε-iter. (sec.)	Total Time (sec.)
w_1=1 w_3=1000 w=10 $\Delta\varepsilon^{sp}$=.05	**Flat**	31	110	24	120	16.30	1242
	L. Flow	33	179	47	532	29.80	3064
w_1=1 w_3=1000 w=10 $\Delta\varepsilon^{sp}$=.1	**Flat**	No convergence of the NR method at ε≈0.90 due to ill-conditioning.					
	L. Flow	26	131	64	685	31.00	3508
w_2=1000 w=10 & w=100 $\Delta\varepsilon^{sp}$=.05	**Flat**	74	263	133	700	17.30	4565
	L. Flow	86	445	214	2081	27.00	10224
w_2=1000 w=10 & w=100 $\Delta\varepsilon^{sp}$=.025	**Flat**	80	294	86	444	16.70	3724
	L. Flow	92	491	158	1582	27.40	8852
w_3=1000 w=10 $\Delta\varepsilon^{sp}$=.05	**Flat**	At ε≈1 trajectory loses optimality and newton method does not converge (type 2 of critical points).					
	L. Flow	At ε=0.99, $\mathbf{qg}_{65}$ is released from its min. limit and the trajectory loses optimality (critical point of type 1).					
w_3=1000 w=10 $\Delta\varepsilon^{sp}$=.025	**Flat**	At ε≈1 trajectory loses optimality and newton method does not converge (type 2 of critical points).					
	L. Flow	At ε=1, $\mathbf{qg}_{65}$ is released from its min. limit and the trajectory loses optimality (critical point of type 1).					

The comparison of the results shown on Tables 6.10-6.12 shows the better performance of the second and third strategies. The difference in CPU time between the

Table 6.11- 118 bus system - linear prediction.

Case	x^0	# Good ε-iter.	# Good NR-iter.	# Trial ε-iter	# Trial NR-iter.	Time per ε-iter. (sec.)	Total time (sec.)
w_1=1 w_3=1000 w=10	Flat	34	110	0	0	15.58	858
	L. Flow	39	208	3	36	24.0	1491
w_2=1000 w=10	Flat	87	286	3	17	17.1	2482
	L. Flow	97	492	10	132	26.2	4669
w_3=1000 w=10	Flat	44	121	2	38	15.6	1156
	L. Flow	At ε=1, the problem loses optimality (critical point of type 1) and Newton method does not converge.					

Table 6.12- 118 bus system - linear prediction & binary search.

Case	x^0	# Good ε-iter.	# Good NR-iter.	# Trial ε-iter	# Trial NR-iter.	Time per ε-iter. (sec.)	Total time (sec.)
w_1=1 w_3=1000 w=10	Flat	36	118	0	0	15.12	847
	L. Flow	40	219	2	25	24.70	1534
w_2=1000 w=10	Flat	92	302	7	30	16.5	2567
	L. Flow	102	510	11	137	23.40	4349
w_3=1000 w=10	Flat	47	134	2	44	16.70	1286
	L. Flow	At ε=1, the trajectory loses optimality (critical point of type 1) and Newton method does not converge.					

binary search based Parametric-OPF and the other two implementations tends to increase with the number of buses and with the type of objective function. For this system, the default increment on ε again proved to be a key factor for the convergence of the strategy using binary search. In addition, the large number of variables here, led to the occurrence of a critical point of type 7 in the case of optimization of the voltage profile. To be able

to optimize the voltage profile, the active generations in all buses except for the slack bus had to be fixed, thus solving only the reactive OPF problem. Even with this simplification of the optimization problem, the binary search mechanism was not successful. Because the last change in the active set occurs at ε=0.9997 (a transformer tap is fixed at the maximum limit), the Parametric-OPF using default increment in ε equal to 0.05 or 0.025 did not make this last change in the optimal active set before reaching ε=1. As a result, when ε is made equal to 1, the proximity of a critical point of type 2 causes the failure of the Newton method. Since the linear prediction based approach could determine all necessary changes in the optimal active set before reaching ε=1, this approach could reach the final solution.

The strategy based on forwards and backwards linear prediction was found to be computationally more expensive for half of the cases tested, in spite of yielding a smaller number of ε-iterations and Newton iterations when compared with the mechanism based on the combination of linear prediction and binary search.

The importance of a good initial solution is noticeable in the tests with this last network, specially for the binary search. Particularly, in the problem of minimizing the voltage deviation from 1.0 p.u., for the 118-bus system, a bad choice for x^0 (far from the flat voltage profile) also led to the failure of the tracking process even when the strategy was based on linear prediction.

It is interesting to note that for some of the tests, the computational time of the 34-bus network was not very different from those of tests with the 118-bus network, suggesting that the performance of the method depends not only on the size of the network but also on the reactive power level and on how heavily loaded the network is.

As a general conclusion, we may say that the overall performance of the binary search is worse than that of the linear prediction, specially for larger and/or more complex systems. Unfortunately, not all cases have an optimal solution and a reformulation of the problem was necessary when testing the method on the last two networks (34 and 118). Even if there is an optimum, in some cases the method is not able to find the solution of

the problem, which shows the importance of a careful choice of $\mathbf{x}^0$ and $\Delta\varepsilon^{sp}$. In spite of this fact, the method can differentiate the various causes for failure and an eventual solution for the various types of critical points which may appear in the optimal trajectories may increase considerably the robustness of the Parametric-OPF algorithm.

Although, during Phase I, the tracking process can be very slow due to the number of changes in the active set (which directly influences the number of good and trial ε-iterations), the tracking process was found to be much faster during Phase II. In Table 6.13 the average number of ε-iterations and Newton iterations are represented for the 34-bus system and the 118-bus system when minimizing the transmission losses in the load tracking mode. In these tests the mechanism composed of linear prediction forwards and binary search backwards was used to control the changes in the optimal active set. The load curve being tracked is presented in Figure 6.2. The load decreases, at first, until 86 percent of the total load and, subsequently, increases until 120 percent of the total load. The load variation between the intervals was either 2 or 1 percent. For the 34-bus system, 1 percent of load variation corresponds to a change in 198.6 MW in the total load, whereas for the 118-bus system, 1 percent of the total load is equal to 42.2 MW. This difference in the total load, together with the high level of reactive power of the 34-bus system, are the main reasons for the similar computational times of the tests.

As can be seen by comparing Tables 6.9 and 6.12 with Table 6.13, *the total CPU times of Phase I, for both test systems, are approximately 10 times the average CPU time for Phase II.* In fact, the computational times obtained for Phase II are not prohibitive in an on-line environment, indicating that, although the Parametric-OPF can be slow when solving the initial OPF problem (with fixed load), it has great potential in the optimal tracking of a load curve.

6.2.2 Tests With Different λ^0

The choice of the initial Lagrange multiplier associated with the equality constraints was arbitrary. Their influence on the convergence of the method was found to be smaller than the influence of $\mathbf{x}^0$. In the Tables below, are shown the results of tests

Table 6.13- Results for Phase II.

System	Case	Average Good ε-iter.	Average Good NR-iter.	Average Trial ε-iter.	Average Trial NR-iter.	Average time per ε-iter. (sec.)	Average total time (sec.)
34-bus	w_2=1000 w=20	13	42	2	7	6.34	116.63
118-bus	w_2=1000 w=10	7	26	1	5	17.31	143.12

done with different λ^0 in three different systems. In the cases presented in the first Table, the objective was to minimize generation cost plus voltage profile deviation from normal. In the case of the second Table, the objective was to minimize transmission losses. In all tests only the binary search mechanism was used to determine the break-points and the initial guess was considered to be an approximate load flow solution (the same used for the tests presented in section 6.2.1). In these tests, the Lagrange multipliers associated with the real and reactive power balance equations (α^0 and β^0, respectively) were varied independently. Here, a "sparse" formulation of the Parametric-OPF problem was used. In this model, the reactive generations are also considered as decision variables (not as functional inequalities) and line flow limits are not considered. In addition, the cost coefficients are different from those used in the previous tests. As a result, the computational times related below are on the average smaller than those presented in the previous Tables (6.1-6.9). However, the influence of λ^0 for both the compact and sparse formulations is similar. In the Tables below, α^* and β^* are the optimal values of these Lagrange multipliers for ε=1 whereas α^{or} and β^{or} correspond to the usual initialization for these Lagrange multipliers (that is, α^0 equal to the average of the generation incremental cost and β^0 equal to 1).

Table 6.14- Optimization of generation cost plus voltage profile with different λ^0.

System	Case	α^0	β^0	# Good ϵ-iter.	# Good NR-iter.	# Trial ϵ-iter.	# Trial NR-iter.	Total time (sec.)
14-bus system	w_1=1, w_3=100, α^{or}= -.43, β^{or}=1, $\alpha^* \approx$ -5, $\beta^* \approx$ 0.1 $\Delta\epsilon$=0.1	α^{or}	β^{or}	12	32	0	0	34
		α^*	β^*	12	33	0	0	35
		-.43	0	12	27	0	0	29
		0	0	12	26	0	0	29
		2	1	12	36	0	0	32
30 bus system	w_1=1, w_3=100, α^{or}=-.2, β^{or}=1, $\alpha^* \approx$ -6, $\beta^* \approx$ -5 $\Delta\epsilon$=0.1	α^{or}	β^{or}	14	40	10	41	107
		α^*	β^*	13	57	7	42	143
		-0.2	0	15	35	10	26	90
		0	0	15	34	10	25	84
		2	1	17	55	15	75	151
34 bus system	w_1=1, w_3=200, w=10, α^{or}=-12, β^{or}=1, $\alpha^* \approx$ -158, $\beta^* \approx$ 1.3 $\Delta\epsilon$=0.05	α^{or}	β^{or}	55	201	64	284	522
		α^*	β^*	59	331	61	394	721
		-12	0	57	199	63	273	513
		0	0	58	159	63	230	453
		2	2	53	264	65	369	660

From the Tables 6.13 and 6.14 it can be seen that the influence of α^0 and β^0 is smaller than the influence of $\mathbf{x}^0$. Although their values affect the convergence of the Newton method, the number of ϵ-iterations is not affected in most of the cases. In addition, it is interesting to notice that making α^0 equal to the average of the generator

Table 6.15- Minimization of transmission losses with different λ^0.

System	Case	α^0	β^0	# Good ε-iter.	# Good NR-iter.	# Trial ε-iter.	# Trial NR-iter.	Total time (sec.)
14-bus system	w_2=100, w=5, α^{or}= **-.43**, β^{or}=**1**, $\alpha^*\approx$ **-110**, $\beta^*\approx$ **0** $\Delta\varepsilon$=0.1	α^{or}	β^{or}	13	36	4	24	56
		α^*	β^*	No convergence of NR method for ε=.1				
		-.43	0	13	38	4	16	50
		0	0	13	38	4	14	48
		2	2	13	39	4	46	81
30 bus system	w_2=100, w=10, α^{or}=**-.2**, β^{or}=**1**, $\alpha^*\approx$ **-112**, $\beta^*\approx$ **-1** $\Delta\varepsilon$=0.1	α^{or}	β^{or}	15	44	18	167	193
		α^*	β^*	17	55	23	346	329
		-0.2	0	18	44	22	62	126
		0	0	18	43	22	61	123
		2	2	15	40	18	95	141
34 bus system	w_2=100, w=10, α^{or}=**-12**, β^{or}=1, $\alpha^*\approx$ **-1030**, $\beta^*\approx$ **9.7** $\Delta\varepsilon$=0.05	α^{or}	β^{or}	46	194	75	420	558
		α^*	β^*	46	730	66	1901	1947
		-12	0	43	167	76	359	501
		0	0	44	136	76	246	413
		2	2	45	283	76	727	830

incremental costs is not the best possible choice even when minimizing the generation costs. Similarly, making the values of α^0 and β^0 equal to their optimal values was the worst initialization for all tested systems (!!) and minimization criteria, whereas α^0=**0** and β^0=**0** were the best choices.

6.2.3 Tests With Different w

To assess the influence of the weighting factor associated with the parameterized quadratic term, some of the tests presented in section 6.2.1 were repeated with a different value for w. For this new set of tests, the objective was the minimization of transmission losses while forwards and backwards linear prediction was used to find the break-points. Also, in all tests $\mathbf{x}^0$ is equal to the flat voltage profile.

Table 6.16- Tests with different weighting factors, w.

System	Case	# Good ϵ-iter.	# Good NR-iter.	# Trial ϵ-iter.	# Trial NR-iter.	Time per iter. (sec.)	Total time (sec.)
14-bus	w_2=1, w=1	21	430	2	53	21.38	598
	w_2=1 w=10	15	39	6	24	6.37	166
30-bus	w_2=1 w=1	16	220	3	11	24.38	658
	w_2=1 w=10	19	49	3	9	8.45	270
34-bus	w_2=1000 w=40	100	322	9	33	7.20	1277
	w_2=1000 w=20	94	302	9	28	7.50	1222
118-bus	w_2=1000 w=200	72	251	8	47	17.30	2368
	w_2=1000 w=10	87	286	3	17	17.10	2482

Table 6.15 shows that the influence of the parameterized weighting factor, w, is in some cases, considerable. For the 14-bus and 30-bus systems, smaller w's yielded a great increase in the number of Newton iterations and consequently of the CPU time, whereas a faster convergence of the program was obtained by choosing a smaller w for

the 34-bus network and a larger w for the 118-bus network. Since this term affects the characteristics of the problem under study, its best value would be a balance between the desirable convexity (and consequently, better convergence of Newton method) and the desirable perturbation of the original problem, which will bring, as a consequence, an increase in the number of ε-iterations.

6.2.4 Tests Considering Line Limits

In all tests presented previously, no line limit was activated during the tracking process. To assess the influence of such constraints on the performance of the Parametric-OPF some tests were repeated with active line limits. In all cases, the mechanism composed of linear prediction plus binary search was used to find the optimal active set with the initial guess of $\mathbf{x}$ equal to the flat voltage profile. The results are presented in Table 6.17. In this Table, $\mathbf{pl}^{cr}$ represents the power flow on that specific line without imposing any limit, whereas **pl** is the limited power flow.

The results of Table 6.17 show that the existence of active power flow limits increases considerably the computational time of the Parametric-OPF. Because of the adoption of restrictive limits on the active generation, for the 14, 30 and 34 bus systems, only mild enforcements of line flows did not lead to critical points of type 3 or 4. Note that the largest increase in the number of iterations and computational time occurred for the 34-bus network, again showing the great difficulties of operating the system, specially when a limit on power flow is imposed. As a result, for all test systems, the final CPU time increases when power flow limits become active in the optimization process.

6.2.5 Tests Considering FACTS Devices

Finally, the influence of Flexible AC Transmission Systems (FACTS) on the convergence of the method was analyzed by repeating some of the previous tests. In this study, only the binary search mechanism was used to obtain the break-points of the optimal trajectory. The initial solution was made equal to the approximate load flow

Table 6.17- Tests with active line flow limits.

System	Case	Line flow limit.	# Good ε-iter.	# Good NR-iter.	# Trial ε-iter.	# Trial NR-iter.	Time per iter.	Total time
14-bus	w_1=1, w_3=100 pl_7=0.62 pl_7^{or}=0.66	**Inact.**	10	26	1	4	5.89	82
		Active	19	55	3	10	7.02	232
30-bus	w_1=1 w_3=100 pl_7=0.71 pl_7^{or}=0.75	**Inact.**	11	24	0	0	9.02	141
		Active	14	37	1	4	10.42	250
34-bus	w_1=200 w_3=1000 w=10 pl_{12}= -16.1 pl_{12}^{or}= -15.2	**Inact.**	74	224	6	19	7.31	885
		Active	137	494	38	151	8.90	2358
118-bus	w_1=1 w_3=1000 w=10 pl_{129}= -1.5 pl_{129}^{or}= -2.1	**Inact.**	34	110	0	0	15.58	858
		Active	37	122	1	5	15.70	926

solution and the initial Lagrange multipliers associated with the equality constraints are the same used in section 6.2.1.

Table 6.18 shows a significant increase in the total CPU time when variable series reactances are considered in the optimization. Besides the increment in the time per ε-iteration, the number of iterations also increase, specially for the 34-bus and 118-bus networks. The difference in CPU time between cases with and without FACTS devices increases when the number of devices augments, mainly because the number of Newton iterations increases. Eventually, the optimization is only possible with the adoption of a large parameterized weighting factor, w, which makes the problem more convex and improves the performance of the Newton method.

Table 6.18- Tests considering variable series reactances.

System	Case	Mode	# Good ε-iter.	# Good NR-iter.	# Trial ε-iter.	# Trial NR-iter.	Time per iter (sec.).	Total time (sec.)
14-bus	w_2=1, w=50 Δε=0.1 test with $\mathbf{xl}_2$	**Fixed**	23	68	4	14	4.70	151
		Variable	24	72	5	26	5.97	209
30-bus	w_2=1 w=50 Δε=0.1 test with $\mathbf{xl}_3$	**Fixed**	26	73	21	70	7.16	444
		Variable	25	70	18	65	8.88	515
34-bus	w_2=1000 w=50 Δε= 0.05 test with $\mathbf{xl}_{20}$	**Fixed**	88	309	177	765	6.2	2069
		Variable	94	352	172	796	8.3	2811
118-bus	w_2=1000 w=10 Δε= 0.05 test with $\mathbf{xl}_{57}$	**Fixed**	74	263	133	700	17.30	4565
		Variable	87	303	165	851	18.9	5894

With this, we finish the discussion of the computational aspects of the Parametric-OPF algorithm. In the next section we present results that are related to the general aspects of the optimal operation of a generation-transmission system.

6.3 Studies on the Optimal Operation of a Power System with the Parametric-OPF.

The use of an optimization program in the active and reactive power optimal dispatch is not trivial. The amount of time that must be spent in introducing an OPF package into an engineering environment has given rise to discussion about the possible savings that can be achieved by operating a generation-transmission system near the

optimum. In addition, the fact that nonlinear based OPF algorithms are not always able to find a solution to the problem of optimal operation the power system has made even more difficult their acceptance by the utilities. The question that has been in researchers' mind is that, since the load flow algorithm is nowadays considered a robust tool and, for this reason, widely used in power utilities, and since there has been great developments in optimization methods in the past decades, why is it so difficult to solve the OPF problem? How to differentiate between an unsolvable case and a case where the algorithm fails to find a solution? These appear to be questions that need to be answered before discussing the possible benefits of having an OPF package in a control centre.

Following this discussion, we here start the discussion of some aspects of the optimal operation of a power system by studying the behaviour of the optimal solutions of the Parametric-OPF problem. Later on, we discuss the benefits of optimal steady state operation.

6.3.1 The Behaviour of the Optimal Power Flow Solutions under Parameter Variations

The first aspect to be analyzed here is related to the difficulties encountered in solving the OPF problem. Because the parametric approach dismembers the problem through the use of the model parameters, it is useful in the study of the optimal behaviour of the solution trajectories both for Phase I and Phase II. To make this analysis, we show in Figures 6.1.a-6.1.i the optimal trajectories of some chosen variables of the 34-bus system and their corresponding Lagrange multipliers. These trajectories correspond to the problem of minimization of transmission losses starting from the flat voltage profile. The results are presented in per unit for a 100 MVA basis.

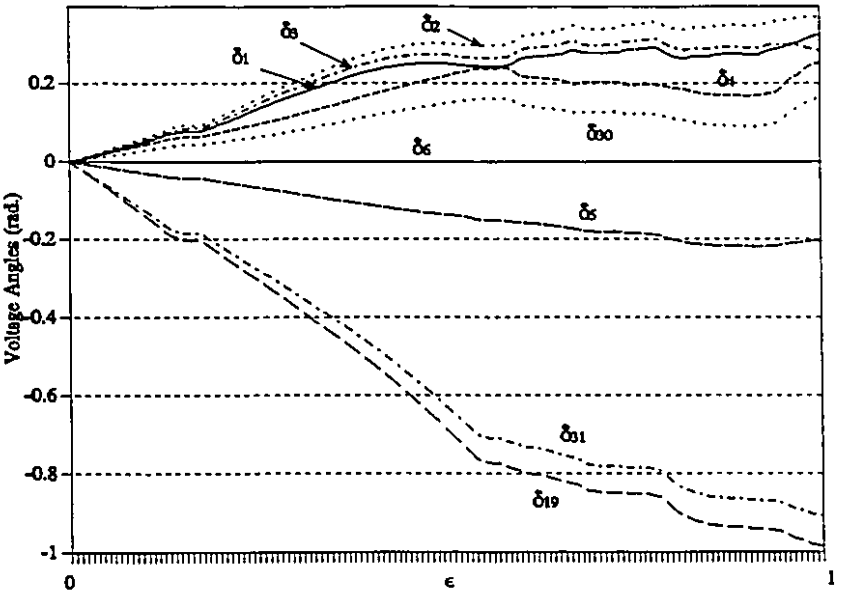

Figure 6.1.a- Voltage angles - Phase I.

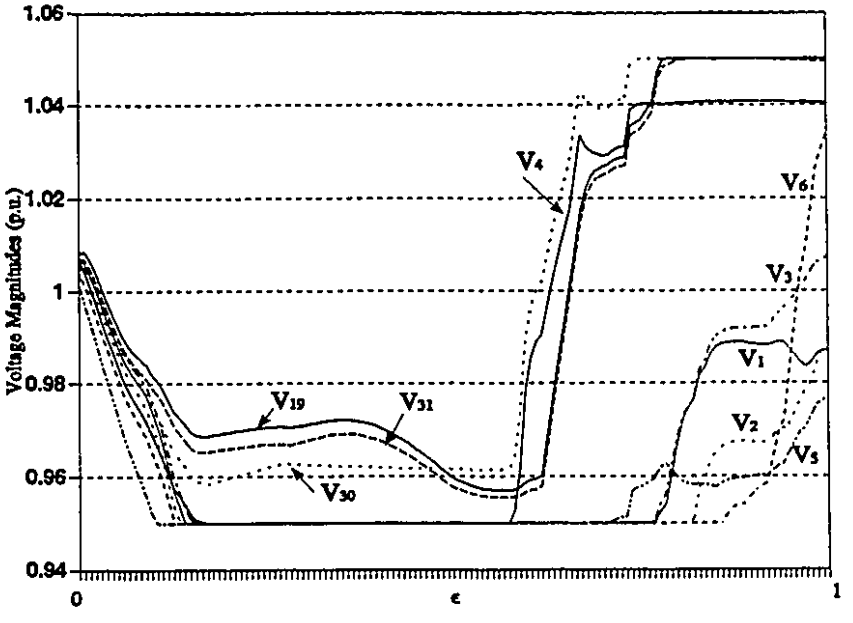

Figure 6.1.b- Voltage magnitudes - Phase I.

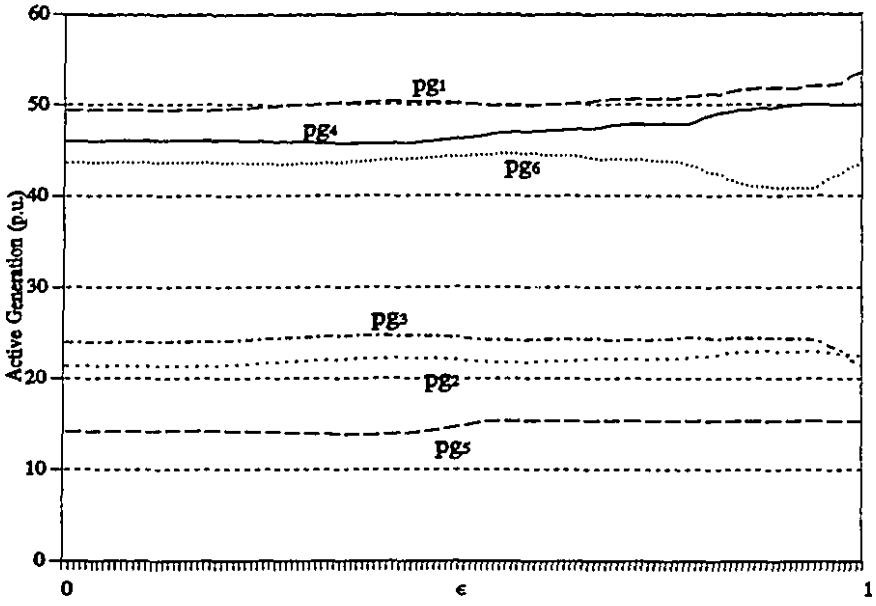

Figure 6.1.c- Active Generation - Phase I.

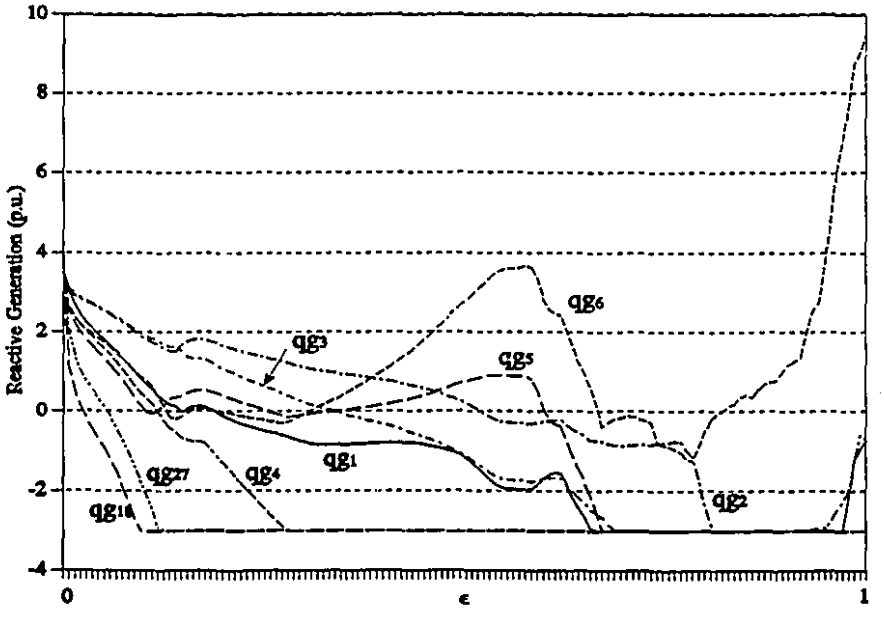

Figure 6.1.d- Reactive generation - Phase I.

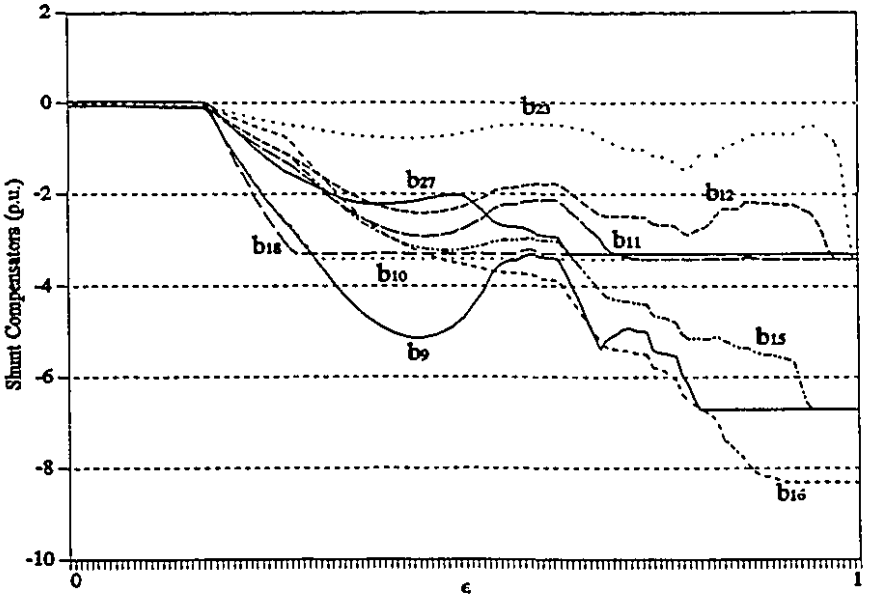

Figure 6.1.e- Shunt compensators - Phase I.

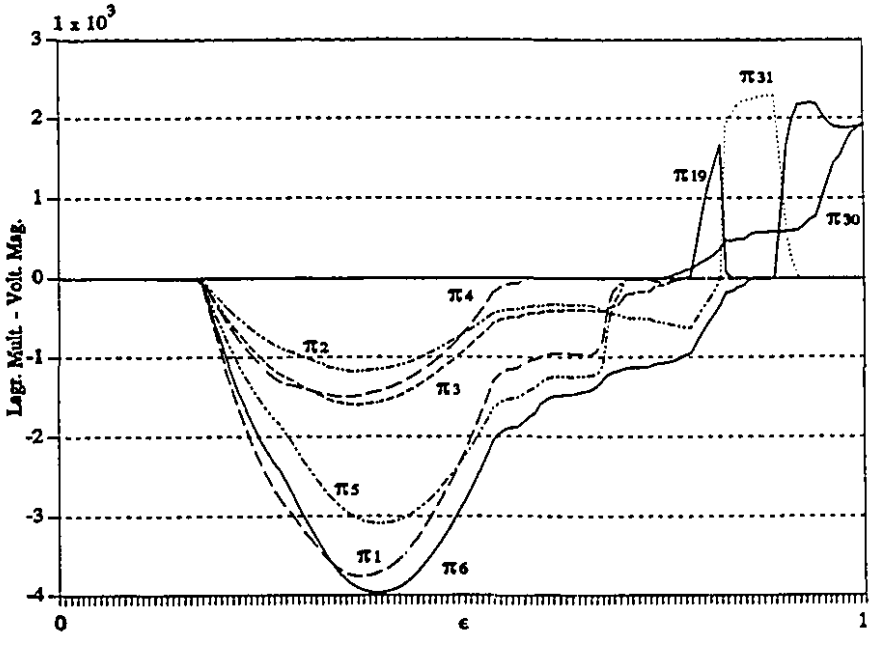

Figure 6.1.f- Lagrange multipliers of voltage magnitudes - Phase I.

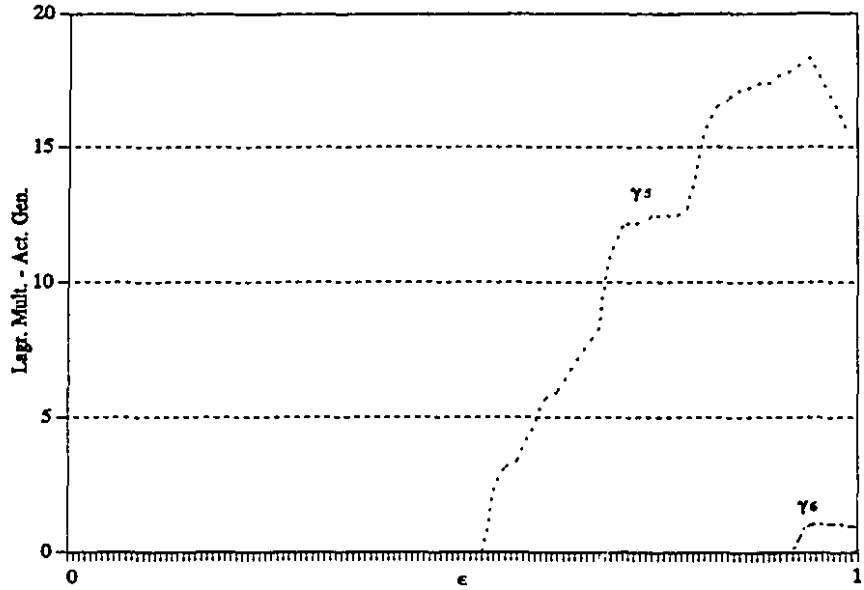

Figure 6.1.g- Lagrange multipliers of active generation - Phase I.

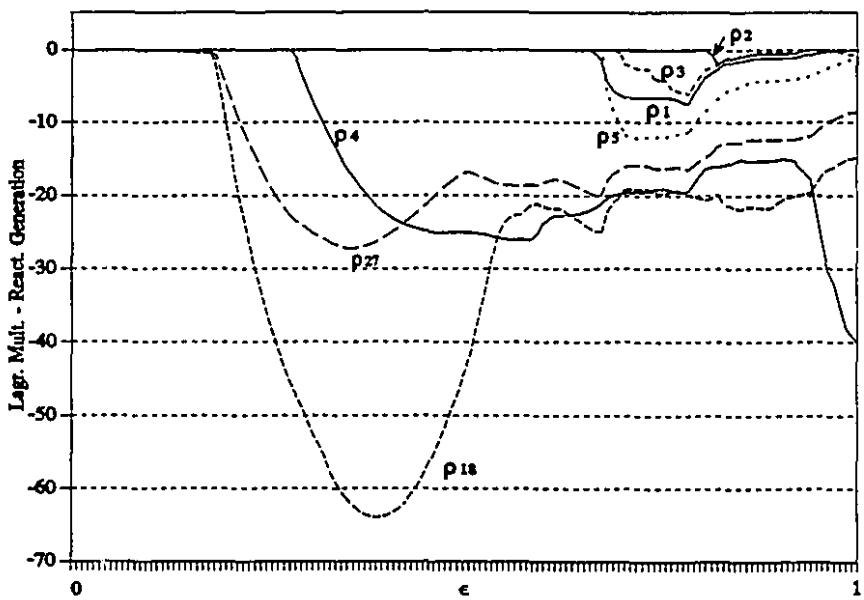

Figure 6.1.h- Lagrange multipliers of reactive generation - Phase I.

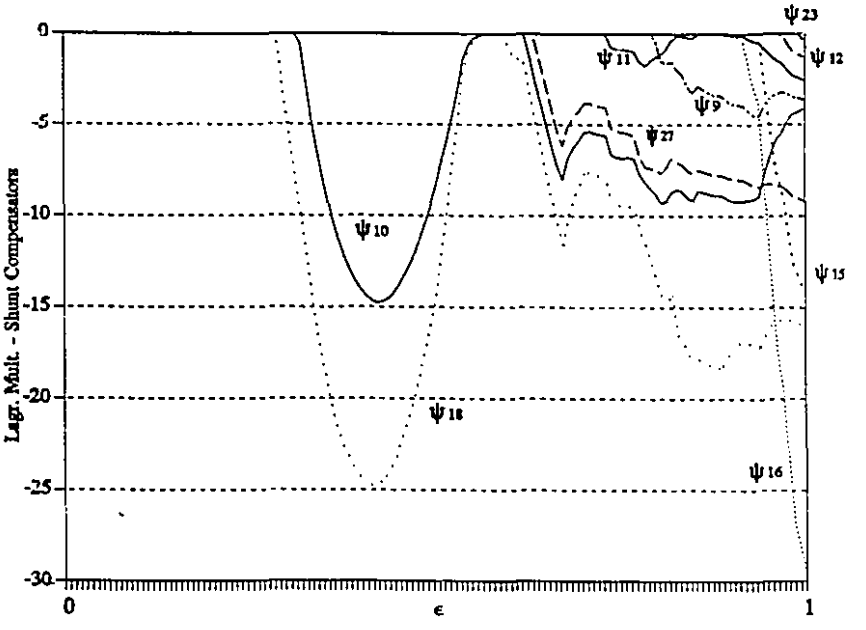

Figure 6.1.i- Lagrange multipliers of shunt compensators - Phase I.

The first noticeable aspect of the solution trajectories is the almost linear behaviour of the voltage angles and active power generation compared with the very nonlinear behaviour of the voltage magnitudes, reactive generation and shunt compensators. This is in accordance with the general knowledge that a reasonably good approximation for the active OPF sub-problem can be achieved with linear models whereas for the reactive sub-problem linear models do not yield reliable results. In addition, this confirms the high level of reactive power and voltage instability of the 34-bus system.

The optimal trajectories of the Lagrange multipliers also give us valuable information about the behaviour of the optimal solutions throughout the optimization process. Specially for the voltage magnitudes and static compensators these Lagrange multipliers show a very erratic behaviour, thus indicating that the "tendency" of such variables to stay fixed changes even with an incremental change in ε. As an example of such behaviour, we refer to Figure 6.1.f where the Lagrange multipliers of the voltage magnitudes are depicted. By the values of some of these Lagrange multipliers we can see, first of all, that the optimal voltage magnitudes are extremely sensitive to parameter variations, thus some of these voltages (fixed at the minimum) at some point of the

tracking have their Lagrange multipliers smaller than -3000 while other voltages (fixed at the maximum) have their Lagrange multipliers larger than 2000. Also notice the behaviour of the Lagrange multipliers of the voltages at bus 19 and 31 around ε=0.9. These two buses are interconnected and as a result their voltage have more or less the same behaviour (see Figure 6.1.b). During the tracking process, $\mathbf{V}_{19}$ is the first to be fixed at its maximum, and the sharp increase of its Lagrange multiplier indicates that such a limit is very severe. However, as soon as $\mathbf{V}_{31}$ reaches its maximum limit, there is an abrupt change in the trajectory of the Lagrange multiplier associated with $\mathbf{V}_{19}$, indicating that these two voltages cannot be fixed at the limit at the same time. Later on, the optimization process "asks" that $\mathbf{V}_{19}$ be fixed once more at its maximum. As a consequence, $\mathbf{V}_{31}$ has to be released almost immediately (as indicated by the abrupt change on the trajectory of its Lagrange multiplier). This sort of behaviour is not uncommon for variables of the reactive OPF sub-problem and it is a very good indication of the difficulties that have been encountered by researchers to solve the OPF. Because of such behaviour, the definition of an optimal active feasible set is a complex task and a wrongly chosen active set can lead to ill-conditioning of the Newton matrix (in this example, it is not possible to increase ε directly to 1 with these two voltages fixed at their maximum and solve the problem because the Newton method does not converge).

In the same way that the parametric approach is able to give us a very good insight into the behaviour of the OPF variables during the optimization process, this method also provides valuable information regarding the behaviour of the optimal solution under variation of the system load.

The next Figures show the optimal solution trajectories of variables of the 34-bus system during Phase II. The objective function used in the tracking is again the transmission losses and the same variables represented in Figures 6.1.a-6.1.e are depicted. During the load tracking the Parametric-OPF followed the load curve represented in Figure 6.2. In the process, all the loads of the system are multiplied by the same load factor (Figure 6.2) which implies that they have different increments. For the 34-bus system, the minimum load that can be attained starting from the optimal solution of Phase

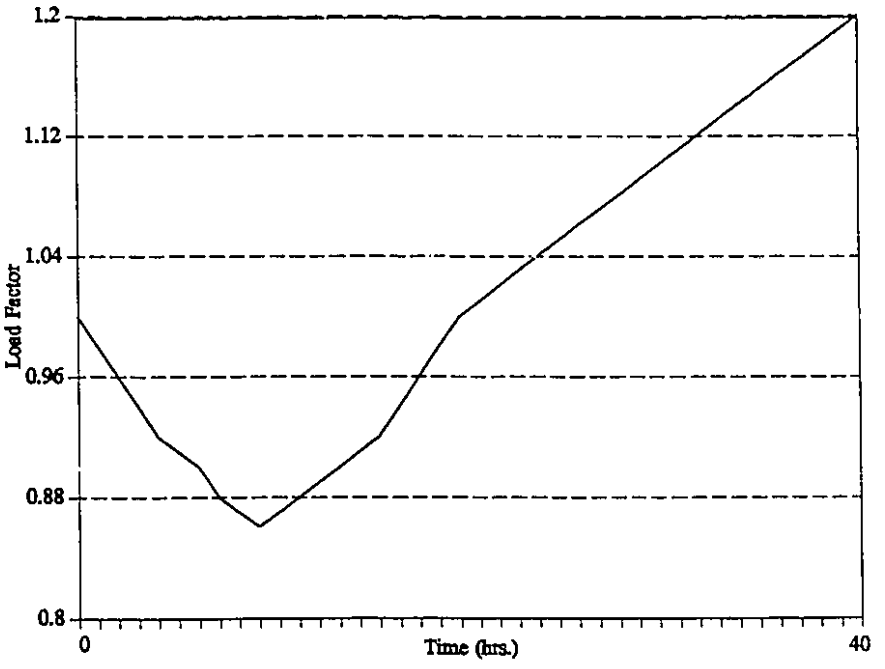

Figure 6.2.- Load factor.

I is equal to 86% of the total load whereas the maximum load that can be supplied is equal to 104% of the total load. Below the minimum limit, the optimal tracking cannot continue without a "jump" to another optimal trajectory because of the occurrence of a critical point of type 1 (saddle point) after the release of a previously fixed variable. The maximum load limit, on the other hand, is defined by the existence of a critical point of type 3 on the optimal trajectory, indicating the loss of structural stability and that the feasible set becomes locally empty beyond this limit. Note that for the 34-bus network, 1% of the total load corresponds to 198 MW.

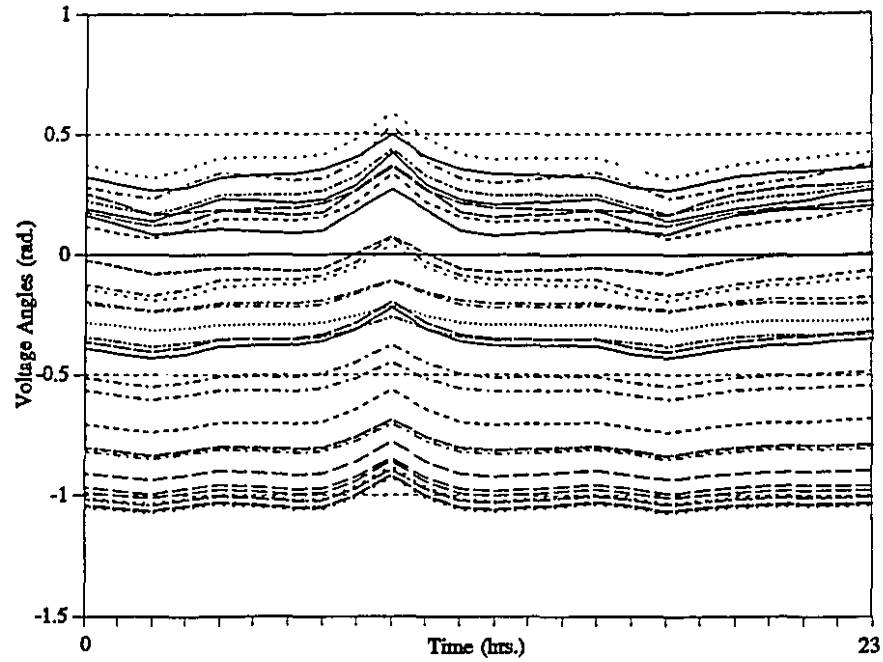

Figure 6.3.a- Voltage angles - Phase II.

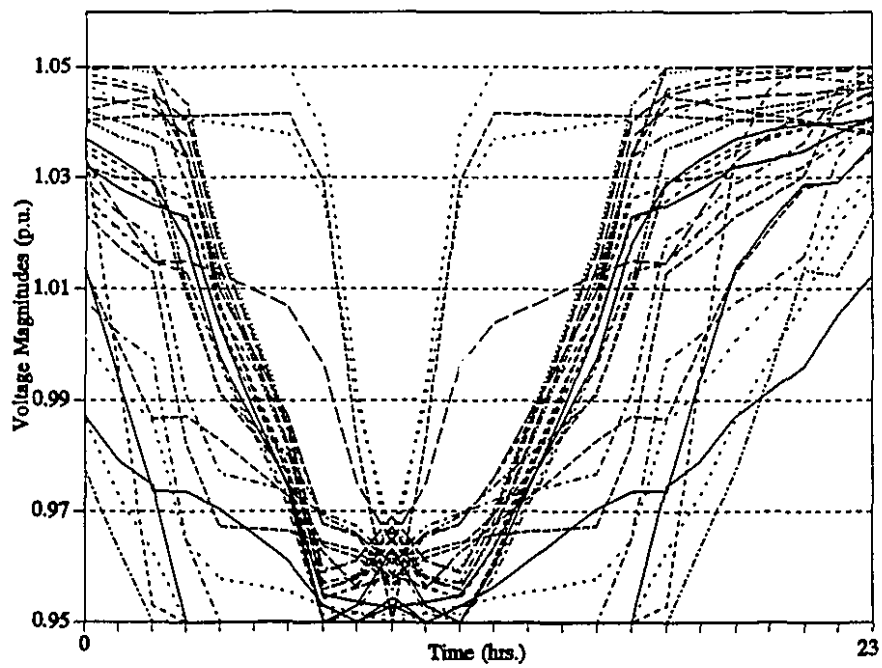

Figure 6.3.b-Voltage magnitudes - Phase II.

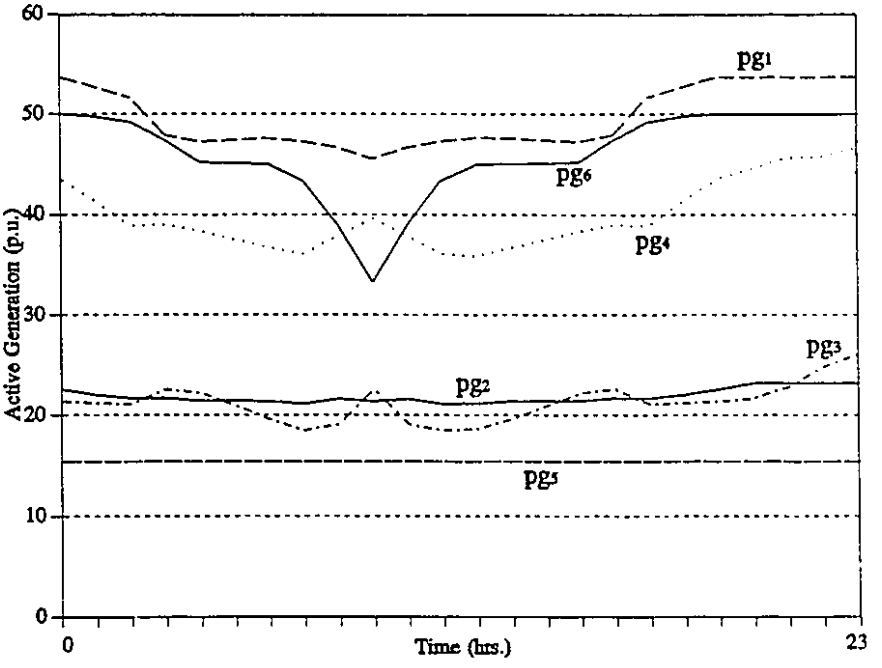

Figure 6.3.c- Active generation - Phase II.

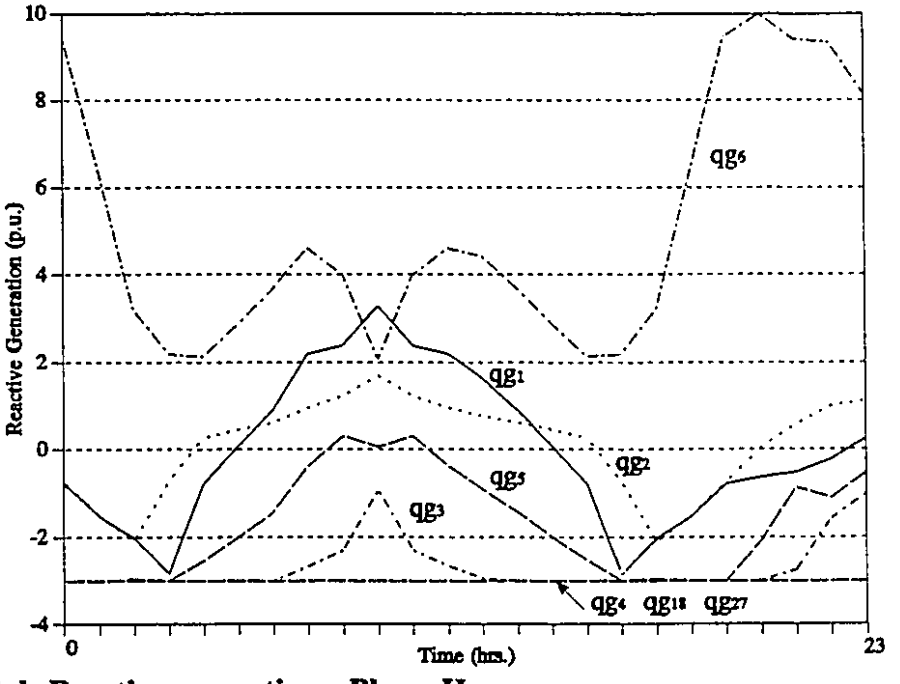

Figure 6.3.d- Reactive generation - Phase II.

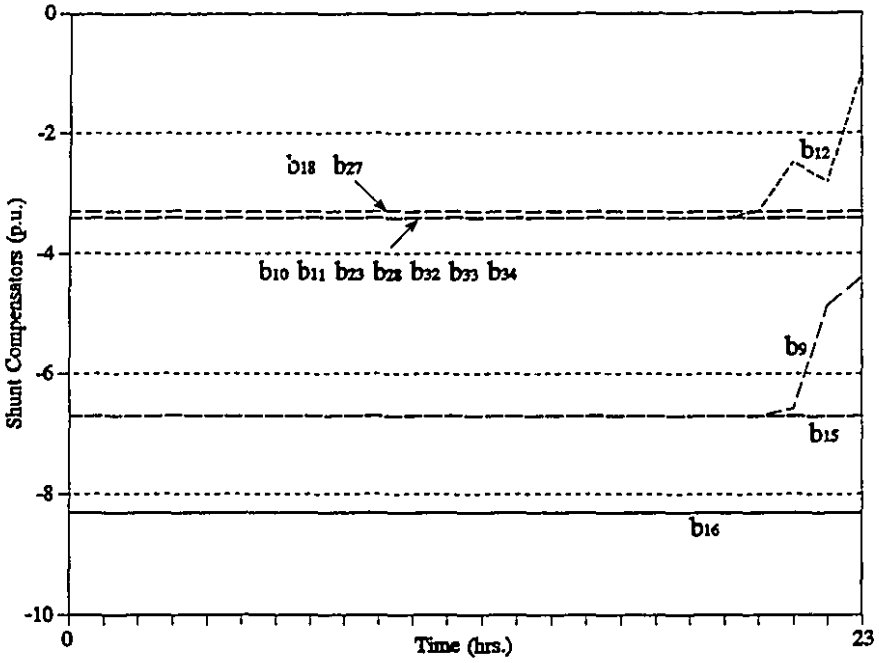

Figure 6.3.e- Shunt compensators - Phase II.

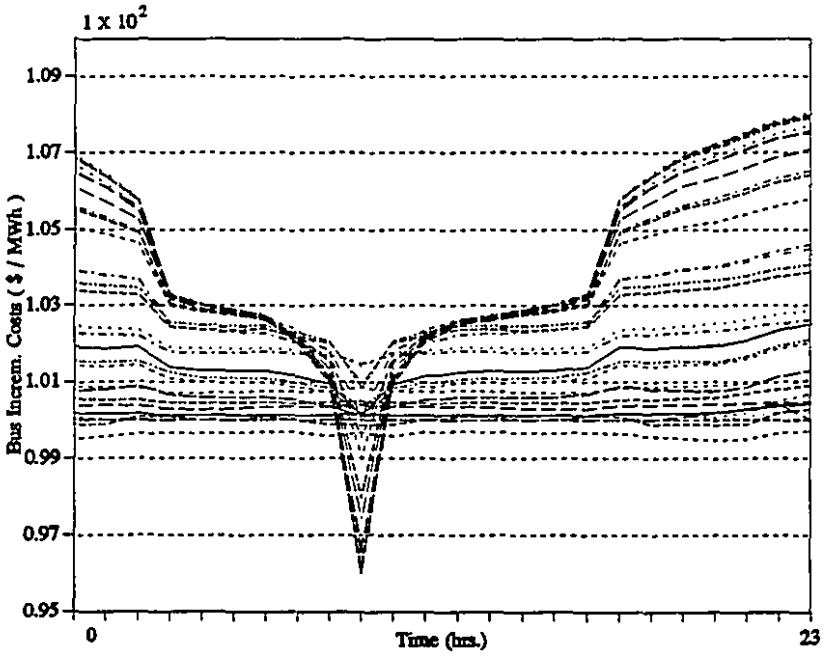

Figure 6.3.f- Bus incremental costs - Phase II.

From Figures 6.3.a-6.3.f, the more nonlinear characteristic of the reactive sub-problem is very noticeable. However, even this part is considerably more linear than it was for Phase I, resulting in a much faster tracking process. It is interesting to notice as well that, for this example, the voltage magnitudes decreased with the load, instead of increasing. This fact is due to the excessive amount of VAr power in the network for low loads. If we allow the shunt compensators to be more inductive, thus absorbing the VAr excess, the voltage magnitudes would drop less with the load. Another interesting fact is the behaviour of the reactive generations, indicating the fine tuning necessary to maintain optimality during the tracking.

Throughout the tracking process, the optimization algorithm kept the shunt compensators constant leaving the optimal control of the voltage magnitudes to the synchronous condensers or generators only. As the load decreases, these var sources cannot keep the voltage magnitudes near the ideal value of 1.0 p.u. and there is a voltage drop in all network. For this system, at low loads it is necessary to disconnect some of the transmission lines in order to keep a good control on the variables.

Notice in Fig. 6.3.f that the bus incremental costs decrease at low load, at the same time remaining more or less the same value for all buses of the system. As the load increases however, some of the bus incremental costs increase more than others, indicating the effect of the higher transmission losses on these values.

6.3.2 Assessing the Effectiveness of Optimizing

To assess the importance of the optimization during the load tracking, the results shown above (Figures 6.3.a-6.3.f) were compared with the results of the load tracking where the objective function was the minimization of the deviation of the current solution from the optimum at 100% of the load. This objective function was chosen to give an idea of the difference in costs between an arbitrary solution which respects all operation limits and an optimal solution in the sense of minimum losses. The results of this second load tracking are shown in Figures 6.4.a-6.4.e below. Also, to have an idea of the savings obtained when tracking the load curve following the minimum loss criterium, the total

active power generated for the minimum loss case (Case I) and for the minimum deviation from an initial solution case (Case II) are represented in Figure 6.5. In addition, Figure 6.6 depicts the MW difference between the total generations of each case studied.

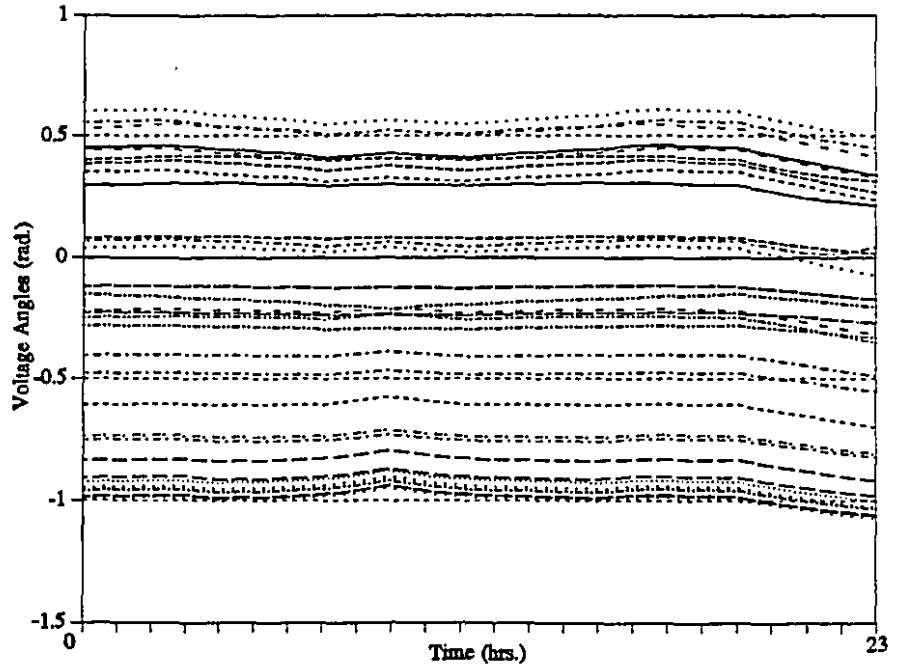

Figure 6.4.a- Voltage angles - feasible solution.

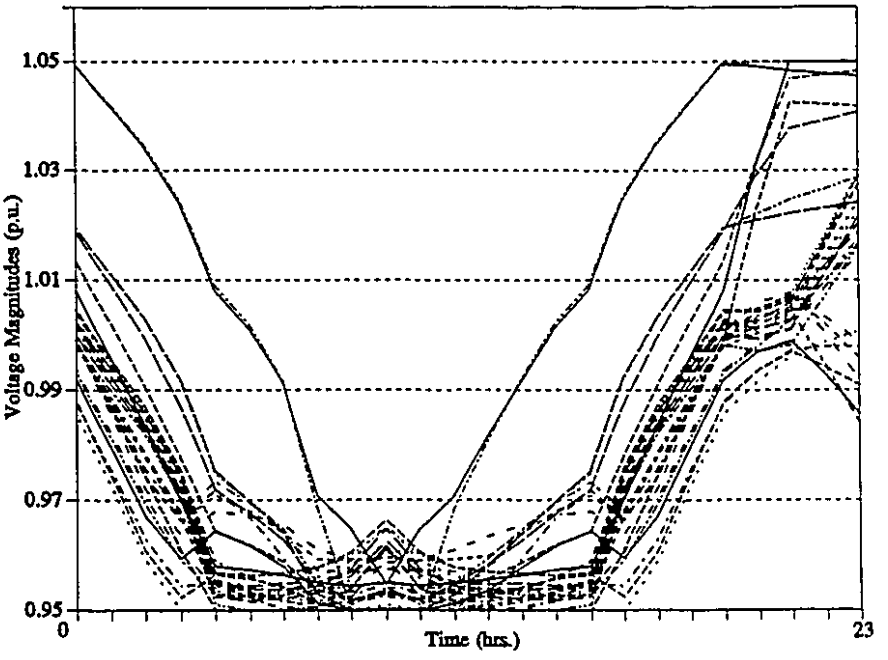

Figure 6.4.b- Voltage magnitudes - feasible solution.

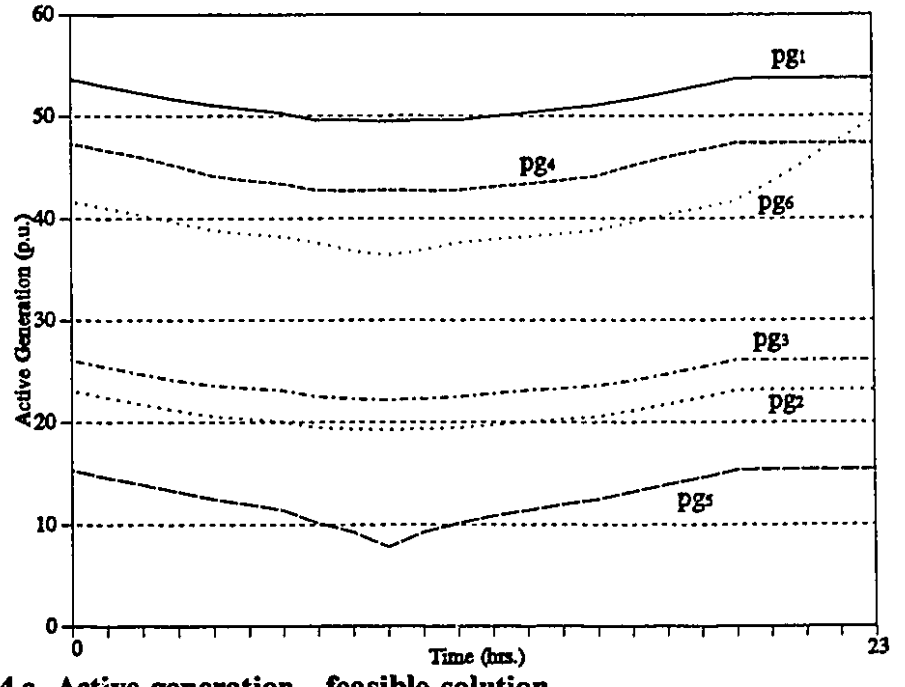

Figure 6.4.c- Active generation - feasible solution.

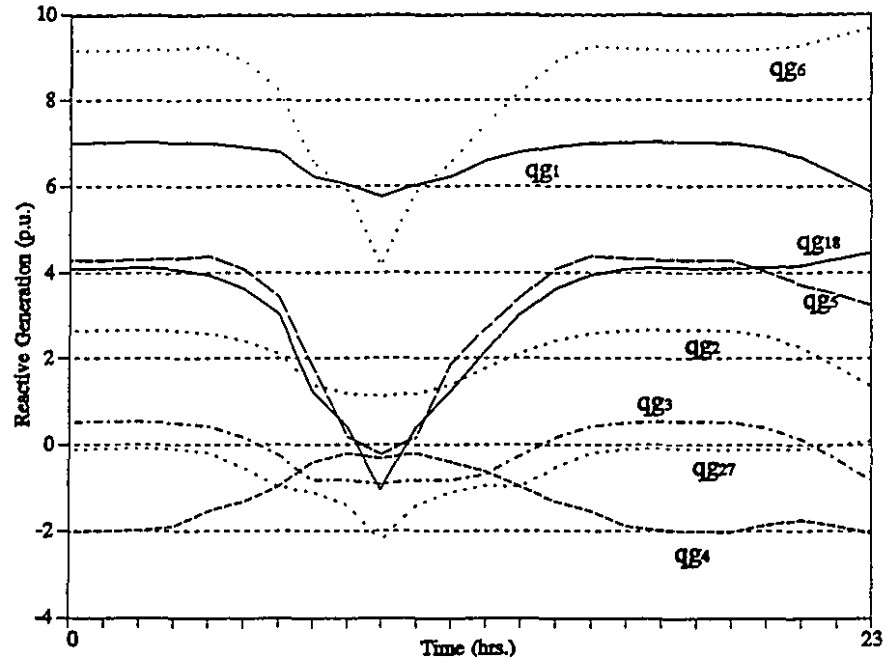

Figure 6.4.d- Reactive generation - feasible solution.

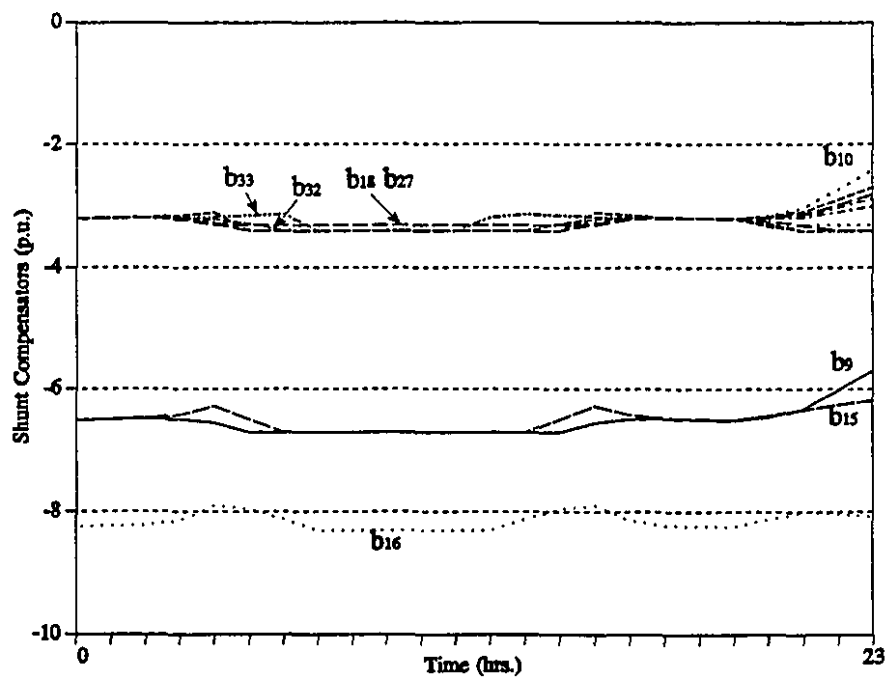

Figure 6.4.e- Shunt compensation - feasible solution.

The comparison of the optimal trajectories of Case I and case II shows, first of all, that the voltage drop which occurs at low load levels is due to a feasibility problem rather than because of the optimization process. In addition, one can notice the difference of the optimal trajectories of the active and reactive generations for cases I and II. While for Case II, all active generations and most of the reactive generations decrease with the load, during Case I this behaviour is not observed and the optimal trajectories are more "erratic", thus indicating the tuning necessary to optimally track the load.

Figure 6.5 depicts the total active generation for cases I and II. As can be seen, the difference is very small, even diminishing at low load levels and high load levels, thus indicating the greater difficulty to perform the optimal operation. This small difference in the absolute value of the total generation was expected since the difference between the cases is due to the transmission losses, which normally is of the order of 2% of the total load.

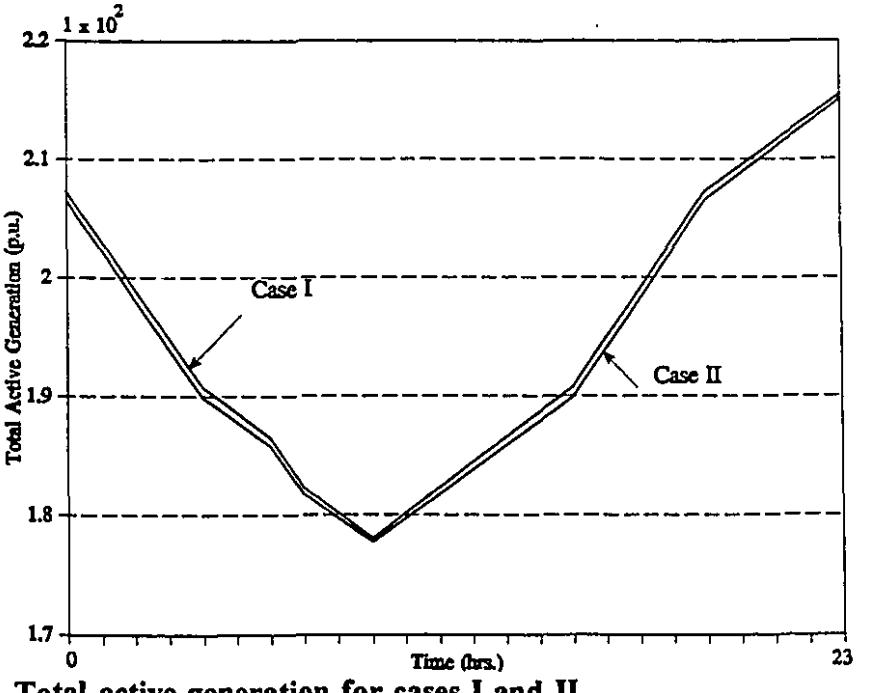

Figure 6.5- Total active generation for cases I and II.

Figure 6.6 represents the difference in MW between the total generations of Case I and Case II. This difference varies from 30.8 MW, at 86% of the total load, until 89.3

MW at 94% of the total load. It is smaller at low load levels and high load levels indicating the reduction of the optimization space. Considering that the cost of building new generation is approximately $4x10^3$\$/kW [Yamayee and Bala Jr., 1994], the capital savings will range from $1.2x10^8$\$ to $3.6x10^8$\$. This gives a good idea of the savings provided by optimally operating (that is, operating with minimum loss) the 34-bus system. Although the absolute value of the losses is very small when comparing to the total load, the savings can be substantial, which justifies the use of an OPF algorithm in on-line operation. These savings will be even greater if one considers fuel or operational costs.

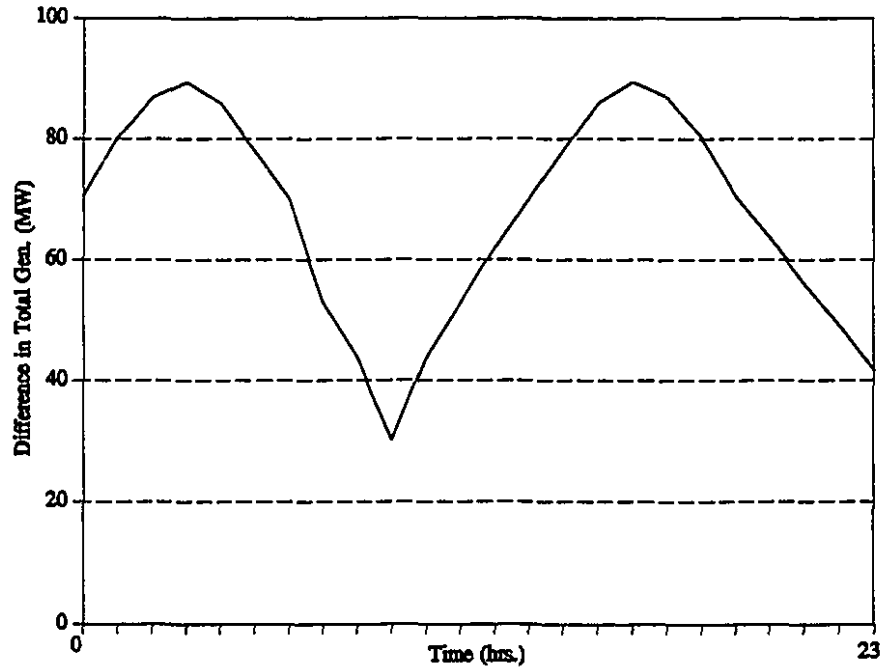

Figure 6.6- Difference in total generation of cases I and II.

Compared with the system incremental cost, SIC, the bus incremental costs (**BIC's**) represented in Figure 6.3.f offer a more precise idea about the cost involved in an energy transaction. In Figure 6.7, we compare some of the **BIC**'s with the system incremental cost for the 34-bus network during the load tracking. For this example, at high load levels $\mathbf{BIC_7}$ and $\mathbf{BIC_8}$ are higher than the system incremental cost (SIC) whereas $\mathbf{BIC_{15}}$ and $\mathbf{BIC_{21}}$ are lower than the SIC. At low load levels, however, the inverse occurs (that is, $\mathbf{BIC_7}$ and $\mathbf{BIC_8}$ are lower than SIC and $\mathbf{BIC_{15}}$ and $\mathbf{BIC_{21}}$ are larger and SIC. Such

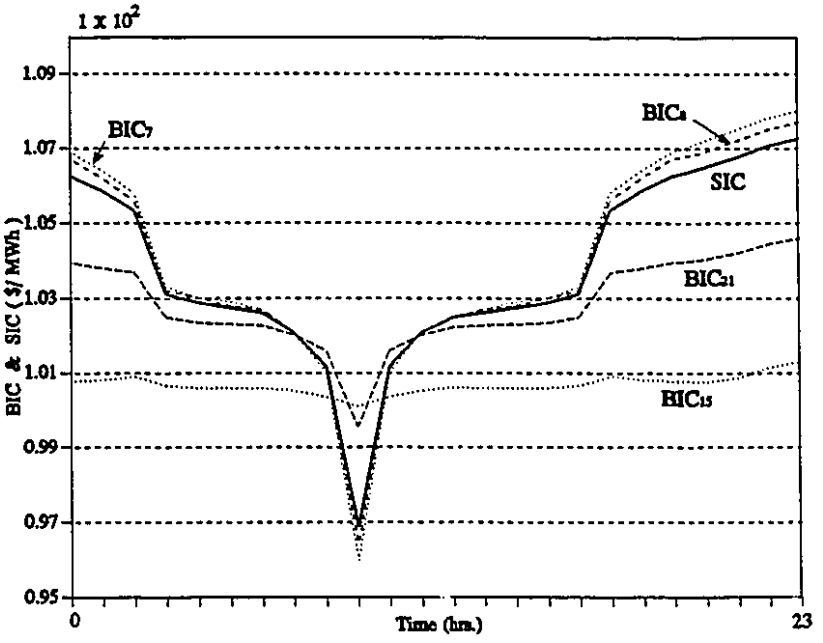

Figure 6.7- System incremental cost & bus incremental costs.

behaviour can be understood if we consider that buses 7 and 8 are situated far from the generating units whereas the opposite occurs with buses 15 and 21. Thus, the transmission losses will yield larger incremental costs at buses 7 and 8 at high load levels and smaller incremental costs at low load levels. For buses 15 and 21, on the other hand, the changes in the transmission losses are very small, therefore they are not very much affected by the variation of the total load. As a result, when considering transmission transactions in this network, both the location of the buses where the transaction occurs and the actual load level of the system have special importance.

6.3.3 Optimal Steady State Behaviour under Line Contingencies

The simulation of line contingencies is important for a definition of an optimal secure operating state. Although, presently, the Parametric-OPF algorithm is not able to solve the secure OPF problem [Carpentier, 1987], possible violations in line flow limits due to line contingencies can be corrected by the algorithm. A single line contingency seldom leads to an "infeasible" OPF case (or, more specifically, to a structurally unstable case), but there are situations where resulting violations in the line flow limits cannot be

corrected, specially if the limits of the active generation present in the neighbourhood of the fault are very tight. Even in the cases where these violations can be corrected, the loadability limit of the system may be reduced. The next Figures show some selected trajectories of the 118-bus system before and after the loss of one its lines during the load tracking process. In the resulting network after the line outage, power flow violations occur and this fact has a considerable effect on the behaviour of all variables of the system. In this example, line 86 is taken out during the load tracking at a load level that is 4% above the initial load. The optimization criterion used in the test is a combination of generation cost and voltage profile deviation from normal. The load curve is increased by 1% between each interval of time. Due to the outage of line 86, the power flow limits of lines 81 and 107 become active. After the line outage and the resulting violations are corrected by applying Phase I, the load tracking proceeds until the load reaches 7% above the initial values. At this point, the occurrence of a critical point of type 3 prevents the tracking to proceed beyond a load level of 7% above the initial one. On the other hand, without the line outage and the power flow violations, the optimal tracking may proceed until the total load is 12% above the initial value. The results are in p.u with a 100 MVA basis.

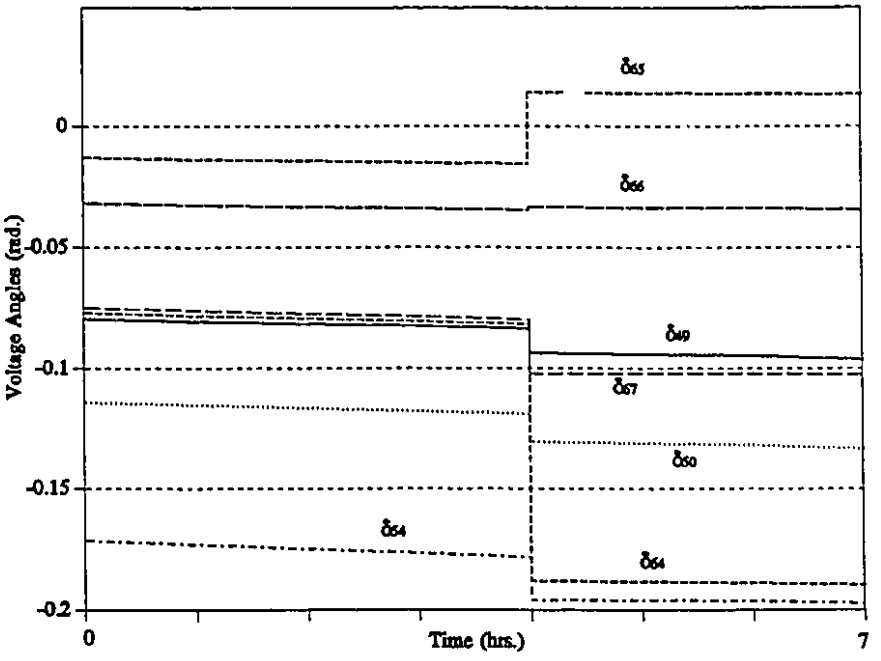

Figure 6.8.a- Voltage angles - Phase II with line contingency.

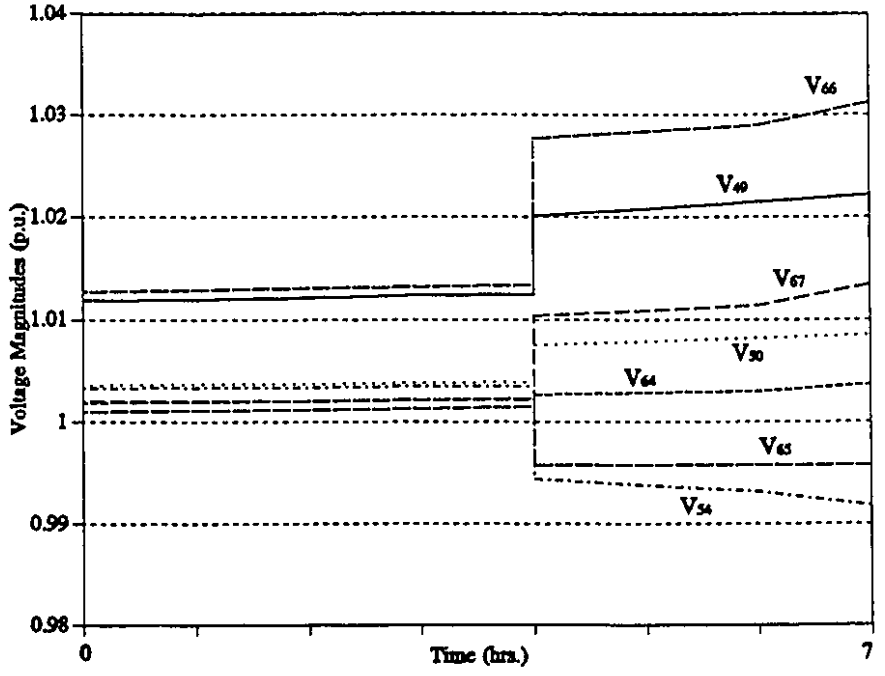

Figure 6.8.b- Voltage magnitudes - Phase II with line contingency.

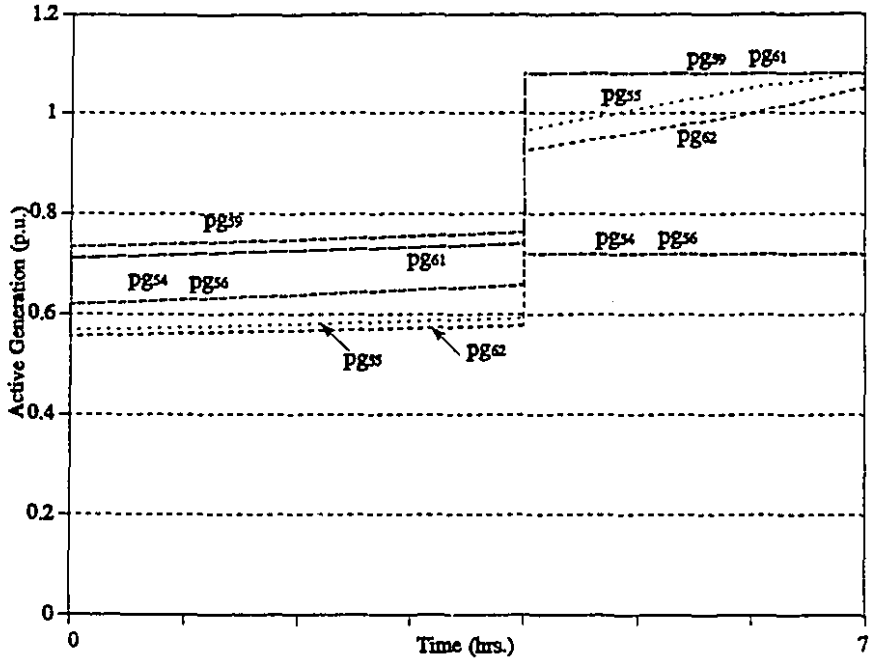

Figure 6.8.c- Active generation - Phase II with line contingency.

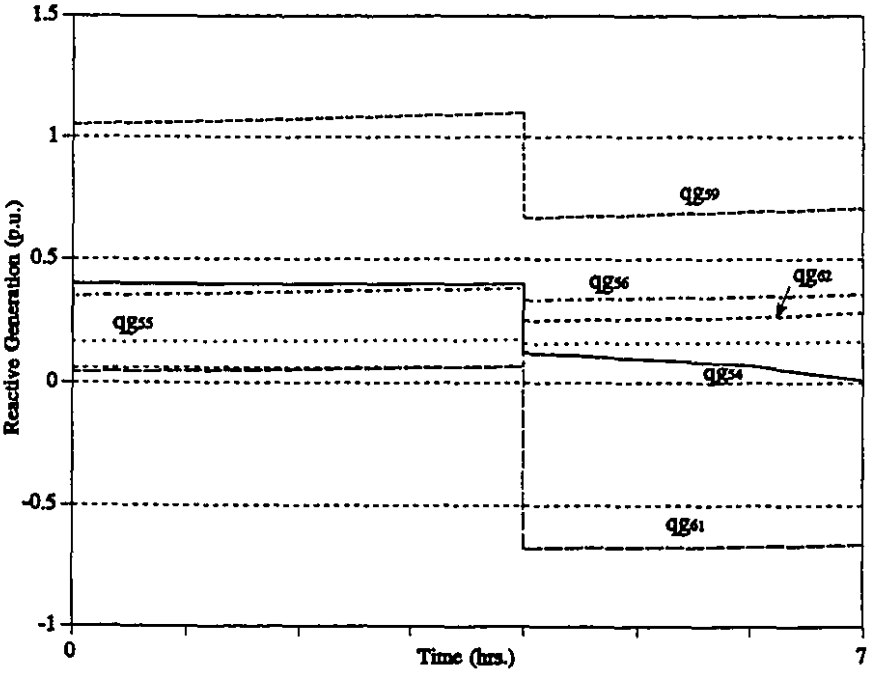

Figure 6.8.d- Reactive generation - Phase II with line contingency.

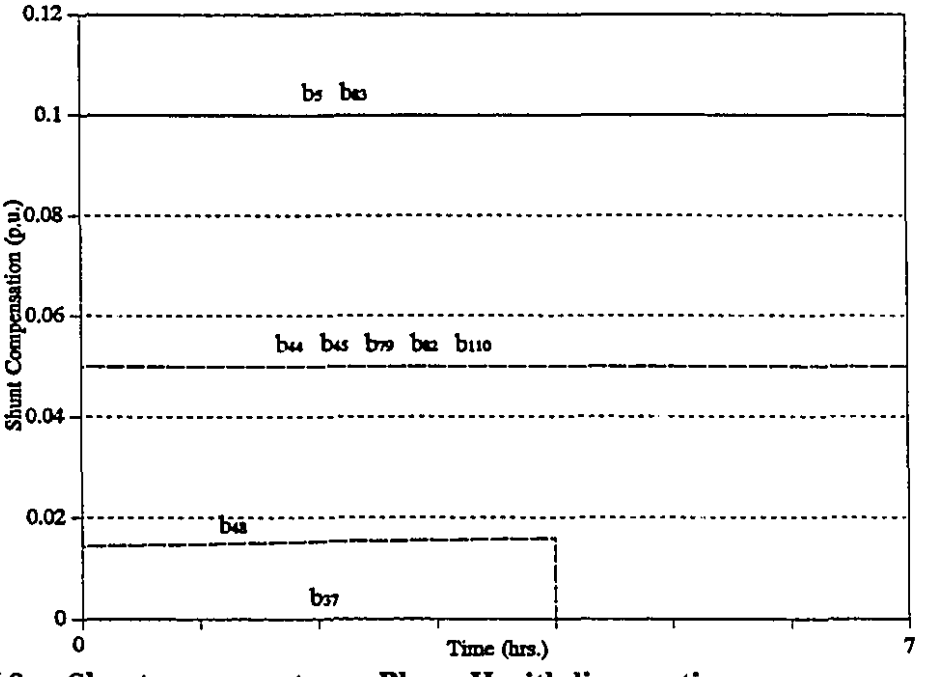

Figure 6.8.e- Shunt compensators - Phase II with line contingency.

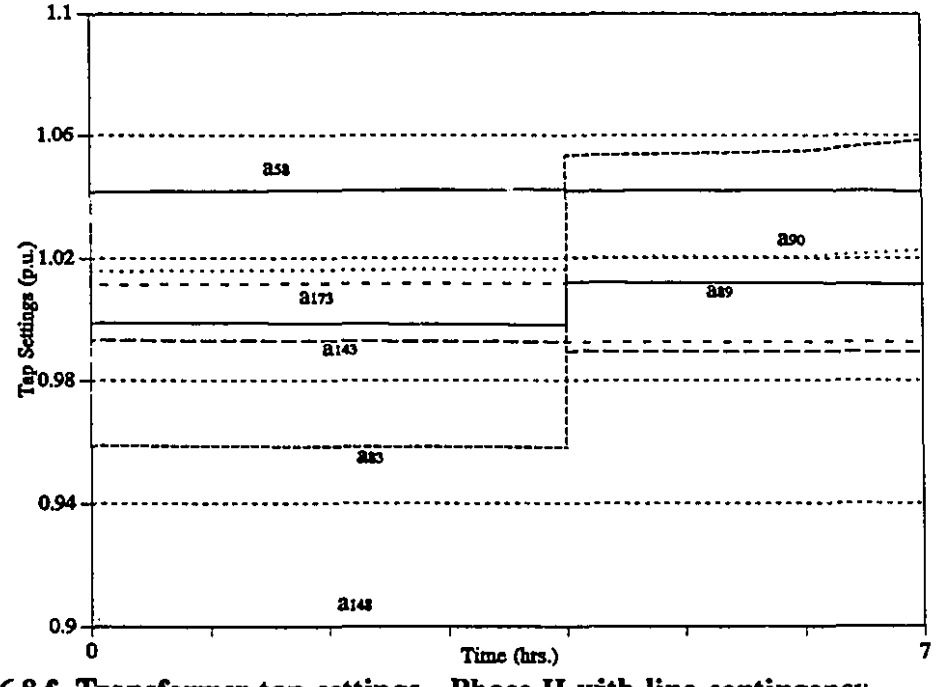

Figure 6.8.f- Transformer tap settings - Phase II with line contingency.

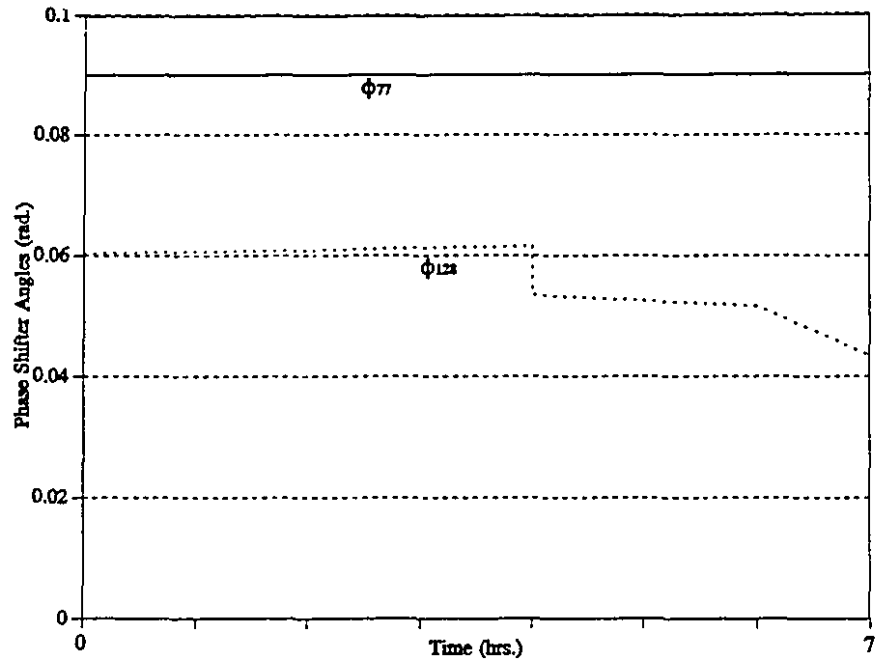

Figure 6.8.g- Phase shifter angles - Phase II with line contingency.

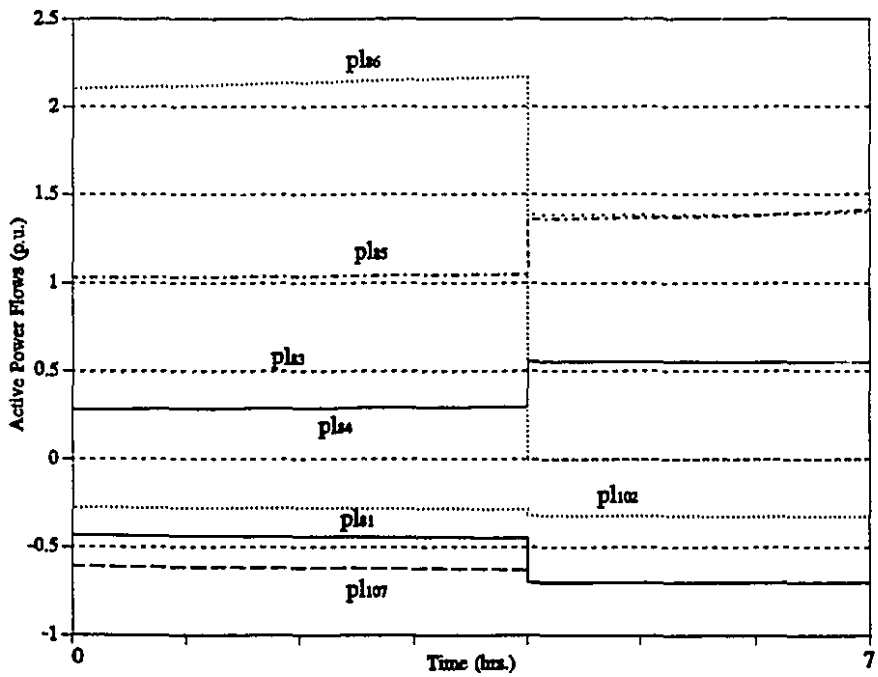

Figure 6.8.h- Power flows - Phase II with line contingency.

The first aspect to be noticed is the very linear behaviour of the optimal trajectories during the tracking, showing the more linear characteristics of 118-bus network when compared with the 34-bus network. Also notice that the line outage does not cause extreme variations in the voltage magnitudes and angles, shunt inductors and phase shifter angles. Transformer tap settings and real and reactive generation experience larger variations. Note that all the variable displayed in the above figures are in a region close to the line outage. As the load is increased towards 8% above the initial value, some of the optimal trajectories approach a quadratic turning point and, at the same time, some Lagrange multipliers assume very large values. This behaviour indicates the proximity of the critical point of type 3 which occurs in a region where the objective function is increasing thus demonstrating that the loadability limit was reached (see Figures 6.9.a-6.9.d).

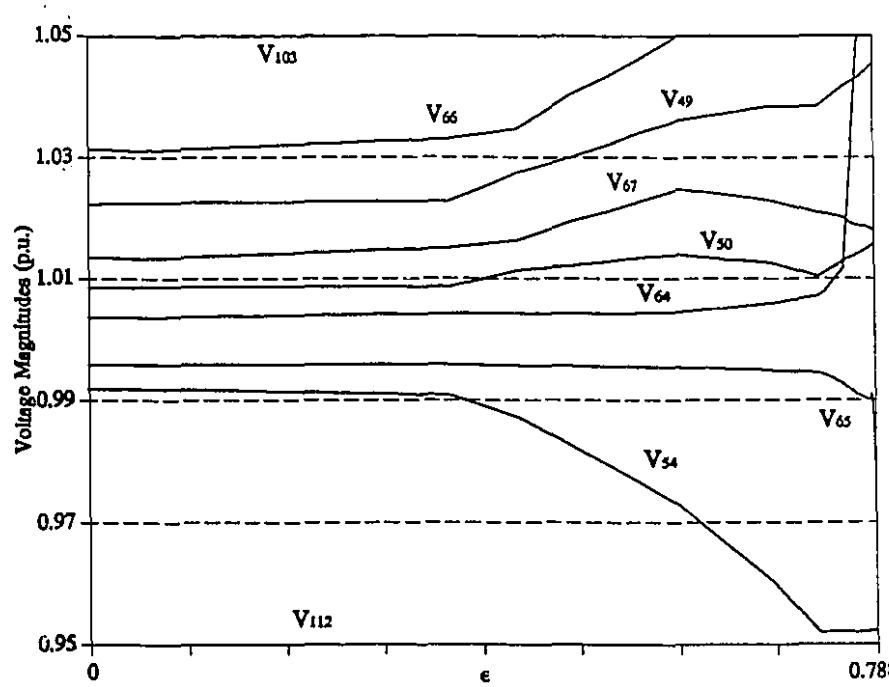

Figure 6.9.a- Voltage magnitudes near critical point of type 3.

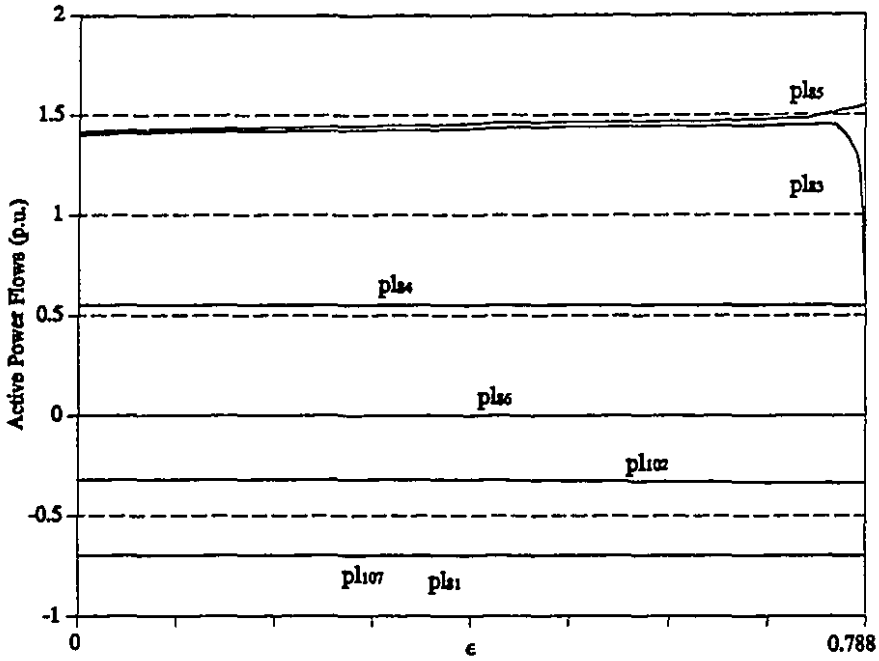

Figure 6.9.b- Power flows near critical point of type 3.

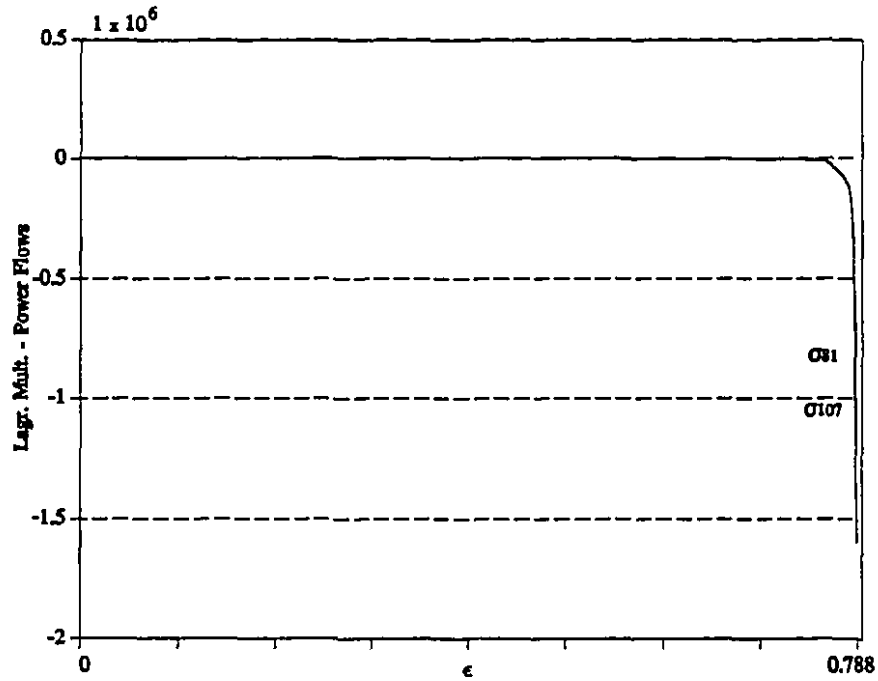

Figure 6.9.c- Lagrange mult. of power flows near critical point of type 3.

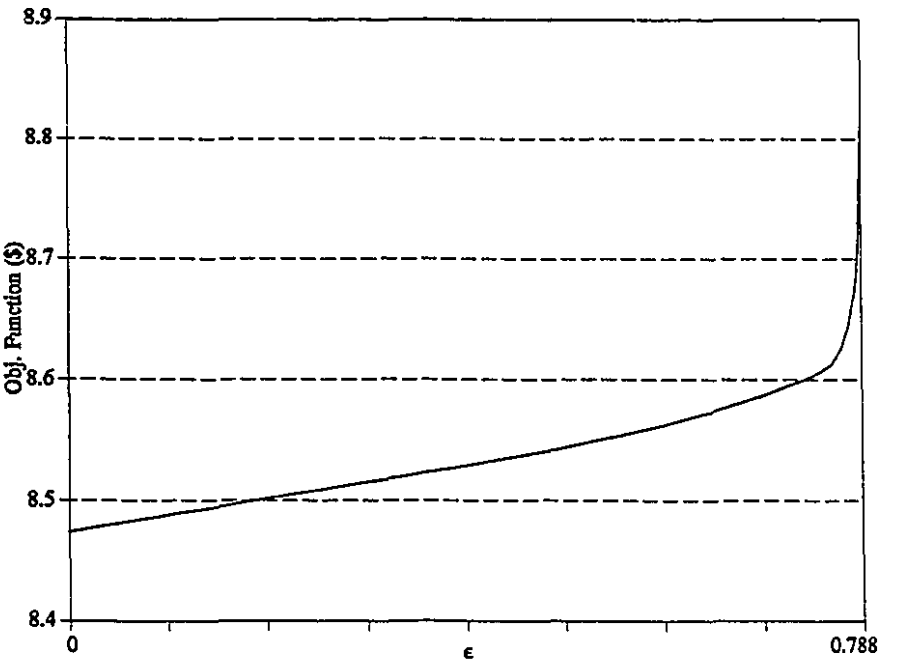

Figure 6.9.d- Objective function near critical point of type 3.

In the test discussed above, the loadability limit of the 118-bus network was determined by the limits imposed on the power flows of line 81 and 107. The FACTS devices were designed to help the power dispatch in special situations such as this. Therefore, next, we analyze the behaviour and performance of the FACTS devices in the same scenario described above.

6.3.4 Studies with FACTS Devices

In an attempt to increase the loadability limit of the system considering the loss of line 86 (approximately 4% less than with the line in), we introduced a FACTS device in each line where the power flow limits are active. The FACTS devices simulated in this case consist of variable series reactances. The devices are supposed to be able to vary the lines reactances by $\mp$ 50%. The same test represented in Figures 6.8.a-6.8.h and 6.9.a-6.9.d was repeated with the FACTS devices in the network. The results are shown below.

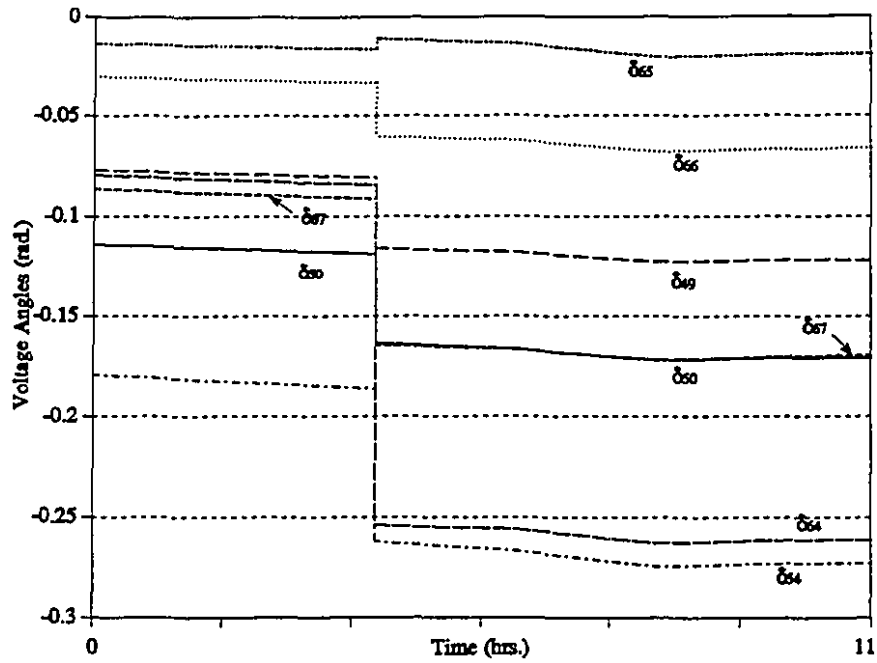

Figure 6.10.a- Voltage angles - Phase II with FACTS devices.

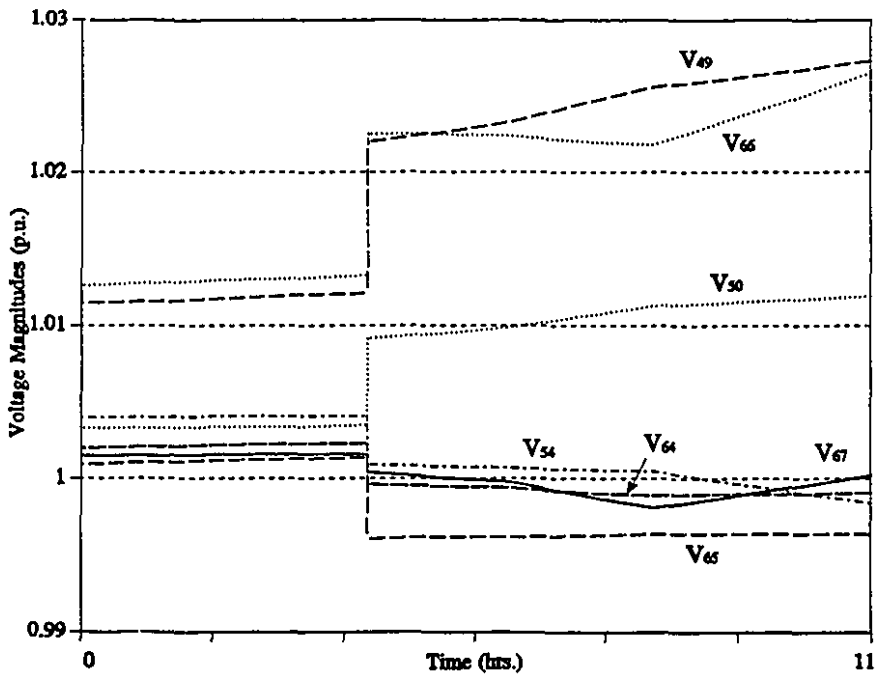

Figure 6.10.b- Voltage magnitudes - Phase II with FACTS devices.

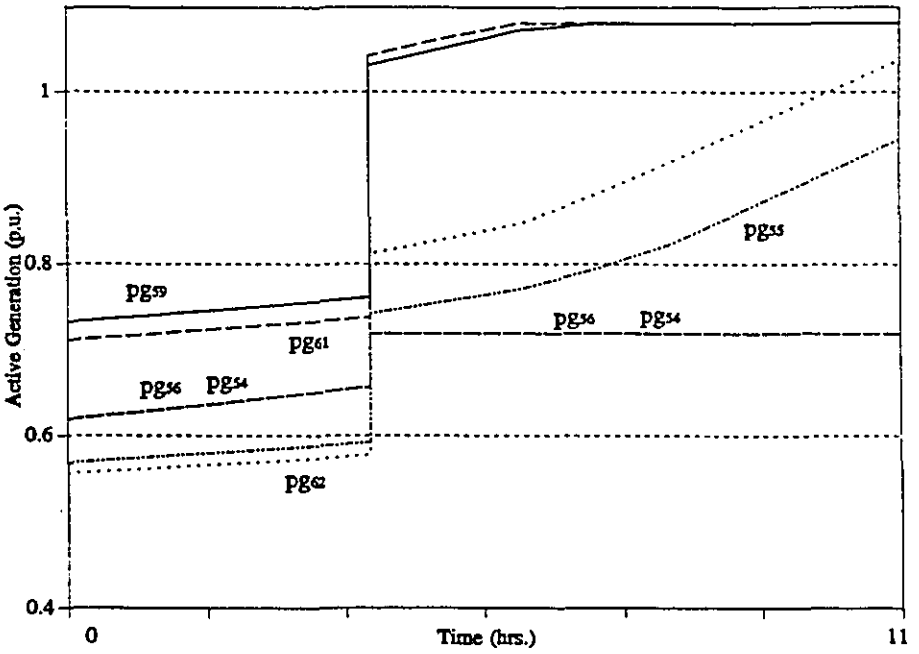

Figure 6.10.c- Active generation - Phase II with FACTS devices.

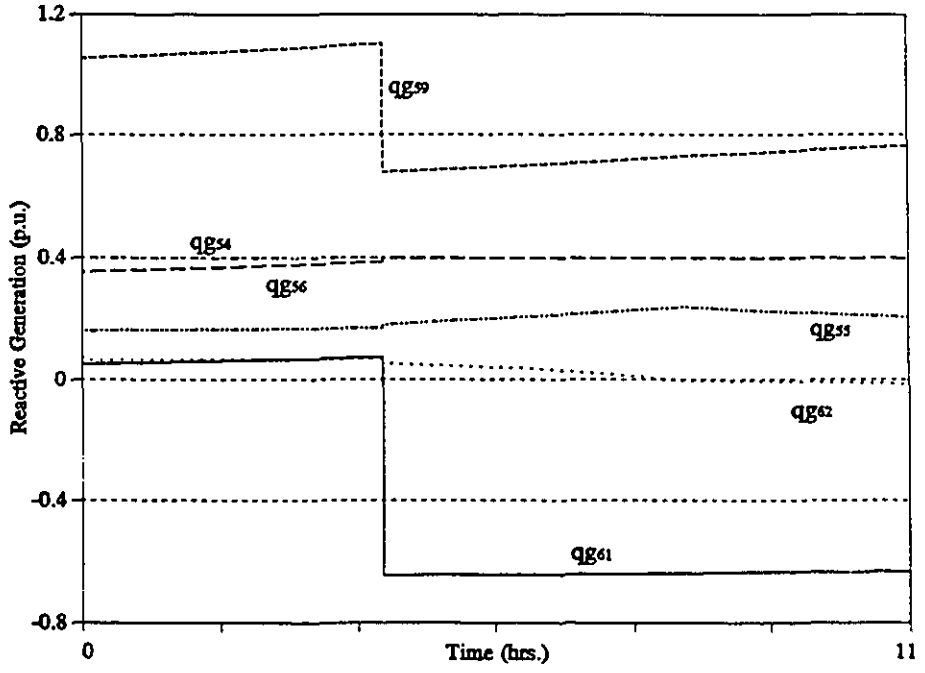

Figure 6.10.d- Reactive generation - Phase II with FACTS devices.

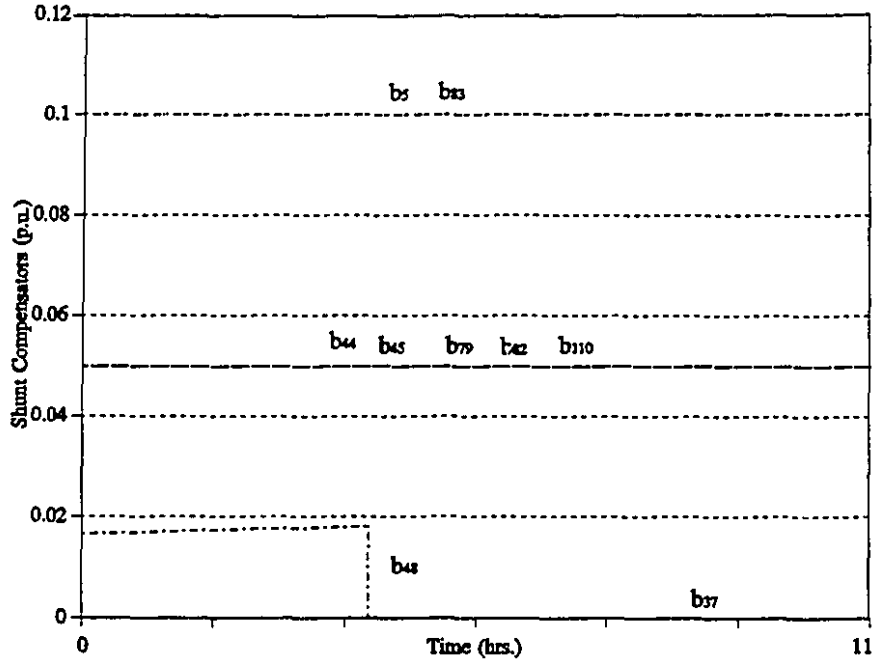

Figure 6.10.e- Shunt compensators - Phase II with FACTS devices.

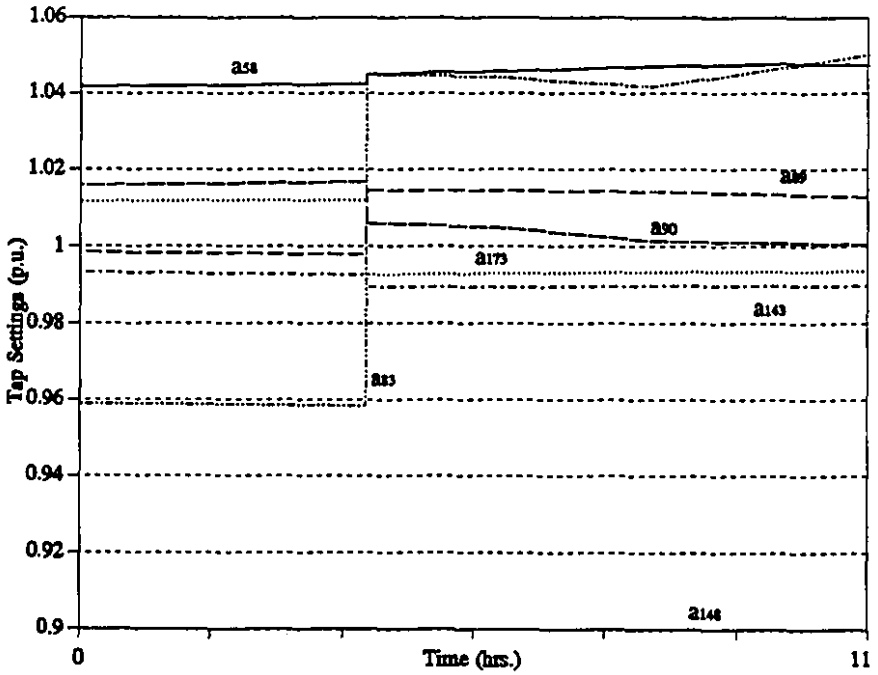

Figure 6.10.f- Transformer tap settings - Phase II with FACTS devices.

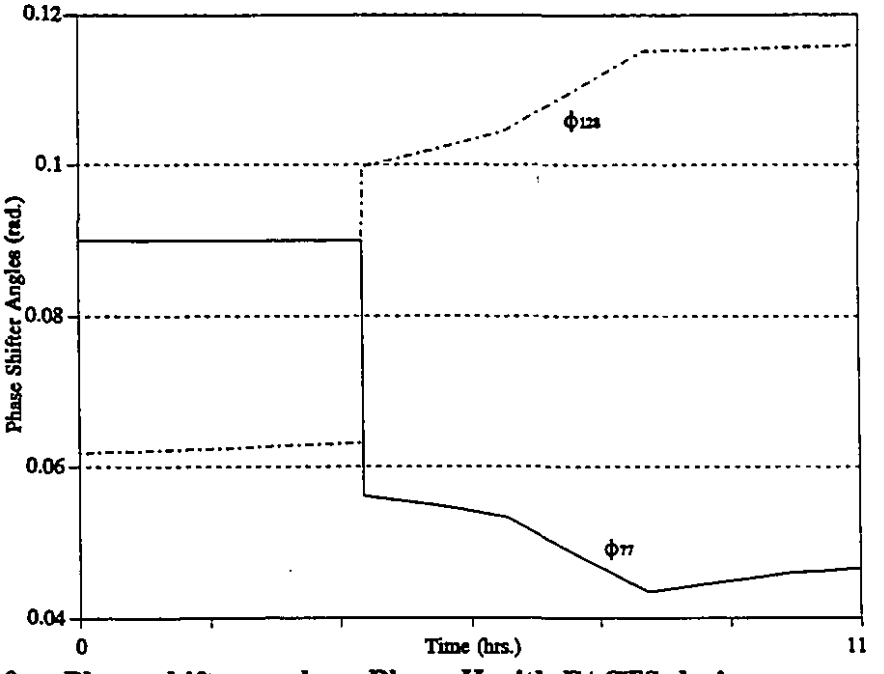

Figure 6.10.g- Phase shifter angles - Phase II with FACTS devices.

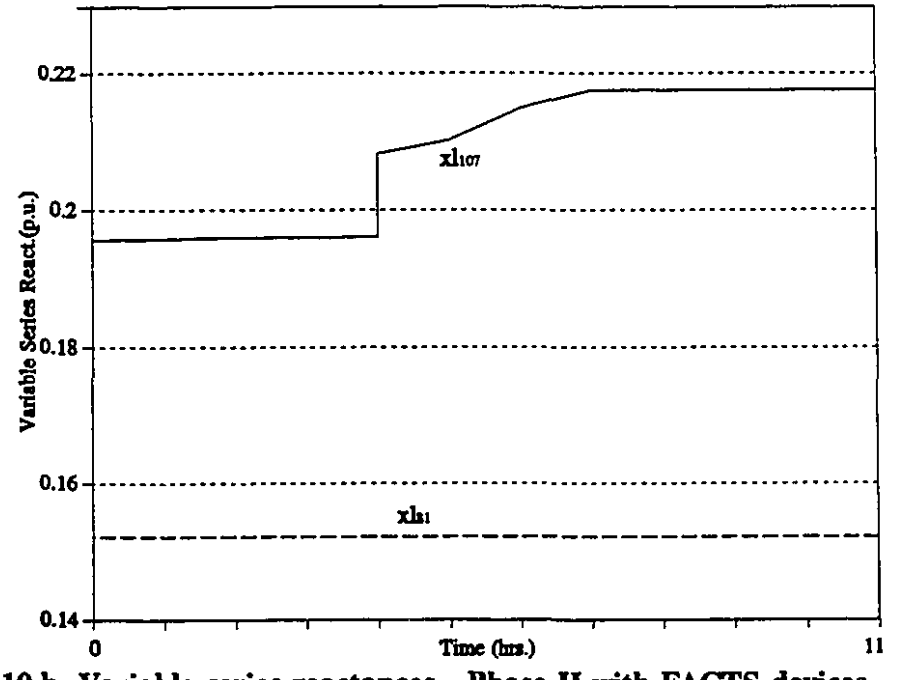

Figure 6.10.h- Variable series reactances - Phase II with FACTS devices.

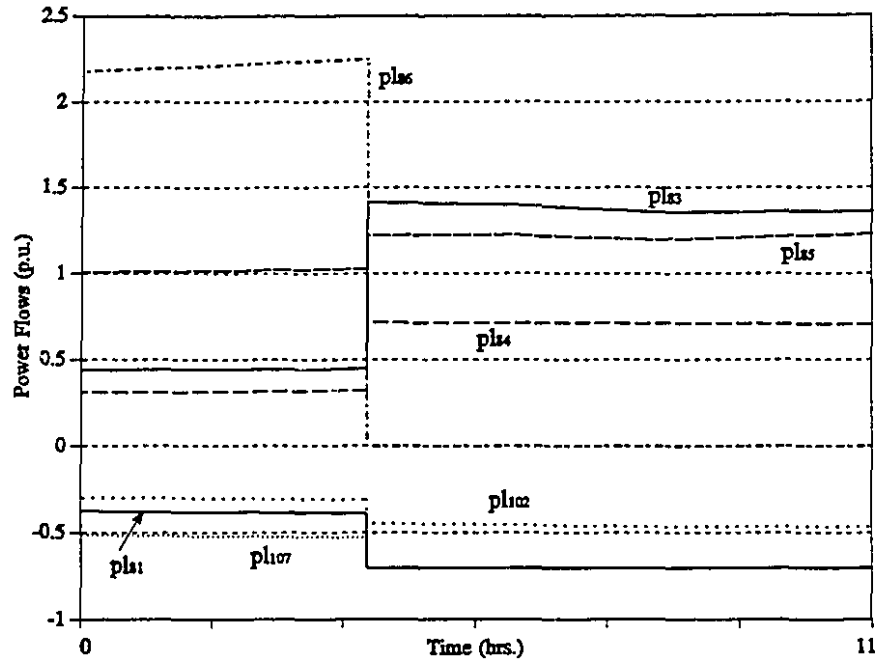

Figure 6.10.i- Power flows - Phase II with FACTS devices.

Figures 6.10.a-6.10.i show that the introduction of FACTS devices on lines 81 and 107 compensates for the severity of the line constraints and enables the tracking process to continue until the total load is 11% above the initial value (that is, the same as without a line outage). As the total load approaches 12% above the initial value, the violation of another line constraint (on line 24) causes the occurrence of a critical point of type 3 in a region where the objective function is increasing. The theory tells us that beyond this load level the feasible set is locally empty. This test demonstrates that such devices are able to enlarge the loadability limit of a system in cases where a contingency occurs.

The presence of FACTS devices in lines 81 and 107 changes the amount of real and reactive power in the region where the line outage occurs. When the FACTS devices are not present, all **pg**'s in the neighbourhood (that is, $\mathbf{pg}_{54}$, $\mathbf{pg}_{55}$, $\mathbf{pg}_{56}$, $\mathbf{pg}_{59}$, $\mathbf{pg}_{61}$ and $\mathbf{pg}_{62}$) reach their maximum limit whereas when the FACTS are introduced, only $\mathbf{pg}_{54}$, $\mathbf{pg}_{56}$, $\mathbf{pg}_{59}$, $\mathbf{pg}_{61}$ are at the maximum, indicating that more power can be transferred from the neighbouring areas of the network. As a result, the tracking can proceed normally

until a higher load level and the loadability limit is defined by the operating limits of another area of the system. This shows that such devices can be used to increase the power transfer capability of a transmission network.

The total initial load of the 118-bus network is equal to 4216 MW. The difference in demand that can be satisfied in the first case (with no FACTS devices) and the second case (with two FACTS devices) is approximately equal to 4% of the total load, or 168.64 MW. Considering that the capital cost of generation is equal to $4x10^3$\$/kW, the savings in generation will be approximately equal to $6.7x10^8$\$. This savings will increase if the operational costs are also considered. Presently, the cost of a FACTS device varies from 50 to 100 \$/kVA, depending on the maximum power flow that the device can withstand [Hingorani, 1993]. The maximum power flows in lines 81 and 107 are equal to 70 MW, therefore, the price of a FACTS device for one of these lines will vary from $3.5x10^6$\$ to $7.0x10^6$\$, which yields a total investment varying from $7.0x10^6$\$ to $1.4x10^7$\$. This justifies the use of the FACTS devices.

Although the FACTS devices may be important for the transmission of power, the optimal control of the variables existing in the FACTS's model proved to be difficult when the system under consideration has a larger amount of reactive power and total load. This is translated in an increase on the number of iterations (see Table 6.1) and/or in the values needed for w to assure an initial optimal solution and a good convergence of the Newton method. A typical example is the case of minimizing generation cost plus voltage profile deviation from 1.0 p.u. for the 34-bus system. Supposing a maximum power flow of 20.2 p.u. for lines 36, 37 and 38, the problem was solved, at first, supposing no FACTS devices and, next, with one of such devices in each line with a limiting transmission capacity. The FACTS were represented by a variable phase shifter (with ϕ varying from -0.1 rad to 0.1 rad) connected in series with a reactance which varies the original value of the line reactance in ±50%. In both cases the Parametric-OPF was able to arrive at the optimal solution, but because of very restrictive active generation capacity, in order to respect the transmission limits imposed, considerable adjustments of the decision variables is necessary, specially on the voltage magnitudes. The total generation cost for the case without FACTS devices ($1.504x10^3$\$/h) was almost the same as the

total generation cost for the case with the FACTS devices, 1.498×10^3 \$/h. The difference in active generation was only 62 MW however a large difference was observed in the optimal voltage magnitudes. Figure 6.11 shows that the use of FACTS devices improved considerably the optimal voltage profile of the 34-bus system considering the line limits described above.

The optimal control of the 3 FACTS devices included in the 34-bus system proved to be a difficult task. Whereas, for the test with no such devices the weighting factor w was made equal to 10, in the presence of FACTS devices this weighting factor had to be above 5000 to assure an initial optimal solution and a good convergence of the Newton method. With the increase in the number of FACTS devices, there is a considerable increase in the number of iterations and larger w's must be used. This can be an obstacle to the optimization of the FACTS variables for larger generation-transmission systems with heavy load and/or high levels of reactive power.

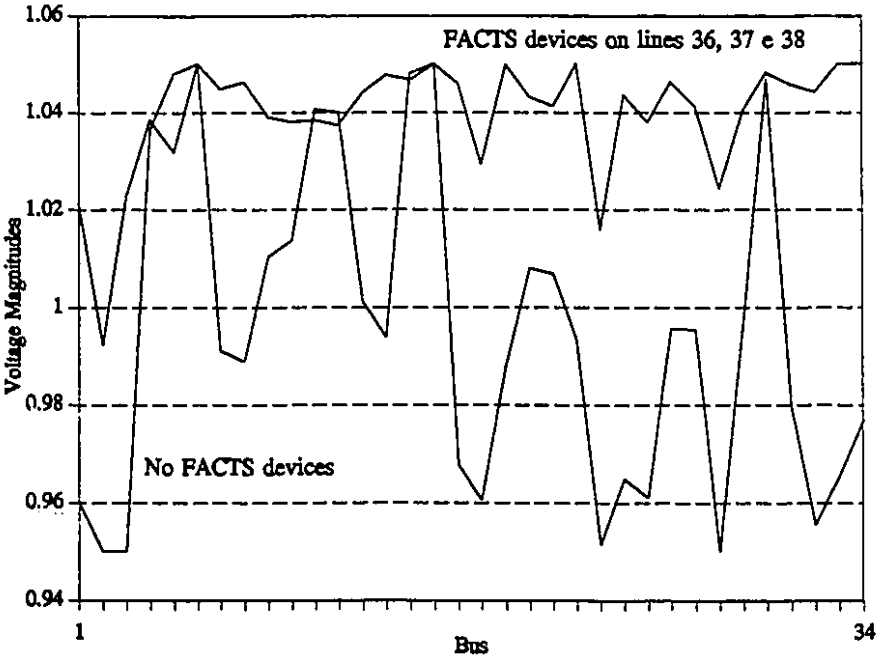

Figure 6.11- Optimal voltage magnitudes with & without FACTS devices.

6.4 Validation of the Results

The results provided by the parametric algorithm were compared with the optimal solution given by a general nonlinear optimization package. Two problems defined with a fixed load were also solved by the nonlinear optimization toolbox of MATLAB 4.0 which is based on sequential quadratic programming. The initial solution guess, $\mathbf{x}^0$, was made equal to the flat voltage profile for the 14-bus system and equal to a load flow solution for the 30-bus network. Since Phase II is a simplification of Phase I, the tests were not repeated for a varying load.

The problem of minimizing the generation cost plus the voltage profile deviation from 1.0 p.u. was solved for the 14-bus and 30-bus systems using both the Parametric - OPF and the optimization toolbox. The tests were made supposing the transformer tap settings fixed and equal to 1.0 p.u..Tables 6.19 and 6.20 show the results for the 14-bus system and 30-bus system, respectively.

The comparison of the results for Phase I show very small differences in the optimal solutions for both the 14-bus system and the 30-bus system. In both cases, the Parametric-OPF provided a slightly better solution. However, if $\mathbf{x}^0$ is made equal to the flat voltage profile, the performance of the optimization toolbox deteriorates for the 30-bus system, yielding an optimal cost of 30.0395$, indicating its dependency of the optimal solution on the initial guess. The proximity of the solutions obtained by the different methods validates the Parametric-OPF results.

In all tests made, the choice of $\mathbf{x}^0$ did not affect the quality of the solution provided by the Parametric-OPF. Although the solution trajectories vary substantially for different $\mathbf{x}^0$, different initial guesses did not lead to different optima, which is an interesting characteristic of the Parametric method.

Table 6.19- Comparison of results - 14-bus system.

14-Bus System										
Bus	**Parametric-OPF** Optimal Cost: 23.9530$					**Optimization Toolbox** Optimal Cost: 24.9091$				
	δ	**V**	**pg**	**qg**	**b**	δ	**V**	**pg**	**qg**	**b**
1	0	1.0260	2.7607	-0.2500	0	0	1.0313	2.7587	-0.2101	0
2	-0.1145	1.0084	0	0.3372	0	-0.1129	1.0122	0	0.3148	
3	-0.2608	0.9928	0	0.4000	0	-0.2581	0.9960	0	0.4000	0
4	-0.2122	0.9918	0	0	0	-0.2096	0.9945	0	0	0
5	-0.1821	0.9951	0	0	0	-0.1798	0.9982	0	0	0
6	-0.2887	1.0102	0	0.2400	0	-0.2864	1.0113	0	0.2400	0
7	-0.2734	1.0028	0	0	0	-0.2704	1.0029	0	0	0
8	-0.2734	1.0001	0	-0.0154	0	-0.2704	0.9998	0	-0.0177	0
9	-0.3049	1.0118	0	0	0.4173	-0.3019	1.0107	0	0	0.3939
10	-0.3077	1.0038	0	0	0	-0.3048	1.0031	0	0	0
11	-0.3010	1.0033	0	0	0	-0.2983	1.0036	0	0	0
12	-0.3054	0.9957	0	0	0	-0.3030	0.9967	0	0	0
13	-0.3074	0.9918	0	0	0	-0.3049	0.9926	0	0	0
14	-0.3254	0.9841	0	0	0	-0.3226	0.9839	0	0	0

Table 6.20- Comparison of results - 30-bus system.

30-Bus System										
Bus	**Parametric-OPF** Optimal Cost: 27.8658$					**Optimization Toolbox** Optimal Cost: 27.8683$				
	δ	V	pg	qg	b	δ	V	pg	qg	b
1	0	1.0500	2.8449	-0.2509	0	0	1.0500	2.8285	-0.2529	0
2	-0.1090	1.0332	0.1838	0.5000	0	-0.1083	1.0334	0.1992	0.5000	0
3	-0.1502	1.0168	0	0	0	-0.1497	1.0169	0	0	0
4	-0.1814	1.0095	0	0	0	-0.1808	1.0096	0	0	0
5	-0.2668	1.0055	0	0.4000	0	-0.2660	1.0057	0	0.4000	0
6	-0.2125	1.0057	0	0	0	-0.2118	1.0058	0	0	0
7	-0.2440	0.9978	0	0	0	-0.2433	0.9980	0	0	0
8	-0.2259	1.0064	0	0.4000	0	-0.2253	1.0066	0	0.4000	0
9	-0.2706	1.0163	0	0	0	-0.2700	1.0163	0	0	0
10	-0.3013	1.0069	0	0	0.1900	-0.3007	1.0069	0	0	0.190
11	-0.2706	1.0473	0	0.1559	0	-0.2700	1.0469	0	0.1542	0
12	-0.2886	1.0153	0	0	0	-0.2880	1.0154	0	0	0
13	-0.2886	1.0474	0	0.2400	0	-0.2880	1.0474	0	0.2400	0
14	-0.3052	1.0003	0	0	0	-0.3046	1.0003	0	0	0
15	-0.3068	0.9960	0	0	0	-0.3061	0.9961	0	0	0
16	-0.2992	1.0043	0	0	0	-0.2986	1.0043	0	0	0
17	-0.3046	1.0006	0	0	0	-0.3040	1.0006	0	0	0
18	-0.3180	0.9872	0	0	0	-0.3174	0.9872	0	0	0
19	-0.3210	0.9853	0	0	0	-0.3204	0.9853	0	0	0
20	-0.3172	0.9899	0	0	0	-0.3166	0.9899	0	0	0
21	-0.3097	0.9938	0	0	0	-0.3090	0.9938	0	0	0
22	-0.3094	0.9943	0	0	0	-0.3087	0.9943	0	0	0
23	-0.3136	0.9859	0	0	0	-0.3129	0.9859	0	0	0
24	-0.3161	0.9811	0	0	0.0430	-0.3154	0.9811	0	0	0.043
25	-0.3074	0.9773	0	0	0	-0.3068	0.9774	0	0	0
26	-0.3154	0.9589	0	0	0	-0.3147	0.9590	0	0	0
27	-0.2972	0.9839	0	0	0	-0.2965	0.9840	0	0	0
28	-0.2236	1.0023	0	0	0	-0.2229	1.0024	0	0	0
29	-0.3204	0.9632	0	0	0	-0.3198	0.9633	0	0	0
30	-0.3372	0.9512	0	0	0	-0.3365	0.9513	0	0	0

6.5 Conclusion

The Parametric-OPF approach proved to be a flexible and reliable method. For Phase I, in spite of the large computational times required, the method enables the resolution of the OPF problem without the recourse of numerous heuristics to find the optimal feasible set. The method was able to find the optimal solution of different test systems, including a very nonlinear network and could track a load curve efficiently during an interval of time. In all cases tested, the optimum did not depend on the initialization, which is a good measure of the reliability of the approach. Although, for some cases the Parametric-OPF was not able to solve the problem, changes in the strategy to find the optimal active feasible set or changes in some initial parameters enabled the finding of an optimal solution (when a single optimum exists). The many difficulties associated with the optimal operation of a generation-transmission system are easily visualized with the parametric approach, specially the occurrence of multiple solutions or unfeasible cases for the OPF problem. Since these difficulties can be differentiated, separate solutions can be proposed for each one, in this way augmenting the reliability of the method. However, it is important to realize that some of the difficulties existing in the parametric approach are inherent in the OPF problem itself and their resolution will benefit other OPF methods. Some of the difficulties that were highlighted by the parametric method are closely related to the optimal operation of a power system (for example, the loss of optimality or structural stability during the load tracking), and the successful adoption of a on-line OPF package depends heavily on their resolution.

Because of its high computational time, the present implementation of the method is not suited to be used in large systems. A more powerful version of the Parametric-OPF will certainly depend on the usage of a faster and more intelligent strategy to find the optimal active set. The challenge here is to conceive such a strategy without recourse to heuristics, which could compromise the positive characteristics of the method (namely, the ability to differentiate the various causes for failure and to provide a good visualization of the optimal behaviour of a generation-transmission system). In addition to this necessary improvement, the development strategies for resolution of the critical points are also crucial, even more so if we think about on-line applications to track a

varying load. This represents a meaningful change in the present way of studying the OPF problem. Nowadays, researchers are mostly concerned with a fast solution of the problem for a fixed load and very little attention was given to the fact that the load varies with time and well posed problems can become unsolvable because of these changes in the system load (unsolvable either because of the inexistence of an optimum or the inexistence of a feasible solution that can be attained without drastic changes in the control variables). This is in fact the meaning of the critical points: the loss of optimality or local feasibility that can occur due to changes in the total load. On-line implementations of an OPF method must be able to deal with such situations.

Even though the Parametric-OPF was not used in real size systems, the tests made proved that the approach provides a very good understanding of the optimal steady state behaviour of a power system. The studies made showed the potential benefits of the optimal operation of a power system in normal operation or considering line outages with or without FACTS devices.

Finally, the tests made with a different optimization method in two different networks validate the optimal solutions provided by the Parametric-OPF.

CHAPTER 7

CONCLUSIONS AND RECOMMENDATIONS FOR FUTURE RESEARCH

7.1 Introduction

This thesis has presented a first implementation of a generalized parametric optimization method to solve the full nonlinear OPF problem. The parametric approach has the characteristic that it can generate a set of optimal solution trajectories rather than a single solution. The main motivation for the use of such an approach was to analyze the behaviour of the optimal solution trajectories during the optimization process. This study showed that, besides providing an innovative means to solve the OPF, the parametric approach also gives a completely new understanding of the problem itself.

The parameterization embeds the OPF model into a broader class of problems characterized by the range of variation of the parameter. Using this formulation, the behaviour of the optimal solution with respect to a change in any parameter existing in the model can be studied. As a direct consequence, a formulation of the OPF problem valid for both fixed or variable load was possible. In addition an algorithm which can be used in both cases was implemented. Generally speaking, one could study the behaviour of the optimal solution with respect to any parameter of the OPF with basically the same algorithm.

7.2 Summary of Results

The following are the main results obtained from the research performed in this thesis:

1. The parametric approach enables the solution of the OPF problem (in principle) starting from any initial solution and permits the exact tracking of a pre-specified load curve.

2. The parameterization gives us a means of solving the OPF problem by systematically tracking the changes in the optimal active set by either a binary search or a linear prediction method.

3. As a result of the systematic tracking, the approach is less subject to problems of ill-conditioning of the Newton matrix, W.

4. In spite of being slow, the Parametric-OPF algorithm is robust. It was tested successfully in different transmission systems for fixed and variable load and, when tested for different initial points, the method always arrived at the same optimum. The results were validated by an optimization algorithm based on sequential quadratic programming.

5. The method permits the visualization of the optimum trajectories created during the solution process, which gives valuable insight about the behaviour of the OPF solution both for both fixed and variable load. From this characteristic and from consideration (2) above it follows that:

    a. The approach permits the identification and prediction of the "critical points" existing in the optimal trajectories. The differentiation of these critical points is useful to the identification of unsolvable cases and, in a more broad perspective, is important for a good understanding of the

optimal steady-state behaviour of a power system in a varying load environment.

b. Regions of *structural stability* could be identified by the method. These regions may be of great importance in practice because they represent intervals of variation of ε for which there is a continuous change in the feasible set.

c. Some conclusions can be drawn about the behaviour of the optimal trajectories: (i) these trajectories are fairly linear between break-points; (ii) clearly the trajectories of the active OPF subproblem are more linear compared with those of the reactive subproblem; (iii) this nonlinear behaviour of the reactive subproblem is mainly due to changes in the active feasible set and (iv) it is evident that there is a linear variation of the OPF variables for a small variation in the system demand.

d. Useful information can also be obtained from the optimal trajectories of the Lagrange multipliers associated to different variables. The changes in their trajectories give an idea about the influence of a newly fixed variable on the "tendency" of other variables to stay at their limits. In particular, these trajectories show the great sensitivity of the reactive subproblem variables to changes in the active set.

e. The trajectories of the Bus Incremental Costs and of the System Incremental Cost as a function of the load can also be provided. These trajectories show that the cost of supplying additional demand depends both on the total system demand at a specific time and on the location of this additional load. Moreover, the study of these sensitivities show that the Bus Incremental Costs provide more reliable information regarding the actual cost of supplying additional load at different buses.

6. The fairly linear characteristics of the optimal trajectories between break-points

accounts for the good performance of the linear prediction based approach implemented in this thesis to follow the changes in the optimal active feasible set throughout the tracking process.

7. The studies regarding FACTS devices show that they can be important to increase the loadability limit of a network and also to improve the quality of the optimal solution.

7.3 Recommendations for Future Research

The following are some points that could be investigated to continue the work that has begun with this thesis:

1. The CPU time of the Parametric-OPF is still prohibitive for on-line use. To improve the performance of the algorithm it is important to conceive faster strategies to define the optimal active feasible set that would not compromise the systematic search made by the algorithm. In addition, faster solvers for the system of KT conditions could be tested, perhaps with sparsity techniques designed specifically for the OPF problem.

2. A new implementation of the Parametric-OPF in a compilable language is necessary to enable tests with real-size transmission networks.

3. The on-line use of this method is also conditioned to the resolution of the critical points that can occur in the optimal trajectories when the load varies.

4. The study of critical points might also be important to formulate a sound theoretical basis for the problem of feasibility of the OPF and Secure-OPF.

5. There are some aspects of the tracking process still not fully understood. We could not disprove the existence of "cycling" in the algorithm (i.e., the existence of variables that continuously are fixed at their limit and subsequently released

delaying the tracking process). An investigation of such an aspect is advisable. Another point that bears investigation is the observed invariance of the optimal solution given by the method for different starting points.

6. Until today no attempt was made to represent discrete variables in parametric approaches. Further research is also needed is this area.

7. Among the interior points optimization methods being developed today is a pathfollowing method. Interior points methods have shown a computational performance comparable to LP based algorithms in the resolution the OPF. It would be interesting to see the performance of such an interior point pathfollowing method in the parameterized OPF problem.

8. Additional studies can also be made regarding the influence of FACTS devices in the optimal steady-state operation of a power system. New (more realistic) models can be tested and more extensive simulations can be carried out to assess the influence of such devices.

APPENDIX A

FORMULATION OF THE OPF PROBLEM

A.1 Mathematical Model for the OPF Problem

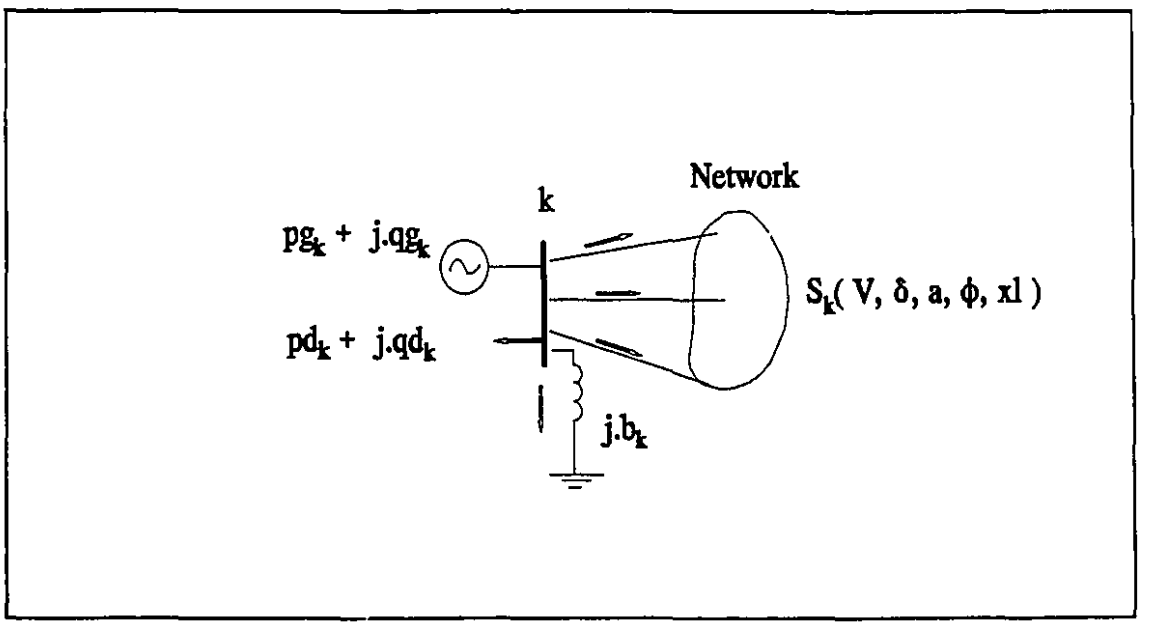

Figure A.1- Power balance at bus k.

Figure (A.1) represents a generic bus k of a transmission system with all "arriving" and "leaving" power. From this figure, it is easy to verify that the energy balance on bus k can be represented as

$$\begin{aligned} pg_k - pd_k - p_k(V,\delta,a,\phi,xl) &= 0 \\ qg_k - qd_k - q_k(V,\delta,a,\phi,xl) + b_k.V_k^2 &= 0 \end{aligned} \qquad \textbf{(A.1)}$$

where $\mathbf{pg}_k$ and $\mathbf{qg}_k$ are the generated power; $\mathbf{pd}_k$ and $\mathbf{qd}_k$ are the connected loads; $\mathbf{b}_k$ represents the variable shunt compensator; **V** and δ are the vectors of bus voltage magnitudes and angles, respectively; **a** is the vector of transformer taps; ϕ is the vector of phase shifter angles and **xl** is the vector of variable series reactances.

The Optimal Power Flow calculation optimizes the static operating condition of a power generation-transmission system. A scalar function is to be minimized subject to many sparse equality and inequality constraints. The equality constraints represent the energy balance in each bus of the network (the basic load flow equations) while the inequalities represent limits on the state and controllable variables, as well as on other dependent variables (e.g., line active flows). Since $\mathbf{pg}_k$ and $\mathbf{qg}_k$ are considered free within limits, in the OPF formulation we can represent both $\mathbf{pg}_k$ and $\mathbf{qg}_k$ in terms of the other variables by using equation (A.1). However, since the OPF is formulated also to optimize the generation cost, we decided to consider $\mathbf{pg}_k$ as a decision variable, while using equation (A.1) to represent the reactive power injections in terms of the other variables of the system. Considering this, the problem can be formulated in a general form as:

$$Min \quad c = w_1 \sum_{i=1}^{nb} c_i(pg_i) + w_2 \sum_{i=1}^{nb} pg_i + w_3 \sum_{i=1}^{nb} (V_i - 1)^2 \tag{A.2}$$

subject to

$$pg_i - pd_i - p_i(V, \delta, a, \phi, xl) = 0, \quad i = 1,...,nb \quad (\alpha_i) \tag{A.3}$$

$$qd_i + q_i(V, \delta, a, \phi, xl) - b_i V_i^2 = 0, \quad i = 1,...,nqgfix \quad (\beta_i) \tag{A.4}$$

$$qg_i^{min} \le q_i(V, \delta, a, \phi, xl) - b_i V_i^2 + qd_i \le qg_i^{max}, \quad i = 1,...,nqgnf \quad (\rho_i^{min}, \rho_i^{max}) \tag{A.5}$$

$$pl_i^{min} \le pl_i(V, \delta, a, \phi, xl) \le pl_i^{max} \quad i = 1,...,nl \quad (\sigma_i^{min}, \sigma_i^{max}) \tag{A.6}$$

$$V_i^{min} \le V_i \le V_i^{max} \quad i = 1,...,nb \quad (\pi_i^{min}, \pi_i^{max}) \tag{A.7}$$

$$b_i^{min} \le b_i \le b_i^{max} \quad i = 1,...,nb \quad (\psi_i^{min}, \psi_i^{max}) \tag{A.8}$$

$$pg_i^{min} \le pg_i \le pg_i^{max} \quad i = 1,...,nb \quad (\gamma_i^{min}, \gamma_i^{max}) \tag{A.9}$$

$$a_i^{min} \le a_i \le a_i^{max} \quad i = 1,...,nl \quad (\xi_i^{min}, \xi_i^{max}) \tag{A.10}$$

$$\phi_i^{min} \le \phi_i \le \phi_i^{max} \quad i = 1,...,nl \quad (\eta_i^{min}, \eta_i^{max}) \tag{A.11}$$

$$xl_i^{min} \le xl_i \le xl_i^{max} \quad i = 1,...,nl \quad (\tau_i^{min}, \tau_i^{max}) \tag{A.12}$$

Where

nb = number of buses in the system;

nl = number of lines in the system;

nqgfix = number of buses with fixed reactive injection (load buses);

nqgnf = number of buses with free reactive injection;

$\mathbf{pg}_i \in \mathbf{R}$ = active power generation at bus i;

$\mathbf{pd}_i \in \mathbf{R}$ = active load at bus i;

$\mathbf{qd}_i \in \mathbf{R}$ = reactive load at bus i;

$\mathbf{b}_i \in \mathbf{R}$ = variable shunt compensator at bus i;

$\mathbf{V} \in \mathbf{R}^{nb}$ = vector of voltage magnitudes;

$\delta \in \mathbf{R}^{nb}$ = vector of voltage angles;

$\mathbf{a} \in \mathbf{R}^{nl}$ = vector of transformer tap settings;

$\phi \in \mathbf{R}^{nl}$ = vector of phase shifter angles;

$\mathbf{xl} \in \mathbf{R}^{nl}$ = vector of variable series reactances;

$\alpha_i \in \mathbf{R}$ = Lagrange multiplier associated to the active power mismatch;

$\beta_i \in \mathbf{R}$ = Lagrange multipliers associated with the reactive power mismatch at the load buses;

$\rho_i^{min}, \rho_i^{max} \in \mathbf{R}$ = Lagrange multipliers associated with the minimum and maximum limits on the reactive generation;

$\sigma_i^{min}, \sigma_i^{max} \in \mathbf{R}$ = Lagrange multipliers associated with the minimum and maximum limits on the line flows;

$\pi_i^{min}, \pi_i^{max} \in \mathbf{R}$ = Lagrange multiplier associated with the minimum and maximum limits on the voltage magnitudes;

$\psi_i^{min}, \psi_i^{max} \in \mathbf{R}$ = Lagrange multiplier associated with the minimum and maximum limits on the shunt compensators;

$\gamma_i^{min}, \gamma_i^{max} \in \mathbf{R}$ = Lagrange multipliers associated with the minimum and maximum limits on the active generation;

$\xi_i^{min}, \xi_i^{max} \in \mathbf{R}$ = Lagrange multipliers associated with the minimum and maximum limits on the transformer tap settings;

$\eta_i^{min}, \eta_i^{max} \in \mathbf{R}$ = Lagrange multipliers associated with the minimum and maximum limits on the phase shifter angles;

$\tau_i^{min}, \tau_i^{max} \in \mathbf{R}$ = Lagrange multipliers associated with the minimum and maximum limits on the variable series reactances;

$\mathbf{c}_i(\mathbf{pg}_i) = \mathbf{aa}_i\, \mathbf{pg}_i + \mathbf{bb}_i\, \mathbf{pg}_i^2$ = generation cost function of bus i.

A.2 Parameterized Model and Optimality Conditions - Phase I

A.2.1 Parameterized Model

Let $x = [\delta^T, V^T, b^T, pg^T, a^T, \phi^T, xl^T]^T$. The Parametric-OPF is formulated from the model given by (A.2)-(A.12). To express the parameterized model we first introduce a Lagrangian function composed only by the equality constraints (A.3) and (A.4). This Lagrangian is defined at the initial guess ($\mathbf{x}^0$, α^0, β^0), supposing that the active and reactive bus load vectors for Phase I are **pd** and **qd**, respectively:

$$\begin{aligned} \mathcal{L}^0 \;=\; & w_1 \sum_{i=1}^{nb} c_i(pg_i^0) + w_2 \sum_{i=1}^{nb} pg_i^0 + w_3 \sum_{i=1}^{nb} (V_i^0 - 1)^2 \\ & + \sum_{i=1}^{nb} \alpha_i^0 [pg_i^0 - pd_i - p_i(V^0, \delta^0, a^0, \phi^0, xl^0)] \\ & + \sum_{i=1}^{nqgfix} \beta_i^0 [qd_i + q_i(V^0, \delta^0, a^0, \phi^0, xl^0) - b_i^0 (V_i^0)^2] \end{aligned} \tag{A.13}$$

Then the Parametric-OPF model can be defined as

$$\begin{aligned} Min \;\; c \;=\; & w_1 \sum_{i=1}^{nb} c_i(pg_i) + w_2 \sum_{i=1}^{nb} pg_i + w_3 \sum_{i=1}^{nb} (V_i - 1)^2 \\ & - (1 - \epsilon) \Bigg\{ \sum_{i=1}^{nb} \left[\left(\frac{\partial \mathcal{L}^0}{\partial \delta_i} \right) \delta_i + \left(\frac{\partial \mathcal{L}^0}{\partial V_i} \right) V_i + \left(\frac{\partial \mathcal{L}^0}{\partial b_i} \right) b_i + \left(\frac{\partial \mathcal{L}^0}{\partial pg_i} \right) pg_i \right] \\ & \qquad + \sum_{i=1}^{nl} \left[\left(\frac{\partial \mathcal{L}^0}{\partial a_i} \right) a_i + \left(\frac{\partial \mathcal{L}^0}{\partial \phi_i} \right) \phi_i + \left(\frac{\partial \mathcal{L}^0}{\partial xl_i} \right) xl_i \right] \\ & - \frac{w}{2} \sum_{i=1}^{nb} \left[(\delta_i - \delta_i^0)^2 + (V_i - V_i^0)^2 + (b_i - b_i^0)^2 + (pg_i - pg_i^0)^2 \right] \\ & \qquad - \frac{w}{2} \sum_{i=1}^{nl} \left[(a_i - a_i^0)^2 + (\phi_i - \phi_i^0)^2 + (xl_i - xl_i^0)^2 \right] \Bigg\} \end{aligned} \tag{A.14}$$

subject to

$$pg_i - pd_i - p_i(V,\delta,a,\phi,xl) - (1-\epsilon)\left[pg_i^0 - pd_i - p_i(V^0,\delta^0,a^0,\phi^0,xl^0)\right] = 0, \quad i=1,...,nb \quad (\alpha_i) \tag{A.15}$$

$$qd_i + q_i(V,\delta,a,\phi,xl) - b_i V_i^2 - (1-\epsilon)\left[qd_i + q_i(V^0,\delta^0,a^0,\phi^0,xl^0) - b_i^0 (V_i^0)^2\right] = 0, \quad i=1,...,nqgfix \quad (\beta_i) \tag{A.16}$$

$$qg_i^{\min} \le q_i(V,\delta,a,\phi,xl) - b_i V_i^2 + qd_i - (1-\epsilon)\Delta qg_i \le qg_i^{\max}, \quad i=1,...,nqgnf \quad (\rho_i^{\min},\rho_i^{\max}) \tag{A.17}$$

$$pl_i^{\min} \le pl_i(V,\delta,a,\phi,xl) - (1-\epsilon)\Delta pl_i \le pl_i^{\max}, \quad i=1,...,nl \quad (\sigma_i^{\min},\sigma_i^{\max}) \tag{A.18}$$

$$V_i^{\min} \le V_i \le V_i^{\max} \quad i=1,...,nb \quad (\pi_i^{\min},\pi_i^{\max}) \tag{A.19}$$

$$b_i^{\min} \le b_i \le b_i^{\max} \quad i=1,...,nb \quad (\psi_i^{\min}\psi_i^{\max}) \tag{A.20}$$

$$pg_i^{\min} \le pg_i \le pg_i^{\max} \quad i=1,...,nb \quad (\gamma_i^{\min},\gamma_i^{\max}) \tag{A.21}$$

$$a_i^{\min} \le a_i \le a_i^{\max} \quad i=1,...,nl \quad (\xi_i^{\min},\xi_i^{\max}) \tag{A.22}$$

$$\phi_i^{\min} \le \phi_i \le \phi_i^{\max} \quad i=1,...,nl \quad (\eta_i^{\min},\eta_i^{\max}) \tag{A.23}$$

$$xl_i^{\min} \le xl_i \le xl_i^{\max} \quad i=1,...,nl \quad (\tau_i^{\min},\tau_i^{\max}) \tag{A.24}$$

A.2.2 Optimality Conditions

For Phase I, the Lagrangian of the parameterized problem is written

$$
\begin{aligned}
\mathcal{L} \;=\; & w_1\sum_{i=1}^{nb} c_i(pg_i) + w_2\sum_{i=1}^{nb} pg_i + w_3\sum_{i=1}^{nb}(V_i-1)^2 \\
& - (1-\epsilon)\left\{\sum_{i=1}^{nb}\left[\left(\frac{\partial \mathcal{L}^0}{\partial \delta_i}\right)\delta_i + \ldots + \left(\frac{\partial \mathcal{L}^0}{\partial pg_i}\right)pg_i\right] + \sum_{i=1}^{nl}\left[\left(\frac{\partial \mathcal{L}^0}{\partial a_i}\right) + \ldots + \left(\frac{\partial \mathcal{L}^0}{\partial xl_i}\right)xl_i\right]\right. \\
& \left. - \frac{w}{2}\sum_{i=1}^{nb}\left[(\delta_i-\delta_i^0)^2 + \ldots + (pg_i-pg_i^0)^2\right] - \frac{w}{2}\sum_{i=1}^{nl}\left[(a_i-a_i^0)^2 + \ldots + (xl_i-xl_i^0)^2\right]\right\} \\
& + \sum_{i=1}^{nb}\alpha_i\{pg_i - pd_i - p_i(V,\delta,a,\phi,xl) - (1-\epsilon)[pg_i^0 - pd_i - p_i(V^0,\delta^0,a^0,\phi^0,xl^0)]\} \\
& + \sum_{i=1}^{nqgfix}\beta_i\{qd_i + q_i(V,\delta,a,\phi,xl) - b_iV_i^2 - (1-\epsilon)[qd_i + q_i(V^0,\delta^0,a^0,\phi^0,xl^0) - b_i^0(V_i^0)^2]\} \\
& + \sum_{i=1}^{nqgnf}\rho_i^{\min}[qd_i + q_i(V,\delta,a,\phi,xl) - b_iV_i^2 - qg_i^{\min} - (1-\epsilon)\Delta qd_i] \\
& + \sum_{i=1}^{nqgnf}\rho_i^{\max}[qd_i + q_i(V,\delta,a,\phi,xl) - b_iV_i^2 - qg_i^{\max} - (1-\epsilon)\Delta qd_i] \\
& + \sum_{i=1}^{nl}\sigma_i^{\min}[pl_i(V,\delta,a,\phi,xl) - pl_i^{\min} - (1-\epsilon)\Delta pl_i] \\
& + \sum_{i=1}^{nl}\sigma_i^{\max}[pl_i(V,\delta,a,\phi,xl) - pl_i^{\max} - (1-\epsilon)\Delta pl_i] \\
& + \sum_{i=1}^{nb}\pi_i^{\min}(V_i - V_i^{\min}) + \sum_{i=1}^{nb}\pi_i^{\max}(V_i - V_i^{\max}) + \sum_{i=1}^{nb}\psi_i^{\min}(b_i - b_i^{\min}) + \sum_{i=1}^{nb}\psi_i^{\max}(b_i - b_i^{\max}) \\
& + \sum_{i=1}^{nb}\gamma_i^{\min}(pg_i - pg_i^{\min}) + \sum_{i=1}^{nb}\gamma_i^{\max}(pg_i - pg_i^{\max}) + \sum_{i=1}^{nl}\xi_i^{\min}(a_i - a_i^{\min}) + \sum_{i=1}^{nl}\xi_i^{\max}(a_i - a_i^{\max}) \\
& + \sum_{i=1}^{nl}\eta_i^{\min}(\phi_i - \phi_i^{\min}) + \sum_{i=1}^{nl}\eta_i^{\max}(\phi_i - \phi_i^{\max}) + \sum_{i=1}^{nl}\tau_i^{\min}(xl_i - xl_i^{\min}) + \sum_{i=1}^{nl}\tau_i^{\max}(xl_i - xl_i^{\max})
\end{aligned}
\tag{A.25}
$$

First Order Optimality Conditions (Kuhn-Tucker Conditions)

A feasible point $x^* = [(\delta^*)^T,(V^*)^T,(b^*)^T,(pg^*)^T,(a^*)^T,(\phi^*)^T,(xl^*)^T]^T$ (i.e., belonging to the set defined by (A.15)-(A.24)) that fulfils LICQ, satisfies the necessary conditions for optimality if it solves the following system of equations for $\upsilon^* = [(\alpha^*)^T,(\beta^*)^T,(\pi^{min*})^T,(\pi^{max*})^T,\ldots,(\tau^{min*})^T,(\tau^{max*})^T]^T$:

$$\left[\frac{\partial^T \mathcal{L}}{\partial \delta}, \frac{\partial^T \mathcal{L}}{\partial V}, \frac{\partial^T \mathcal{L}}{\partial b}, \frac{\partial^T \mathcal{L}}{\partial pg}, \frac{\partial^T \mathcal{L}}{\partial a}, \frac{\partial^T \mathcal{L}}{\partial \phi}, \frac{\partial^T \mathcal{L}}{\partial xl}\right]^T = 0 \qquad \textbf{(A.26)}$$

$$\begin{aligned}(\rho_i^{min})^*[qd_i + q_i(\delta^*,V^*,a^*,\phi^*,xl^*) - b_i^*(V_i^*)^2 - qg_i^{min} - (1-\epsilon)\Delta qg_i] = 0\\ (\rho_i^{max})^*[qd_i + q_i(\delta^*,V^*,a^*,\phi^*,xl^*) - b_i^*(V_i^*)^2 - qg_i^{max} - (1-\epsilon)\Delta qg_i] = 0\end{aligned} \quad i=1,..,nqgnf \qquad \textbf{(A.27)}$$

$$\begin{aligned}(\sigma_i^{min})^*[pl_i(\delta^*,V^*,a^*,\phi^*,xl^*) - pli^{min} - (1-\epsilon)\Delta pl_i] &= 0\\ (\sigma_i^{max})^*[pl_i(\delta^*,V^*,a^*,\phi^*,xl^*) - pl_i^{max} - (1-\epsilon)\Delta pl_i] &= 0\end{aligned} \quad i=1,\ldots,nl \qquad \textbf{(A.28)}$$

$$\begin{aligned}(\pi_i^{min})^*(V_i^* - V_i^{min}) &= 0\\ (\pi_i^{max})^*(V_i^* - V_i^{max}) &= 0\end{aligned} \quad i=1,\ldots,nb \qquad \textbf{(A.29)}$$

$$\begin{aligned}(\psi_i^{min})^*(b_i^* - b_i^{min}) &= 0\\ (\psi_i^{max})^*(b_i^* - b_i^{max}) &= 0\end{aligned} \quad i=1,\ldots,nb \qquad \textbf{(A.30)}$$

$$\begin{aligned}(\gamma_i^{min})^*(pg_i^* - pg_i^{min}) &= 0\\ (\gamma_i^{max})^*(pg_i^* - pg_i^{max}) &= 0\end{aligned} \quad i=1,\ldots,nb \qquad \textbf{(A.31)}$$

$$\begin{aligned}(\xi_i^{min})^*(a_i^* - a_i^{min}) &= 0\\ (\xi_i^{max})^*(a_i^* - a_i^{max}) &= 0\end{aligned} \quad i=1,\ldots,nl \qquad \textbf{(A.32)}$$

$$\begin{aligned}(\eta_i^{min})^*(\phi_i^* - \phi_i^{min}) &= 0 \\ (\eta_i^{max})^*(\phi_i^* - \phi_i^{max}) &= 0\end{aligned} \quad i=1,...,nl \tag{A.33}$$

$$\begin{aligned}(\tau_i^{min})^*(xl_i^* - xl_i^{min}) &= 0 \\ (\tau_i^{max})^*(xl_i^* - xl_i^{max}) &= 0\end{aligned} \quad i=1,...,nl \tag{A.34}$$

Where

$$\begin{aligned}&(\rho_i^{min})^* \le 0,\ (\sigma_i^{min})^* \le 0\ ,(\pi_i^{min})^* \le 0,\ (\psi_i^{min})^* \le 0, \\ &(\gamma_i^{min})^* \le 0,\ (\xi_i^{min})^* \le 0,\ (\eta_i^{min})^* \le 0,\ (\tau_i^{min})^* \le 0\end{aligned} \tag{A.35}$$

$$\begin{aligned}&(\rho_i^{max})^* \ge 0,\ (\sigma_i^{max})^* \ge 0,\ (\pi_i^{max})^* \ge 0,\ (\psi_i^{max})^* \ge 0, \\ &(\gamma_i^{max})^* \ge 0,\ (\xi_i^{max})^* \ge 0,\ (\eta_i^{max})^* \ge 0,\ (\tau_i^{max})^* \ge 0\end{aligned} \tag{A.36}$$

and for $\forall\ \alpha_i^*,\ \beta_i^*$.

Second Order Optimality Conditions

A point $\mathbf{z}^* = [\mathbf{x}^*, \upsilon^*]$ satisfies the second order (sufficient) optimality conditions if , at $\mathbf{z} = \mathbf{z}^*$ the hessian matrix,

$$H = \begin{bmatrix} \frac{\partial^2 \mathcal{L}}{\partial \delta^2} & \frac{\partial^2 \mathcal{L}}{\partial \delta \partial V} & 0 & 0 & \frac{\partial^2 \mathcal{L}}{\partial \delta \partial a} & \frac{\partial^2 \mathcal{L}}{\partial \delta \partial \phi} & \frac{\partial^2 \mathcal{L}}{\partial \delta \partial xl} \\ \frac{\partial^2 \mathcal{L}}{\partial V \partial \delta} & \frac{\partial^2 \mathcal{L}}{\partial V^2} & \frac{\partial^2 \mathcal{L}}{\partial V \partial b} & 0 & \frac{\partial^2 \mathcal{L}}{\partial V \partial a} & \frac{\partial^2 \mathcal{L}}{\partial V \partial \phi} & \frac{\partial^2 \mathcal{L}}{\partial V \partial xl} \\ 0 & \frac{\partial^2 \mathcal{L}}{\partial b \partial V} & \frac{\partial^2 \mathcal{L}}{\partial b^2} & 0 & 0 & 0 & 0 \\ 0 & 0 & 0 & \frac{\partial^2 \mathcal{L}}{\partial pg^2} & 0 & 0 & 0 \\ \frac{\partial^2 \mathcal{L}}{\partial a \partial \delta} & \frac{\partial^2 \mathcal{L}}{\partial a \partial V} & 0 & 0 & \frac{\partial^2 \mathcal{L}}{\partial a^2} & \frac{\partial^2 \mathcal{L}}{\partial a \partial \phi} & \frac{\partial^2 \mathcal{L}}{\partial a \partial xl} \\ \frac{\partial^2 \mathcal{L}}{\partial \phi \partial \delta} & \frac{\partial^2 \mathcal{L}}{\partial \phi \partial V} & 0 & 0 & \frac{\partial^2 \mathcal{L}}{\partial \phi \partial a} & \frac{\partial^2 \mathcal{L}}{\partial \phi^2} & \frac{\partial^2 \mathcal{L}}{\partial \phi \partial xl} \\ \frac{\partial^2 \mathcal{L}}{\partial xl \partial \delta} & \frac{\partial^2 \mathcal{L}}{\partial xl \partial V} & 0 & 0 & \frac{\partial^2 \mathcal{L}}{\partial xl \partial a} & \frac{\partial^2 \mathcal{L}}{\partial xl \partial \phi} & \frac{\partial^2 \mathcal{L}}{\partial xl^2} \end{bmatrix} \quad \text{(A.37)}$$

is positive definite on the null space of the jacobian J defined as

$$J = \begin{bmatrix} -\frac{\partial p}{\partial \delta} & -\frac{\partial p}{\partial V} & 0 & Id & -\frac{\partial p}{\partial a} & -\frac{\partial p}{\partial \phi} & -\frac{\partial p}{\partial xl} \\ \frac{\partial q_K}{\partial \delta} & \frac{\partial q_K}{\partial V} & \frac{\partial q_K}{\partial b} & 0 & \frac{\partial q_K}{\partial a} & \frac{\partial q_K}{\partial \phi} & \frac{\partial q_K}{\partial xl} \\ \frac{\partial q_{N_0}}{\partial \delta} & \frac{\partial q_{N_0}}{\partial V} & \frac{\partial q_{N_0}}{\partial b} & 0 & \frac{\partial q_{N_0}}{\partial a} & \frac{\partial q_{N_0}}{\partial \phi} & \frac{\partial q_{N_0}}{\partial xl} \\ \frac{\partial pl_{N_0}}{\partial \delta} & \frac{\partial pl_{N_0}}{\partial V} & 0 & 0 & \frac{\partial pl_{N_0}}{\partial a} & \frac{\partial pl_{N_0}}{\partial \phi} & \frac{\partial pl_{N_0}}{\partial xl} \end{bmatrix} \quad \text{(A.38)}$$

where the index **K** stands for the set of buses with fixed reactive injection, N_0 stands for the set of active inequalities associated with Lagrange multipliers different from 0 (for q(.) this includes all buses with generation at the limit) and **Id** is the identity matrix.

Therefore, a point $\mathbf{z}^*=(\mathbf{x}^*, \upsilon^*)$ satisfies the second order optimality conditions if, for $\mathbf{y} \neq \mathbf{0}$ such that

$$Jy = 0 \tag{A.39}$$

we have

$$y^T Hy > 0 \tag{A.40}$$

A.3 Parameterized Model and Optimality Conditions - Phase II

A.3.1 Parameterized Model

During Phase II the system load is supposed to vary linearly with ε. For the load tracking, the optimal solution corresponding to a specific load level $\mathbf{d}^0$ is used as the initial solution to track the load variation until the next level $\mathbf{d}^0+\Delta\mathbf{d}^0$. Since the initial solution is an optimal solution, it is not necessary to parameterize the objective function. However, to improve the convergence of the Newton method, the parameterized quadratic term is kept also during the load tracking. Since the parameterization affects the load, all constraints of power balance on the buses of the system need to be parameterized (this includes the power balance constraints on the load buses and the limits on the reactive generation). The active power flow limits, since they do not depend directly on the bus loads, are not parameterized.

Supposing that the vectors of real and reactive load associated with the initial solution $\mathbf{x}^0$ are $\mathbf{pd}^0$ and $\mathbf{qd}^0$, respectively, the Parametric-OPF for Phase II is defined

$$Min \quad c = w_1 \sum_{i=1}^{nb} c_i(pg_i) + w_2 \sum_{i=1}^{nb} pg_i + w_3 \sum_{i=1}^{nb} (V_i - 1)^2$$

$$+ (1 - \epsilon)\left\{ \frac{w}{2} \sum_{i=1}^{nb} \left[(\delta_i - \delta_i^0)^2 + (V_i - V_i^0)^2 + (b_i - b_i^0)^2 + (pg_i - pg_i^0)^2 \right] \right. \tag{A.41}$$

$$\left. + \frac{w}{2} \sum_{i=1}^{nl} \left[(a_i - a_i^0)^2 + (\phi_i - \phi_i^0)^2 + (xl_i - xl_i^0)^2 \right] \right\}$$

subject to

$$pg_i - (pd_i^0 + \epsilon \Delta pd_i^0) - p_i(V, \delta, a, \phi, xl) = 0, \quad i = 1,...,nb \quad (\alpha_i) \tag{A.42}$$

$$qd_i^0 + \epsilon \Delta qd_i^0 + q_i(V, \delta, a, \phi, xl) - b_i V_i^2 = 0, \quad i = 1,...,nqgfix \quad (\beta_i) \tag{A.43}$$

$$qg_i^{\min} \le q_i(V, \delta, a, \phi, xl) - b_i V_i^2 + qd_i^0 + \epsilon \Delta qd_i^0 \le qg_i^{\max}, \quad i = 1,...,nqgnf \quad (\rho_i^{\min}, \rho_i^{\max}) \tag{A.44}$$

$$pl_i^{\min} \le pl_i(V, \delta, a, \phi, xl) \le pl_i^{\max}, \quad i = 1,...,nl \quad (\sigma_i^{\min}, \sigma_i^{\max}) \tag{A.45}$$

$$V_i^{\min} \le V_i \le V_i^{\max} \quad i = 1,...,nb \quad (\pi_i^{\min}, \pi_i^{\max}) \tag{A.46}$$

$$b_i^{\min} \le b_i \le b_i^{\max} \quad i = 1,...,nb \quad (\psi_i^{\min}, \psi_i^{\max}) \tag{A.47}$$

$$pg_i^{\min} \le pg_i \le pg_i^{\max} \quad i = 1,...,nb \quad (\gamma_i^{\min}, \gamma_i^{\max}) \tag{A.48}$$

$$a_i^{\min} \le a_i \le a_i^{\max} \quad i = 1,...,nl \quad (\xi_i^{\min}, \xi_i^{\max}) \tag{A.49}$$

$$\phi_i^{\min} \le \phi_i \le \phi_i^{\max} \quad i = 1,...,nl \quad (\eta_i^{\min}, \eta_i^{\max}) \tag{A.50}$$

$$xl_i^{\min} \le xl_i \le xl_i^{\max} \quad i = 1,...,nl \quad (\tau_i^{\min}, \tau_i^{\max}) \tag{A.51}$$

A.3.2 Optimality Conditions

The Lagrangian of the parameterized problem is written

$$
\begin{aligned}
\mathcal{L} \;=\; & w_1\sum_{i=1}^{nb} c_i(pg_i) + w_2\sum_{i=1}^{nb} pg_i + w_3\sum_{i=1}^{nb}(V_i-1)^2 \\
& + (1-\epsilon)\left\{\frac{w}{2}\sum_{i=1}^{nb}\left[(\delta_i-\delta_i^0)^2+\ldots+(pg_i-pg_i^0)^2\right] + \frac{w}{2}\sum_{i=1}^{nl}\left[(a_i-a_i^0)^2+\ldots+(xl_i-xl_i^0)^2\right]\right\} \\
& + \sum_{i=1}^{nb}\alpha_i\{pg_i-(pd_i^0+\epsilon\Delta pd_i^0)-p_i(V,\delta,a,\phi,xl)\} \\
& + \sum_{i=1}^{nqgfix}\beta_i\{qd_i^0+\epsilon\Delta qd_i^0+q_i(V,\delta,a,\phi,xl)-b_iV_i^2\} \\
& + \sum_{i=1}^{nqgnf}\rho_i^{\min}[qd_i^0+\epsilon\Delta qd_i^0+q_i(V,\delta,a,\phi,xl)-b_iV_i^2-qg_i^{\min}] \\
& + \sum_{i=1}^{nqgnf}\rho_i^{\max}[qd_i^0+\epsilon\Delta qd_i^0+q_i(V,\delta,a,\phi,xl)-b_iV_i^2-qg_i^{\max}] \\
& + \sum_{i=1}^{nl}\sigma_i^{\min}[pl_i(V,\delta,a,\phi,xl)-pl_i^{\min}] + \sum_{i=1}^{nl}\sigma_i^{\max}[pl_i(V,\delta,a,\phi,xl)-pl_i^{\max}] \\
& + \sum_{i=1}^{nb}\pi_i^{\min}(V_i-V_i^{\min}) + \sum_{i=1}^{nb}\pi_i^{\max}(V_i-V_i^{\max}) + \sum_{i=1}^{nb}\psi_i^{\min}(b_i-b_i^{\min}) + \sum_{i=1}^{nb}\psi_i^{\max}(b_i-b_i^{\max}) \\
& + \sum_{i=1}^{nb}\gamma_i^{\min}(pg_i-pg_i^{\min}) + \sum_{i=1}^{nb}\gamma_i^{\max}(pg_i-pg_i^{\max}) + \sum_{i=1}^{nl}\xi_i^{\min}(a_i-a_i^{\min}) + \sum_{i=1}^{nl}\xi_i^{\max}(a_i-a_i^{\max}) \\
& + \sum_{i=1}^{nl}\eta_i^{\min}(\phi_i-\phi_i^{\min}) + \sum_{i=1}^{nl}\eta_i^{\max}(\phi_i-\phi_i^{\max}) + \sum_{i=1}^{nl}\tau_i^{\min}(xl_i-xl_i^{\min}) + \sum_{i=1}^{nl}\tau_i^{\max}(xl_i-xl_i^{\max})
\end{aligned}
\tag{A.52}
$$

First Order Optimality Conditions (Kuhn-Tucker Conditions)

For Phase II, a feasible point $x^* = [(\delta^*)^T,(V^*)^T,(b^*)^T,(pg^*)^T,(a^*)^T,(\phi^*)^T,(xl^*)^T]^T$ (i.e., belonging to the set defined by (A.42)-(A.51)) that fulfils LICQ, satisfies the necessary conditions for optimality if it solves the following system of equations for $\upsilon^* = [(\alpha^*)^T,(\beta^*)^T,(\pi^{\min *})^T,(\pi^{\max *})^T,\ldots,(\tau^{\min *})^T,(\tau^{\max *})^T]^T$:

$$\left[\frac{\partial^T \mathcal{L}}{\partial \delta}, \frac{\partial^T \mathcal{L}}{\partial V}, \frac{\partial^T \mathcal{L}}{\partial b}, \frac{\partial^T \mathcal{L}}{\partial pg}, \frac{\partial^T \mathcal{L}}{\partial a}, \frac{\partial^T \mathcal{L}}{\partial \phi}, \frac{\partial^T \mathcal{L}}{\partial xl}\right]^T = 0 \tag{A.53}$$

$$\begin{aligned}(\rho_i^{\min})^*[qd_i^0 + \epsilon \Delta qd_i^0 + q_i(\delta^*, V^*, a^*, \phi^*, xl^*) - b_i^*(V_i^*)^2 - qg_i^{\min}] = 0 \\ (\rho_i^{\max})^*[qd_i^0 + \epsilon \Delta qd_i^0 + q_i(\delta^*, V^*, a^*, \phi^*, xl^*) - b_i^*(V_i^*)^2 - qg_i^{\max}] = 0\end{aligned} \quad i = 1,..,nqgnf \tag{A.54}$$

$$\begin{aligned}(\sigma_i^{\min})^*[pl_i(\delta^*, V^*, a^*, \phi^*, xl^*) - pli^{\min}] = 0 \\ (\sigma_i^{\max})^*[pl_i(\delta^*, V^*, a^*, \phi^*, xl^*) - pl_i^{\max}] = 0\end{aligned} \quad i = 1,...,nl \tag{A.55}$$

$$\begin{aligned}(\pi_i^{\min})^*(V_i^* - V_i^{\min}) = 0 \\ (\pi_i^{\max})^*(V_i^* - V_i^{\max}) = 0\end{aligned} \quad i = 1,...,nb \tag{A.56}$$

$$\begin{aligned}(\psi_i^{\min})^*(b_i^* - b_i^{\min}) = 0 \\ (\psi_i^{\max})^*(b_i^* - b_i^{\max}) = 0\end{aligned} \quad i = 1,...,nb \tag{A.57}$$

$$\begin{aligned}(\gamma_i^{\min})^*(pg_i^* - pg_i^{\min}) = 0 \\ (\gamma_i^{\max})^*(pg_i^* - pg_i^{\max}) = 0\end{aligned} \quad i = 1,...,nb \tag{A.58}$$

$$\begin{aligned}(\xi_i^{\min})^*(a_i^* - a_i^{\min}) = 0 \\ (\xi_i^{\max})^*(a_i^* - a_i^{\max}) = 0\end{aligned} \quad i = 1,...,nl \tag{A.59}$$

$$\begin{aligned}(\eta_i^{\min})^*(\phi_i^* - \phi_i^{\min}) = 0 \\ (\eta_i^{\max})^*(\phi_i^* - \phi_i^{\max}) = 0\end{aligned} \quad i = 1,...,nl \tag{A.60}$$

$$\begin{aligned}(\tau_i^{\min})^*(xl_i^* - xl_i^{\min}) = 0 \\ (\tau_i^{\max})^*(xl_i^* - xl_i^{\max}) = 0\end{aligned} \quad i = 1,...,nl \tag{A.61}$$

Where

$$(\rho_i^{min})^* \le 0,\ (\sigma_i^{min})^* \le 0\ ,(\pi_i^{min})^* \le 0,\ (\psi_i^{min})^* \le 0,$$
$$(\gamma_i^{min})^* \le 0,\ (\xi_i^{min})^* \le 0,\ (\eta_i^{min})^* \le 0,\ (\tau_i^{min})^* \le 0 \quad \textbf{(A.62)}$$

$$(\rho_i^{max})^* \ge 0,\ (\sigma_i^{max})^* \ge 0,\ (\pi_i^{max})^* \ge 0,\ (\psi_i^{max})^* \ge 0,$$
$$(\gamma_i^{max})^* \ge 0,\ (\xi_i^{max})^* \ge 0,\ (\eta_i^{max})^* \ge 0,\ (\tau_i^{max})^* \ge 0 \quad \textbf{(A.63)}$$

and for $\forall\ \alpha_i^*,\ \beta_i^*$.

Second Order Optimality Conditions

The second order optimality conditions represented by equations (A.37)-(A.40) are also valid here. Since the parameterized quadratic term existing in the objective function is the same for both models, the expression of the hessian $\boldsymbol{H}$ and of the jacobian $\boldsymbol{J}$ are the same for both Phase I and Phase II. The main difference between the two models appears on the first order optimality conditions. These differences become clear if we derive the expressions existing in equations (A.26) and (A.53).

A.3 Derivatives of the Lagrangians of Phase I and Phase II

The differences between the expressions of equation (A.26) and (A.53) are due to the parameterized term linear in $\mathbf{x}$ that appear in the objective function during Phase I. The expressions of the derivatives shown below are also valid for Phase II if the terms in $\mathcal{L}^0$ are disregarded.

A.3.1 First Order Derivatives

For Phase I, the first order derivatives existing on the optimality conditions (equation (A.14)) are:

$$\frac{\partial \mathcal{L}}{\partial V_k} = 2w_3(V_k - 1) - \sum_{i=1}^{nb} \alpha_i \frac{\partial p_i}{\partial V_k}(V,\delta,a,\phi,xl) + \sum_{i=1}^{nqgfix} \beta_i \frac{\partial q_i}{\partial V_k}(V,\delta,a,\phi,xl)$$
$$- 2\beta_k V_k b_k + \sum_{i=1}^{nqgnf} \rho^{\min} \frac{\partial q_i}{\partial V_k}(V,\delta,a,\phi,xl) - 2\rho_k^{\min} b_k V_k$$
$$+ \sum_{i=1}^{nqgnf} \rho_i^{\max} \frac{\partial q_i}{\partial V_k}(V,\delta,a,\phi,xl) - 2\rho_k^{\max} b_k V_k + \sum_{i=1}^{nl} \sigma_i^{\min} \frac{\partial pl_i}{\partial V_k}(V,\delta,a,\phi,xl) \quad \text{(A.64)}$$
$$+ \sum_{i=1}^{nl} \sigma_i^{\max} \frac{\partial pl_i}{\partial V_k}(V,\delta,a,\phi,xl) + \pi_k^{\min} + \pi_k^{\max} - (1-\epsilon)\left[\frac{\partial \mathcal{L}^0}{\partial V_k} - w(V_k - V_k^0)\right]$$

$$\frac{\partial \mathcal{L}}{\partial \delta_k} = -\sum_{i=1}^{nb} \alpha_i \frac{\partial p_i}{\partial \delta_k}(V,\delta,a,\phi,xl) + \sum_{i=1}^{nqgfix} \beta_i \frac{\partial q_i}{\partial \delta_k}(V,\delta,a,\phi,xl)$$
$$+ \sum_{i=1}^{nqgnf} \rho_i^{\min} \frac{\partial q_i}{\partial \delta_k}(V,\delta,a,\phi,xl) + \sum_{i=1}^{nqgnf} \rho_i^{\max} \frac{\partial q_i}{\partial \delta_k}(V,\delta,a,\phi,xl)$$
$$+ \sum_{i=1}^{nl} \sigma_i^{\min} \frac{\partial pl_i}{\partial \delta_k}(V,\delta,a,\phi,xl) + \sum_{i=1}^{nl} \sigma_i^{\max} \frac{\partial pl_i}{\partial \delta_k}(V,\delta,a,\phi,xl) \quad \text{(A.65)}$$
$$- (1-\epsilon)\left[\frac{\partial \mathcal{L}^0}{\partial \delta_k} - w(\delta_k - \delta_k^0)\right]$$

$$\frac{\partial \mathcal{L}}{\partial b_k} = -\beta_k V_k^2 - \rho_k^{\min} V_k^2 - \rho_k^{\max} V_k^2 + \psi_k^{\min} + \psi_k^{\max}$$
$$- (1-\epsilon)\left[\frac{\partial \mathcal{L}^0}{\partial b_k} - w(b_k - b_k^0)\right] \quad \text{(A.66)}$$

$$\frac{\partial \mathcal{L}}{\partial pg_k} = w_1 \frac{dc_k}{pg_k}(pg_k) + w_2 + \alpha_k + \gamma_k^{\min} + \gamma_k^{\max} - (1-\epsilon)\left[\frac{\partial \mathcal{L}^0}{\partial pg_k} - w(pg_k - pg_k^0)\right] \tag{A.67}$$

$$\begin{aligned}\frac{\partial \mathcal{L}}{\partial a_k} = & -\sum_{i=1}^{nb} \alpha_i \frac{\partial p_i}{\partial a_k}(V,\delta,a,\phi,xl) + \sum_{i=1}^{nqgfix} \beta_i \frac{\partial q_i}{\partial a_k}(V,\delta,a,\phi,xl) \\ & + \sum_{i=1}^{nqgnf} \rho_i^{\min} \frac{\partial q_i}{\partial a_k}(V,\delta,a,\phi,xl) + \sum_{i=1}^{nqgnf} \rho_i^{\max} \frac{\partial q_i}{\partial a_k}(V,\delta,a,\phi,xl) \\ & + \sum_{i=1}^{nl} \sigma_i^{\min} \frac{\partial pl_i}{\partial a_k}(V,\delta,a,\phi,xl) + \sum_{i=1}^{nl} \sigma_i^{\max} \frac{\partial pl_i}{\partial a_k}(V,\delta,a,\phi,xl) \\ & + \xi_k^{\min} + \xi_k^{\max} - (1-\epsilon)\left[\frac{\partial \mathcal{L}^0}{\partial a_k} - w(a_k - a_k^0)\right]\end{aligned} \tag{A.68}$$

$$\begin{aligned}\frac{\partial \mathcal{L}}{\partial \phi_k} = & -\sum_{i=1}^{nb} \alpha_i \frac{\partial p_i}{\partial \phi_k}(V,\delta,a,\phi,xl) + \sum_{i=1}^{nqgfix} \beta_i \frac{\partial q_i}{\partial \phi_k}(V,\delta,a,\phi,xl) \\ & + \sum_{i=1}^{nqgnf} \rho_i^{\min}(V,\delta,a,\phi,xl) + \sum_{i=1}^{nqgnf} \rho_i^{\max} \frac{\partial q_i}{\partial \phi_k}(V,\delta,a,\phi,xl) \\ & + \sum_{i=1}^{nl} \sigma_i^{\min} \frac{\partial pl_i}{\partial \phi_k}(V,\delta,a,\phi,xl) + \sum_{i=1}^{nl} \sigma_i^{\max} \frac{\partial pl_i}{\partial \phi_k}(V,\delta,a,\phi,xl) \\ & + \eta_k^{\min} + \eta_k^{\max} - (1-\epsilon)\left[\frac{\partial \mathcal{L}^0}{\partial \phi_k} - w(\phi_k - \phi_k^0)\right]\end{aligned} \tag{A.69}$$

$$\begin{aligned}\frac{\partial \mathcal{L}}{\partial xl_k} &= -\sum_{i=1}^{nb} \alpha_i \frac{\partial p_i}{\partial xl_k}(V,\delta,a,\phi,xl) + \sum_{i=1}^{nqgfix} \beta \frac{\partial q_i}{\partial xl_k}(V,\delta,a,\phi,xl) \\ &+ \sum_{i=1}^{nqgnf} \rho_i^{\min} \frac{\partial q_i}{\partial xl_k}(V,\delta,a,\phi,xl) + \sum_{i=1}^{nqgnf} \rho_i^{\max} \frac{\partial q_i}{\partial xl_k}(V,\delta,a,\phi,xl) \\ &+ \sum_{i=1}^{nl} \sigma_i^{\min} \frac{\partial pl_i}{\partial xl_k}(V,\delta,a,\phi,xl) + \sum_{i=1}^{nl} \sigma_i^{\max} \frac{\partial pl_i}{\partial xl_k}(V,\delta,a,\phi,xl) \\ &+ \tau_k^{\min} + \tau_k^{\max} - (1-\epsilon)\left[\frac{\partial \mathcal{L}^0}{\partial xl_k} - w(xl_k - xl_k^0)\right]\end{aligned} \tag{A.70}$$

A.3.2 Second Order Derivatives:

The second order derivatives appearing in (A.37) for both Phase I and Phase II are:

$$\begin{aligned}\frac{\partial^2 \mathcal{L}}{\partial V_k V_l} &= diag(2w_3) - \sum_{i=1}^{nb} \frac{\partial^2[\alpha_i p_i(V,\delta,a,\phi,xl)]}{\partial V_k V_l} + \sum_{i=1}^{nqgfix} \frac{\partial^2[\beta_i q_i(V,\delta,a,\phi,xl)]}{\partial V_k V_l} \\ &+ \sum_{i=1}^{nqgnf} \frac{\partial^2[\rho_i^{\min} q_i(V,\delta,a,\phi,xl)]}{\partial V_k V_l} + \sum_{i=1}^{nqgnf} \frac{\partial^2[\rho_i^{\max} q_i(V,\delta,a,\phi,xl)]}{\partial V_k V_l} \\ &- \sum_{i=1}^{nl} \frac{\partial^2[\sigma_i^{\min} pl_i(V,\delta,a,\phi,xl)]}{\partial V_k V_l} + \sum_{i=1}^{nl} \frac{\partial[\sigma_i^{\max} pl_i(V,\delta,a,\phi,xl)]}{\partial V_k V_l} \\ &- diag(2.\beta_k.b_k) - diag(2.\rho_k^{\min}.b_k) - diag(2.\rho_k^{\max}.b_k) + (1-\epsilon)w\end{aligned} \tag{A.71}$$

$$\frac{\partial^2 \mathcal{L}}{\partial \delta_k \delta_l} = -\sum_{i=1}^{nb} \frac{\partial^2 [\alpha_i p_i(V,\delta,a,\phi,xl)]}{\partial \delta_k \delta_l} + \sum_{i=1}^{nqgfix} \frac{\partial^2 [\beta_i q_i(V,\delta,a,\phi,xl)]}{\partial \delta_k \delta_l}$$
$$+ \sum_{i=1}^{nqgnf} \frac{\partial^2 [\rho_i^{\min} q_i(V,\delta,a,\phi,xl)]}{\partial \delta_k \delta_l} + \sum_{i=1}^{nqgnf} \frac{\partial^2 [\rho_i^{\max} q_i(V,\delta,a,\phi,xl)]}{\partial \delta_k \delta_l} \qquad \text{(A.72)}$$
$$+ \sum_{i=1}^{nl} \frac{\partial^2 [\sigma_i^{\min} pl_i(V,\delta,a,\phi,xl)]}{\partial \delta_k \delta_l} + \sum_{i=1}^{nl} \frac{\partial^2 [\sigma_i^{\max} pl_i(V,\delta,a,\phi,xl)]}{\partial \delta_k \delta_l}$$
$$+ (1-\epsilon)w$$

$$\frac{\partial^2 \mathcal{L}}{\partial V_k \delta_l} = -\sum_{i=1}^{nb} \frac{\partial^2 [\alpha_i p_i(V,\delta,a,\phi,xl)]}{\partial V_k \delta_l} + \sum_{i=1}^{nqgfix} \frac{\partial^2 [\beta_i q_i(V,\delta,a,\phi,xl)]}{\partial V_k \delta_l}$$
$$+ \sum_{i=1}^{nqgnf} \frac{\partial^2 [\rho_i^{\min} q_i(V,\delta,a,\phi,xl)]}{\partial V_k \delta_l} + \sum_{i=1}^{nqgnf} \frac{\partial^2 [\rho_i^{\max} q_i(V,\delta,a,\phi,xl)]}{\partial V_k \delta_l} \qquad \text{(A.73)}$$
$$+ \sum_{i=1}^{nl} \frac{\partial^2 [\sigma_i^{\min} pl_i(V,\delta,a,\phi,xl)]}{\partial V_k \delta_l} + \sum_{i=1}^{nl} \frac{\partial^2 [\sigma_i^{\max} pl_i(V,\delta,a,\phi,xl)]}{\partial V_k \delta_l}$$

$$\frac{\partial^2 \mathcal{L}}{\partial V_k b_l} = -diag(2\beta_k V_k) - diag(2\rho_k^{\min} V_k) - diag(2\rho_k^{\max} V_k) \qquad \text{(A.74)}$$

$$\frac{\partial^2 \mathcal{L}}{\partial b_k^2} = (1-\epsilon)w \qquad \text{(A.75)}$$

$$\frac{\partial^2 \mathcal{L}}{\partial pg_k^2} = w_1 \frac{d^2 c_k(pg_k)}{dpg_k^2} + (1-\epsilon)w \qquad \text{(A.76)}$$

$$\frac{\partial^2 \mathcal{L}}{\partial a_k a_l} = -\sum_{i=1}^{nb} \frac{\partial^2 [\alpha_i p_i(V,\delta,a,\phi,xl)]}{\partial a_k a_l} + \sum_{i=1}^{nqgfix} \frac{\partial^2 [\beta_i q_i(V,\delta,a,\phi,xl)]}{\partial a_k a_l}$$
$$+ \sum_{i=1}^{nqgnf} \frac{\partial^2 [\rho_i^{\min} q_i(V,\delta,a,\phi,xl)]}{\partial a_k a_l} + \sum_{i=1}^{nqgnf} \frac{\partial^2 [\rho_i^{\max} q_i(V,\delta,a,\phi,xl)]}{\partial a_k a_l} \quad \text{(A.77)}$$
$$+ \sum_{i=1}^{nl} \frac{\partial^2 [\sigma_i^{\min} pl_i(V,\delta,a,\phi,xl)]}{\partial a_k a_l} + \sum_{i=1}^{nl} \frac{\partial^2 [\sigma_i^{\max} pl_i(V,\delta,a,\phi,xl)]}{\partial a_k a_l}$$
$$+ (1-\epsilon)w$$

$$\frac{\partial^2 \mathcal{L}}{\partial a_k V_l} = -\sum_{i=1}^{nb} \frac{\partial^2 [\alpha_i p_i(V,\delta,a,\phi,xl)]}{\partial a_k V_l} + \sum_{i=1}^{nqgfix} \frac{\partial^2 [\beta_i q_i(V,\delta,a,\phi,xl)]}{\partial a_k V_l}$$
$$+ \sum_{i=1}^{nqgnf} \frac{\partial^2 [\rho_i^{\min} q_i(V,\delta,a,\phi,xl)]}{\partial a_k V_l} + \sum_{i=1}^{nqgnf} \frac{\partial^2 [\rho_i^{\max} q_i(V,\delta,a,\phi,xl)]}{\partial a_k V_l} \quad \text{(A.78)}$$
$$+ \sum_{i=1}^{nl} \frac{\partial^2 [\sigma_i^{\min} pl_i(V,\delta,a,\phi,xl)]}{\partial a_k V_l} + \sum_{i=1}^{nl} \frac{\partial^2 [\sigma_i^{\max} pl_i(V,\delta,a,\phi,xl)]}{\partial a_k V_l}$$

$$\frac{\partial^2 \mathcal{L}}{\partial a_k \delta_l} = -\sum_{i=1}^{nb} \frac{\partial^2 [\alpha_i p_i(V,\delta,a,\phi,xl)]}{\partial a_k \delta_l} + \sum_{i=1}^{nqgfix} \frac{\partial^2 [\beta_i q_i(V,\delta,a,\phi,xl)]}{\partial a_k \delta_l}$$
$$+ \sum_{i=1}^{nqgnf} \frac{\partial^2 [\rho_i^{\min} q_i(V,\delta,a,\phi,xl)]}{\partial a_k \delta_l} + \sum_{i=1}^{nqgnf} \frac{\partial^2 [\rho_i^{\max} q_i(V,\delta,a,\phi,xl)]}{\partial a_k \delta_l} \quad \text{(A.79)}$$
$$+ \sum_{i=1}^{nl} \frac{\partial^2 [\sigma_i^{\min} pl_i(V,\delta,a,\phi,xl)]}{\partial a_k \delta_l} + \sum_{i=1}^{nl} \frac{\partial^2 [\sigma_i^{\max} pl_i(V,\delta,a,\phi,xl)]}{\partial a_k \delta_l}$$

$$\frac{\partial^2 \mathcal{L}}{\partial \phi_k \phi_l} = -\sum_{i=1}^{nb} \frac{\partial^2 [\alpha_i p_i(V,\delta,a,\phi,xl)]}{\partial \phi_k \phi_l} + \sum_{i=1}^{nqgfix} \frac{\partial^2 [\beta_i q_i(V,\delta,a,\phi,xl)]}{\partial \phi_k \phi_l} + \sum_{i=1}^{nqgnf} \frac{\partial^2 [\rho_i^{\min} q_i(V,\delta,a,\phi,xl)]}{\partial \phi_k \phi_l} + \sum_{i=1}^{nqgnf} \frac{\partial^2 [\rho_i^{\max} q_i(V,\delta,a,\phi,xl)]}{\partial \phi_k \phi_l} + \sum_{i=1}^{nl} \frac{\partial^2 [\sigma_i^{\min} pl_i(V,\delta,a,\phi,xl)]}{\partial \phi_k \phi_l} + \sum_{i=1}^{nl} \frac{\partial^2 [\sigma_i^{\max} pl_i(V,\delta,a,\phi,xl)]}{\partial \phi_k \phi_l} + (1-\epsilon)w \tag{A.80}$$

$$\frac{\partial^2 \mathcal{L}}{\partial \phi_k V_l} = -\sum_{i=1}^{nb} \frac{\partial^2 [\alpha_i p_i(V,\delta,a,\phi,xl)]}{\partial \phi_k V_l} + \sum_{i=1}^{nqgfix} \frac{\partial^2 [\beta_i q_i(V,\delta,a,\phi,xl)]}{\partial \phi_k V_l} + \sum_{i=1}^{nqgnf} \frac{\partial^2 [\rho_i^{\min} q_i(V,\delta,a,\phi,xl)]}{\partial \phi_k V_l} + \sum_{i=1}^{nqgnf} \frac{\partial^2 [\rho_i^{\max} q_i(V,\delta,a,\phi,xl)]}{\partial \phi_k V_l} + \sum_{i=1}^{nl} \frac{\partial^2 [\sigma_i^{\min} pl_i(V,\delta,a,\phi,xl)]}{\partial \phi_k V_l} + \sum_{i=1}^{nl} \frac{\partial^2 [\sigma_i^{\max} pl_i(V,\delta,a,\phi,xl)]}{\partial \phi_k V_l} \tag{A.81}$$

$$\frac{\partial^2 \mathcal{L}}{\partial \phi_k \delta_l} = -\sum_{i=1}^{nb} \frac{\partial^2 [\alpha_i p_i(V,\delta,a,\phi,xl)]}{\partial \phi_k \delta_l} + \sum_{i=1}^{nqgfix} \frac{\partial^2 [\beta_i q_i(V,\delta,a,\phi,xl)]}{\partial \phi_k \delta_l} + \sum_{i=1}^{nqgnf} \frac{\partial^2 [\rho_i^{\min} q_i(V,\delta,a,\phi,xl)]}{\partial \phi_k \delta_l} + \sum_{i=1}^{nqgnf} \frac{\partial^2 [\rho_i^{\max} q_i(V,\delta,a,\phi,xl)]}{\partial \phi_k \delta_l} + \sum_{i=1}^{nl} \frac{\partial^2 [\sigma_i^{\min} pl_i(V,\delta,a,\phi,xl)]}{\partial \phi_k \delta_l} + \sum_{i=1}^{nl} \frac{\partial^2 [\sigma_i^{\max} pl_i(V,\delta,a,\phi,xl)]}{\partial \phi_k \delta_l} \tag{A.82}$$

$$\frac{\partial^2 \mathcal{L}}{\partial \phi_k a_l} = -\sum_{i=1}^{nb} \frac{\partial^2 [\alpha_i p_i(V,\delta,a,\phi,xl)]}{\partial \phi_k a_l} + \sum_{i=1}^{nqgfix} \frac{\partial^2 [\beta_i q_i(V,\delta,a,\phi,xl)]}{\partial \phi_k a_l} + \sum_{i=1}^{nqgnf} \frac{\partial^2 [\rho_i^{\min} q_i(V,\delta,a,\phi,xl)]}{\partial \phi_k a_l} + \sum_{i=1}^{nqgnf} \frac{\partial^2 [\rho_i^{\max} q_i(V,\delta,a,\phi,xl)]}{\partial \phi_k a_l} + \sum_{i=1}^{nl} \frac{\partial^2 [\sigma_i^{\min} pl_i(V,\delta,a,\phi,xl)]}{\partial \phi_k a_l} + \sum_{i=1}^{nl} \frac{\partial^2 [\sigma_i^{\max} pl_i(V,\delta,a,\phi,xl)]}{\partial \phi_k a_l} \tag{A.83}$$

$$\frac{\partial^2 \mathcal{L}}{\partial xl_k V_l} = -\sum_{i=1}^{nb} \frac{\partial^2 [\alpha_i p_i(V,\delta,a,\phi,xl)]}{\partial xl_k V_l} + \sum_{i=1}^{nqgfix} \frac{\partial^2 [\beta_i q_i(V,\delta,a,\phi,xl)]}{\partial xl_k V_l} + \sum_{i=1}^{nqgnf} \frac{\partial^2 [\rho_i^{\min} q_i(V,\delta,a,\phi,xl)]}{\partial xl_k V_l} + \sum_{i=1}^{nqgnf} \frac{\partial^2 [\rho_i^{\max} q_i(V,\delta,a,\phi,xl)]}{\partial xl_k V_l} + \sum_{i=1}^{nl} \frac{\partial^2 [\sigma_i^{\min} pl_i(V,\delta,a,\phi,xl)]}{\partial xl_k V_l} + \sum_{i=1}^{nl} \frac{\partial^2 [\sigma_i^{\max} pl_i(V,\delta,a,\phi,xl)]}{\partial xl_k V_l} \tag{A.84}$$

$$\frac{\partial^2 \mathcal{L}}{\partial xl_k \delta_l} = -\sum_{i=1}^{nb} \frac{\partial^2 [\alpha_i p_i(V,\delta,a,\phi,xl)]}{\partial xl_k \delta_l} + \sum_{i=1}^{nqgfix} \frac{\partial^2 [\beta_i q_i(V,\delta,a,\phi,xl)]}{\partial xl_k \delta_l} + \sum_{i=1}^{nqgnf} \frac{\partial^2 [\rho_i^{\min} q_i(V,\delta,a,\phi,xl)]}{\partial xl_k \delta_l} + \sum_{i=1}^{nqgnf} \frac{\partial^2 [\rho_i^{\max} q_i(V,\delta,a,\phi,xl)]}{\partial xl_k \delta_l} + \sum_{i=1}^{nl} \frac{\partial^2 [\sigma_i^{\min} pl_i(V,\delta,a,\phi,xl)]}{\partial xl_k \delta_l} + \sum_{i=1}^{nl} \frac{\partial^2 [\sigma_i^{\max} pl_i(V,\delta,a,\phi,xl)]}{\partial xl_k \delta_l} \tag{A.85}$$

$$\frac{\partial^2 \mathcal{L}}{\partial xl_k a_l} = -\sum_{i=1}^{nb} \frac{\partial^2 [\alpha_i p_i(V,\delta,a,\phi,xl)]}{\partial xl_k a_l} + \sum_{i=1}^{nqgfix} \frac{\partial^2 [\beta_i q_i(V,\delta,a,\phi,xl)]}{\partial xl_k a_l} + \sum_{i=1}^{nqgnf} \frac{\partial^2 [\rho_i^{\min} q_i(V,\delta,a,\phi,xl)]}{\partial xl_k a_l} + \sum_{i=1}^{nqgnf} \frac{\partial^2 [\rho_i^{\max} q_i(V,\delta,a,\phi,xl)]}{\partial xl_k a_l} + \sum_{i=1}^{nl} \frac{\partial^2 [\sigma_i^{\min} pl_i(V,\delta,a,\phi,xl)]}{\partial xl_k a_l} + \sum_{i=1}^{nl} \frac{\partial^2 [\sigma_i^{\max} pl_i(V,\delta,a,\phi,xl)]}{\partial xl_k a_l} \tag{A.86}$$

$$\frac{\partial^2 \mathcal{L}}{\partial xl_k \phi_l} = -\sum_{i=1}^{nb} \frac{\partial^2 [\alpha_i p_i(V,\delta,a,\phi,xl)]}{\partial xl_k \phi_l} + \sum_{i=1}^{nqgfix} \frac{\partial^2 [\beta_i q_i(V,\delta,a,\phi,xl)]}{\partial xl_k \phi_l} + \sum_{i=1}^{nqgnf} \frac{\partial^2 [\rho_i^{\min} q_i(V,\delta,a,\phi,xl)]}{\partial xl_k \phi_l} + \sum_{i=1}^{nqgnf} \frac{\partial^2 [\rho_i^{\max} q_i(V,\delta,a,\phi,xl)]}{\partial xl_k \phi_l} + \sum_{i=1}^{nl} \frac{\partial^2 [\sigma_i^{\min} pl_i(V,\delta,a,\phi,xl)]}{\partial xl_k \phi_l} + \sum_{i=1}^{nl} \frac{\partial^2 [\sigma_i^{\max} pl_i(V,\delta,a,\phi,xl)]}{\partial xl_k \phi_l} \tag{A.87}$$

$$\frac{\partial^2 \mathcal{L}}{\partial xl_k xl_l} = -\sum_{i=1}^{nb} \frac{\partial^2 [\alpha_i p_i(V,\delta,a,\phi,xl)]}{\partial xl_k xl_l} + \sum_{i=1}^{nqgfix} \frac{\partial^2 [\beta_i q_i(V,\delta,a,\phi,xl)]}{\partial xl_k xl_l} + \sum_{i=1}^{nqgnf} \frac{\partial^2 [\rho_i^{\min} q_i(V,\delta,a,\phi,xl)]}{\partial xl_k xl_l} + \sum_{i=1}^{nqgnf} \frac{\partial^2 [\rho_i^{\max} q_i(V,\delta,a,\phi,xl)]}{\partial xl_k xl_l} + \sum_{i=1}^{nl} \frac{\partial^2 [\sigma_i^{\min} pl_i(V,\delta,a,\phi,xl)]}{\partial xl_k xl_l} + \sum_{i=1}^{nl} \frac{\partial^2 [\sigma_i^{\max} pl_i(V,\delta,a,\phi,xl)]}{\partial xl_k xl_l} + (1-\epsilon)w \tag{A.88}$$

The remaining second order derivatives are zero.

APPENDIX B

MATRIX FORMULATION AND DERIVATIVES

B.1 Power Injections and Power Flows in Matrix Form

The current on the line between two busses k and l, with voltages VC_k and VC_l, of a system (Figure B.1) is given by

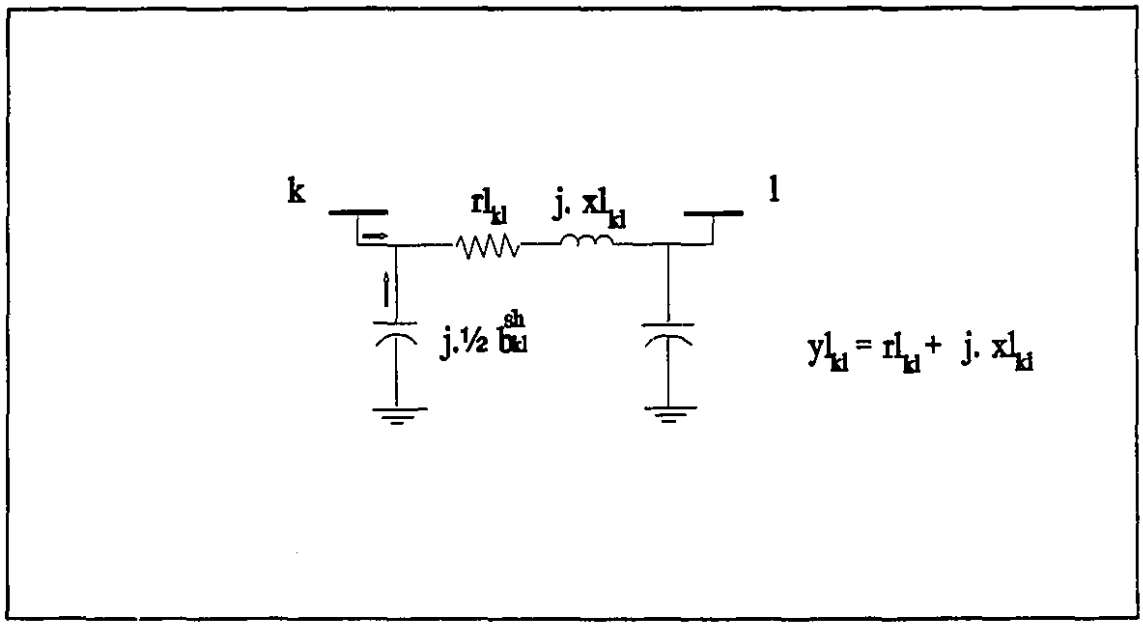

Figure B.1-Line current.

$$IC_{kl} = yl_{kl}.(VC_k - VC_l) + j.b_{kl}^{sh}.VC_k \qquad \textbf{(B.1)}$$

where

$$VC_k = V_k.\exp(j.\delta_k)$$
$$VC_l = V_l.\exp(j.\delta_l) \qquad \textbf{(B.2)}$$

For this line, the complex power flow is, thus, represented by

$$S_{kl} = VC_k.IC_{kl}^* = VC_k.yl_{kl}^*.(VC_k^* - VC_l^*) - j.\frac{1}{2}VC_k.VC_k^*.b_{kl}^{sh} \qquad \textbf{(B.3)}$$

If an ideal transformer is connected between busses k and l (Figure A.2), the current starting at each bus will be

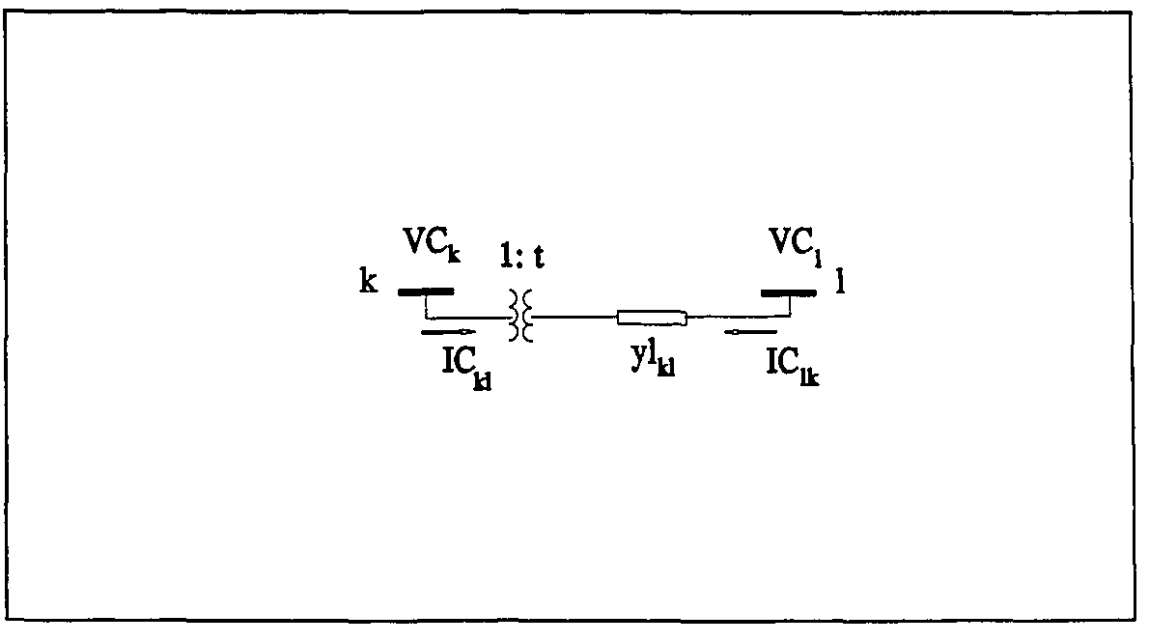

Figure B.2- Transformer current.

$$IC_{kl} = |t_{kl}|^2.yl_{kl}.VC_k - t_{kl}^*.yl_{kl}.VC_l$$
$$IC_{lk} = -t_{kl}.yl_{kl}.VC_k + yl_{kl}.VC_l \qquad \textbf{(B.4)}$$

where

$$t_{kl} = a_{kl}.\exp(j.\phi_{kl}) \tag{B.5}$$

Since $\mathbf{IC}_{kl}$ is different from $\mathbf{IC}_{lk}$, only one is chosen to be monitored during the solution of the problem. Here, the current $\mathbf{IC}_{kl}$ was chosen. The power flow through this transformer will then be

$$S_{kl} = VC_k.IC_{kl}^* = VC_k.|t_{kl}|^2.yl_{kl}^*.VC_k^* - VC_k.t_{kl}.yl_{kl}.VC_l^* \tag{B.6}$$

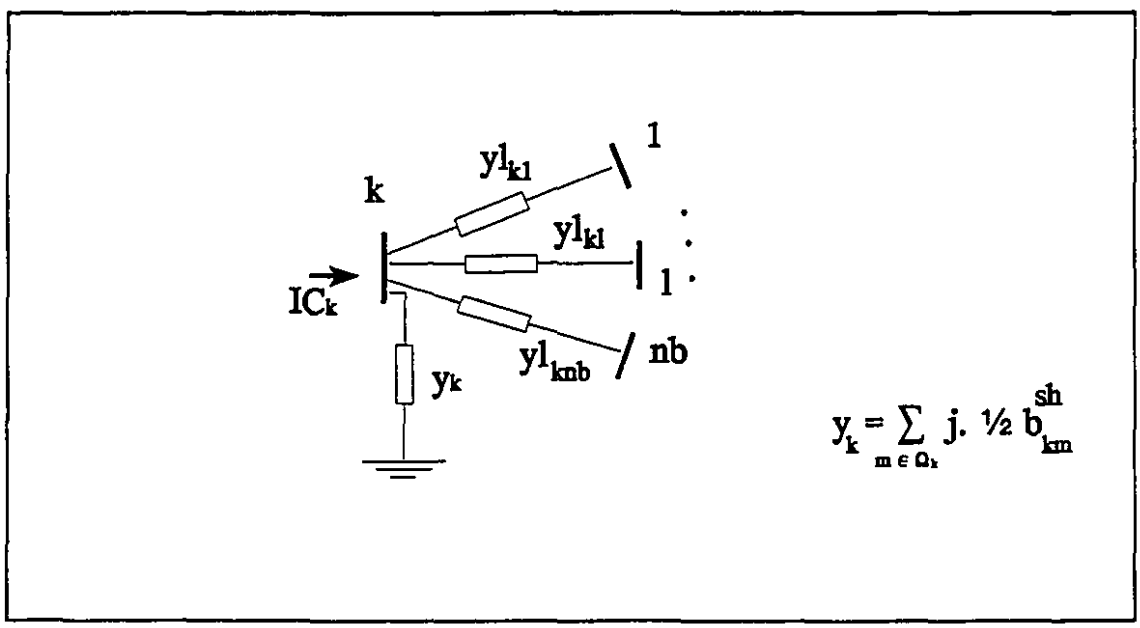

Figure B.3- Bus current injection.

The current injection at a bus k (Figure B.3) is given by

$$IC_k = VC_k.(y_k + \sum_{m=1,m\neq k}^{nb} yl_{km}) + \sum_{m=1,m\neq k}^{nb} (-yl_{km}).VC_m \tag{B.7}$$

Using (B.7) a expression for the vector of current injections **IC** and an expression for the vector of complex power injections **S** can be derived. To represent the complex power injection in matrix form, let us first define the admittance matrix **Y** as

$$Y = \begin{array}{c} \\ k \\ l \end{array} \begin{array}{c} \begin{array}{ccc} k & & l \end{array} \\ \begin{bmatrix} \sum_{m \in \Omega_k} (\|t_{km}\|^2 . yl_{km} + j.\frac{1}{2}.b_{km}^{sh}) & \cdots & -t_{kl}^{*}.yl_{kl} \\ -t_{lk}.yl_{lk} & \cdots & \sum_{m \in \Omega_l} (yl_{lm} + j.\frac{1}{2}.b_{lm}^{sh}) \end{bmatrix} \end{array} \qquad \textbf{(B.8)}$$

where Ω_k and Ω_l are the sets of all busses connected to bus k and l (excluding bus k and l), respectively.

Using **Y**, and defining **VC** as the vector of complex bus voltages, the vector of complex power injections is given by

$$S = VC.diag(IC^*) = VC.diag(Y^*.VC^*) = diag(VC).Y^*.VC^* \qquad \textbf{(B.9)}$$

where

$$VC = diag(V).\exp(j.\delta) = diag(\exp(j.\delta)).V \qquad \textbf{(B.10)}$$

and where **V** and δ are the vectors of voltage magnitudes and angles, respectively.

To represent the complex power flows on lines or transformers in matrix form, first we define the bus-line incidence matrix **A**, the "starting bus-line" incidence matrix **Af** and the "ending bus-line" incidence matrix **At** respectively, as

$$A = [A_{ij}] \quad where \quad A_{ij} = \begin{cases} 1 & if \quad i = ifrom(j) \\ -1 & if \quad i = ito(j) \\ 0 & otherwise \end{cases}$$

$$Af = [Af_{ij}] \quad where \quad Af_{ij} = \begin{cases} 1 & if \quad i = ifrom(j) \\ 0 & otherwise \end{cases} \qquad \textbf{(B.11)}$$

$$At = [At_{ij}] \quad where \quad At_{ij} = \begin{cases} 1 & if \quad i = ito(j) \\ 0 & otherwise \end{cases}$$

Let $\mathbf{b}^{sh}$ be the vector of line shunt reactances, **Yl** the vector of lines and transformers series admittances and **t** the vector of complex transformer ratios. Using matrices **Af** and **At**, the complex power flows through lines are expressed

$$\begin{aligned} Sl = {} & diag(Af^T.VC).diag(Yl^*).diag[Af - At]^T.VC^* \\ & -j.\frac{1}{2}.diag(Af^T.VC).diag(b^{sh})(Af^T.VC^*) \end{aligned} \qquad \textbf{(B.12)}$$

Whereas the power flow trough transformers are

$$Sl = diag(Af^T.VC).diag(Yl^*).diag(t).[Af.diag(t^*) - At]^T.VC^* \qquad \textbf{(B.13)}$$

where

$$t = diag(a).\exp(j.\phi) = diag(\exp(j.\phi)).a \qquad \textbf{(B.14)}$$

with **a** and ϕ being the vectors of transformer tap settings and phase shifter angles.

Since the second term of equation (B.12) affects only the reactive power, the active power flows both through lines (with **t=1**) and transformers are represented in matrix form as

$$pl = real\{diag(Af^T.VC).diag(Yl^*).diag(t)[Af.diag(t^*) - At]^T.VC^*\} \quad \textbf{(B.15)}$$

If, in equation (B.8), the transformer ratios t_{kl} are all equal to 1, **Y** is a symmetric matrix and can be expressed in terms of the bus-line incidence matrix **A**:

$$Y = A.diag(Yl).A^T + \frac{1}{2}.diag(j.abs(A).b^{sh}) \quad \textbf{(B.16)}$$

When the transformer ratios are complex, **Y** is no longer symmetric. Nevertheless, it can still be represented as a matrix multiplication of the form

$$Y = [Af.diag(t^*) - At].diag(Yl).[Af.diag(t) - At]^T + \frac{1}{2}.diag(j.abs(A).b^{sh}) \quad \textbf{(B.17)}$$

Equation (B.17) can substitute **Y** in equation (B.9), giving an "extended" expression for the complex power injections:

$$S = diag(VC).\{[Af.diag(t^*) - At].diag(Yl).[Af.diag(t) - At]^T + \frac{1}{2}.diag(j.abs(A).b^{sh})\}^*.VC^* \quad \textbf{(B.18)}$$

or

$$S = diag(VC).\{[Af.diag(t) - At].diag(Yl^*).[Af.diag(t^*) - At]^T - \frac{1}{2}diag(j.abs(A).b^{sh})\}.VC^* \quad \textbf{(B.19)}$$

This equation will be useful when obtaining the derivatives of **S** with respect to the transformer ratios and series reactances.

B.2 Derivatives of the Expressions of Complex Power Injection

B.2.1 First Order Derivative of S

The vector of complex power injections, S, can be represented concisely in terms of the system admittance matrix and the vector complex voltages. This representation is used here to obtain the first and second derivatives of S with respect to the voltage magnitudes and angles. However, the derivatives of S with respect to the transformer taps, phase shifter angles and series reactance can be obtained in a matrix form only by using the "extended" expression for S of equation (B.19).

The real and imaginary parts of the derivatives of S with respect to the decision variables are the expressions of the derivatives of the active and reactive injections appearing in the optimality conditions of the problem.

The derivatives of the complex voltage vector with respect to its magnitudes and angles are, respectively,

$$\frac{\partial VC}{\partial V} = diag(\exp(j.\delta)) \qquad \textbf{(B.20)}$$

$$\frac{\partial VC}{\partial \delta} = j.diag(VC) \qquad \textbf{(B.21)}$$

Thus, the first derivative of the complex power vector with respect to the voltage magnitude vector is expressed as

$$\frac{\partial S}{\partial V} = diag(VC).Y^*.\frac{\partial VC^*}{\partial V} + diag(Y^*.VC^*).\frac{\partial VC}{\partial V} \qquad \textbf{(B.22)}$$

or

$$\frac{\partial S}{\partial V} = diag(VC).Y^*.diag(\exp(-j.\delta)) + diag(Y^*.VC^*).diag(\exp(j.\delta)) \quad \textbf{(B.23)}$$

In the same way, the first derivative of the complex power injection vector with respect with the voltage angles vector is given by

$$\frac{\partial S}{\partial \delta} = j.[diag(Y^*.VC^*).diag(VC) - diag(VC).Y^*.diag(VC^*)] \quad \textbf{(B.24)}$$

The derivatives of t with respect to the transformer tap settings and phase shifter angles are, respectively,

$$\frac{\partial t}{\partial a} = diag(\exp(j.\phi)) \quad \textbf{(B.25)}$$

and

$$\frac{\partial t}{\partial \phi} = j.diag(t) \quad \textbf{(B.26)}$$

Then, from (B.19),

$$\frac{\partial S}{\partial a} = diag(VC).\frac{\partial}{\partial a}\{[Af.diag(t) - At].diag(Yl)^*.[Af.diag(t^*) - At]^T.VC^*\} \quad \textbf{(B.27)}$$

or

$$\frac{\partial S}{\partial a} = diag(VC).\{Af.diag(Yl^*)[diag(Af^T VC^*).diag(2.a) - diag(At^T.VC^*).diag(\exp(j.\phi))] - At.diag(Yl^*).diag(Af^T.VC^*).diag(\exp(-j.\phi))\} \quad \textbf{(B.28)}$$

And, in the same way,

$$\frac{\partial S}{\partial \phi} = diag(VC).\frac{\partial}{\partial \phi}\{[Af.diag(t) - At].diag(Yl^*).[Af.diag(t^*) - At]^T.VC^*\} \quad \textbf{(B.29)}$$

or

$$\begin{aligned}\frac{\partial S}{\partial \phi} &= j.diag(VC).[At.diag(Yl^*)diag(Af^T.VC^*).diag(t^*) \\ &\quad - Af.diag(Yl^*).diag(At^T.VC^*).diag(t)]\end{aligned} \quad \textbf{(B.30)}$$

The conjugate series admittance of a line kl of the network, $\mathbf{yl}^*_{kl}$, is

$$yl^*_{kl} = \frac{rl_{kl}}{rl^2_{kl} + xl^2_{kl}} + j\frac{xl_{kl}}{rl^2_{kl} + xl^2_{kl}} \quad \textbf{(B.31)}$$

where $\mathbf{rl}_i$ and $\mathbf{xl}_i$ are the resistance and series reactance of line i. Thus, the derivative of $\mathbf{yl}^*$ will be

$$\frac{\partial yl^*_{kl}}{\partial xl_{kl}} = -\frac{2.rl_{kl}.xl_{kl}}{(rl^2_{kl} + xl^2_{kl})^2} + j.\frac{rl^2_{kl} - xl^2_{kl}}{(rl^2_{kl} + xl^2_{kl})^2} \quad \textbf{(B.32)}$$

And the derivative of **S** with respect to **xl** will be

$$\begin{aligned}\frac{\partial S}{\partial xl} &= diag(VC).[Af.diag(t) - At]. \\ &diag\{[diag(t^*).Af^T - At^T].VC^*\}.diag\left(\frac{\partial Yl^*}{\partial xl}\right)\end{aligned} \quad \textbf{(B.33)}$$

B.2.2 Second Order Derivative of S

Since the first derivatives are matrices, the second derivatives would be tensors. To facilitate their expressions, these derivatives are obtained in terms of an arbitrary

multiplicative vector **k**. Following the same steps as above we have

$$\frac{\partial^2(S^T.k)}{\partial V^2} = \frac{\partial}{\partial V}\{[diag(VC).Y^*.diag(\exp(-j.\delta)) + diag(Y^*.V^*).diag(\exp(j.\delta))]^T.k\} \quad \textbf{(B.34)}$$

or

$$\frac{\partial^2(S^T.k)}{\partial V^2} = diag(\exp(-j.\delta)).(Y^*)^T.diag(\exp(j.\delta)).diag(k) + diag(k).diag(\exp(j.\delta)).Y^*.diag(\exp(-j.\delta)) \quad \textbf{(B.35)}$$

In the same way,

$$\frac{\partial^2(S^T.k)}{\partial \delta^2} = \frac{\partial}{\partial \delta}\{j.[diag(Y^*.VC).diag(VC) - diag(VC).Y^*.diag(VC^*)]^T.k\} \quad \textbf{(B.36)}$$

or

$$\frac{\partial^2(S^T.k)}{\partial \delta^2} = -diag(Y^*.VC^*).diag(VC).diag(k) + diag(k).diag(VC).Y^*.diag(VC^*) + diag(VC^*).(Y^*)^T.diag(VC).diag(k) - diag[(Y^*)^T.diag(VC).k].diag(VC^*) \quad \textbf{(B.37)}$$

And

$$\frac{\partial^2(S^T.k)}{\partial \delta \partial V} = \frac{\partial}{\partial V}\{j.[diag(Y^*.VC^*).diag(VC) - diag(VC).Y^*.diag(VC^*)]^T k\} \quad \textbf{(B.38)}$$

or

$$\begin{aligned}\frac{\partial^2(S^T.k)}{\partial\delta\,\partial V} &= j.diag(Y^*.VC^*).diag(\exp(j.\delta)).diag(k)\\ &+ j.diag(k).diag(VC).Y^*.diag(\exp(-j.\delta))\\ &- j.diag(VC^*).(Y^*)^T.diag(\exp(j.\delta)).diag(k)\\ &- j.diag[(Y^*)^T.diag(VC).k].diag(\exp(-j.\delta))\end{aligned} \tag{B.39}$$

To obtain the second derivative of S with respect to V and a, we first substitute Y from equation (B.17) in equation (B.23). The second derivative is then represented

$$\begin{aligned}\frac{\partial^2(S^T.k)}{\partial V\partial a} &= \frac{\partial}{\partial a}\{\{diag(VC).[Af.diag(t) - At].diag(Yl^*)\\ &.[Af.diag(t^*) - At]^T diag(\exp(-j.\delta)) + diag\{[Af.diag(t) - At]\\ &.diag(Yl^*).[Af.diag(t^*) - At]^T.VC^*\}.diag(\exp(j.\delta))\}^T k\}\end{aligned} \tag{B.40}$$

or

$$\begin{aligned}\frac{\partial^2(S^T.k)}{\partial V\partial a} &= diag(\exp(-j.\delta))\\ &.\{[Af.diag(2.a) - At.diag(\exp(j.\phi))].diag[Af^T.diag(k).VC]\\ &+ Af.diag(\exp(-j.\phi)).diag[At^T.diag(k).VC]\}.diag(Yl^*)\\ &+ diag(\exp(j.\delta)).diag(k).\{[Af.diag(2.a) - At.diag(\exp(-j.\phi))]\\ &.diag(Af^T.VC^*) - Af.diag(\exp(-j.\phi)).diag(At^T.VC^*)\}.diag(Yl^*)\end{aligned} \tag{B.41}$$

Following the same steps, the second derivative of S with respect to V and ϕ is

$$\begin{aligned}\frac{\partial^2(S^T.k)}{\partial V\partial\phi} &= j.diag(\exp(-j.\delta))\\ &.[Af.diag(t^*) - At.diag(t)].diag(Yl^*).diag[Af^T.diag(k).VC]\\ &- j.diag(\exp(j.\delta)).diag(k).Af.diag(At^T.VC^*).diag(t).diag(Yl^*)\\ &+ j.diag(\exp(j.\delta)).diag(k)At.diag(Af^T.VC^*).diag(t^*).diag(Yl^*)\end{aligned} \tag{B.42}$$

Substituting (B.17) into equation (B.24), the first derivative of S with respect to δ can be used to obtain the expression of the second derivative of S with respect to δ and **a**:

$$\begin{aligned}\frac{\partial^2(S^T.k)}{\partial\delta\,\partial a} = \frac{\partial}{\partial a}\{\{-j.diag(VC).\{[Af.diag(t^*) - At].diag(Yl^*)\\ .[Af.diag(t) - At]^T\}^*.diag(VC^*) + diag\{\{[Af.diag(t^*) - At]\\ .diag(Yl^*).[Af.diag(t) - At]^T.VC\}^*\}.diag(VC)\}^T k\}\end{aligned} \tag{B.43}$$

Giving

$$\begin{aligned}&\frac{\partial^2(S^T.k)}{\partial\delta\,\partial a} =\\ &-j.diag(VC^*)\{[Af.diag(2.a) - At.diag(\exp(j.\phi))].diag[Af^T.diag(k).VC]\\ &- Af.diag(\exp(-j.\phi)).diag[At^T.diag(k).VC]\}.diag(Yl^*)\\ &+ j.diag(VC).diag(k).\{[Af.diag(2.a) - At.diag(\exp(-j.\phi))].diag(Af^T.VC^*)\\ &- Af.diag(\exp(j.\phi)).diag(At^T.VC^*)\}.diag(Yl^*)\end{aligned} \tag{B.44}$$

In the same way, the second derivative of S with respect to δ and ϕ can be obtained by substituting (B.17) into (B.24) and deriving for ϕ:

$$\begin{aligned}&\frac{\partial^2(S^T.k)}{\partial\delta\,\partial\phi} =\\ &\quad\{diag(VC).\{Af.diag[At^T.diag(k).VC].diag(t^*)\\ &\quad - At.diag[Af^T.diag(k).VC].diag(t)\}\\ &\quad + diag(VC).diag(k).\{Af.diag(At^T.VC^*).diag(t)\\ &\quad - At.diag(Af^T.VC^*).diag(t^*)\}\}.diag(Yl^*)\end{aligned} \tag{B.45}$$

Finally, the second derivatives of S with respect to **a**, ϕ and **a** & ϕ can be obtained directly from the first derivatives (equations (B.28) and (B.30)):

$$\frac{\partial^2(S^T.k)}{\partial a^2} = \tag{B.46}$$
$$diag(2).diag(Af^T.VC^*).diag(Yl^*).diag[Af^T.diag(k).VC]$$

$$\frac{\partial^2(S^T.k)}{\partial a \partial \phi} = j.diag(Af^T.VC^*).diag(Yl^*).diag[At^T.diag(k).VC]. \tag{B.47}$$
$$diag(\exp(-j.\phi)) - diag(At^T.VC^*).diag(Yl^*).$$
$$diag[At^T.diag(k).VC].diag(\exp(j.\phi))$$

and

$$\frac{\partial^2(S^T.k)}{\partial \phi^2} = diag(At^T.VC^*).diag(Yl^*).diag[Af^T.diag(k).VC]. \tag{B.48}$$
$$diag(t) + diag(Af^T.VC^*).diag(Yl^*).$$
$$diag[At^T.diag(k).VC].diag(t^*)$$

The second derivatives of **S** with respect to **xl** and **V**, δ, **a** and ϕ can be obtained from (B.33). Then, for **V**,

$$\frac{\partial^2(S^T.k)}{\partial xl \partial V} = \frac{\partial}{\partial V}\{\{diag(VC).[Af.diag(t) - At]. \tag{B.49}$$
$$diag\{[diag(t^*).Af^T - At^T].VC^*\}.diag\left(\frac{\partial Yl^*}{\partial xl}\right)\Big\}^T k\Big\}$$

or

$$\frac{\partial^2(S^T.k)}{\partial xl \partial V} = diag\left(\frac{\partial Yl^*}{\partial xl}\right).\{diag\{[diag(t^*).Af^T - At^T].VC^*\}. \tag{B.50}$$
$$[diag(t).Af^T - At^T].diag(k).diag(\exp(j.\delta))$$
$$+ diag\{[diag(t).Af^T - At^T].diag(k).VC\}.$$
$$[diag(t^*).Af^T - At^T].diag(\exp(-j.\delta))\}$$

For δ,

$$\begin{aligned}\frac{\partial^2(S^T.k)}{\partial xl\,\partial\delta} = j.diag\left(\frac{\partial Yl^*}{\partial xl}\right).\{diag\{[diag(t^*).Af^T - At^T].VC^*\}. \\ [diag(t).Af^T - At^T].diag(k).diag(VC) \\ - diag\{[diag(t).Af^T - At^T].diag(k).VC\}. \\ [diag(t^*).Af^T - At^T].diag(VC^*)\}\end{aligned} \tag{B.51}$$

For **a**,

$$\begin{aligned}\frac{\partial^2(S^T.k)}{\partial xl\,\partial a} = diag\left(\frac{\partial Yl^*}{\partial xl}\right).\{diag\{[diag(t^*).Af^T - At^T].VC^*\}. \\ diag[Af^T.diag(k).VC].diag(\exp(j.\phi)) \\ + diag\{[diag(t).Af^T - At^T].diag(k).VC\}. \\ diag(Af^T.VC^*).diag(\exp(-.j.\phi))\}\end{aligned} \tag{B.52}$$

And for ϕ,

$$\begin{aligned}\frac{\partial^2(S^T.k)}{\partial xl\,\partial\phi} = j.diag\left(\frac{\partial Yl^*}{\partial xl}\right).\{diag\{[diag(t^*).Af^T - At^T].VC^*\}. \\ diag[Af^T.diag(k).VC].diag(t) \\ - diag\{[diag(t).Af^T - At^T].diag(k).VC\}. \\ diag(Af^T.VC^*).diag(t^*)\}\end{aligned} \tag{B.53}$$

The second derivative of **S** with respect to **xl** is a function of the second derivative of $\mathbf{Yl}^*$ with respect to **xl**. From (B.32) we have

$$\frac{\partial^2(yl_{kl}^*)}{\partial xl_{kl}^2} = 2.r_{kl}.\left[\frac{4.xl_{kl}^2}{(rl_{kl}^2 + xl_{kl}^2)^3} - \frac{1}{(rl_{kl}^2 + xl_{kl}^2)^2}\right] - j.2.xl_{kl}\left[\frac{2.(rl_{kl}^2 - xl_{kl}^2)}{(rl_{kl}^2 + xl_{kl}^2)^3} + \frac{1}{(rl_{kl}^2 + xl_{kl}^2)^2}\right] \quad \textbf{(B.54)}$$

And, from (B.33),

$$\frac{\partial^2(S^T.k)}{\partial xl^2} = diag\{[diag(t^*).Af^T - At^T].VC^*\}. diag\{[diag(t).Af^T - At^T].diag(k).VC\}.\left(\frac{\partial^2(Yl^*)}{\partial xl^2}\right) \quad \textbf{(B.55)}$$

B.3 Derivatives of the Power Flows

The active power flows through lines or transformers can be represented by the general expression (B.15). To obtain the expression of the derivatives, first we define

$$Sl_1 = diag(Af^T.VC).diag(Yl^*).diag(t).[diag(t^*).Af^T - At^T].VC^* \quad \textbf{(B.56)}$$

The real part of the derivatives of $\mathbf{Sl_1}$ with respect to the state variables are the expressions needed to compute the optimality conditions for the real power flows.

B.3.1 First Order Derivatives of the Power Flows

The first derivatives of $\mathbf{Sl_1}$ are:

$$\frac{\partial Sl_1}{\partial V} =$$

$$diag(Af^T.VC).diag(Yl^*).diag(t).[diag(t^*).Af^T - At^T].diag(\exp(-j.\delta)) \quad \textbf{(B.57)}$$
$$+ diag(Yl^*).diag(t).diag\{[diag(t^*).Af^T - At^T].VC^*\}.Af^T.diag(\exp(j.\delta))$$

$$\frac{\partial Sl_1}{\partial \delta} = -j.diag(Af^T.VC).diag(Yl^*).diag(t).[diag(t^*).Af^T - At^T].diag(VC^*) \quad \textbf{(B.58)}$$
$$+ j.diag(Yl^*).diag(t).diag\{[diag(t^*).Af^T - At^T].VC^*\}.Af^T.diag(VC)$$

$$\frac{\partial Sl_1}{\partial a} = diag(Af^T.VC).diag(Yl^*).diag(Af^T.VC^*).diag(2.a) \quad \textbf{(B.59)}$$
$$-diag(Af^T.VC).diag(Yl^*).diag(At^T.VC^*).diag(\exp(j.\phi))$$

$$\frac{\partial Sl_1}{\partial \phi} = -j.diag(Af^T.VC).diag(Yl^*).diag(At^T.VC^*).diag(t) \quad \textbf{(B.60)}$$

and

$$\frac{\partial Sl_1}{\partial xl} = diag(Af^T.VC).$$
$$diag(t).diag\{[diag(t^*).Af^T - At^T]VC^*\}.diag\left(\frac{\partial Yl^*}{\partial xl}\right) \quad \textbf{(B.61)}$$

which is a function of (B.32).

B.3.2 Second Order Derivatives of the Power Flows

The second derivatives of Sl_1 are:

$$\frac{\partial^2(Sl_1^T.k)}{\partial V^2} = diag(\exp(-j.\delta)).[Af.diag(t^*) - At].diag(t).$$
$$diag(Yl^*).diag(k).Af^T.diag(\exp(j.\delta)) + diag(\exp(j.\delta)).Af.$$
$$diag(k).diag(Yl^*).diag(t).[diag(t^*).Af^T - At^T].diag(\exp(-j.\delta)) \quad \text{(B.62)}$$

$$\frac{\partial^2(Sl_1^T.k)}{\partial \delta^2} = diag(VC^*).[Af.diag(t^*) - At].diag(t).$$
$$diag(Yl^*).diag(k).Af^T.diag(VC) - diag\{[Af.diag(t^*) - At].$$
$$diag(t).diag(Yl^*).diag(Af^T.VC).k\}.diag(VC^*) + diag(VC).$$
$$Af.diag(k).diag(Yl^*).diag(t).[diag(t^*).Af^T - At^T].diag(VC^*)$$
$$-diag\{Af.diag(k).diag(Yl^*).diag(t)[diag(t^*).Af^T - At^T].VC^*\}.diag(VC) \quad \text{(B.63)}$$

$$\frac{\partial^2(Sl_1^T.k)}{\partial \delta \partial V} = -j.diag(VC^*).[Af.diag(t^*) - At].$$
$$diag(t).diag(Yl^*).diag(k).Af^T.diag(\exp(j.\delta))$$
$$-j.diag\{[Af.diag(t^*) - At].diag(t).diag(Yl^*).$$
$$diag(Af^T.VC).k\}.diag(\exp(-j.\delta)) + j.diag(VC).$$
$$Af.diag(k).diag(Yl^*).diag(t).[diag(t^*).Af^T - At^T].$$
$$diag(\exp(-j.\delta)) + j.diag\{Af.diag(k).diag(Yl^*).diag(t).$$
$$[diag(t^*).Af^T - At^T].VC^*\}.diag(\exp(j.\delta)) \quad \text{(B.64)}$$

$$\frac{\partial^2(Sl_1^T.k)}{\partial a^2} = \tag{B.65}$$

$$diag(2).diag(Af^T.VC^*).diag(Yl^*).diag(Af^T.VC).diag(k)$$

$$\begin{aligned}\frac{\partial^2(Sl_1^T.k)}{\partial a \partial V} &= diag(2.a).diag(Af^T.VC^*).diag(Yl^*).diag(k).Af^T.diag(\exp(j.\delta)) \\ &+ diag(2.a).diag(Yl^*).diag(k).diag(Af^T.VC).Af^T.diag(\exp(-j.\delta)) \\ &- diag(\exp(j.\phi)).diag(At^T.VC^*).diag(Yl^*).diag(k).Af^T.diag(\exp(j.\delta)) \\ &- diag(\exp(j.\phi)).diag(Yl^*).diag(k).diag(Af^T.VC).At^T.diag(\exp(-j.\delta))\end{aligned} \tag{B.66}$$

$$\begin{aligned}\frac{\partial^2(Sl_1^T.k)}{\partial a \partial \delta} &= j.diag(2.a).diag(Af^T.VC^*).diag(Yl^*).diag(k).Af^T.diag(VC) \\ &- j.diag(2.a).diag(Yl^*).diag(k).diag(Af^T.VC).Af^T.diag(VC^*) \\ &- j.diag(\exp(j.\phi)).diag(At^T.VC^*).diag(Yl^*).diag(k).diag(k).Af^T.diag(VC) \\ &+ j.diag(\exp(j.\phi)).diag(Yl^*).diag(k).adiag(Af^T.VC).At^T.diag(VC^*)\end{aligned} \tag{B.67}$$

$$\frac{\partial^2(Sl_1^T.k)}{\partial \phi^2} = diag(Af^T.VC).diag(Yl^*).diag(At^T.VC^*).diag(k).diag(t) \tag{B.68}$$

$$\frac{\partial^2(Sl_1^T.k)}{\partial \phi \partial V} = \tag{B.69}$$

$$\begin{aligned}&-j.diag(t).diag(At^T.VC^*).diag(Yl^*).diag(k).Af^T.diag(\exp(j.\delta)) \\ &-j.diag(t).diag(Yl^*).diag(k).diag(Af^T.VC).At^T.diag(\exp(-j.\delta))\end{aligned}$$

$$\frac{\partial^2(Sl_1^T.k)}{\partial\phi.\partial.\delta} = diag(t).diag(At^T.VC^*).diag(Yl^*).diag(k).$$
$$Af^T.diag(VC) - j.diag(t).diag(Yl^*).diag(k).$$
$$diag(Af^T.VC^*).At^T.\ diag(VC^*) \tag{B.70}$$

$$\frac{\partial^2(Sl_1^T.k)}{\partial\phi\partial a} = -j.diag(Af^T.VC).diag(Yl^*).$$
$$diag(At^T.VC^*).diag(k).diag(\exp(j.\phi)) \tag{B.71}$$

$$\frac{\partial^2(Sl_1^T.k)}{\partial V\partial xl} = diag(\exp(-.\delta)).[Af^T.diag(t^*) - At].$$
$$diag(t).diag(Af^T.VC).diag(k).diag\left(\frac{\partial Yl^*}{\partial xl}\right)$$
$$+ diag(\exp(j.\delta)).Af.diag(k).diag(t).$$
$$diag\{[diag(t^*).Af^T - At^T].VC^*\}.diag\left(\frac{\partial Yl^*}{\partial xl}\right) \tag{B.72}$$

$$\frac{\partial(Sl_1^T.k)}{\partial\delta\,\partial xl} = -\,j.diag(VC^*).[Af.diag(t^*) - At].$$
$$diag(t).diag(Af^T.VC).diag(k).diag\left(\frac{\partial Yl^*}{\partial xl}\right)$$
$$+ j.diag(VC).Af.diag(k).diag(t).$$
$$diag\{[diag(t^*).Af^T - At^T].VC^*\}.diag\left(\frac{\partial Yl^*}{\partial xl}\right) \tag{B.73}$$

$$\frac{\partial^2(Sl_1^T.k)}{\partial a \partial xl} = diag(2.a).diag(Af^T.VC^*).diag(Af^T.VC).$$
$$diag(k).diag\left(\frac{\partial Yl^*}{\partial xl}\right) - diag(\exp(j.\phi)). \qquad \textbf{(B.74)}$$
$$diag(At^T.VC^*).diag(Af^T.VC).diag(k).diag\left(\frac{\partial Yl^*}{\partial xl}\right)$$

$$\frac{\partial^2(Sl_1^T.k)}{\partial \phi \partial xl} = -j.diag(t).diag(At^T.VC^*).$$
$$diag(Af^T.VC).diag(k).diag\left(\frac{\partial Yl^*}{\partial xl}\right) \qquad \textbf{(B.75)}$$

$$\frac{\partial^2(Sl_1^T.k)}{\partial xl^2} = diag(t).diag(Af^T.VC).diag(k).$$
$$diag\{[diag(t^*).Af^T - At^T].VC^*\}.diag\left(\frac{\partial^2 Yl^*}{\partial xl^2}\right) \qquad \textbf{(B.76)}$$

APPENDIX C

BEHAVIOUR OF THE OPTIMAL SOLUTIONS NEAR A SINGULARITY OF MATRIX $W(z,\varepsilon)$

When tracking the OPF optimal solutions as the parameter varies, critical points on the optimal trajectories occur where the jacobian of the KT conditions (defined for the active set) is singular. In addition, since in the Newton method the same jacobian matrix is involved, near the point of singularity, the parametric algorithm is not able to find the solution of the KT conditions. This is so because of the ill-conditioning of $W(z,\varepsilon)$ near such type of critical points. In this appendix, we present some results about the behaviour of the optimal trajectories near the singular points.

A point belonging to the optimal trajectory must solve the KT equations derived for the Lagrangian function, $\mathcal{L}$, (equation (3.9)) . These equations can be defined as

$$\left[\begin{array}{l} \dfrac{\partial \mathcal{L}}{\partial x}(z,\epsilon) = \dfrac{\partial c}{\partial x}(x,\epsilon) + \dfrac{\partial^T g}{\partial x}(x,\epsilon)\lambda + \dfrac{\partial^T h_{L_0}}{\partial x}(x,\epsilon)\mu_{L_0} \\ \dfrac{\partial \mathcal{L}}{\partial \lambda}(z,\epsilon) = g(x,\epsilon) \\ \dfrac{\partial \mathcal{L}}{\partial \mu_{L_0}}(z,\epsilon) = h_{L_0}(x,\epsilon) \end{array}\right] = \frac{\partial \mathcal{L}}{\partial z}(z,\epsilon) = 0 \quad \text{(C.1)}$$

The behaviour of (C.1) around an arbitrary a point $(\bar{z},\bar{\epsilon})$ is given by

$$d\left[\frac{\partial \mathcal{L}}{\partial z}\right] = \left[W(\bar{z},\bar{\epsilon}) \ , \ \frac{\partial^2 \mathcal{L}}{\partial z \partial \epsilon}(\bar{z},\bar{\epsilon})\right]\begin{bmatrix} dz \\ d\epsilon \end{bmatrix} + Q\left(\begin{bmatrix} dz \\ d\epsilon \end{bmatrix}\right) = 0 \qquad \text{(C.2)}$$

where $W(\bar{z},\bar{\epsilon}) \in \mathbb{R}^{(nv+m+p \times nv+m+p)}$ is the jacobian of the KT conditions (that is, the derivative of the KT conditions with respect to **z**) and **Q**(.) is an expression containing terms in $[dz^T, d\varepsilon]^T$ of second and possibly higher orders. As long as at $(\bar{z},\bar{\epsilon})$ the jacobian of the KT equations is non-singular, for small variations in ε, the higher order term of equation (C.2) is negligible and we can express the variation in **z** as

$$dz = -W(\bar{z},\bar{\epsilon})^{-1}\left(\frac{\partial^2 \mathcal{L}}{\partial z \partial \epsilon}(\bar{z},\bar{\epsilon})\right)d\epsilon \qquad \textbf{(C.3)}$$

If, otherwise, at $(\bar{z},\bar{\epsilon})$, the matrix $W(\bar{z},\bar{\epsilon})$ is singular, the variation on the KT solutions for a small variation of the parameter cannot be obtained by (C.3). To obtain the behaviour of **z** near a singular point, the higher order term of equation (C.1), **Q**(.), must be considered. To derive the expression of **dz**, first of all, note that, at $(\bar{z},\bar{\epsilon})$ there exists a non-zero vector **v** such that:

$$W(\bar{z},\bar{\epsilon})v = 0 \qquad \textbf{(C.4)}$$

and, since $W(\bar{z},\bar{\epsilon})$ is symmetric,

$$v^T W(\bar{z},\bar{\epsilon}) = 0 \qquad \textbf{(C.6)}$$

Assume, for simplicity, that the null space of $W(\bar{z},\bar{\epsilon})$ has dimension one. Then, associated with $W(\bar{z},\bar{\epsilon})$ there also exists a range space, spanned by the nv+m+p-1 independent vectors $\{\mathbf{u}_i\}$ perpendicular to **v**. Let these vectors be represented by the (nv+m+p) by (nv+m+p-1) matrix **U**.

The solution **dz** of equation (C.2) for small increments **dε** characterizes the optimal power flow solution behaviour near a singularity. Taking the second order term of (C.2) into consideration we have

$$d\left[\frac{\partial \mathcal{L}}{\partial z}\right] = \left[W\ ,\ \frac{\partial^2 \mathcal{L}}{\partial z \partial \epsilon}\right]\begin{bmatrix} dz \\ d\epsilon \end{bmatrix} + \begin{bmatrix} dz \\ d\epsilon \end{bmatrix}^T \begin{bmatrix} \left[\frac{\partial^3 \mathcal{L}}{\partial z^3} dz\right] + \frac{\partial^3 \mathcal{L}}{\partial z^2 \partial \epsilon} d\epsilon \\ \frac{\partial^3 \mathcal{L}}{\partial z^2 \partial \epsilon} dz + \frac{\partial^3 \mathcal{L}}{\partial z \partial \epsilon^2} d\epsilon \end{bmatrix} = 0 \qquad \text{(C.6)}$$

Let dz be represented by two components, one along the null space of the jacobian, v, and another perpendicular to it:

$$dz = v d\theta + U d\omega \qquad \text{(C.7)}$$

Substituting (C.7) into (C.6) and disregarding the term in $(d\varepsilon)^2$ yields,

$$\begin{aligned} &WU d\omega + \frac{\partial^2 \mathcal{L}}{\partial z \partial \epsilon} d\epsilon + \left[\frac{\partial^3 \mathcal{L}}{\partial z^3} v d\theta\right] v d\theta + \left[\frac{\partial^3 \mathcal{L}}{\partial z^3} v d\theta\right] U d\omega + \left[\frac{\partial^3 \mathcal{L}}{\partial z^3} U d\omega\right] v d\theta \\ &+ \left[\frac{\partial^3 \mathcal{L}}{\partial z^3} U d\omega\right] U d\omega + 2\frac{\partial^3 \mathcal{L}}{\partial z^2 \partial \epsilon} v d\theta d\epsilon + 2\frac{\partial^3 \mathcal{L}}{\partial z^2 \partial \epsilon} U d\omega d\epsilon = 0 \end{aligned} \qquad \text{(C.8)}$$

To solve (C.8) we neglect the terms in $d\theta.d\varepsilon$, $d\omega.d\varepsilon$, $d\theta.d\omega$ and $(d\omega)^2$ (this step is justified later on). Thus,

$$WU d\omega + \frac{\partial^2 \mathcal{L}}{\partial z \partial \epsilon} d\epsilon + \left[\frac{\partial^3 \mathcal{L}}{\partial z^3} v d\theta\right] v d\theta = 0 \qquad \text{(C.9)}$$

Multiplying (C.9) by v^T and using (C.5) yields

$$v^T \frac{\partial^2 \mathcal{L}}{\partial z \partial \epsilon} d\epsilon + v^T \left[\frac{\partial^3 \mathcal{L}}{\partial z^3} v\right] v (d\theta)^2 = 0 \qquad \text{(C.10)}$$

which can be solved for $d\theta$:

$$d\theta = \pm\sqrt{-v^T\frac{\partial^2 \mathcal{L}}{\partial z\partial \epsilon}\left\{v^T\left[\frac{\partial^3 \mathcal{L}}{\partial z^3}v\right]v\right\}^{-1}}\,d\epsilon \qquad \text{(C.11)}$$

For $d\varepsilon \geq 0$, equation (C.11) has a solution if and only if $v^T\frac{\partial^2 \mathcal{L}}{\partial z\partial \epsilon}\left\{v^T\left[\frac{\partial^3 \mathcal{L}}{\partial z^3}v\right]v\right\}^{-1} \leq 0$. Additionally, around $(\bar{z},\bar{\epsilon})$, the optimal trajectories can be represented by a parabola whose maximum point is $(\bar{z},\bar{\epsilon})$.

If we substitute (C.11) into (C.9) we can find the value of $d\omega$:

$$WUd\omega = -\frac{\partial^2 \mathcal{L}}{\partial z\partial \epsilon}d\epsilon + \left\{\left[\frac{\partial^3 \mathcal{L}}{\partial z^3}v\right]v\right\}v^T\frac{\partial^2 \mathcal{L}}{\partial z\partial \epsilon}\left\{v^T\left[\frac{\partial^3 \mathcal{L}}{\partial z^3}v\right]v\right\}^{-1}d\epsilon \qquad \text{(C.12)}$$

Since $\mathbf{v}^T W=0$, the vector on the right hand side of (C.12) is perpendicular to $\mathbf{v}$, that is, this vector belongs to the range space of W. Consequently (C.12) can be solved for $d\omega$ giving

$$d\omega = [U^T W(\bar{x},\bar{\epsilon})\,U]^{-1}U^T dz' \qquad \text{(C.13)}$$

where

$$dz' = -\frac{\partial^2 \mathcal{L}}{\partial z\partial \epsilon}d\epsilon + \left\{\left[\frac{\partial^3 \mathcal{L}}{\partial z^3}v\right]v\right\}v^T\frac{\partial^2 \mathcal{L}}{\partial z\partial \epsilon}\left\{v^T\left[\frac{\partial^3 \mathcal{L}}{\partial z^3}v\right]v\right\}^{-1}d\epsilon \qquad \text{(C.14)}$$

As a conclusion, the behaviour of the OPF solution neat the singularity of the jacobian of the KT conditions is characterized by:

(i)- The solution of the KT equations can be represented locally by a parabola with maximum at $(\bar{z},\bar{\epsilon})$.

(ii)- It is composed of the sum of two components $v d\theta$ and $U d\omega$. The first term has a unique direction but its magnitude is affected by $d\theta$ (equation (C.11)).

(iii)- The second term is orthogonal to the first.

(iv)- The square root term also indicates the direction along which there exists a solution.

(v)- The square root tends to dominate the behaviour near the singularity of W, yielding relatively large changes in z for small changes in ε.

(vi)- The terms neglected in equation (C.8) are of order 2 and 1.5 in $d\varepsilon$, while the retained ones are of order 1. This justifies their elimination in equation (C.9).

APPENDIX D

RESOLUTION OF CRITICAL POINTS TYPE 4

A Type 4 critical point $(\bar{x},\bar{\epsilon})$ is characterized by the existence of more active inequalities than free variables. Therefore, the jacobian of the active constraints, J, in this situation has more rows than columns. Since this jacobian is rank deficient (from equation (3.37)), we have that the matrix $W(\bar{z},\bar{\epsilon})$ is singular at this point, in the same way that it occurs with type 3 critical points. Since we have more active constraints than free variables, to proceed with the tracking process, we must find an optimal sub-set of this set of active constraints. Because equation (3.37) holds, we can take at least one active inequality from the active set. To ensure optimality over the remaining active set, we must consider the sign of the Lagrange multipliers of the remaining active inequalities and the value of the released inequality for $\varepsilon > \bar{\epsilon}$. In other words, supposing that $\mathbf{h}_p$ is the new inequality that is just to become active at $(\bar{x},\bar{\epsilon})$ and that $\mathbf{h}_q$ is the inequality to be deleted from the active set, we must have, for $\Delta\varepsilon > 0$,

$$\begin{aligned} &\mu_l > 0,\ l \in L_0(\bar{x},\bar{\epsilon}),\ l \neq q \\ &h_q(\bar{x} + \Delta x, \bar{\epsilon} + \Delta\epsilon) \leq 0 \end{aligned} \qquad \textbf{(D.1)}$$

To derive the expressions of $\mu_l \in L_0(\bar{x},\bar{\epsilon})$, l≠q and $\mathbf{h}_q$, let J be the jacobian defined for the m+p-1 constraints initially active at $(\bar{x},\bar{\epsilon})$. From the KT equations we have that

$$\begin{aligned} \frac{\partial c}{\partial x}(\bar{x},\bar{\epsilon}) + J^T\begin{bmatrix}\lambda_{old}\\ \mu_{old}\end{bmatrix} &= 0 \\ g_k(\bar{x},\bar{\epsilon}) &= 0,\ k \in K \\ h_l(\bar{x},\bar{\epsilon}) &= 0,\ l \in L_0(\bar{x},\bar{\epsilon}) \end{aligned} \tag{D.2}$$

where $\lambda_{old} \in \mathbb{R}^m$ and $\mu_{old} \in \mathbb{R}^{(p-1)}$ correspond to the initially m+p-1 active constraints.

Since J is a square matrix, the first equation of (D.2) can be solved for $[\lambda_{old}^T, \mu_{old}^T]^T$, yielding

$$\begin{bmatrix}\lambda_{old}\\ \mu_{old}\end{bmatrix} = (J^T)^{-1}\frac{\partial c}{\partial x}(\bar{x},\bar{\epsilon}) \tag{D.3}$$

Since $\mathbf{h}_p$ was the last inequality to reach its limit, we want to verify if replacing a previously fixed inequality constraint, $\mathbf{h}_q$, with $\mathbf{h}_p$ will give us an optimal active set. Let J' be the jacobian defined after $\mathbf{h}_q$ is replaced by $\mathbf{h}_p$, this jacobian will have the form:

$$J' = \begin{bmatrix} \partial g_1/\partial x \\ \vdots \\ \partial g_m/\partial x \\ \partial h_1/\partial x \\ \vdots \\ \partial h_q/\partial x \\ \partial h_{q+1}/\partial x \\ \vdots \\ \partial h_{p-1}/\partial x \end{bmatrix} - \begin{bmatrix} 0 \\ \vdots \\ 0 \\ 0 \\ \vdots \\ \partial h_q/\partial x - \partial h_p/\partial x \\ 0 \\ \vdots \\ 0 \end{bmatrix} \leftarrow qth\ position \tag{D.4}$$

where the first term on the right-hand side of equation (D.4) is the jacobian defined for a fixed $\mathbf{h}_q$ (without considering $\mathbf{h}_p$), J, and the second term is the change in the original jacobian, ΔJ.

The new set of Lagrange multipliers $[\lambda_{new}^T, (\mu_{new})^T]^T$ (defined for the new set of active constraints), is, therefore,

$$\begin{bmatrix} \lambda_{new} \\ \mu_{new} \end{bmatrix} = [(J')^T]^{-1} \frac{\partial c}{\partial x}(\bar{x}, \bar{\epsilon}) \tag{D.5}$$

The value of the released inequality, $\mathbf{h}_q$, for ϵ near $\bar{\epsilon}$ can be approximated by

$$h_q(\bar{x} + dx, \bar{\epsilon} + d\epsilon) = h_q(\bar{x}, \bar{\epsilon}) + \frac{\partial^T h_q}{\partial x} dx + \frac{\partial h_q}{\partial \epsilon} d\epsilon \tag{D.6}$$

Now, since the new set of active constraints must remain active for ϵ near $\bar{\epsilon}$, we have

$$d\begin{bmatrix} g(x,\epsilon) \\ h_{new}(x,\epsilon) \end{bmatrix} = J' dx + \begin{bmatrix} \frac{\partial g}{\partial \epsilon} \\ \frac{\partial h_{new}}{\partial \epsilon} \end{bmatrix} d\epsilon = 0$$

which gives

$$dx = -(J')^{-1} \begin{bmatrix} \frac{\partial g}{\partial x} \\ \frac{\partial h_{new}}{\partial x} \end{bmatrix} d\epsilon \tag{D.7}$$

and where $\mathbf{h}_{new}$ is the new vector of active inequalities.

Substituting (D.7) into (D.6) we can obtain an expression for the derivative of $\mathbf{h}_q$, which must be less or equal to zero to guarantee non-violation of the maximum limit:

$$dh_q = \left\{ -\frac{\partial^T h_q}{\partial x}(J')^{-1} \begin{bmatrix} \frac{\partial g}{\partial \epsilon} \\ \frac{\partial h_{new}}{\partial \epsilon} \end{bmatrix} + \frac{\partial h_q}{\partial \epsilon} \right\} d\epsilon \leq 0 \qquad \textbf{(D.8)}$$

To solve equations (D.5) and (D.8) we can apply the matrix inversion lemma for J'. First of all, note that ΔJ can be represented as

$$\Delta J = r_q . e_q^T \qquad \textbf{(D.9)}$$

where $\mathbf{e}_q \in \mathbb{R}^{(m+p-1)}$ is a column vector with 1 in the q*th* position and zeros elsewhere and

$$r_q = \left[\frac{\partial h_q}{\partial x} - \frac{\partial h_p}{\partial x} \right]$$

Therefore, the inverse of J' can be represented as

$$(J')^{-1} = J^{-1} - \frac{(J^{-1}) r_q e_q^T (J^{-1})}{1 + r_q^T (J^{-1}) e_q} \qquad \textbf{(D.10)}$$

Substituting (D.10) into (D.5) we have

$$\begin{bmatrix} \lambda_{new} \\ \mu_{new} \end{bmatrix} = \begin{bmatrix} \lambda_{old} \\ \mu_{old} \end{bmatrix} - \left[\frac{(J^{-1}) r_q e_q^T}{1 + r_q^T (J^{-1}) e_q} \right] \begin{bmatrix} \lambda_{old} \\ \mu_{old} \end{bmatrix} \qquad \textbf{(D.11)}$$

The new Lagrange multipliers associated with the inequality constraints, $\boldsymbol{\mu}_{new}$, can then be tested using equation (D.11). Note that in this equation, the only elements that vary are the vectors $\mathbf{r}_q$ and $\mathbf{e}_q$, which are defined for each $\mathbf{h}_q$ that we try to release. Note, as well, that on the q*th* position of $\boldsymbol{\mu}_{new}$ we have the Lagrange multiplier associated with $\mathbf{h}_p$, whereas, in the q*th* position of $\boldsymbol{\mu}_{old}$ we have the Lagrange multiplier associated with

In the same way, the value of the released inequality, $\mathbf{h}_q$ can be obtained from

$$dh_q = \left\{ -\frac{\partial^T h_q}{\partial x}\left[J^{-1} - \frac{(J^{-1})r_q e_q^T (J^{-1})}{1 + r_q^T (J^{-1}) e_q}\right]\begin{bmatrix} \frac{\partial g}{\partial \epsilon} \\ \frac{\partial h_{new}}{\partial \epsilon} \end{bmatrix} + \frac{\partial h_q}{\partial \epsilon} \right\} d\epsilon \qquad \textbf{(D.12)}$$

Once more, some of the terms in (D.12) will remain constant throughout the calculations; only varying $\mathbf{h}_q$, $\mathbf{h}_{new}$ and $\mathbf{r}_q$.

Equations (D.11) and (D.12) can be used to test if some inequality constraint $\mathbf{h}_q$ can be released when $\mathbf{h}_p$ is fixed at its limit. Equation (D.11) can be used to verify the first condition of (D.1), while equation (D.12) can be used to verify the second condition of (D.1). Since, initially, there are p-1 active inequalities and since, for every trial (where $\mathbf{h}_q$ is substituted by $\mathbf{h}_p$), equations (D.11) and (D.12) must be solved, then up to 2(p-1) equations must be solved to find a inequality to be released when $\mathbf{h}_p$ is fixed.

APPENDIX E

TESTS SYSTEMS DATA

E.1 Remarks

All data is given in per unit with a basis of 100 MVA. The power flow limits were arbitrarily chosen. In the Tables showing the generation data, *aa* and *bb* are the cost coefficients associated with the linear and quadratic terms of the generation cost function, $c_i(pg_i)$, respectively. The constant term of $c_i(pg_i)$ was always supposed to be equal to zero.

E.2 5-bus System

Table E.1

Line data						
Line No.	From	To	r	xl	bsh	Max. flow
1	1	2	0.0420	0.1680	0.0300	1.1600
2	2	3	0.0310	0.1260	0.0200	0.5000
3	3	5	0.0530	0.2100	0.0150	0.3000
4	3	4	0.0840	0.3360	0.0120	0.2100
5	4	5	0.0630	0.2520	0.0110	0.2780
6	5	1	0.0310	0.1260	0.0100	0.6000

Table E.2

Bus data						
Bus No.	V^{min}	V^{max}	b^{min}	b^{max}	pd	qd
1	0.9500	1.0500	0.000	0.000	0.6500	0.3000
2	0.9500	1.0500	0.000	0.000	1.1500	0.6000
3	0.9500	1.0500	0.000	0.000	0.7000	0.4000
4	0.9500	1.0500	0.000	0.000	0.7000	0.3000
5	0.9500	1.0500	0.000	0.000	0.8500	0.4000

Table E.3

Generation data						
Bus No.	pg^{min}	pg^{max}	qg^{min}	qg^{max}	aa	bb
1	0.000	3.700	-1.0500	2.0500	0.500	1.000
3	0.000	2.160	-1.000	1.000	1.000	2.000
4	0.000	2.000	-1.000	1.000	0.500	0.500

E.3- 14-bus System

Table E.4

Line data						
Line No.	From	To	r	xl	bsh/2	Max. Flow
1	1	2	0.01938	0.05917	0.0264	2.500
2	1	5	0.05403	0.22304	0.0246	1.320
3	2	3	0.04699	0.19797	0.0219	1.300
4	2	4	0.05811	0.17632	0.0187	1.100
5	2	5	0.05695	0.17388	0.0170	1.050
6	3	4	0.06701	0.17103	0.0173	1.050
7	5	4	0.01335	0.04211	0.0064	1.500
8	4	7	0.0000	0.20912	0.0000	2.000
9	4	9	0.0000	0.55618	0.0000	1.600
10	5	6	0.0000	0.25202	0.0000	1.500
11	6	11	0.09498	0.19890	0.0000	1.100
12	6	12	0.12291	0.25581	0.0000	1.040
13	6	13	0.06615	0.13027	0.0000	1.100
14	7	8	0.0000	0.17615	0.0000	1.600
15	7	9	0.0000	0.11001	0.0000	1.600
16	9	10	0.03181	0.08450	0.0000	1.100
17	9	14	0.12711	0.27038	0.0000	1.200
18	10	11	0.08205	0.19207	0.0000	1.200
19	12	13	0.22092	0.19988	0.0000	1.200
20	13	14	0.17093	0.34802	0.0000	1.200

Table E.5

Bus data						
Bus No.	V^{min}	V^{max}	b^{min}	b^{max}	pd	qd
1	0.95	1.05	0.0000	0.0000	0.0000	0.0000
2	0.95	1.05	0.0000	0.0000	0.2170	0.1270
3	0.95	1.05	0.0000	0.0000	0.9420	0.1900
4	0.95	1.05	0.0000	0.0000	0.4780	-0.0390
5	0.95	1.05	0.0000	0.0000	0.0760	0.0160
6	0.95	1.05	0.0000	0.0000	0.1120	0.0750
7	0.95	1.05	0.0000	0.0000	0.0000	0.0000
8	0.95	1.05	0.0000	0.0000	0.0000	0.0000
9	0.95	1.05	-0.4200	0.4200	0.2950	0.1660
10	0.95	1.05	0.0000	0.0000	0.0900	0.0580
11	0.95	1.05	0.0000	0.0000	0.0350	0.0180
12	0.95	1.05	0.0000	0.0000	0.0610	0.0160
13	0.95	1.05	0.0000	0.0000	0.1350	0.0580
14	0.95	1.05	0.0000	0.0000	0.1490	0.0500

Table E.6

Generation data						
Bus No.	pg^{min}	pg^{max}	qg^{min}	qg^{max}	aa	bb
1	0.000	5.000	-0.250	5.000	8.600	0.008
2	0.000	0.500	-0.400	0.500	10.500	0.040
3	0.000	0.000	0.000	0.400	0.000	0.000
6	0.000	0.000	-0.050	0.240	0.000	0.000
8	0.000	0.000	-0.050	0.240	0.000	0.000

E.4 30-bus System

Table E.7

Generation data						
Bus No.	pg^{min}	pg^{max}	qg^{min}	qg^{max}	aa	bb
1	0.000	5.000	-3.000	5.000	8.000	0.200
2	0.000	0.500	-0.400	0.500	10.000	0.100
5	0.000	0.000	-0.400	0.400	0.000	0.000
8	0.000	0.000	-0.100	0.400	0.000	0.000
11	0.000	0.000	-0.060	0.240	0.000	0.000
13	0.000	0.000	-0.060	0.240	0.000	0.000

Table E.8

Transformer tap data				
Line No.	From	To	a^{min}	a^{max}
11	6	9	0.900	1.100
12	6	10	0.900	1.100
15	4	12	0.900	1.100
36	28	27	0.900	1.100

Table E.9

Line data						
Line No.	From	To	r	xl	bsh/2	Max. flow
1	1	2	0.0192	0.0575	0.0264	2.5000
2	1	3	0.0452	0.1852	0.0204	1.6500
3	2	4	0.0570	0.1737	0.0184	1.6500
4	3	4	0.0132	0.0379	0.0042	1.9000
5	2	5	0.0472	0.1983	0.0209	1.3200
6	2	6	0.0581	0.1763	0.0187	1.3000
7	4	6	0.0119	0.0414	0.0045	1.7000
8	5	7	0.0460	0.1160	0.0102	1.6500
9	6	7	0.0267	0.0820	0.0085	1.6500
10	6	8	0.0120	0.0420	0.0045	1.6500
11	6	9	0.000	0.2080	0.0000	1.8000
12	6	10	0.000	0.5560	0.0000	1.8000
13	9	11	0.000	0.2080	0.0000	1.6500
14	9	10	0.000	0.1100	0.0000	1.3000
15	4	12	0.000	0.2560	0.0000	2.3000
16	12	13	0.000	0.1400	0.0000	2.9000
17	12	14	0.1231	0.2559	0.0000	1.6500
18	12	15	0.0662	0.1304	0.0000	1.3200
19	12	16	0.0945	0.1987	0.0000	1.6500
20	14	15	0.2210	0.1997	0.0000	1.6500
21	16	17	0.0824	0.1923	0.0000	1.3200
22	15	18	0.1070	0.2185	0.0000	1.3200
23	18	19	0.0639	0.1292	0.0000	1.3200
24	19	20	0.0340	0.0680	0.0000	1.3200
25	10	20	0.0936	0.2090	0.0000	1.1600
26	10	17	0.0324	0.0845	0.0000	1.3200
27	10	21	0.0348	0.0749	0.0000	1.3200
28	10	22	0.0727	0.1499	0.0000	1.1600
29	21	22	0.0116	0.0236	0.0000	1.3200
30	15	23	0.1000	0.2020	0.0000	1.3200
31	22	24	0.1150	0.1790	0.0000	1.3200
32	23	24	0.1320	0.2700	0.0000	1.1600
33	24	25	0.1885	0.3292	0.0000	1.1600
34	25	26	0.2544	0.3800	0.0000	1.1600
35	25	27	0.1093	0.2087	0.0000	1.1600
36	28	27	0.000	0.3960	0.0000	2.2000
37	27	29	0.2198	0.4153	0.0000	1.1600
38	27	30	0.3202	0.6027	0.0000	1.1600
39	29	30	0.2399	0.4533	0.0000	1.1600
40	8	28	0.0636	0.2000	0.0214	1.1600
41	6	28	0.0169	0.0599	0.0065	1.1600

Table E.10

Bus data						
Bus No.	V^{min}	V^{max}	b^{min}	b^{max}	pd	qd
1	0.95	1.05	0.000	0.000	0.000	0.000
2	0.95	1.05	0.000	0.000	0.217	0.127
3	0.95	1.05	0.000	0.000	0.024	0.012
4	0.95	1.05	0.000	0.000	0.076	0.016
5	0.95	1.05	0.000	0.000	0.942	0.190
6	0.95	1.05	0.000	0.000	0.000	0.000
7	0.95	1.05	0.000	0.000	0.228	0.109
8	0.95	1.05	0.000	0.000	0.300	0.300
9	0.95	1.05	0.000	0.000	0.000	0.000
10	0.95	1.05	-0.190	0.190	0.058	0.02
11	0.95	1.05	0.000	0.000	0.000	0.000
12	0.95	1.05	0.000	0.000	0.112	0.075
13	0.95	1.05	0.000	0.000	0.000	0.000
14	0.95	1.05	0.000	0.000	0.062	0.016
15	0.95	1.05	0.000	0.000	0.082	0.025
16	0.95	1.05	0.000	0.000	0.035	0.018
17	0.95	1.05	0.000	0.000	0.090	0.058
18	0.95	1.05	0.000	0.000	0.032	0.009
19	0.95	1.05	0.000	0.000	0.095	0.034
20	0.95	1.05	0.000	0.000	0.022	0.007
21	0.95	1.05	0.000	0.000	0.175	0.112
22	0.95	1.05	0.000	0.000	0.000	0.000
23	0.95	1.05	0.000	0.000	0.032	0.016
24	0.95	1.05	-0.043	0.043	0.087	0.067
25	0.95	1.05	0.000	0.000	0.000	0.000
26	0.95	1.05	0.000	0.000	0.035	0.023
27	0.95	1.05	0.000	0.000	0.000	0.000
28	0.95	1.05	0.000	0.000	0.000	0.000
29	0.95	1.05	0.000	0.000	0.024	0.009
30	0.95	1.05	0.000	0.000	0.106	0.019

E.5 34-bus System

Table E.11

Generation data						
Bus No.	pg^{min}	pg^{max}	qg^{min}	qg^{max}	aa	bb
1	0.00	53.70	-3.00	10.00	7.00	0.001
2	0.00	23.20	-3.00	10.00	7.50	0.003
3	0.00	26.10	-3.00	10.00	7.50	0.003
4	0.00	47.40	-3.00	10.00	7.20	0.002
5	0.00	15.40	-3.00	10.00	7.70	0.004
6	0.00	50.00	-3.00	10.00	7.00	0.001
18	0.00	0.00	-3.00	10.00	0.00	0.00
27	0.00	0.00	-3.00	10.00	0.00	0.00

Table E.12.a

Line data						
Line No.	From	To	r	xl	bsh	Max flow
1	1	28	0.00005	0.00269	0	120.000
2	2	23	0.00004	0.00643	0.1360	100.000
3	3	25	0.00010	0.00444	0	100.000
4	4	30	0.00003	0.00226	-0.0340	150.000
5	5	11	0.00014	0.00898	-0.0610	77.000
6	6	12	0.00014	0.00581	0	120.000
7	7	8	0.00008	0.00185	0.7380	55.000
8	7	13	0.00023	0.00681	2.5760	45.000
9	7	14	0.00006	0.00150	0.6260	102.000
10	7	26	0.00011	0.00314	1.3740	50.000
11	8	19	0.00009	0.00255	1.1230	37.000
12	8	20	0.00055	0.01307	5.5530	53.000
13	8	18	0.00053	0.01493	6.6410	46.000
14	9	10	0.00007	0.00172	0.6890	100.000
15	9	13	0.00023	0.00692	2.8010	101.000
16	9	13	0.00023	0.00692	2.8010	101.000
17	9	11	0.00078	0.02295	9.8210	30.000
18	9	11	0.00078	0.02295	9.2810	30.000
19	9	11	0.00094	0.02253	9.9290	31.000
20	10	12	0.00101	0.02434	10.878	28.000
21	10	20	0.00010	0.00228	0.9530	100.000
22	11	12	0.00013	0.00379	1.5460	100.000
23	11	15	0.00045	0.01042	4.4020	67.000
24	11	15	0.00045	0.01042	4.4020	67.000
25	12	15	0.00048	0.01126	4.7660	62.000
26	12	21	0.00068	0.01517	6.4880	46.000
27	13	14	0.00027	0.00851	3.6790	82.000
28	13	29	0.00015	0.00426	1.8390	100.000
29	14	22	0.00009	0.00279	1.2250	100.000
30	15	16	0.00058	0.01351	5.7550	51.000
31	15	16	0.00058	0.01351	5.7540	51.000
32	15	16	0.00058	0.01351	5.7540	51.000

Table E.12.b

Line data (cont.)						
Line No.	From	To	r	xl	bsh	Max. flow
33	16	30	0.00060	0.01411	6.0180	49.000
34	16	30	0.00060	0.01411	6.0180	49.000
35	16	30	0.00060	0.01411	6.0180	49.000
36	17	18	0.00054	0.01608	7.2820	43.000
37	17	18	0.00054	0.01610	7.2670	43.000
38	17	18	0.00054	0.01647	7.5980	42.000
39	17	32	0.00044	0.01311	5.8550	53.000
40	17	32	0.00044	0.01311	5.8560	53.000
41	17	32	0.00049	0.01422	6.5520	49.000
42	17	34	0.00012	0.00345	1.5130	100.000
43	18	19	0.00050	0.01513	6.8060	46.000
44	18	31	0.00037	0.01059	4.8650	66.000
45	19	22	0.00019	0.00551	2.4260	127.000
46	19	31	0.00016	0.00471	2.0640	148.000
47	20	21	0.00052	0.01149	4.8620	60.000
48	20	26	0.00045	0.01083	4.6110	64.000
49	20	27	0.00053	0.01561	6.7450	44.000
50	21	27	0.00024	0.00709	3.1110	80.000
51	23	24	0.00022	0.00622	2.8050	90.000
52	23	28	0.00032	0.00942	4.1280	74.000
53	24	25	0.00025	0.00706	3.1820	90.000
54	24	25	0.00025	0.00706	3.1820	90.000
55	24	33	0.00045	0.01318	5.8770	53.000
56	24	33	0.00045	0.01318	5.8770	53.000
57	27	34	0.00039	0.01155	5.1380	60.000
58	27	34	0.00039	0.01155	5.1380	60.000
59	28	32	0.00055	0.01649	7.4560	42.000
60	28	32	0.00055	0.01649	7.4580	42.000
61	28	32	0.00055	0.01649	7.5310	42.000
62	32	33	0.00007	0.01900	0.8560	36.000
63	33	34	0.00048	0.01387	6.3980	50.000
64	33	34	0.00048	0.01387	6.3980	50.000

Table E.13

Bus data						
Bus No.	V^{min}	V^{max}	b^{min}	b^{max}	pd	qd
1	0.95	1.05	0.00	0.00	0.0000	0.0000
2	0.95	1.05	0.00	0.00	0.0000	0.0000
3	0.95	1.05	0.00	0.00	0.0000	0.0000
4	0.95	1.05	0.00	0.00	0.0000	0.0000
5	0.95	1.05	0.00	0.00	0.0000	0.0000
6	0.95	1.05	0.00	0.00	0.0000	0.0000
7	0.95	1.05	0.00	0.00	32.0326	4.0382
8	0.95	1.05	0.00	0.00	27.8528	0.7733
9	0.95	1.05	-6.70	6.60	24.7537	-6.5129
10	0.95	1.05	-3.40	3.30	9.1963	-0.0082
11	0.95	1.05	-3.40	3.30	0.0000	0.0000
12	0.95	1.05	-3.40	3.30	0.0000	0.0000
13	0.95	1.05	0.00	0.00	11.6150	0.4902
14	0.95	1.05	0.00	0.00	21.3966	0.1042
15	0.95	1.05	-6.70	6.60	2.4618	0.4492
16	0.95	1.05	-8.30	8.25	1.1464	0.2127
17	0.95	1.05	0.00	0.00	3.7194	-0.7294
18	0.95	1.05	-3.40	3.30	0.0000	0.0000
19	0.95	1.05	0.00	0.00	17.4624	-1.0848
20	0.95	1.05	0.00	0.00	7.8867	-0.2046
21	0.95	1.05	0.00	0.00	4.7270	1.9766
22	0.95	1.05	0.00	0.00	8.0475	0.5300
23	0.95	1.05	-3.40	3.30	0.0000	0.0000
24	0.95	1.05	0.00	0.00	0.0000	0.0000
25	0.95	1.05	0.00	0.00	0.0000	0.0000
26	0.95	1.05	0.00	0.00	11.1031	-0.4204
27	0.95	1.05	-3.40	3.30	0.0000	0.0000
28	0.95	1.05	-3.40	3.30	0.0000	0.0000
29	0.95	1.05	0.00	0.00	12.0500	1.1311
30	0.95	1.05	0.00	0.00	0.6000	0.1100
31	0.95	1.05	0.00	0.00	2.6449	0.3130
32	0.95	1.05	-3.40	3.30	0.0000	0.0000
33	0.95	1.05	-3.40	3.30	0.0000	0.0000
34	0.95	1.05	-3.40	3.30	0.0000	0.0000

E.6 118-bus System

Table E.14

Transformer tap data				
Line No.	From	To	a^{min}	a^{max}
51	86	87	0.900	1.100
58	81	80	0.900	1.100
83	65	66	0.900	1.100
89	64	61	0.900	1.100
90	63	59	0.900	1.100
143	30	17	0.900	1.100
148	26	25	0.900	1.100
173	8	5	0.900	1.100

Table E.15

Phase shifters data				
Line No.	From	To	ϕ^{min}	ϕ^{max}
77	69	68	-0.090	0.090
128	38	37	-0.5236	0.5236

Table E.16.a

Line data						
Line No.	From	To	r	xl	bsh	Max. flow
1	118	76	0.01640	0.05440	0.01356	1.370
2	118	75	0.01450	0.04810	0.01198	1.370
3	117	12	0.03290	0.14000	0.03580	1.370
4	116	68	0.00034	0.00405	0.16400	4.055
5	115	114	0.00230	0.01040	0.00276	1.370
6	115	27	0.01640	0.07410	0.01972	1.370
7	114	32	0.01350	0.06120	0.01628	1.370
8	113	32	0.06150	0.20300	0.05180	1.370
9	113	17	0.00913	0.03010	0.00768	1.370
10	112	110	0.0247	0.06400	0.06200	1.370
11	111	110	0.02200	0.07550	0.02000	1.370
12	110	109	0.02780	0.07620	0.02020	1.370
13	110	103	0.03906	0.18130	0.04610	1.370
14	109	108	0.01050	0.02880	0.00760	1.370
15	108	105	0.02610	0.07030	0.01844	1.370
16	107	106	0.05300	0.18300	0.04720	1.370
17	107	105	0.05300	0.18300	0.04720	1.370
18	106	105	0.01400	0.05470	0.01434	1.370
19	106	100	0.06050	0.22900	0.06200	1.370
20	105	104	0.00994	0.03780	0.00986	1.370
21	105	103	0.05350	0.16250	0.04080	1.370
22	104	103	0.04660	0.15840	0.04070	1.370
23	104	100	0.04510	0.20400	0.05410	1.370
24	103	100	0.01600	0.05250	0.05360	2.050
25	102	101	0.02460	0.11200	0.02940	1.370
26	102	92	0.01230	0.05590	0.01464	1.370
27	101	100	0.02770	0.12620	0.03280	1.370
28	100	99	0.01800	0.08130	0.02160	1.370
29	100	98	0.03970	0.17900	0.04760	1.370
30	100	94	0.01780	0.05800	0.06040	2.055
31	100	92	0.06480	0.29500	0.07720	1.370
32	99	80	0.04540	0.20600	0.05460	1.370
33	98	80	0.02380	0.10800	0.02860	1.370
34	97	96	0.01730	0.08850	0.02400	1.370
35	97	80	0.01830	0.09340	0.02540	1.370
36	96	95	0.01710	0.05470	0.01474	1.370

Table E.16.b

Line data (cont.)						
Line No.	From	To	r	xl	bsh	Max. flow
37	96	94	0.02690	0.08690	0.02300	4.055
38	96	82	0.01620	0.05300	0.05440	1.370
39	96	80	0.03560	0.18200	0.04940	1.370
40	95	94	0.01320	0.04340	0.01110	1.370
41	94	93	0.02230	0.07320	0.01876	1.370
42	94	92	0.04810	0.15800	0.04060	1.370
43	93	92	0.02580	0.08480	0.02180	1.370
44	92	91	0.03870	0.12720	0.03268	1.370
45	92	89	0.00799	0.03829	0.09620	2.370
46	91	90	0.02540	0.08360	0.02140	1.370
47	90	89	0.01638	0.06517	0.15880	1.370
48	89	88	0.01390	0.07120	0.01934	1.370
49	89	85	0.02390	0.17300	0.04700	1.370
50	88	85	0.02000	0.10200	0.02760	1.370
51	86	87	0.00000	0.20740	0.00000	2.150
52	86	85	0.03500	0.12300	0.02760	1.370
53	85	84	0.03020	0.06410	0.01234	1.370
54	85	83	0.04300	0.14800	0.03480	1.370
55	84	83	0.06250	0.13200	0.02580	1.370
56	83	82	0.01120	0.03665	0.03796	1.370
57	82	77	0.02980	0.08530	0.08174	1.370
58	81	80	0.00000	0.03700	0.00000	4.225
59	81	68	0.00175	0.02020	0.80800	2.015
60	80	79	0.01560	0.07040	0.01870	1.370
61	80	77	0.01088	0.03321	0.07000	2.055
62	79	78	0.00546	0.02440	0.00648	1.370
63	78	77	0.00376	0.01240	0.01264	1.370
64	77	76	0.04440	0.14800	0.03680	1.370
65	77	75	0.06010	0.19990	0.04978	1.370
66	77	69	0.03090	0.10100	0.10380	1.370
67	75	74	0.01230	0.04060	0.01034	1.370
68	75	70	0.04280	0.14100	0.03600	1.370
69	75	69	0.04050	0.12200	0.12400	1.370
70	74	70	0.04010	0.13230	0.03368	1.370
71	73	71	0.00866	0.04540	0.01178	1.370
72	72	71	0.0446	0.18000	0.04444	1.370

Table E.16.c

Line data (cont.)						
Line No.	From	To	r	xl	bsh	Max. flow
73	72	24	0.04880	0.19600	0.04880	1.370
74	71	70	0.00882	0.03550	0.00878	1.370
75	70	69	0.03000	0.12700	0.12200	1.370
76	70	24	0.10221	0.41150	0.10198	1.370
77	69	68	0.00000	0.03700	0.00000	6.225
78	69	49	0.09850	0.32400	0.08280	1.370
79	69	47	0.08440	0.27780	0.07092	1.370
80	68	65	0.00138	0.01600	0.63800	4.150
81	67	66	0.02240	0.10150	0.02682	1.370
82	67	62	0.02580	0.11700	0.03100	1.370
83	65	66	0.00000	0.03700	0.00000	6.225
84	66	62	0.04820	0.21800	0.05780	1.370
85	66	49	0.00900	0.04595	0.04960	2.055
86	65	64	0.00269	0.03020	0.38000	6.225
87	65	38	0.00901	0.09860	1.04600	2.055
88	64	63	0.00172	0.02000	0.21600	4.150
89	64	61	0.00000	0.02680	0.00000	6.225
90	63	59	0.00000	0.03860	0.00000	2.055
91	62	61	0.00824	0.03760	0.00980	2.055
92	62	60	0.01230	0.05610	0.01468	1.370
93	61	60	0.00264	0.01350	0.01456	1.370
94	61	59	0.03280	0.15000	0.03880	1.370
95	60	59	0.03170	0.14500	0.03760	1.370
96	59	56	0.04070	0.12243	0.11050	1.370
97	59	55	0.04739	0.21580	0.05646	1.370
98	59	54	0.05030	0.22930	0.05980	1.370
99	58	56	0.03430	0.09660	0.02420	1.370
100	58	51	0.02550	0.07190	0.01788	1.370
101	57	56	0.03430	0.09660	0.02420	1.370
102	57	50	0.04740	0.13400	0.03320	1.370
103	56	55	0.00488	0.01510	0.00374	1.370
104	56	54	0.00275	0.00955	0.00732	2.055
105	55	54	0.01690	0.07070	0.02020	1.370
106	54	53	0.02630	0.12200	0.03100	1.370
107	54	49	0.03993	0.14507	0.14680	1.370
108	53	52	0.04050	0.16350	0.04058	1.370

Table E.16.d

Line data (cont.)						
Line No.	From	To	r	xl	bsh	Max. flow
109	52	51	0.02030	0.05880	0.01396	1.370
110	51	49	0.04860	0.13700	0.03420	1.370
111	50	49	0.02670	0.07520	0.01874	1.370
112	49	48	0.01790	0.05050	0.01258	1.370
113	49	47	0.01910	0.06250	0.01604	1.370
114	49	45	0.06840	0.18600	0.04440	1.370
115	49	42	0.03575	0.16150	0.17200	1.370
116	48	46	0.06010	0.18900	0.04720	1.370
117	47	46	0.03800	0.12700	0.03160	1.370
118	46	45	0.04000	0.13560	0.03320	1.370
119	45	44	0.02240	0.09010	0.02240	1.370
120	44	43	0.06080	0.24540	0.06068	1.370
121	43	34	0.04130	0.16810	0.04226	2.055
122	42	41	0.04100	0.13500	0.03440	1.370
123	42	40	0.05550	0.18300	0.04660	1.370
124	41	40	0.01450	0.04870	0.01222	2.055
125	40	39	0.01840	0.06050	0.01552	2.055
126	40	37	0.05930	0.16800	0.04200	1.370
127	39	37	0.03210	0.10600	0.02700	1.370
128	38	37	0.00000	0.03750	0.00000	4.150
129	38	30	0.00464	0.05400	0.42200	6.225
130	37	35	0.01100	0.04970	0.01318	1.370
131	37	34	0.00256	0.00940	0.00984	2.055
132	37	33	0.04150	0.14200	0.03660	1.370
133	36	35	0.00224	0.01020	0.00268	1.370
134	36	34	0.00871	0.02680	0.00568	1.370
135	34	19	0.07520	0.24700	0.06320	1.370
136	33	15	0.03800	0.12440	0.03194	1.370
137	32	31	0.02980	0.09850	0.02510	1.370
138	32	27	0.02290	0.07550	0.01926	1.370
139	32	23	0.03170	0.11530	0.11730	1.370
140	31	29	0.01080	0.03310	0.00830	1.370
141	31	17	0.04740	0.15630	0.03990	1.370
142	30	26	0.00799	0.08600	0.90800	6.225
143	30	17	0.00000	0.03880	0.96000	4.225
144	30	8	0.00431	0.05040	0.51400	6.225

Table E.16.e

Line data (cont.)						
Line No.	From	To	r	xl	bsh	Max. flow
145	29	28	0.02370	0.09430	0.02380	1.370
146	28	27	0.01913	0.08550	0.02160	1.370
147	27	25	0.03180	0.16300	0.17640	1.370
148	26	25	0.00000	0.03820	0.00000	8.000
149	25	23	0.01560	0.08000	0.08640	2.055
150	24	23	0.01350	0.04920	0.04980	1.370
151	23	22	0.03420	0.15900	0.04040	1.370
152	22	21	0.02090	0.09700	0.02460	1.370
153	21	20	0.01830	0.08490	0.02160	1.370
154	20	19	0.02520	0.11700	0.02980	1.370
155	19	18	0.01119	0.04930	0.01142	1.370
156	19	15	0.01200	0.03940	0.01010	1.370
157	18	17	0.01230	0.05050	0.01298	2.055
158	17	16	0.04540	0.18010	0.04660	1.370
159	17	15	0.01320	0.04370	0.04440	1.370
160	16	12	0.02120	0.08340	0.02140	1.370
161	15	14	0.05950	0.19500	0.05020	1.370
162	15	13	0.07440	0.24440	0.06268	1.370
163	14	12	0.02150	0.07070	0.01816	1.370
164	13	11	0.02225	0.07310	0.01876	1.370
165	12	11	0.00595	0.01960	0.00502	1.370
166	12	7	0.00862	0.03400	0.00874	1.370
167	12	3	0.04840	0.16000	0.04060	1.370
168	12	2	0.01870	0.06160	0.01572	1.370
169	11	5	0.02030	0.06820	0.01738	1.370
170	11	4	0.02090	0.06880	0.01748	1.370
171	10	9	0.00258	0.03220	1.2300	6.225
172	9	8	0.00244	0.03050	1.16200	6.225
173	8	5	0.00000	0.02670	0.00000	6.225
174	7	6	0.00459	0.02080	0.00550	1.370
175	6	5	0.01190	0.05400	0.01426	1.370
176	5	4	0.00176	0.00798	0.00210	2.055
177	5	3	0.02410	0.10800	0.02840	1.370
178	3	1	0.01290	0.04240	0.01082	1.370
179	2	1	0.03030	0.09990	0.02540	1.370

Table E.17.a

Bus data						
Bus No.	V^{min}	V^{max}	b^{min}	b^{max}	pd	qd
1	0.950	1.050	0.000	0.000	0.510	0.270
2	0.950	1.050	0.000	0.000	0.200	0.090
3	0.950	1.050	0.000	0.000	0.390	0.100
4	0.950	1.050	0.000	0.000	0.390	0.120
5	0.950	1.050	0.000	0.100	0.000	0.000
6	0.950	1.050	0.000	0.000	0.520	0.220
7	0.950	1.050	0.000	0.000	0.190	0.020
8	0.950	1.050	0.000	0.000	0.280	0.000
9	0.950	1.050	0.000	0.000	0.000	0.000
10	0.950	1.050	0.000	0.000	0.000	0.000
11	0.950	1.050	0.000	0.000	0.700	0.230
12	0.950	1.050	0.000	0.000	0.470	0.100
13	0.950	1.050	0.000	0.000	0.340	0.160
14	0.950	1.050	0.000	0.000	0.140	0.010
15	0.950	1.050	0.000	0.000	0.900	0.300
16	0.950	1.050	0.000	0.000	0.250	0.100
17	0.950	1.050	0.000	0.000	0.110	0.030
18	0.950	1.050	0.000	0.000	0.600	0.340
19	0.950	1.050	0.000	0.000	0.450	0.250
20	0.950	1.050	0.000	0.000	0.180	0.030
21	0.950	1.050	0.000	0.000	0.140	0.080
22	0.950	1.050	0.000	0.000	0.100	0.050
23	0.950	1.050	0.000	0.000	0.070	0.030
24	0.950	1.050	0.000	0.000	0.130	0.000
25	0.950	1.050	0.000	0.000	0.000	0.000
26	0.950	1.050	0.000	0.000	0.000	0.000
27	0.950	1.050	0.000	0.000	0.710	0.130
28	0.950	1.050	0.000	0.000	0.170	0.070
29	0.950	1.050	0.000	0.000	0.240	0.040
30	0.950	1.050	0.000	0.000	0.000	0.000
31	0.950	1.050	0.000	0.000	0.360	0.270
32	0.950	1.050	0.000	0.000	0.590	0.230
33	0.950	1.050	0.000	0.000	0.230	0.090
34	0.950	1.050	0.000	0.000	0.590	0.260
35	0.950	1.050	0.000	0.000	0.330	0.090
36	0.950	1.050	0.000	0.000	0.310	0.170

Table E.17.b

Bus data (cont.)						
Bus No.	V^{min}	V^{max}	b^{min}	b^{max}	pd	qd
37	0.950	1.050	0.000	0.050	0.000	0.000
38	0.950	1.050	0.000	0.000	0.000	0.000
39	0.950	1.050	0.000	0.000	0.270	0.110
40	0.950	1.050	0.000	0.000	0.660	0.230
41	0.950	1.050	0.000	0.000	0.370	0.100
42	0.950	1.050	0.000	0.000	0.960	0.230
43	0.950	1.050	0.000	0.000	0.180	0.070
44	0.950	1.050	0.000	0.050	0.160	0.080
45	0.950	1.050	0.000	0.050	0.530	0.220
46	0.950	1.050	0.000	0.000	0.090	0.100
47	0.950	1.050	0.000	0.000	0.340	0.000
48	0.950	1.050	0.000	0.100	0.200	0.110
49	0.950	1.050	0.000	0.000	0.870	0.300
50	0.950	1.050	0.000	0.000	0.170	0.040
51	0.950	1.050	0.000	0.000	0.170	0.080
52	0.950	1.050	0.000	0.000	0.180	0.050
53	0.950	1.050	0.000	0.000	0.230	0.110
54	0.950	1.050	0.000	0.000	1.130	0.320
55	0.950	1.050	0.000	0.000	0.630	0.220
56	0.950	1.050	0.000	0.000	0.840	0.180
57	0.950	1.050	0.000	0.000	0.120	0.030
58	0.950	1.050	0.000	0.000	0.120	0.030
59	0.950	1.050	0.000	0.000	2.770	1.130
60	0.950	1.050	0.000	0.000	0.780	0.030
61	0.950	1.050	0.000	0.000	0.000	0.000
62	0.950	1.050	0.000	0.000	0.770	0.140
63	0.950	1.050	0.000	0.000	0.000	0.000
64	0.950	1.050	0.000	0.000	0.000	0.000
65	0.950	1.050	0.000	0.000	0.000	0.000
66	0.950	1.050	0.000	0.000	0.390	0.180
67	0.950	1.050	0.000	0.000	0.280	0.070
68	0.950	1.050	0.000	0.000	0.000	0.000
69	0.950	1.050	0.000	0.000	0.000	0.000
70	0.950	1.050	0.000	0.000	0.660	0.200
71	0.950	1.050	0.000	0.000	0.000	0.000
72	0.950	1.050	0.000	0.000	0.120	0.000

Table E.17.c

Bus data (cont.)						
Bus No.	V^{min}	V^{max}	b^{min}	b^{max}	pd	qd
73	0.950	1.050	0.000	0.000	0.060	0.000
74	0.950	1.050	0.000	0.000	0.680	0.270
75	0.950	1.050	0.000	0.000	0.470	0.110
76	0.950	1.050	0.000	0.000	0.680	0.360
77	0.950	1.050	0.000	0.000	0.610	0.280
78	0.950	1.050	0.000	0.000	0.710	0.260
79	0.950	1.050	0.000	0.050	0.390	0.320
80	0.950	1.050	0.000	0.000	1.300	0.260
81	0.950	1.050	0.000	0.000	0.000	0.000
82	0.950	1.050	0.000	0.050	0.540	0.270
83	0.950	1.050	0.000	0.100	0.200	0.100
84	0.950	1.050	0.000	0.000	0.110	0.070
85	0.950	1.050	0.000	0.000	0.240	0.150
86	0.950	1.050	0.000	0.000	0.210	0.100
87	0.950	1.050	0.000	0.000	0.000	0.000
88	0.950	1.050	0.000	0.000	0.480	0.100
89	0.950	1.050	0.000	0.000	0.000	0.000
90	0.950	1.050	0.000	0.000	1.630	0.420
91	0.950	1.050	0.000	0.000	0.100	0.000
92	0.950	1.050	0.000	0.000	0.650	0.100
93	0.950	1.050	0.000	0.000	0.120	0.070
94	0.950	1.050	0.000	0.000	0.300	0.160
95	0.950	1.050	0.000	0.000	0.420	0.310
96	0.950	1.050	0.000	0.000	0.380	0.150
97	0.950	1.050	0.000	0.000	0.150	0.090
98	0.950	1.050	0.000	0.000	0.340	0.080
99	0.950	1.050	0.000	0.000	0.420	0.000
100	0.950	1.050	0.000	0.000	0.370	0.180
101	0.950	1.050	0.000	0.000	0.220	0.150
102	0.950	1.050	0.000	0.000	0.050	0.030
103	0.950	1.050	0.000	0.000	0.230	0.160
104	0.950	1.050	0.000	0.000	0.380	0.250
105	0.950	1.050	0.000	0.000	0.310	0.260
106	0.950	1.050	0.000	0.000	0.430	0.160
107	0.950	1.050	0.000	0.000	0.500	0.120
108	0.950	1.050	0.000	0.000	0.020	0.010

Table E.17.d

Bus data (cont.)						
Bus No.	V^{min}	V^{max}	b^{min}	b^{max}	pd	qd
109	0.950	1.050	0.000	0.000	0.080	0.030
110	0.950	1.050	0.000	0.050	0.390	0.300
111	0.950	1.050	0.000	0.000	0.000	0.000
112	0.950	1.050	0.000	0.000	0.680	0.130
113	0.950	1.050	0.000	0.000	0.060	0.000
114	0.950	1.050	0.000	0.000	0.080	0.030
115	0.950	1.050	0.000	0.000	0.220	0.070
116	0.950	1.050	0.000	0.000	1.840	0.000
117	0.950	1.050	0.000	0.000	0.200	0.080
118	0.950	1.050	0.000	0.000	0.330	0.100

Table E.18.a

Generation data						
Bus No.	pg^{min}	pg^{max}	qg^{min}	qg^{max}	aa	bb
1	0.700	1.800	-0.230	1.150	60.73	127.70
4	0.800	2.170	-0.400	1.200	48.90	78.60
6	0.400	1.080	-0.500	0.500	69.60	195.60
8	0.800	2.170	-3.500	2.200	77.30	68.00
10	0.400	2.000	-2.000	3.400	50.19	45.97
12	0.400	1.080	0.150	0.750	80.30	193.20
15	0.300	0.720	-0.800	0.400	151.30	120.40
18	0.300	0.720	-0.600	1.400	151.30	120.40
19	0.400	1.080	-0.150	0.750	136.70	124.60
24	0.300	0.720	-0.400	2.400	151.30	120.40
25	0.800	2.170	-2.240	3.000	39.40	78.40
26	1.200	3.240	-4.000	2.250	63.85	69.90
27	0.300	0.720	-0.080	0.400	151.30	120.40
31	0.300	0.720	-0.150	0.400	151.30	120.40
32	0.300	0.720	-0.200	0.600	151.30	120.40
34	0.400	1.080	-0.400	0.750	136.70	124.60
36	0.400	1.080	-1.000	1.000	67.50	206.60
40	0.300	0.720	-0.500	0.500	151.30	120.40
42	0.400	1.080	-0.150	0.750	136.70	124.60
46	0.300	0.720	-0.080	0.400	151.30	120.40
49	0.800	2.170	-0.240	1.200	77.30	68.00
54	0.300	0.720	-0.080	0.400	151.30	120.40
55	0.400	1.080	-0.150	0.750	80.30	193.20
56	0.300	0.720	-0.080	0.400	151.30	120.40
59	0.400	1.080	-0.850	2.000	67.80	154.60

Table E.18.b

Generation data (cont.)						
Bus No.	pg^{min}	pg^{max}	qg^{min}	qg^{max}	aa	bb
61	0.400	1.080	-1.650	1.650	67.80	154.60
62	0.400	1.080	-0.150	0.750	63.60	201.60
65	0.800	2.160	-3.000	1.500	46.33	104.10
66	1.200	3.240	-0.450	2.000	42.13	72.93
69	1.600	4.340	-2.000	2.000	59.97	39.85
70	0.300	0.720	-0.800	0.400	15.13	120.40
72	0.300	0.720	-0.080	0.400	15.13	120.40
73	0.300	0.720	-0.080	0.400	15.13	120.40
74	0.400	1.080	-0.150	0.750	80.30	193.20
76	0.400	1.080	-0.150	0.750	80.30	193.20
77	0.300	0.720	-0.400	0.400	151.30	120.40
80	1.200	3.250	-3.000	2.250	31.49	76.87
85	0.400	1.080	-0.150	0.750	67.80	154.60
87	0.400	1.080	-0.400	0.750	80.30	193.20
89	1.200	2.250	-0.450	2.200	58.13	71.76
90	0.800	2.170	-2.000	1.500	48.90	78.60
91	0.300	0.720	-0.240	1.200	151.30	120.40
92	0.400	1.080	-0.150	0.750	136.70	124.60
99	0.300	0.720	-0.080	0.400	151.30	120.40
100	0.400	4.000	-0.480	2.400	28.20	46.20
103	0.000	4.000	-0.480	2.400	36.82	45.98
104	0.000	2.080	-0.150	0.750	136.70	124.60
105	0.000	2.080	-0.150	0.750	136.70	124.60
107	0.000	2.080	-0.150	0.750	67.80	154.60

REFERENCES

Power Systems

Abdul-Rahman, K.H. and Shahidehpour, S.M.; "A Fuzzy-Based Optimal Reactive Power Control". IEEE Trans. on Power Systems, Vol. 8, No. 2, May 1993, pp. 662-670.

Ajjarapu, V. and Christy, C.; "The Continuation Power Flow: A Tool for Steady State Voltage Stability Analysis". IEEE Trans. on Power Systems, Vol. 7, No. 1, February 1992, p. 416-423.

Almeida, K.C.; Galiana, F.D. and Soares, S.; "A General Parametric Optimal Power Flow". Proc. of the Power Industry Computer Application Conference, Phoenix, USA, May 1993, pp. 66-73.

Almeida, K.C.; Galiana, F.D. and Soares, S.; "A Nonlinear Parametric Approach for Optimal Load Tracking", Proc. of the 11th Power Systems Computation Conference, Avignon, France, August 1993, pp. 1257-1264.

Alsaç, O.; Bright, J.; Prais, M. and Stott, B.; "Further Developments in LP-Based Optimal Power Flow". IEEE Trans. on Power Systems, Vol. 5, No. 3, August 1990, pp. 697-711.

Aoki, K. and Satoh, T.; "Economic Dispatch with Network Security Constraints Using Parametric Quadratic Programming". IEEE Trans. on Power Apparatus and Systems, Vol. 101, No. 12, December 1982, pp. 4548-4556.

Bacher, R. and Van Meeteren, H.P.; "Real-Time Optimal Power Flow in Automatic Generation Control". IEEE Trans. on Power Systems, Vol. 3, No 4, November 1988, pp. 1518-1529.

Balu, N. et al.; "On-Line Power System Security Analysis". Proceedings of the IEEE, Vol. 80, No. 2, February 1992, pp. 262-280.

Baughman, M.L. and Siddiqi, S.N.; "Real-Time Pricing of Reactive Power: Theory and Case Study Results". IEEE Trans. on Power Systems, Vol. 6, No. 1, February 1991, pp. 23-29.

Bertram, T.J.; Kendall, D.D. and Dangelmaier, L.C.; "An Integrated Package for Real-Time Security Enhancement". IEEE Trans. on Power Systems, Vol. 5, No. 2, May 1990, pp. 592-600.

Bjelogrlić, M.; Ćalović, M.S.; Ristanović, P.M. and Babić, B.S.; "Application of Newton's Optimal Power Flow in Voltage/Reactive Power Control". IEEE Trans. on Power Systems, Vol. 5, No. 4, November 1990, pp. 1447-1454.

Blanchon, G.; Dodu, J.C.; Merlin, A.; "Developing a New Tool for Real Time Control in Order to Coordinate the Regulation of Reactive Power and Voltage Schedule in Large Scale EHV Power Systems". Proceedings of Symposium of CIGRÉ, Florence, Italy, 1983, paper 209-01.

Blanchon, G.; Dodu, J.C. and Merlin, A.; "New Developments of the Reactive Power Flow Optimization Model Used at EDF". Proceedings of the 8th Power Systems Computation Conference - PSCC, Helsinky, Finland, September 1984, pp.427-434.

Bridenbaugh, C.J.; Dimascio, D.A. and D'Aquila, R.; "Voltage Control Improvement Through Capacitor and Transformer Tap Optimization". IEEE Trans. on Power Systems, Vol. 7, No. 1, February 1992, pp. 222-227.

Burchett, R.C.; Happ, H.H. and Vierath, D.R.; "Quadratically Convergent Optimal Power Flow". IEEE Trans. on Power Apparatus and Systems, Vol. 103, No. 11, November 1984, pp. 3267 - 3275.

Burchett, R.C.; Happ, H.H.; Merrit, W.C. and Saylor, C.H.; "Security Dispatching". Proceedings of CIGRÉ, 32nd Session, 28 August / 3 September, 1988, paper 39-03.

Cañizares, C.A. and Alvarado, F.L.; "Point of Collapse and Continuation Methods for Large AC/DC Systems". IEEE Trans. on Power Systems, Vol. 8, No. 1, February 1993, pp. 1-8.

Carpentier, J.L.; "Contribuition à l'Étude du Dispatching Économique". Bulletin de la Societé Française des Electriciens, Ser. 8, Vol. 3, 1962, pp. 431-447.

Carpentier, J.L.; "Differential Injections Method: A General Method for Secure and Optimal Load Flows". Proceedings of the Power Industry Computation Conference, Mineapolis, USA, 1973, pp. 255-262.

Carpentier, J.L.; Cotto, G.; Niederlander, P.L.; "New Concepts for Automatic Generation Control in Electric Power Systems Using Parametric Quadratic Programming". Proceedings of the IFAC Symposium on Real Time Digital Control Applications, Guadalajara, Mexico, January 1983, pp. 595-600.

Carpentier, J.L.; "Towards a Secure and Optimal Automatic Operation of Power Systems". Proceedings of the Power Systems Computer Application Conference, Montreal, Canada, May 1987, pp. 2-37.

Carpentier, J.L.; "Extended Security Constrained Optimal Power Flow, a Basic Tool for an Integrated Secure Economic Operation". Proceedings of the 11th Power Systems Computation Conference, Avignon, France, August 1993, pp. 1265-1277.

Chang, S.-K.; Marks, G.E. and Kato, K.; "Optimal Real Time Voltage Control". IEEE Trans. on Power Systems, Vol. 5, No. 3, August 1990, pp. 750-756.

Chowdhury, B.H. and Rahman, S.; "A Review of Recent Advances in Economic Dispatch". IEEE Trans. on Power Systems, Vol. 5, No. 4, November 1990, pp.1248-1257.

Cicoria, R.; Migliardi, P. and Maranino, P.; "Knowledge Based Methodologies Versus Conventional Optimization Algorithms: Applications to Reactive Power Compensation". Proceedings of the 11th Power Systems Computation Conference, Avignon, France, August 1993, Vol. 1, pp. 411-418.

Crisan, O. and Mohtadi, M.A.; "Efficient Identification of Binding Inequality Constraints in the Optimal Power Flow Newton Approach". IEE Proceedings-C, Vol. 139, No. 5, September 1992, pp. 365-370.

da Costa, G.R.M. and Santos Jr., A.; "A Quasi-Newton Version in the Augmented Lagrangian Approach to Solve the Optimal Power Flow". Proceedings of the IFAC Symposium on Control of Power Plants and Power Systems, Munich, Germany, March 1992, pp. 37-40.

Deeb, N.I. and Shahidehpour, S.M.; "Linear Reactive Power Optimization in a Large Power Network Using the Decomposition Approach". IEEE Trans. on Power Systems, Vol. 5, No. 2, May 1990, pp.428-434.

Denzel, D.; Edwin, K.W.; Graf, F.-R. and Glavitsch, H.; "Optimal Power Flow and Its Real-Time Application at the RWE Energy Control Centre". Proceedings of CIGRÉ, 32nd Session, 28 August/ 3 September 1988, paper 39-19

Dias, L.G. and El-Hawary, M.E.; "Effects of Active and Reactive Power Modelling in Optimal Load Flow Studies". IEE Proceedings-C, Vol. 136, No. 5, September 1989, pp. 259-263.

Dias, L.G. and El-Hawary, M.E.; "Effects of Load Modelling in Security Constrained OPF Studies". IEEE Trans. on Power Systems, Vol. 6, No. 1, February 1991, pp. 87-93.

Dillon, T.S.; "Rescheduling, Constrained Participation Factors and Parameter Sensitivity in the Optimal Power Flow Problem". IEEE Trans. on Power Apparatus and Systems, Vol. 100, No. 5, May 1981, pp. 2628-2634.

Dommel, H.W. and Tinney, W.F,; "Optimal Power Flow Solutions". IEEE Trans. on Power Apparatus and Systems, Vol. 87, No. 10, October 1968, pp. 1866-1876.

El-Hawary, M.E. and Mbamalu, G.A.N.; "A Comparison of Probabilistic Perturbation and Deterministic Based Optimal Power Flow Solutions". IEEE Trans. on Power Systems, Vol. 6, No. 3, August 1991, pp. 1099-1105.

Fahmideh-Vojdani, A.; Analysis and Continuous Simulation of Secure-Economic Operation of Power Systems, Ph.D. Thesis, Dept. of Electrical Engineering, McGill University, 1982.

Fahmideh-Vojdani, A. and Galiana, F.D.; "The Continuation Method and its Application in System Planning and Operation" Proceedings of CIGRÉ, Florence, Italy, 1983, paper 102-04.

Fahd, G. and Sheblé, G.B.; "Optimal Power Flow Emulation of Interchange Brokerage Systems Using Linear Programming". IEEE Trans. on Power Systems, Vol. 7, No. 2, May 1992, pp. 497-504.

Fouad, A.A. and Jianzhong, T.; "Stability Constrained Optimal Rescheduling of Generation". IEEE Trans. on Power Systems, Vol. 8, No. 1, February 1993, pp. 105-112.

Galiana, F.D.; Fahmideh-Vojdani, A.; Huneault, M. and Juman, M.; "Optimal Power System Dispatch Through the Continuation Method: Variation of Functional Inequality Limits". Proc. of IEEE Int. Symposium on Circuits and Systems, Newport Beach, USA, May 1983, pp. 1192-1197.

Galiana, F.D. and Zeng, Z.C., "Analysis of the Load Flow Behaviour Near a Jacobian Singularity". IEEE Transactions on Power Systems, Vol. 7, No. 3, August 1992, pp. 1362-1369.

Granville, S.; "Optimal Reactive Dispatch Through Interior Points Methods". IEEE Transactions on Power Systems, Vol. 9, No. 1, February 1994, pp. 136-146.

Gribik, P.R.; Shirmohammadi, D.; Hao, S. and Thomas, C.L.; "Optimal Power Flow Sensitivity Analysis". IEEE Trans. on Power Systems, Vol. 5, No. 3, August 1990, pp. 969-976.

Habibollazahdeh, H.; Luo, G.X. and Semlyen, A.; "Hydrothermal Optimal Power Flow Based on a Combined Linear and Nonlinear Programming Methodology". IEEE Trans. on Power Systems, Vol. 4, No. 2, May 1989, pp. 530-537.

Happ, H.H.; "Optimal Power Dispatch - A Comprehensive Survey". IEEE Trans. on Power Apparatus and Systems, Vol. 96, No. 3, May-June 1977, pp. 841-850.

Heinz, D.; Haubrich, H.-J. and Stelzner, P.; "Online Application of an Extended Optimal Power Flow Algorithm at the VEW Power System Control Center". Proc. of IFAC Symposium on Control of Power Plants and Power Systems, Munich, Germany, March 1992, pp. 1249-1255.

Hingorani, N.G.; "FACTS - Flexible AC Transmission System". AC and DC Power Transmission (Conf. Publ. No. 345), London, UK, September 1991, pp. 1-7.

Hingorani, N.G.; "Flexible AC Transmission". IEEE Spectrum, April 1993, pp. 40-45.

Hong, Y.-Y.; Sun, D.I.; Lin, S.-Y. and Lin, C.-J.; "Multi-Year Multi-Case Optimal VAR Planning". IEEE Trans. on Power Systems, Vol. 5, No. 4, November 1990, pp. 1294-1301.

Hong, Y.-Y.; "Enhanced Newton Optimal Power Flow Approach: Experiences in Taiwan Power System". IEE Proceedings-C, Vol. 139, No. 3, May 1992, pp. 205-210.

Hong, Y.-Y; Liao, C.-M. and T.-G. Lu; "Application of Newton Optimal Power Flow to Assessment of VAR Control Sequences on Voltage Security: Case Studies for a Practical Power System". IEE Proceedings-C, Vol. 140, No. 6, November 1993, pp. 539-544.

Huneault, M.; An Investigation of the Solution to the Optimal Power Flow Problem Incorporating Continuation Methods, Ph.D. Thesis Dept. of Electrical Engineering, McGill University, 1988.

Huneault, M. and Galiana, F.D.; "An Investigation of the Solution to the Optimal Power Flow Problem Incorporating Continuation Methods". IEEE Trans. on Power Systems, Vol. 5, No. 1, February 1990, pp. 103-110.

Huneault, M. and Galiana, F.D.; "A Survey of the Optimal Power Flow Literature". IEEE Trans. on Power Systems, Vol.6, No. 2, May 1991, pp. 762-770.

Iba, K.; "Reactive Power Optimization by Genetic Algorithm". Proc. of the Power Industry Computer Application Conference, Phoenix, USA, May 1993, pp. 195-201.

Innorta, M. and Marannino, P.; "Advance Dispatch Procedures for the Centralized Control of Real Power". Proceedings of the Power Industry Computer Applications Conference, 1985, pp. 188-194.

Innorta, M.; Marannino, P.; Granelli, G.P.; Montagna, M. and Silvestri, A.; "Security Constrained Dynamic Dispatch of Real Power for Thermal Groups". Proceedings of the Power Industry Computer Applications (PICA) Conference, Montreal, Canada, 1987, pp. 407-413.

Kellermann, W.; El-Din, H.M.; Graham, C.E. and Maria, G.A.; "Optimization of Fixed Transformer Settings in Bulk Electricity Systems". IEEE Trans. on Power Systems, Vol. 6, No. 3, August 1991, pp. 1126-1132.

Kirschen, D.S. and Van Meeteren, H.P.; "MW/ Voltage Control in a Linear Programming Based Optimal Power Flow". IEEE Trans. on Power Systems, Vol. 3, No. 2, May 1988, pp. 481-489.

Le Du, A.; "Pour un Réseau Électrique Plus Performant: le Project FACTS". Revue Générale d' Electricité, No. 6, June 1992, pp. 105-121.

Lee, K.Y.; Mohtadi, M.A.; Ortiz, J.L. and Park, Y.M.; "Optimal Operation of Large-Scale Power Systems". IEEE Trans. on Power Systems, Vol. 3, No. 2, May 1988, pp. 413-420.

Lereverend, B.K.; Fong, C.C.; Lau, P.C.K. and Winter,W.H.; "Trade-Off Decisions in Cost and Reliability for Power System Operation" Proceedings of CIGRÉ, 33rd Session, 1990, paper 39-203.

Li, Y.Z. and David, A.K.; "Pricing Reactive Power Conveyance" IEE Proceedings-C, Vol. 140, No. 3, May 1993, pp. 174-180.

Liu, W.-H.E.; Papalexopolous, A.D. and Tinney, W.F.; "Discrete Shunt Controls in a Newton Optimal Power Flow". IEEE Trans. on Power Systems, Vol. 7, No. 4, November 1992, pp. 1509-1518.

Lu, C.N.; Chen, S.S and Ong, C.M.; "The Incorporation of HVDC Equations in Optimal Power Flow Methods Using Sequential Quadratic Programming". IEEE Trans. on Power Systems, Vol. 3, No. 3, August 1988, pp. 1005-1011.

Luo, G.X.; Habibollahzadeh, H. and Semlyen, A.; "Short-Term Hydro-Thermal Dispatch Detailed Model And Solutions". IEEE Trans. on Power Systems, Vol. 4, No. 4, October 1989, pp. 1452-1460.

Maliszewski, R.M.; Pasternack, B.M.; Chamia, M.; frank, H.; Scherer Jr. and Paulsson, L.; "Power Control in a Highly Integrated Transmission Network". Proceedings of CIGRÉ, 33rd Session, 1990, paper 37-303.

Maria, G.A. and Findlay, J.A.; "A Newton Optimal Power Flow Program for Ontario Hydro EMS". IEEE Trans. on Power Systems, Vol. 2, No. 3, August 1987, pp. 576-584.

Meisel, J.; "System Incremental Cost Calculations Using the Participation Factor Load-Flow Formulation". IEEE Trans. on Power Systems, Vol. 8, No. 1, February 1993, pp. 357-363.

Miranda, V. and Saraiva, J.T.; "Fuzzy Modelling of Power System Optimal Load Flow". IEEE Trans. on Power Systems, Vol. 7, No. 2, May 1992, pp. 843-849.

Monticelli, A.; Load Flow in Power System Networks. Edgard Blücher, 1983 (in portuguese).

Monticelli, A.; Pereira, M.V.F. and Granville, S.; "Security-Constrained Optimal Power Flow with Post-Contingency Corrective Rescheduling". IEEE Transactions on Power Systems, Vol. 2, No. 1, February 1987, pp. 175-182.

Monticelli, A. and Liu, W.-H.E.; "Adaptative Movement Penalty Method for the Newton Optimal Power Flow". IEEE Trans. on Power Systems, Vol. 7, No. 1, February 1992, pp. 334-342.

Mukerji, R.; Neugebauer, W.; Ludorf, R.P. and Catelli, A.; "Evaluation of Wheeling and Non-Utility Generation (NUG) Options Using Optimal Power Flows". IEEE Trans. on Power Systems, Vol. 7, No. 1, February 1992, pp. 201-207.

Nanda, J.; Khotari, D.P. and Srivastava, S.C.; "New Optimal Power Dispatch Algorithm Using Fletcher's Quadratic Programming Method". IEE Proceedings-C, Vol. 136, No. 3, May 1989, pp. 153-161.

Okumura, K.; Kishima, A. and Fujita, T.; "Computation of Multiple Solutions of Load-Flow Equations by Simplicial Subdivision Homotopy Method". Electrical Engineering in Japan, Vol. 109, No. 3, May-June 1989, pp. 59-67.

Papalexopoulos, A.D.; Imparato, C.F. and Wu, F.F.; "Large-Scale Optimal Power Flow: Effects of Initialization, Decoupling & Discretization". IEEE Trans. on Power Systems, Vol. 4, No. 2, May 1989, pp. 748-759; correction on Vol. 4, No. 4, November 1989, pp. 1236-1237.

Papalexopoulos, A.D.; Hao, S.; Liu, E. and Alaywan, Z.; "Cost/ Benefit Analysis of an Optimal Power Flow: The PG&E Experience". Proc. of the Power Industry Computer Application Conference, Phoenix, USA, May 1993, pp. 82-88.

Peschon, J.; Piercy, D.S.; Tinney, W.F.; Tveit, O.J. and Cuénod, M.; "Optimum Control of Reactive Power Flow", IEEE Transactions of PAS, Vol. 87, No. 1, January, 1968, pp. 40-48.

Ponrajah, R.; The Minimum Cost Optimal Power Flow Problem Solved Via the Restart Homotopy Continuation Method, Ph.D. Thesis, Dept. of Electrical Engineering, McGill University, 1987.

Ponrajah, R.A. and Galiana, F.D.; "The Minimum Cost Optimal Power Flow Problem Solved Via the Restart Homotopy Continuation Method". IEEE Trans. on Power Systems, Vol. 4, No. 1, February 1989, pp. 139-148.

Rehn, C.; Bubenko, J.A. and Sjelvgren, D.; "Voltage Optimization Using Augmented Lagrangian Functions and Quasi-Newton Techniques". IEEE Trans. on Power Systems, Vol. 4, No. 4, October 1989, pp. 1470-1483.

Rice, R.E.; Grady, W.M.; Lesso, W.G.; Noyola, A.H. and Connoly, M.E.; "Power Generation Scheduling Through Use of Generalized Network Flow Programming". IEE Proceedings-C, Vol. 138, No. 1, January 1991, pp. 39-46.

Salgado, R.; Brameller, A. and Aitchison, P.; "Optimal Power Flow Solutions Using the Gradient Projection Method, Part I and Part II". IEE Proceedings-C, Vol. 137, No. 6, November 1990, pp. 424-435.

Santos Jr., A.; Deckmann, S. and Soares, S.; "A Dual Augmented Lagrangian Approach for Optimal Power Flow". IEEE Trans. on Power Systems, Vol. 3, No. 3, August 1988, pp. 1020-1025.

Saraiva, J.T.; Miranda, V. and Pinto, L.M.V.G.; "Impact on Some Planning Decisions from a Fuzzy Modelling of Power Systems". Proc. of the Power Industry Computer Application Conference, Phoenix, USA, May 1993, pp. 327-333.

Sasson, A.; "Nonlinear Programming Solutions for Load-Flow, Minimum Loss, and Economic Dispatching Problems". IEEE Trans. on Power Apparatus and Systems, Vol. 88, No. 4, April 1969, pp.399-408.

Sasson, A.M.; Viloria, F. and Aboytes, F.; "Optimal Load Flow Solution Using the Hessian Matrix". Proc. of the Power Industry Computer Application Conference, May 1971, pp. 203-209.

Schnyder, G. and Glavitsch, H.; "Integrated Security Control Using an Optimal Power Flow and Switching Concepts". IEEE Trans. on Power Systems, Vol. 3, No. 2, May 1988, pp. 782-788.

Schnyder, G. and Glavitsch, H.; "Security Enhancement Using an Optimal Switching Power Flow". IEEE Trans. on Power Systems, Vol. 5, No. 2, May 1990, pp. 674-681.

Shirmohammadi, D.; Rajagopalan, C.; Alward, E.R. and Thomas, C.L.; "Cost of Transmission Transactions: An Introduction". IEEE Transactions on Power Systems, Vol. 6, No. 4, November 1991, pp. 1546-1556.

Stott, B. and Hobson, E.; "Power System Security Control Calculations Using Linear Programming, Part I and Part II". IEEE Trans. on Power Apparatus and Systems, Vol. 97, No. 5, Sept-Oct. 1978, pp. 1713-1731.

Stott, B.; Alsaç, O and Marinho, J.L.; "The Optimal Power Flow Problem". Proc. of the SIAM Conference, Seattle, Washington, 1980, pp. 327-351.

Stott, B.; Alsaç, O. and Monticelli, A.J.; "Security Analysis and Optimization". Proceedings of the IEEE, Vol. 75, No. 12, december 1987, pp.1623-1644.

Sun, D.I.; Ashley, B.; Brewer, B.; Hughes, A. and Tinney, W.F.; "Optimal Power Flow by Newton Approach". IEEE Trans. on Power Apparatus and Systems, Vol. 103, No. 10, October 1984, pp. 2864-2875.

Sun, D.I.; Hu, T.-I.; Lin, G.-S.; Lin, C.-J. and Chen, C.-M.; "Experiences with Implementing Optimal Power Flow for Reactive Scheduling in the Taiwan Power System". IEEE Trans. on Power Systems, Vol. 3, No. 3, August 1988, pp. 1193-1120.

Talukdar, S. and Ramesh, V.C.; "A Multi-Agent Technique for Contingency Constrained Optimal Power Flows". Proc. of the Power Industry Computer Application Conference, Phoenix, USA, May 1993, pp. 188-194.

Taranto, G.N.; Pinto, L.M.V.G. and Pereira, M.V.F.; "Representation of FACTS Devices in Power System Economic Dispatch". IEEE Trans. on Power Apparatus and Systems, Vol. 7, No. 2, May 1992, pp. 572-576.

Terra, L.D.B. and Short, M.J.; "Security-Constrained Reactive Power Dispatch". IEEE Trans. on Power Systems, Vol. 6, No. 1, February 1991, pp. 109-117.

Thomas, R.J.; Barnard, R.D. and Meisel, J.; "The Generation of Quasi Steady-State Load-Flow Trajectories and Multiple Singular Points Solutions". IEEE Transactions on Power Apparatus and Systems, Vol. 90, No. 5, September/October, 1971, pp. 1967-1973

Tinney, W.F.; Bright, J.M.; Demaree, K.D. and Hughes, B.A.; "Some Deficiencies in Optimal Power Flow". IEEE Trans. on Power Systems, Vol. 3, No. 2, May 1988, pp. 676-683.

Tomsovic, K.; "A Fuzzy Linear Programming Approach to the Reactive Power/ Voltage Control Problem". IEEE Trans. on Power Systems, Vol. 7, No. 1, February 1992, pp. 287-293.

Vaahedi, E. and El-Din, H.M.Z.; "Considerations in Applying Optimal Power Flow to Power System Operation". IEEE Trans. on Power Systems, Vol. 4, No. 2, May 1989, pp. 694-703.

Venkatesh, S.V.; Liu, W.-H.E. and Papalexopoulos, A.D.; "A Least Squares Solution for Optimal Power Flow Sensitivity Calculation". IEEE Trans. on Power Systems, Vol. 7, No. 3, August 1992, pp. 1394-1401.

Wu, Y.; Debs, A. and Marsten, R.; "A Direct Nonlinear Predictor-Corrector Primal-Dual Interior Point Method for Optimal Power Flows". Proc. of the Power Industry Computer Application Conference, Phoenix, USA, May 1993, pp. 138-145.

Yokoyama, R.; Bae, S.H.; Morita, T. and Sasaki, H.; "Multiobjective Optimal Generation Dispatch Based on Probability Security Criteria". IEEE Trans. on Power Systems, Vol. 3, No. 1, February 1988, pp. 317-324.

Optimization Theory

Fiacco, A.; Introduction to Sensitivity and Stability Analysis in Nonlinear Programming. Mathematics in Science and Engineering Vol. 165, Academic Press, 1983.

Garcia, C.B. and Zangwill, W.I.; Pathways to Solutions, Fixed Points and Equilibria. Prentice Hall, 1981.

Gauvin, J.; "A Necessary and Sufficient Regularity Condition To Have Bounded Multipliers in Nonconvex Programming". Mathematical Programming, No. 12, 1977, pp. 136-138.

Guddat, J.; Wacker, H. and Zulehner, W.; "On Imbedding and Parametric Optimization - A Concept of a Globally Convergent Algorithm for Nonlinear Optimization Problems". Mathematical Programming Study, No. 21, 1984, pp.79-96.

Guddat, J.; Jongen, H.Th. and Rueckmann, J.; "On Stability and Stationary Points in Nonlinear Optimization". Journal of the Autralian Mathematical Society Series B, No. 28, 1986, pp.36-56.

Guddat, J.; Jongen, H.Th. and Nowack, F.; "Parametric Optimization: Pathfollowing with Jumps". Approximation and Optimization - Lecture Notes in Mathematics, No. 1354, Springer-Verlag, 1988, pp. 43-53.

Guddat, J.; Guerra Vazquez, F. and Jongen, H.Th.; Parametric Optimization: Singularities, Pathfollowing and Jumps, John Wiley & Sons, 1990.

Jongen, H.Th.; Jonker, P. and Twilt, F.; "One-Parameter Families of Optimization Problems: Equality Constraints". Journal of Optimization Theory and Applications, Vol. 48, No. 1, January 1986, pp. 141-161.

Jongen, H.Th.; Jonker, P. and Twilt, F.; "Critical Sets in Parametric Optimization". Mathematical Programming, No. 34, 1986, pp. 333-353.

Kojima, M.; "Strongly Stable Stationary Solutions in Nonlinear Programs". Proceedings of the Symposium of Analysis and Computation of Fixed Points, Madison, USA, 1979, pp. 93-138.

Luenberger, D.; Linear and Nonlinear Optimization - Second Edition; Addison-Wesley, 1984.

Poore, A.B. and Tiahrt, C.A.; "Bifurcation Problems in Nonlinear Paramtric Programming". Mathematical Programming, No. 39, 1987, pp. 189-205.

Zlobec, S.; "Input Optimization: I. Optimal Realizations of Mathematical Models". Mathematical Programming, No. 31, 1985, pp. 245-268.